Hazard and **Risk** Assessment

for

Induced Seismicity in Groningen

Interim Update November 2015

Contents

1 Management Summary

Summary

Conclusions

- This update to the May 2015 Probabilistic Hazard and Risk Assessment (PHRA) evaluates the risk from failure of buildings as a result of induced earthquakes due to gas production from the Groningen field. This information is intended to be used to access the acceptability of the risk compared to the risk norm, and to determine the appropriate mitigation measures to ensure continued safety of people in the Groningen gas field region.
- Key conclusions of the November 2015 updated PHRA include:
  - This November 2015 PHRA update shows that no houses exceed a risk of 10^{-4} (i.e. consistent with the criteria proposed by the Meijdam Cie) for a 33 bcm/annum scenario for 2016 - 2021.
  - Longer term (2017-2021) the scope of the structural upgrading program, required to remain within the acceptable levels of risk as advised by the Meijdam Committee, will depend on further reduction of the uncertainties around the risk. The program at the current assessment for a 33 Bcm/annum scenario comprises some 5,000 buildings.
  - Based on continued gas production at a rate of 33 Bcm/annum, after 2021 each year no more than a few hundred additional buildings are likely to require upgrading. The total size of the structural ugrading program also depends on the effectiveness with which these buildings can be identified through inspection. As a consequence, buildings that don't require upgrading might actually be upgraded. Therefore the actual scope of the upgrading program will be larger.
  - Hazard maps indicate a smaller geographical area is exposed to significant (> 0.25g PGA) ground accelerations for 2016 – 2021 than was projected for the same period in the May 2015 PHRA report. The reduced hazard area is consistent with the KNMI Hazard map update published in October 2015 and now reflects the improved methodology used to predict ground motion, based on the detailed description of the soil layers in the Groningen field area.
  - For the first time it is possible to match a fully probabilistic risk assessment to an established risk norm. This outcome was achieved by comprehensive studies of building materials and construction in the area, advanced fragility modelling and the results of a shake table test of a Groningen-type terraced house built with representative materials and building methods.
  - The studies into building fragility conclude that in general buildings built in the 1960s and 70s are much stronger than originally thought. Especially, SiCa bricks that are often used for load bearing interior walls have a greater resilience to earthquakes than previously estimated.
- All studies supporting this assessment have been reviewed through an independent peer review process conducted to international scientific standards.

Background to this Study

- A Study and Data Acquisition Plan describes the objectives and interdependencies of all the studies and research efforts into induced seismicity being undertaken by and on behalf of NAM. The plan was first shared with SodM and the Ministry of Economic Affairs (Ref. 2) in November 2012 and was made public in early 2013.
- As part of the original Study and Data Acquisition plan, a probabilistic hazard and risk assessment (PHRA) for the Groningen gas field region was proposed. The original probabilistic hazard assessment (PHA) and scenario based risk assessment for the Groningen field were published in December 2013 as part of the 2013 Winningplan update. The next update to the PHRA will underpin the Winningsplan submission for the Groningen field in mid 2016.
- The six-monthly updates provide insight into the progress of the assessment of the hazard and risk versus the assessment that underpinned the 2013 Winningsplan update.
- NAM continues with its Study and Data Acquisition Plan which:
  - is based on specific evidence and targeted data
  - has many Dutch and international experts involved, including from academia, university laboratories, independent experts, commercial parties and consultants.
  - is subject to an extensive voluntary assurance and verification program, through an independent peer review process conducted to international scientific standards.

New in this November 2015 update:

A Deeper Level of Analysis and more data specific to Groningen

- Revised static and dynamic reservoir modelling (with improved history match to production, pressure and subsidence data)
- Improved seismic model.
- A major update of the equation used to predict ground motion. The updated equation incorporates factors including area-specific details of shallow sub-surface and soils. Data from the newly available geophone network contributed to this.
- New data on strength of buildings and building materials from lab tests, tests in pilot houses and shake table testing conducted in Italy. This was used to update building fragility relationships.
- Updated exposure to risk for people reflecting more comprehensive work on collapse hazard. Furthermore, the risk of falling objects outside of buildings has also been studies.
- This work has resulted in the first quantified probabilistic risk assessment by location. In the previous May 2015 update the risk data were qualitative, as the results had not been fully calibrated to sufficient actual data.

Study Scope

- In this update, NAM has evaluated both the risk in the near term (2016-2017), the measures necessary to maintain risk within acceptable levels in the period 2016-2021. The risk levels have been assessed against the criteria that have been proposed by the Meijdam Committee.
- This evaluation has been done for three production scenarios: 33, 27 and 21 Bcm/annum.

Further work

- Study and data acquisition work will continue to improve understanding of the specific hazard and risk situation in the Groningen field area and will continue to be progressed for the foreseeable future.
- The main work planned between now and the PHRA update for the mid 2016 Winningsplan update is as follows:
  - Continue the experiments and studies to understand the fragility of buildings. Incorporate additional data from field and building tests.
  - Conduct an expert panel to establish the maximum magnitude for earthquakes in the Groningen field.
  - Further refine GMPE and seismological model.
- Independent external oversight for the studies supporting the Hazard and Risk Assessment in the Winningsplan 2016 is provided by the Scientific Advisory Committee (SAC), chaired by L. van Geuns, which was installed by the Minister of Economic Affairs (EZ).
- Many activities are aimed primarily at preparing the hazard and risk assessment for the Winningsplan 2016, but many further activities aim to develop a broader understanding of the physics of induced earthquakes. These activities will not be completed by mid-2016, but may provide the further insights and a broader foundation for the hazard and risk assessment of Winningsplan 2016.

Reader's Guide

This report presents the October 2015 update of the Hazard and Risk Assessment. Data presented in this report should be read or interpreted with due caution taking into account the remaining scientific uncertainties and further calibration, refining of models and validation taking place in 2016 towards the new winningsplan 2016. Further data will have to be incorporated and studies will have to be completed and the remainder of 2015 and 2016. This means that there are still some uncertainties present in this update that will be further addressed in the 2016 Winningsplan. As part of the Winningsplan a "meet- en regel protocol" was established in 2013. The results presented in this report are supported by data acquisition in the Groningen field area. The "meet-en regel protocol" ensures the continuous data acquisition and monitoring needed for Hazard and Risk management.

The structure of the report follows the causal chain from gas production to hazard (chapter 3) and from hazard to risk (chapters 6 - 9). In chapter 3 the technical foundation to the prediction of the seismic hazard resulting from the production of gas from the reservoir is presented. The impact of the gas production on the reservoir pressure, water table rise in the reservoir and the rock compaction are discussed. A summary of the modelling of compaction, subsidence, seismicity and the accelerations, due to the earthquakes, are provided. Emphasis is put on the latest data gathering, modelling and on the new insights derived from this data.

Chapter 4 presents the earthquake hazard metric chosen and in chapter 5 the hazard maps are presented.

Similarly, chapter 6 provides insight into the risk, given the hazard presented earlier. Chapter 7 describes the program for structural upgrading to mitigate future damage and increase safety of

people in the area. Chapter 8 presents a number of significant earthquake risk metrics and in chapter 9 the risk maps and results are presented.

Additional chapters deal with risk for industrial site and infra-structure and with the link between the hazard and risk assessment and the monitoring protocol.

In the main text references will be given to detailed technical reports, where more in-depth descriptions of underlying studies and results of the data acquisition have been documented. These reports can be downloaded from the "onderzoeksrapporten"-page at the NAM website; www.namplatform.nl. This page (Fig. 1.1) can be directly accessed through this link;

http://feitenencijfers.namplatform.nl/onderzoeksrapporten/.

Each of the reports is prefaced by a short introduction explaining the place of the research in the larger study and data acquisition program, the vintage of the research and the assurance provided by external experts. A browse function is available to quickly locate the report of interest.

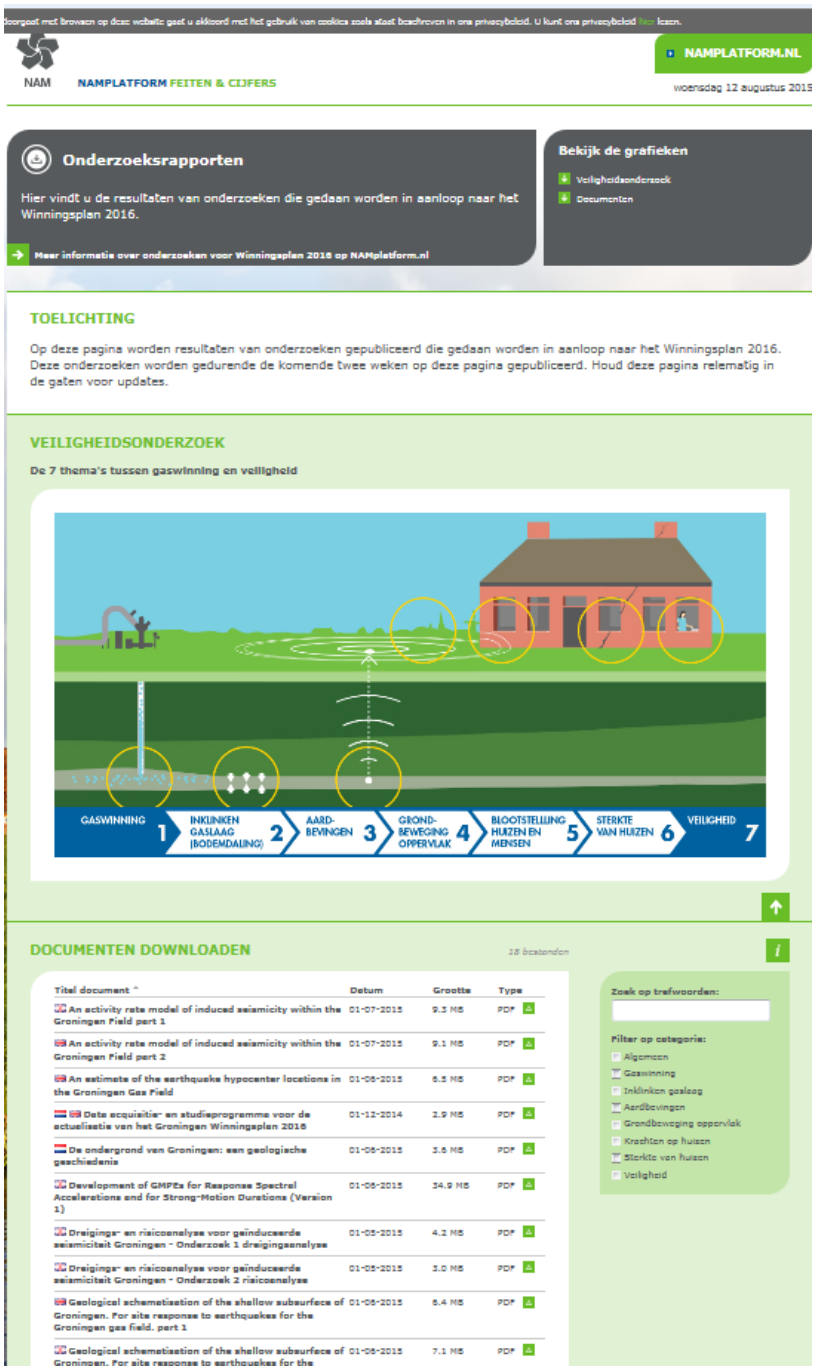

Figure 1.1 *Technical reports prepared as part of the NAM research program into induced seismicity in Groningen can be downloaded from the "onderzoeksrapporten"-page at the NAM website; www.namplatform.nl.*

2 Introduction

Groningen Gas Field

The Groningen field was discovered by the well at Slochteren (SLO-1) in 1959. After this discovery, a public-private partnership - between the NAM, its shareholders, DSM (now EBN) and the Dutch government - was set up. The objective of this 'Maatschap' was, and is, to pursue a joint policy in order to explore and exploit the gas accumulations within the boundaries of the Groningen concession.

The partners in this Maatschap felt a sense of urgency in the development and marketing of the Groningen gas, as it was estimated that there was only a limited window of opportunity for the utilization of this resource. It was generally thought that nuclear energy would replace fossil fuel within the near future.

The field was initially developed by several production clusters in the southern part of the field. At the time, the full extent of the field was not known and it was thought that the entire field could be produced through these southern clusters. However, additional appraisal drilling in the Northern part of the field proved that the Groningen gas volumes were larger than previously assumed. After completion of the appraisal, it was realized the Groningen field is one of the largest gas fields in the world. Furthermore, pressure measurements in these appraisal wells indicated that the Northern part was declining in pressure with a significant delay (Figure 2.1), hence additional production clusters in the North were required. In the early seventies, the rapid development of the field continued with several production clusters added in the Northern part of the field. In total 29 gas production and processing locations (clusters and overslagen) were built.

Currently, the gas is produced through 20 processing locations (clusters), each cluster consists of 8 to 12 wells, gas treatment facilities and compressors. A detailed description of the facilities in the Groningen field can be found in the Winningsplan update of 2013 (Ref. 4). The production from the field causes the reservoir pressure to decline in a same manner as seen in most other gas fields (Fig. 2.1).

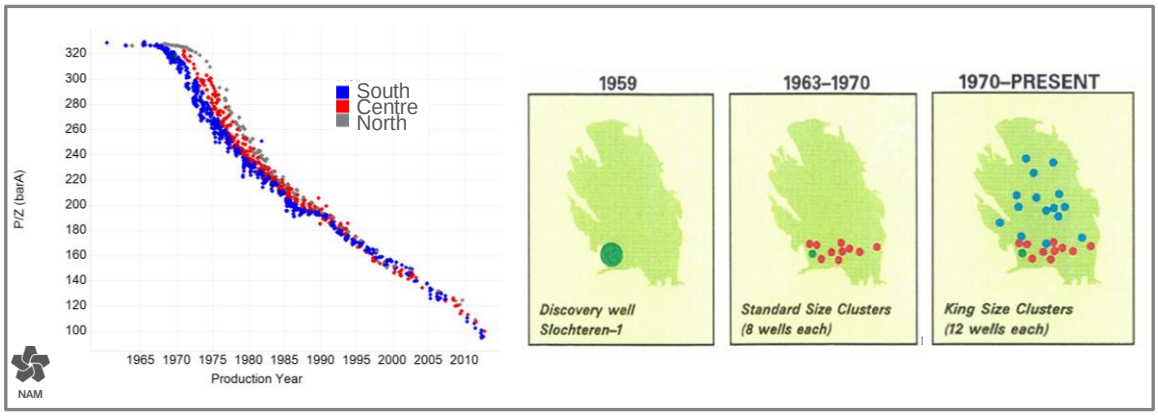

Figure 2.1 *Phased development of Groningen field and historical pressures. This pressure data is available on Feiten en Cijfers at www.namplatform.nl.*

After the first oil crisis in 1973, the Dutch government realized that nuclear energy would not replace fossil fuels within a foreseeable time frame and the rapid depletion of the Groningen field was not considered desirable any longer (Ref. 1). Therefore, the Small Fields Policy was introduced,

which intended to stimulate the exploration and development of smaller gas reservoirs onshore and offshore in The Netherlands and thus conserving the Groningen gas as a strategic energy reserve.

Under the policy, there are legal obligations for Gasunie to connect the field to the grid on socialized tariffs and for GasTerra (previously: Gasunie) to buy the gas against a market price, if the producer chooses to offer it to GasTerra. This resulted in a favorable business environment for the development of Small Fields and effectively a new role for the Groningen field as a swing producer.. Any gas found will be connected to the grid by Gasunie Transport Services and can be offered to GasTerra, who has the obligation to purchase the gas at reasonable terms and conditions.

The development of small fields resulted in a decrease of Groningen gas production and an increase of the surplus production capacity of the Groningen field. NAM has always maintained the high capacity so the Groningen field could be operated as the swing producer and benefit from peak demand periods. In order for the Minister of Economic Affairs to oversee the effectiveness of the small fields policy, it also required detailed annual monitoring reports from Gasunie Transport Services and GasTerra. The impact of the Small Fields Policy is illustrated in Figure 2.2.

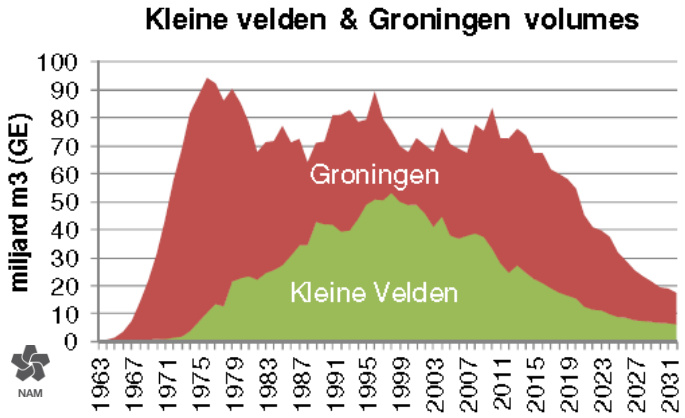

Figure 2.2 Annual contribution to gas production by the Groningen field and small gas fields ("kleine velden")

The production philosophy for the Groningen field has been to balance the production from the various clusters in the Groningen field to keep pressure differences in the field at a minimum. This philosophy follows the principles of prudent operatorship and was first formalized in the Groningen Winningsplan 2003. In practice, this meant that the clusters in the North of the field, where the cluster density is lower and therefore in-place volumes per cluster are larger, were produced throughout the year whilst clusters in the South of the field were only produced when required (i.e. mainly in winter). An exceptions to this is the relatively small South-Western part of the field where the reservoir pressure decline is lower than in the main area of the Groningen field. At some future moment in time, additional production wells may be considered to deplete this area in line with the Groningen main field.

Towards the end of the 1980's, when the Groningen field produced at full capacity, it became clear that compression at production clusters was required to have sufficient capacity available in winter, as compression allows the wells to be produced at reduced wellhead pressures. At the same time, market predictions indicated that during the summer months the gas production from the small fields would be larger than market demand, even with Groningen producing at minimum flow.

This situation resulted in a decision to delay the installation of compression on the Groningen clusters and to develop three Under Ground Storages (UGS): two by NAM in Norg and Grijpskerk, and one by Amoco (later BP and currently TAQA) in Alkmaar. These UGS's are considered part of the

Groningen system and are effectively managed as an extension of the Groningen main field. These were designed to have a high production capacity (security of supply in winter) in combination with a large volume shifting capacity, i.e. the option to have the excess gas produced in summer to be injected into a storage facility. This is illustrated in Figure 2.3.

In recent years, gas demand has increased whilst the contribution of the small gas fields was steadily declining (Figure 2.3). Simultaneously, as a consequence of the declining pressure and production capacity of the Groningen field, the UGS fields have been used more frequently to accommodate the fluctuating seasonal market demand. This led to the decision to expand the Norg UGS which was completed in 2013. Another way to maintain sufficient production capacity in the Groningen field is to install additional (2nd stage) compression at the Groningen production clusters. The first cluster to have 2nd stage compression installed was Schaapbulten in 2014.

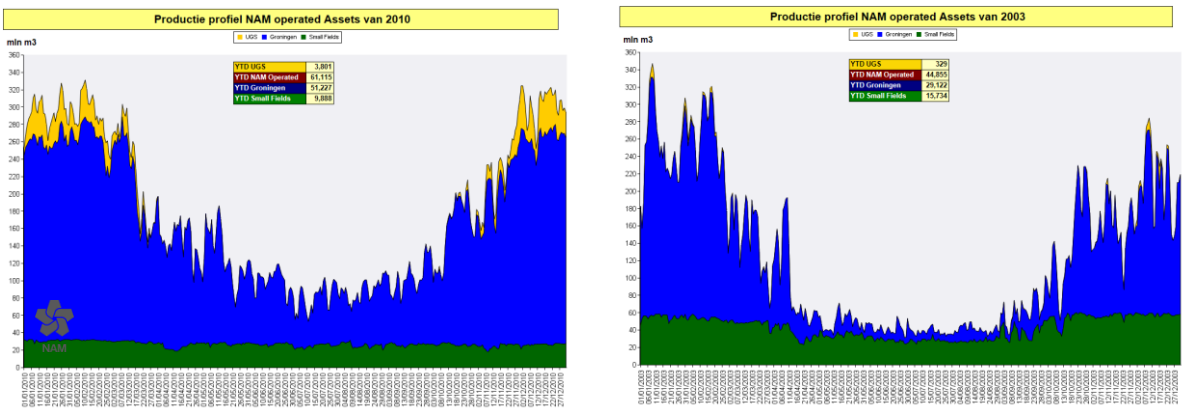

Figure 2.3 *Intra-year production of NAM, 2003 versus 2010. (Small gas fields in green, Groningen main field in blue and the UGSs in yellow)*

History of induced earthquakes in Groningen

Since 1986, relatively small earthquakes have been recorded near producing gas fields in the provinces of Groningen, Drenthe and Noord-Holland and in northern Germany. Initially, the relationship to gas production was not clear. Also the associated consequences were expected to be limited.

A multidisciplinary study was initiated by the Ministry of Economic Affairs in the early 1990's, which was guided by a Scientific Advisory Committee (SAC) that focused on the relationship between gas production and earthquakes. It was concluded that the observed earthquakes were indeed of non-tectonic origin and most likely induced by reservoir depletion (i.e. gas production). The relationship between the earthquakes and gas production was confirmed with the publication of the report in 1993. An agreement was set up between NAM and the Royal Dutch Meteorological Institute (KNMI) to install a borehole seismometer network in the Groningen area. The network has been active since 1995 and was designed to detect earthquakes, pinpoint their locations and quantify their magnitudes. Additional accelerometers were installed in areas with highest earthquake frequency. The network showed a gradual increase in seismic activity, particularly after 2003. Figure 2.4 lists a number of key historical events associated with production-induced seismicity in the Netherlands.

1986	First induced earthquake observed (Assen M= 2.8)
Early '90	Multidisciplinary Study (1993) concluded:
	"Earthquakes in North-Netherlands are induced by gas production"
1995	Seismic network operational
1995	KNMI estimates a maximum magnitude for Groningen: M_{max}= 3.3
1995	Agreement between NAM, Groningen and Drenthe on damage claim handling
1997	Roswinkel earthquake with M= 3.4
1998	KNMI adjusts estimate of maximum magnitude: M_{max}= 3.8-4.0
2001	Establishment of Tcbb (Technische commissie bodembeweging):
2003	Technisch Platform Aardbevingen (TPA) established
2004	KNMI adjusts estimate of maximum magnitude: M_{max}= 3.9
2004	First Probabilistic Seismic Hazard Analysis by TNO and KNMI
2006	Westeremden earthquake with M= 3.4
2009	Calibration study by TNO (Damage analysis)
2011	Deltares assesses the Building Damage in Loppersum and confirms M_{max}= 3.9
2012	Huizinge earthquake with M= 3.6

Figure 2.4 Timeline events before the earthquake of 16th August in Huizinge

Three factors triggered a renewed focus on, and widespread attention for, the issue of seismicity induced by gas production in Groningen. First, the earthquake near Huizinge (16th August 2012) with magnitude M_w=3.6 was experienced as more intense and with a longer duration than previous earthquakes in the same area. Significantly more building damage was reported as a result of this earthquake compared to previous earthquakes. Second, a general realization developed that seismicity in the Groningen area had increased over the last years. Third and most important, studies by SodM, KNMI and NAM concluded that the uncertainty associated with the earthquake hazard in the Groningen field was larger than previously thought. It was recognized that the earthquakes are not just a nuisance but could pose a potential safety risk as well.

The people living in the Groningen field area have been confronted with an increasing intensity of the effects of induced earthquakes. This has been the source of anxiety and frustration among the community. NAM, the ministry of Economic Affairs, State Supervision on Mines (SodM) and the National Coordinator Groningen, together with other stakeholders, are now facing the challenge of formulating a response to the induced earthquakes. To this end, the currently existing instruments for assessing and mitigating these effects – as set down in mining regulations, risk policies and, for example, building codes – are being extended and made fit-for-purpose.

Study and Data Acquisition Plan

NAM reacted to these developments by taking a wide range of measures, including a long-term research program to increase the understanding of the relationship between gas production and safety and to test the effectiveness of mitigation measures. This "Study and Data Acquisition Plan"

describes the objectives and interdependencies of all study and research efforts into induced seismicity undertaken by NAM. The plan was first shared with SodM and the Ministry of Economic Affairs (Ref. 2) in November 2012 and was made public early 2013.

Regular updates on the study progress were reported to the advisory committees of the Minister of Economic Affairs (TBO; Technische Begeleidingscommissie Ondergrond and SAC; Scientific Advisory Committee), the supervisory body (SodM) and their advisors (TNO-AGE and KNMI). The most recent update was issued in March 2015 (Ref. 14).

The main objectives of the Study and Data Acquisition Plan are to:

1. Understand the impact of the earthquake hazard on buildings and other structures and the subsequent impact on safety of the community,
2. Perform a fully integrated Hazard and Risk Assessment for the Groningen region, with all uncertainties fully and consistently recognised and quantified,
3. Identify, evaluate and develop mitigation options to reduce risk:
   - Production measures, i.e. changes in the production from the field
   - Pressure maintenance options, i.e. measures to reduce the impact of production on pressure reduction in the field
   - An optimised Structural Upgrading program:
     - Identify highest risk buildings and/or building elements
     - Establish optimal structural upgrading methodologies
   - Measures for industry and infrastructure.

Other objectives are to:

4. Address different scientific views, and initiate additional studies and/or data acquisition to create consensus amongst the knowledge institutes,
5. Effectively monitor subsidence and seismicity,
6. Continuously improve our understanding of the physical mechanism leading to induced seismicity and the resulting hazard,
7. Reduce the uncertainty in the hazard and risk assessment.

To achieve these objectives, NAM has mobilised the aid of several universities, knowledge institutes and laboratories and sought the assistance and advice from external experts for each relevant expertise area. The main institutes supporting the research are listed in Appendix A, while the most prominent experts and their roles are listed in Appendix B. The total cost of the study and data acquisition program for the 3-year period between the two updates in 2013 and 2016 of the original winningsplan, is estimated to be close to € 100 mln.[1] This program is reviewed every 6 months and adjusted as necessary. The plan serves to support decision- and policy-making, acknowledging that additional (non-technical) factors also have to be taken into account in selecting an appropriate response (Ref. 18).

Scope and Expertise Required

To be able to assess the current situation and take measures to ensure safety for those living above the Groningen field, the full causal chain from gas production to the fragility of buildings and the consequence for people needs to be understood. The NAM research program therefore covers

[1] The costs of the studies carried out in 2012 and 2013 exceed 10 mln €.

different areas as listed below. Together with renowned experts, a conscious choice was made to develop scientifically sound models that are as close to reality as possible. The methodology of probabilistic modelling – Probabilistic Hazard and Risk Assessment, or PHRA – is commonly used in the modelling of earthquake hazard and risk. This is of particular importance for areas such as Groningen where data was scarce.

The hazard from induced seismicity in the area is expressed as the probability that earthquakes will occur and cause ground movement. Understanding the hazard requires insight into the interplay between reservoir pressure, reservoir compaction and the generation of seismicity at faults. The risk associated with induced earthquakes is the probability that people and buildings are exposed to negative consequences. This requires insight into how earthquakes cause the ground surface to shake, the response of buildings to these movements and the possible impact on people (Fig. 2.5).

The research areas included in the Study and Data Acquisition Plan are:

- Changing reservoir pressure (depletion) in response to gas production
- Reservoir compaction in response to pressure depletion,
- Generation of seismicity at faults (earthquakes) due to reservoir compaction,
- Movement of the ground surface, due to earthquakes,
- Response of buildings to the movement of the ground,
- Negative impact on people in or near buildings, caused by damage or collapse of a building.

By looking into all these areas, an integrated view will emerge of the possible consequences of gas production from the Groningen field. The impact is expressed in risk metrics, such as local individual risk, but also possible damage. This type of information is of critical importance to be able to take decisions on future gas production to take measures to mitigate the associated risks for people and buildings in the Groningen region. It must be noted however that risk metrics are estimates, which will change over time when more data becomes available.

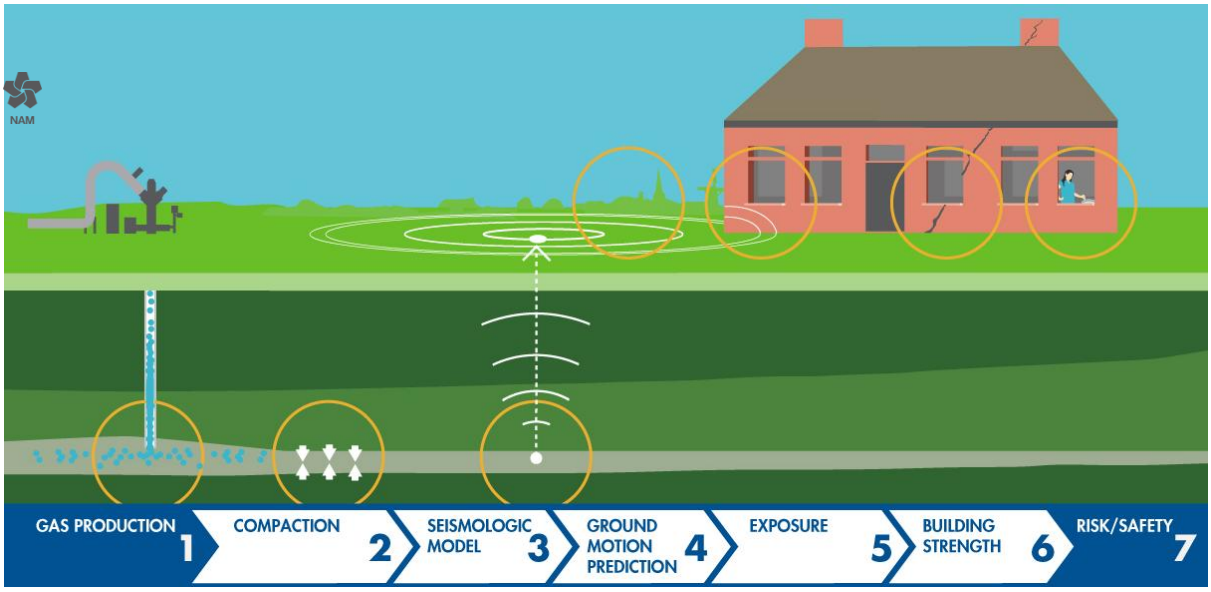

Figure 2.5 Causal chain from gas production to safety of people in or near a building.

The first part of this causal chain requires detailed knowledge of the deep geology of the gas reservoir. The second part requires knowledge of the buildings and presence of people in the Groningen area. Areas of required knowledge and expertise range from geology to civil engineering.

Assurance

NAM has a vested interest in the hazard and risk assessment and in the implementation of measures to ensure that acceptable safety levels are maintained. It is important that the research studies carried out by or on behalf of NAM are subjected to a strict assurance regime, comprising both internal reviews and various types of external and fully independent reviews and verification.

The following assurance steps are applied to the Study and Data Acquisition activities and their outcomes:

- Internal Technical Assurance - review is carried out by internal experts from NAM and its shareholders on those areas where in-house knowledge is available. This especially holds for geology, geophysics and petroleum engineering disciplines.
- Independent review covering the complete work scope is also carried out by external experts.. The assurance of research that concerns geology, geophysics and petroleum engineering, is carried out by the consultancy company SGS Horizon. Reputable academics have reviewed the other parts of the research (see Appendix B).
- The Minister of Economic Affairs has set up a Scientific Advisory Committee (as successor of the initial TBO and TBB) to provide another layer of independent scientific assurance.
- Reports will be publicly shared for scrutiny by experts from various stakeholders, among which NGO's (also see the Reader's Guide in this document).
- The studies are reviewed by the supervisory body SodM and her advisors TNO-AGE and KNMI. SodM has engaged international experts to provide technical advice.
- Raw data is made available at the "feiten en cijfers" page of the website www.namplatform.nl. Larger data volumes are available on request and shared with reputable (research) institutes that are working on induced seismicity (within legal limitations concerning, for instance, privacy and remit legislation).
- Innovative research is being published in peer-reviewed scientific journals.

This multi-layer assurance program has the objective to provide confidence that the outcomes and results are scientifically robust. Furthermore, finalised study reports are made available and published into the public domain at the website; www.namplatform.nl. The reports can be downloaded from the following web-page:

http://feitenencijfers.namplatform.nl/onderzoeksrapporten/

Reviews of these reports and comments can be shared through the NAM-platform website.

Winningsplan 2013

As stipulated in Article 35 of the Mining Act (2002), NAM has to submit a winningsplan to obtain a permit to produce gas from the Groningen field. This document describes the production plan for the field, and its impact on the environment. In more detail, NAM shares the expected remaining quantity of gas, how long it will take to produce this gas, how much will be produced annually, how much subsidence and seismicity is caused by the production and what measures are taken to minimise these and prevent possible damage.

The first winningsplan for this field dates from 2003, with an update issued in 2007. The 2013 Winningsplan update (issued November 2013) was the first document to include a new methodology to estimate hazard and risk from induced seismicity . This new methodology was in line with NAM's own internal safety standards. It stressed the important role of monitoring, and made reference to national and international analogues where possible.

At that time, an urgent need was felt for a better understanding of the hazard and risk caused by the induced earthquakes in Groningen, therefore the Study and Data Acquisition Plan was established. First results were to be included in an Addendum to the Winningsplan requested by the Minister of Economic Affairs for November 2013. The earthquakes in Groningen have many unique features and the relatively short timeline did not allow for sufficient data gathering in Groningen, let alone for preparation of a tailored hazard assessment for Groningen based on any new data. Available knowledge from tectonically active regions was used instead and adjusted to the Groningen situation as much as possible. This was an inherently conservative approach, with subsequent updates of the hazard assessment more likely to be adjusted downwards than upwards. This was considered to be an appropriate and prudent approach given the limited knowledge of the subject at that stage.

The hazard assessment carried out was fully probabilistic. The risk assessment was not probabilistic, but based on a deterministic study on the impact of "worst case events" in the Loppersum area of the field.

The Minister of Economic Affairs had appointed the TBO advisory committee (Technische Begeleidingscommissie Ondergrond) to oversee the technical studies and provide independent advice on the hazard assessment. Three 2-day workshops were held in 2013 with the TBO, to share and discuss the study results. All study results were compiled in November 2013 into a single document, the Addendum to the Winningsplan 2013 (Ref. 5). A separate TBB advisory committee (Technische Begeleidingscommissie Bovengrond) was appointed to oversee the risk assessment.

Winningsplan 2016

The Study and Data Acquisition Plan included an extensive data acquisition program. A good part of the program has now been executed and an extensive set of specific Groningen data is now available. These data are the basis of the hazard and risk assessment carried out to support Winningsplan 2016. This is different from the hazard assessment for Winningsplan 2013 which was largely based on experience from tectonic earthquakes as mentioned in the foregoing. To provide external assurance the Minister installed the Groningen Scientific Advisory Committee (SAC) in 2014.

The proposed risk assessment methodology for the Winningsplan 2016 was shared with the Groningen Scientific Advisory Committee in October 2014. The Minister of Economic Affairs has tasked the committee Meijdam (Ref. 37) to develop a national policy on risks associated with induced earthquakes. This policy will be used (Ref. 18) to assess the Winningsplan 2016. Additional supporting elements include a national annex to the Eurocode 8 Building Code that addresses the fragility of buildings.

Intermediate results of all the study work in preparation of the Winningsplan 2016 are reported and shared each half year with SodM and her advisors TNO and KNMI and the SAC. These reports are also available at www.namplatform.nl. The previous progress report of May 2015 is considered to

be Version 1 of the more detailed hazard and risk assessment, the current November 2015 report is Version 2.

Some of the activities outlined in the Study and Data Acquisition Plan are not directly supporting the Hazard and Risk Assessment of Winningsplan 2016, since results will not be available in time. They mainly serve to increase the understanding of physical processes in support of future hazard and risk assessments. An example is the planned laboratory experimental programme on the Zeerijp-3A core to investigate rupture and compaction processes in reservoir rock. Results may be included in a future update of this report.

Hazard and Risk Update end-2014

On September 30, 2014 an earthquake of Magnitude 2.8 was registered with an epicentre in Ten Boer, east of the city of Groningen. This event triggered a parliamentary debate where concerns were raised about a possible shifting of risk contours towards the city of Groningen as a result of the production constraints imposed on the Loppersum area. Following up on this concern, the minister of Economic Affairs requested an updated renewed assessment of the earthquake hazard for the Groningen gas field with a specific focus on the south-western part of the Groningen field. This area straddles the eastern extension of the municipality of Groningen. The Eemskanaal cluster is the production facility closest to the city and is located in this area.

A new set of seismic hazard maps was generated for the area, based on the latest production figures for the Eemskanaal cluster, and incorporating several improvements in the static and dynamic models (Ref. 19). The assessment concluded however that, independent of the compaction model used, the impact of the production level of the Eemskanaal Cluster on the hazard was limited.

In January 2015, four regional production caps were introduced by the Minister of Economic Affairs (see section Production Caps). This is based on an advice from SodM.

Hazard and Risk Update mid-2015

An updated hazard and risk assessment was published by NAM in mid 2015, based on two studies. Study 1 on "Hazard Assessment" addressed the 'technical' hazard elements that support the risk methodology. This work had advanced substantially since December 2013, now incorporating a seismological model and a compaction model based on the inversion of subsidence data. Study 2 on Risk Assessment for the first time introduced a fully probabilistic risk assessment. The results could only be used qualitatively at that stage, since further studies and more data were needed for quantitative calibration; these data will be acquired through response measurements at the geophone network locations and shake-table tests of a typical Groningen terraced house.

3 From Gas Production to Hazard

The causal chain from gas production to seismic hazard and risk was introduced in Chapter 2. The current chapter further elaborates on the constituent steps of the chain and the work undertaken to better understand these steps. The induced seismicity and the response of buildings in the Groningen field area to seismic agitation is unique. First, this is because induced seismicity due to gas extraction is not a very common phenomenon, and second because buildings in the Groningen field area were not specifically designed and constructed to withstand agitation by earthquakes. Consequently, there is limited relevant experience and only scarce scientific literature available as a starting point for detailed studies.

The main prohibitive factor for increasing our understanding of the induced seismicity and response of buildings in Groningen field area to the seismic agitation was the lack of Groningen specific data.. A large part of the research effort over the past years therefore involved the collection of new data in the Groningen field.

The following data acquisition activities and experimental programs were carried out:

- Extension of the geophone network with some 70 locations to cover the full field and its immediate surroundings.
    - Each location has a 200 m deep well with geophones installed at 50 m depth intervals,
    - Placement of an accelerometer at each of the locations.
- Drilling of two new dedicated deep geophone wells in the Groningen field.
    - Extensive wireline logging and pressure measurements in new wells, including acquisition of shear and pressure wave velocity data over the full well length,
    - Real-time compaction monitoring device (fibre-optic) was installed in Zeerijp-3A well,
    - Coring of a large section of the gas- and water bearing part of the Rotliegend and of the Carboniferous formations in Zeerijp-3A.
- Placement of 10 GPS stations to better monitor subsidence.
- Gravimetric survey over the full field area.

This chapter subsequently reports on the research into a) the production of the Groningen gas field, b) the compaction of the soil below the Groningen gas field, c) the prediction of the ground motion, and d) the seismological or hazard model.

The current Hazard Assessment (or PSHA – probabilistic seismic hazard assessment) incorporates a number of additional features compared to the interim assessment of May 2015:

- An interim update of the reservoir model of the Groningen field has been made with an improved porosity model and an extension of the model towards the west. Further refinements will be included in the Winningsplan 2016 update.
- The history match of the field has been improved, towards the periphery, by extending the matching procedure from matching reservoir pressure and water rise to also include subsidence.
- The prediction of ground motion now also specifically takes into account the local shallow sub-surface and soil, whereas previously a simpler generic model was used.

- A distribution for the maximum magnitude of the earthquakes has been incorporated.
- Improved compaction modelling based on inversion of the subsidence data, using both levelling surveys and satellite data (InSAR).

Groningen gasfield Models

Groningen model update 2015

This section discusses the models built for characterizing the Groningen gas reservoir. The models comprise both the gas-bearing rock interval (or reservoir) and its immediately adjacent and underlying water bearing equivalents (the aquifers). The static model describes the structural framework, i.e. the top and base surfaces, natural faults and internal layering, and the reservoir properties such as porosity and permeability. The dynamic model describes the flow of gas and water through the reservoir formations when gas is produced through wells.

Groningen Field Review 2012

The current version of the Groningen static model (built with Petrel software) is referred to as the Groningen Field Review model 2012 (GFR2012 in short). Work on this model was started in 2009 and the model was released in December 2011. Early 2012 the model was presented to SodM and TNO. The objective of the model was to serve as a fit-for-purpose static basis for the construction of a dynamic model. The combined static and dynamic models served to support a number of planned major investment decisions associated with the installation of 2nd and 3rd stage compression, and with the development of some of the peripheral areas of the Groningen field. The new models resulted in a significant improvement of the history match compared to the previous models dating from 2003. Hence, they were used for the evaluation of production scenarios for business planning purposes, and for the compilation and maturation of a portfolio of development opportunities. The models also served as input for the calculation of compaction and subsidence.

Rationale for the Groningen interim model update 2015

Adequate and fit-for-purpose static and dynamic models of the Groningen are required for providing history-matched reservoir pressures, and for evaluating different production scenarios and their associated pressure forecasts. These are direct input for the hazard and risk assessment to be included in the Winningsplan 2016.

Several factors have led NAM to prepare an update of the Groningen static and dynamic model in 2015. These factors include:

- The availability of new data acquired since the last model update (further detailed below),
- Changing requirements for the model with increased focus on parameters controlling compaction, subsidence and production-induced seismicity,
- Opportunity to use and incorporate new developments in modelling software,
- Suggestions from model reviews by internal and external reviewers,
- Opportunity to improve the history match by combined pressure, water rise and subsidence matching,

The updated models serve as input for dynamic modelling (history-matching), subsidence and compaction modelling and the evaluation of production forecast scenarios.

Static Model update details

The following reservoir data has become available since 2012:

- Seismic data for the entire northern Netherlands have been reprocessed following the latest developments in processing algorithms,

- New wireline log data from wells Borgsweer-5, Zeerijp-2 and Zeerijp-3, which have all been logged extensively. A standard logging suite has been acquired in the Bedum-5 well just outside the Groningen field (Fig 3.1).
- V_clay and porosity logs from all wells included in the model have been quality-controlled, which has resulted in removal or adjustment of outlier values
- A new set of permeability logs has been prepared, by applying different porosity-permeability relationships for the gas zone and the water zone. This has resulted in slightly lower permeabilities for the water zone and (very) slightly higher permeabilities for the gas-saturated parts of the field.

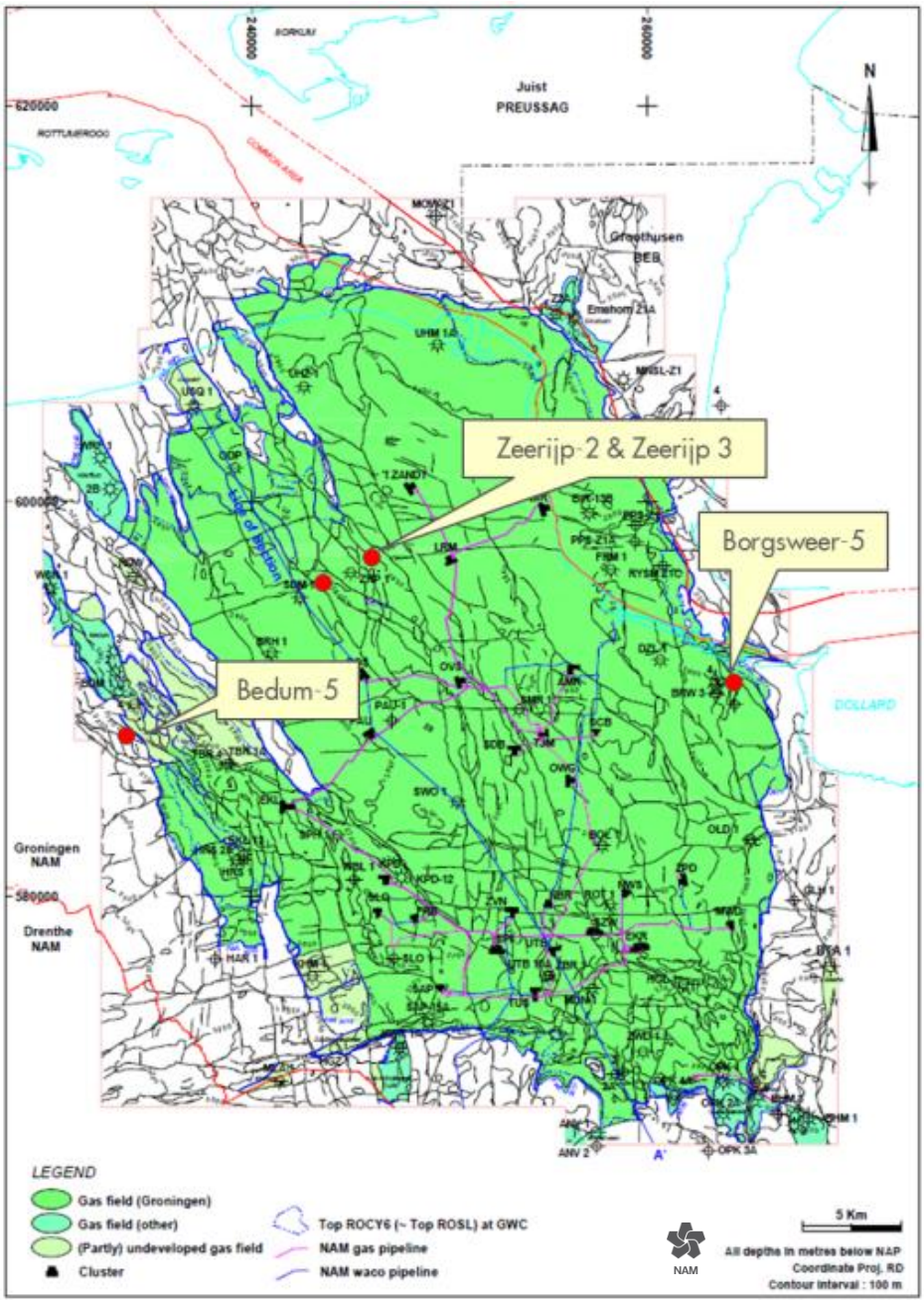

Figure 3.1. General map of the Groningen Field indicating the wells drilled since GFR 2012.

The following modelling activities have been carried out in order to improve the model frame work, i.e. the subdivision of the reservoir into layers, voxels and fault compartments:

- The model area has been extended to cover part of the main aquifers west of the Groningen field. (Figs 3.2 and 3.3) This allows for a numerical evaluation of the dynamic behavior of the aquifers, particularly around the city of Groningen. In the 2012 models, only analytical aquifers were included.
- The newly reprocessed seismic cube has been interpreted to yield a slightly revised Top_Rotliegend horizon, which forms the top surface of the reservoir model. Only 5 wells were excluded from the well tying process (compared to more than 100 excluded wells in 2012).The newly processed seismic cube was used to extensively quality-control the fault model included in the GFR2012 static model, both in terms of fault geometries and structural consistency. Reviews have been carried out by structural geology and seismic interpretation experts. It was concluded that the GFR2012 fault model is adequate and fit-for-purpose, and that a new fault mapping and interpretation effort on the new seismic will not result in an improved fault description.
- In the pillar gridding process for creating a top_reservoir horizon from the new Top_Rotliegend surface, fault connections were simplified and unnecessary detail was removed, resulting in an improved model grid
- The number of layers in each reservoir zone has been revised to create a consistent cell thickness distribution throughout the model.

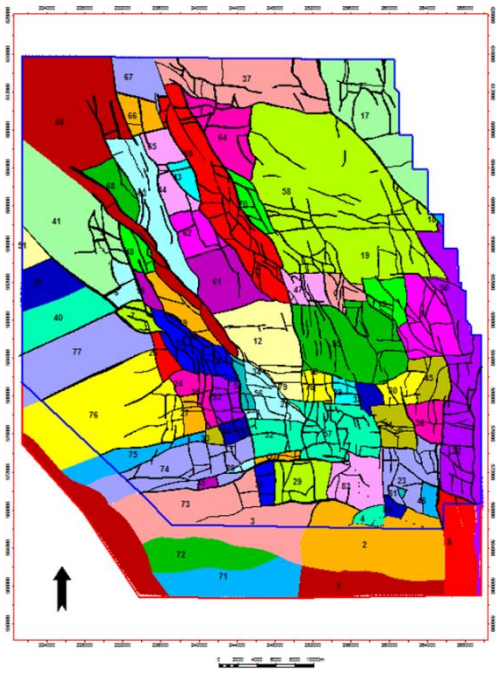

Figure 3.2 *(left) Topographic map showing the expanded boundary polygon with relevant Fields and populations.*

Figure 3.3 *(right) GFR 2015 Segment map, indicating the new segments to the west of the Groningen Field.*

Other activities have been geared towards improving the reservoir property models, of which a selection is presented below. Activities related to the porosity model in specific areas have been

more extensive. They are treated in a separate section, because of its particular importance for compaction and subsidence modelling.

- A new set of trend maps has been prepared, based on wireline log measurements from a selection of representative wells. The new maps have smoother trends and are considered to better represent the depositional trends inferred from core observations and regional geology.
- Recent developments in modelling software have brought improved functionality for data analysis (e.g., nested variograms), interpolation algorithms, sequential Gaussian simulation, and so on.
- A review was carried out on the cut-off values used to convert V_clay logs into Net-to-Gross curves, and on the associated uncertainties. The cut-off values applied in the GFR2012 were taken from an evaluation carried out in 2003 on a small number of selected core intervals. The same methodology was tested again on cores covering the full extent of the Groningen field, also incorporating the results of an ongoing sedimentological study on lithofacies of the same core material (also see section on porosity modelling). It was concluded that the values applied in 2012 were accurate and fit-for-purpose, but that the associated uncertainty ranges need to be widened.
- The methodology for deriving a permeability model is the same as in 2012, but the input permeability logs have changed (as described above). Work is still in progress, but the average permeability in the water-saturated zones is expected to slightly decrease, whilst in the gas-saturated zone it will slightly increase.

Several new approaches have been followed to evaluate the porosity distribution in the model area. Data sets such as acoustic impedance, subsidence measured at surface, and facies distribution, are thought to provide a proxy for reservoir porosity, but are measured independently from the wireline porosity logs. It has been investigated how these secondary data sources can help constrain the porosity distribution, particularly in areas with limited well coverage. This will allow for the creation of multiple porosity scenarios, and to a better evaluation of the uncertainties in the porosity distribution.

- The use of acoustic impedance data (AI in short) has been tested with an AI cube derived in 2003. The method involves resampling of the AI cube in Petrel at the resolution of the reservoir zones, then extract AI values per zone at the well locations, and compare with wireline log porosities at the same scale. Cross-plotting shows a linear relation between the two, with a high correlation coefficient. This relation has been applied to convert the AI property in a pseudo-porosity property, which can be used in turn to constrain the porosity away from well control.
- Simultaneously, a new seismic inversion study has been kicked off using the newly reprocessed seismic data and specifically inverting for porosity. The results of this study are expected to become available in November 2015, and will then be incorporated in the porosity modelling following the method described above.
- A different approach for porosity modeling is being tested on the basis of a lithofacies model. The concept assumes a relation between lithofacies and reservoir properties (porosity, permeability) where each lithofacies type has a distinctive set of properties. Building a detailed facies model and populating it with the characteristic property sets derived for each

lithofacies should then yield an alternative porosity model. Previous attempts to follow this approach showed disappointing results. Nevertheless, a new effort was kicked off by revisiting core material from some 25 wells in the Groningen field. Core descriptions were reviewed in very much detail by applying a simplified and fit-for-purpose lithofacies scheme. However, preliminary attempts to establish distinctive property sets per lithofacies have not yielded equivocal results. Hence, the feasibility of the lithofacies approach has not been demonstrated yet, but more testing is currently being pursued.

- A third approach is tested using subsidence measured by levelling and satellite surveys. This concept assumes a relation between reservoir porosity and reservoir compaction, and between reservoir compaction and subsidence at surface. Hence, measured subsidence can be considered as an indicator for reservoir porosity. A complication with this method is the scale of observation. Subsidence at surface hypothetically relates to the cumulative pore height of the depleting interval (gas-bearing and water-bearing), and cannot be used to resolve the porosity distribution at a reservoir layer, or even reservoir zone scale.

  Note that subsidence data will be used in the dynamic modeling realm (see next chapter). Assuming a relation with cumulative vertical depleting pore height and pressure depletion, subsidence can be used as a matching parameter in the history matching process.

The aforementioned extension of the model area towards the West and South poses a challenge on the construction of property models, and particularly of the porosity model. Modelling algorithms such as Sequential Gaussian Simulation make use of a conditional property distribution derived from upscaled wireline log data. Such a distribution can only be representative for the area covered by the well penetrations. In the extended Groningen model, more than 95% from all the well data is derived from well locations within the Groningen closure. The model area outside the closure only has very few well penetrations. Therefore, several tests have been performed to evaluate the most efficient way of incorporating porosity proxy information in the modelling workflow, such that both the areas within and outside the Groningen closure are populated with representative values.

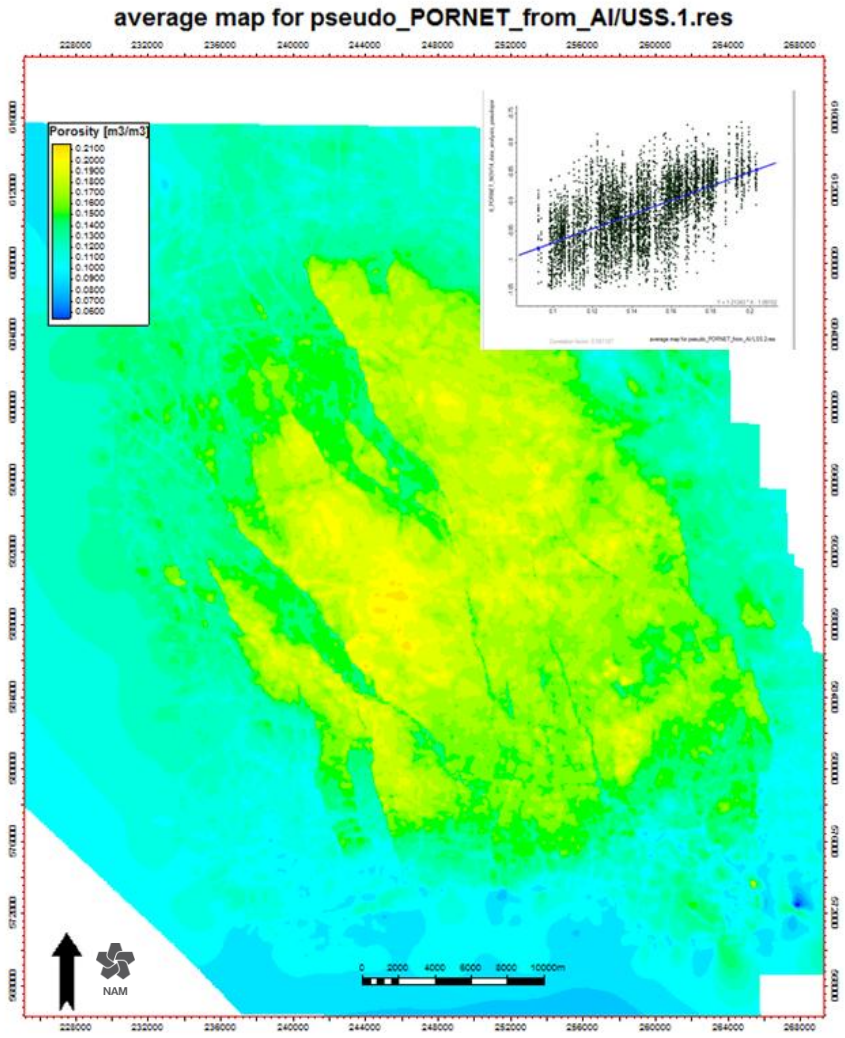

Figure 3.4 *USS.1.res pseudo porosity average map has a good correlation coefficient with Net porosity and can be used for populating the 3D grid away from well control.*

Groningen dynamic model status update 2015

Background

For the Technical Addendum to the Winningsplan Groningen 2013 two subsurface realisations of the Groningen field were used. These models were labelled as G1 and G2:

- The G2 model was the best history matched dynamic model with respect to the reservoir pressure data (SPTG and RFT) and gas-water contact movements (PNL logs). The G2 model assumed weak northern aquifers and had a mismatch with subsidence data in the Northwestern part of the model area.
- A subsurface realisation (G1) with moderately strong northern aquifers showed an improved subsidence match but resulted in a poorer contact movements match (PNL data).

Hence both models had their own shortcomings. The GFR2015 dynamic model update aimed to achieve a good match on pressure and contact data, and simultaneously match the subsidence data, i.e. to have one single model to adequately represent pressure, water rise and compaction behaviour of the reservoir.

Extended grid

The GFR2015 model builds on the insights gained from the GFR2003 and GFR2012 models. A major change relates to an extension of the model area to the West and South, based on the following considerations:

- The previous static model was built for business planning and development purposes, and therefore mainly focusing on the area within the Groningen field. However, for geomechanical studies and subsidence calculations it is important to also put emphasis on the area outside of the Groningen closure.
- Subsidence in the greater Groningen area, including the city of Groningen, is not only affected by the pressure depletion in the main Groningen gas field, but also by pressure depletion in adjacent aquifers and surrounding smaller fields. To improve the forecast of subsidence in this greater area, an extended subsurface model is required.
- There are more options for subsidence calculations when historical and forecasted pressure values are available on an extended numerical grid. Previously, aquifer pressure values were provided via analytical correlations.

The extension of the numerical model means that data from the other wells had to be included in the model. It also required additional efforts in the history matching process. The new extended model now includes the following small fields in the Groningen area, for which calibration is required:

1. Annerveen-Veendam
2. Bedum
3. Bedum South
4. Midlaren
5. Rodewolt
6. Usquert
7. Zuidwending East
8. Feerwerd
9. Warffum
10. Rodewolt
11. Kiel-Windeweer

All available data for these fields were included in the history matching process following the same approach as for the main Groningen field. Also, newly drilled Groningen wells like Borgsweer-5 and Zeerijp-2 and 3A, and an older non-Groningen well Sauwerd-1 were included in the extended model. The 2012 and 2015 models are compared in Figure 3.5, with initial distribution of gas shown in blue.

“Base case grid” - GFR 2015 initial static model	“Extended grid” - GFR 2015 static model with additional cells in the aquifers and land fields for the SS calculation purposes

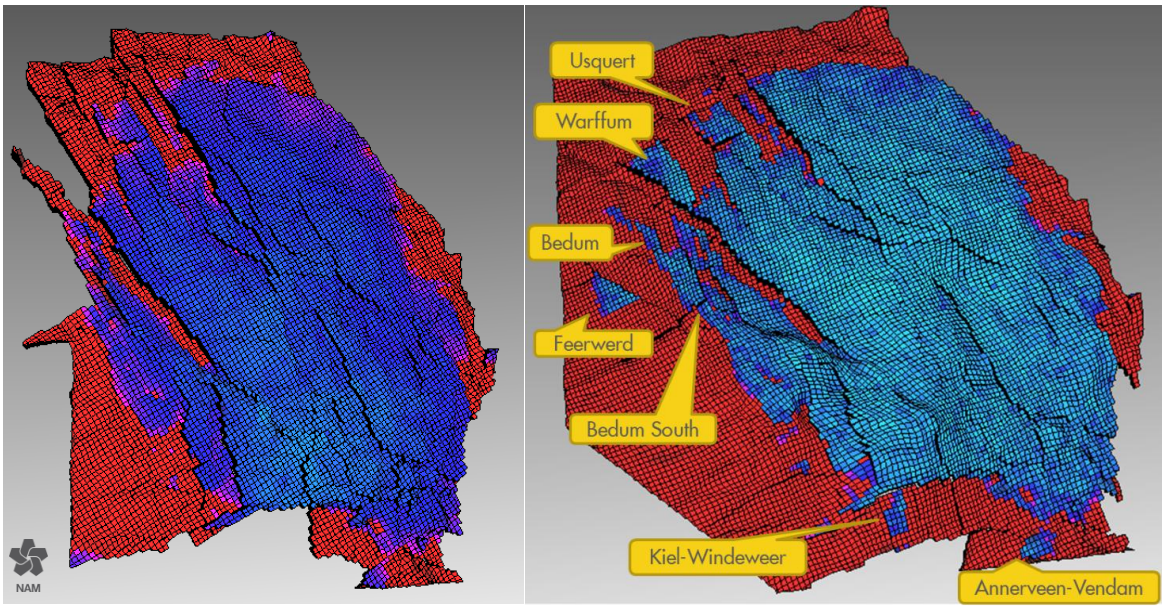

Figure 3.5 GFR2012 and GFR2015 grid boundary comparison. Small fields surrounding the Groningen field are located within this model area. Field names are indicated.

Modelling workflow and main changes

The inputs to the GFR2015 model that are new or that have been changed from GFR 2012 are:

- GFR2015 extended static model
- New subsidence proxy calculation and match quality indicator (normalised RMSE for subsidence) in Mores
- New definition of dynamic compartments of the Groningen field (reviewed free-water levels and PVT regions)
- Newly assigned analytical aquifers, and a different approach to tuning analytical aquifer parameters for history matching and uncertainty evaluation
- Revised capillary pressure vs. saturation functions
- Revised fluid (PVT) properties
- More constrained history matching workflow, with three matching parameters instead of two.

The revised model input properties are explained in more details in Appendix C.

Subsidence proxy

One of the main objectives of the GFR2015 dynamic model update is to also achieve a subsidence match, in addition to the more conventional match on reservoir pressure and gas-water contact movements. The approach for the subsidence history matching process has been to build an approximate, fast and integrated subsidence proxy in Mores. The proxy guides the history matching and is used in the uncertainty management workflow (for more details see Appendix C).

Dynamic compartments

The Groningen reservoir is divided into compartments based on faults and structure, gas quality, formation pressures (RFT) and free-water-levels (FWL). Groningen compartments all seem to be in pressure communication, but different FWLs and gas qualities are observed. To honour the variability in reservoir data, different dynamic model compartments were defined and used for model initialisation regions (FWLs), PVT models and aquifers assignments. The smaller fields included in the model also represent separate compartments (See Appendix C).

Aquifers

Aquifers may play an important role in Groningen reservoir late life production and ultimate recovery. Aquifers are also causing the gas-water contacts to move and influence the PNL history match. Some aquifers could be important for subsidence matching (Lauwerszee) and may be constrained by subsidence data. Ten aquifers have a certain influence on the Groningen field. Some of the aquifers are now included in the extended model area, and some had to be split into smaller compartments in order to have a better control over the pressure changes and water rise. More details on aquifer modelling are given in Appendix C.

Assisted History Matching Workflow

The GFR 2015 dynamic model is constrained by the following historical data:

- Production and injection data as controlling parameters
- Pressure data including SP(T)Gs, CITHPs, BUs and RFTs
- PNL data (water rise)
- Subsidence data

Fluid composition data is not directly used in the history-matching process, but the changing gas composition in certain wells was evaluated during the analysis of the reservoir behaviour.

The subsidence data was matched using the subsidence proxy calculation and match quality indicator as described above. An example of Mores output using this proxy is shown on Figure 3.8.

The best matched “reference” model was manually tuned based on the general understanding of the reservoir dynamics and results from the previous Groningen field reviews. The behaviour of the surrounding Land asset fields and their interference with the main Groningen field had to be newly analysed and understood. Assisting tools such as Adjoint were also utilised in order to test the possible alternative options of the reservoir dynamics. Then the reference model was used as an input for the Assisted History Matching (AHM) workflow. This workflow serves to investigate many realisations with different variables and hence gives an insight into the various history matching possibilities.

The history match quality from resulting runs was assessed on the basis of three main criteria:

- Reservoir pressure
- Water rise behaviour (PNL)
- Compaction (Subsidence)

The model that was finally chosen is very well matched on all three parameters with a very small difference in Gas Initially In Place (GIIP) values between the GFR 2012 model and the new static and dynamic models. Currently, alternative history matching options are being considered and local improvements are being implemented. The Spotfire tool was used to analyse the large set of data and found to be extremely useful. Local match quality indicators suggest that additional local tuning parameters are required, e.g. an exact value of fault transmissibility in order to minimise the RMS in certain areas as shown in Figure 3.21. A few examples of the history model match quality can be seen in the figures below.

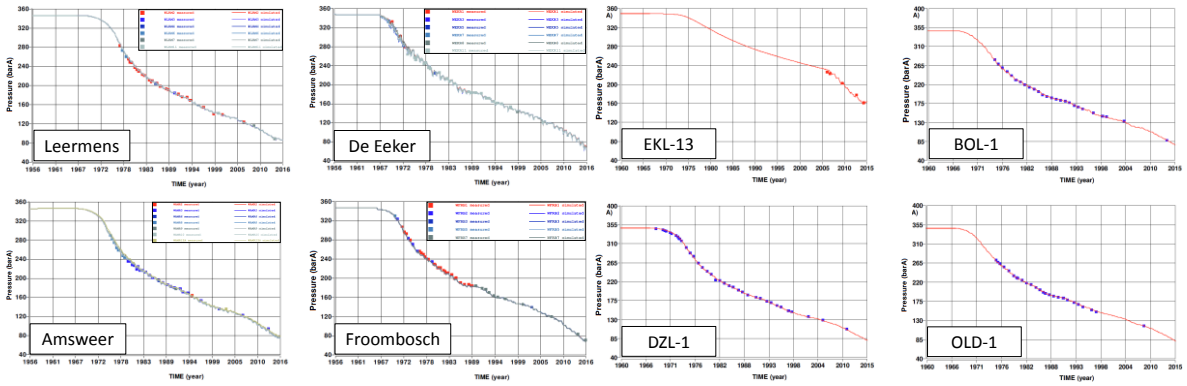

Figure 3.6 Reservoir pressure history match quality for a few typical Groningen clusters, Eemskanaal 13 and some observation wells

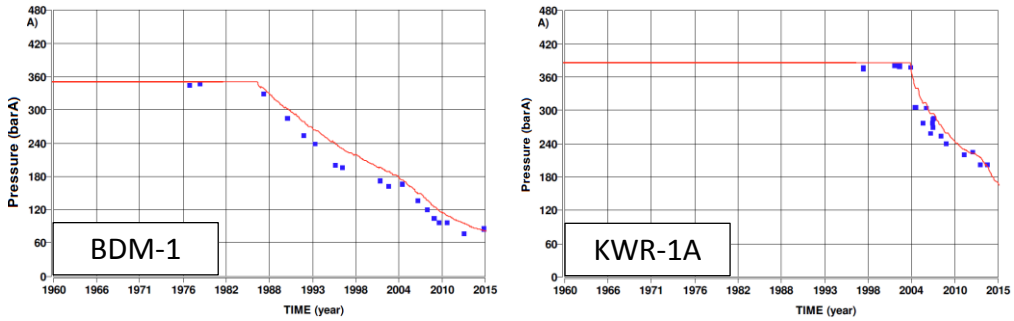

Figure 3.7 Reservoir pressure history match quality of some wells drilled in smaller fields located around the Groningen field.

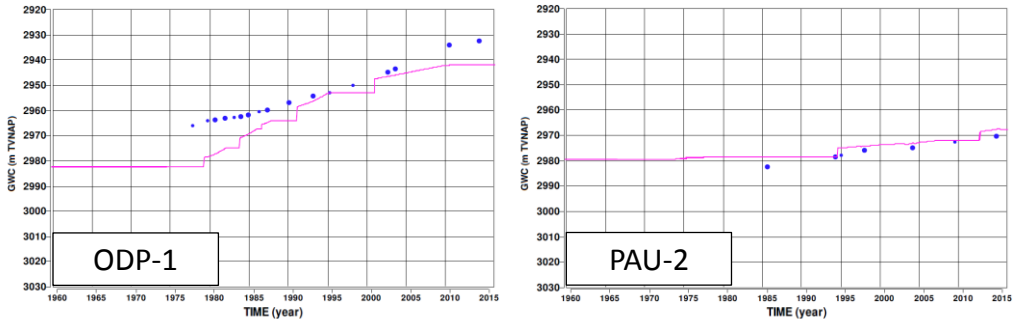

Figure 3.18 History match quality on water rise (PNL) using some example wells.

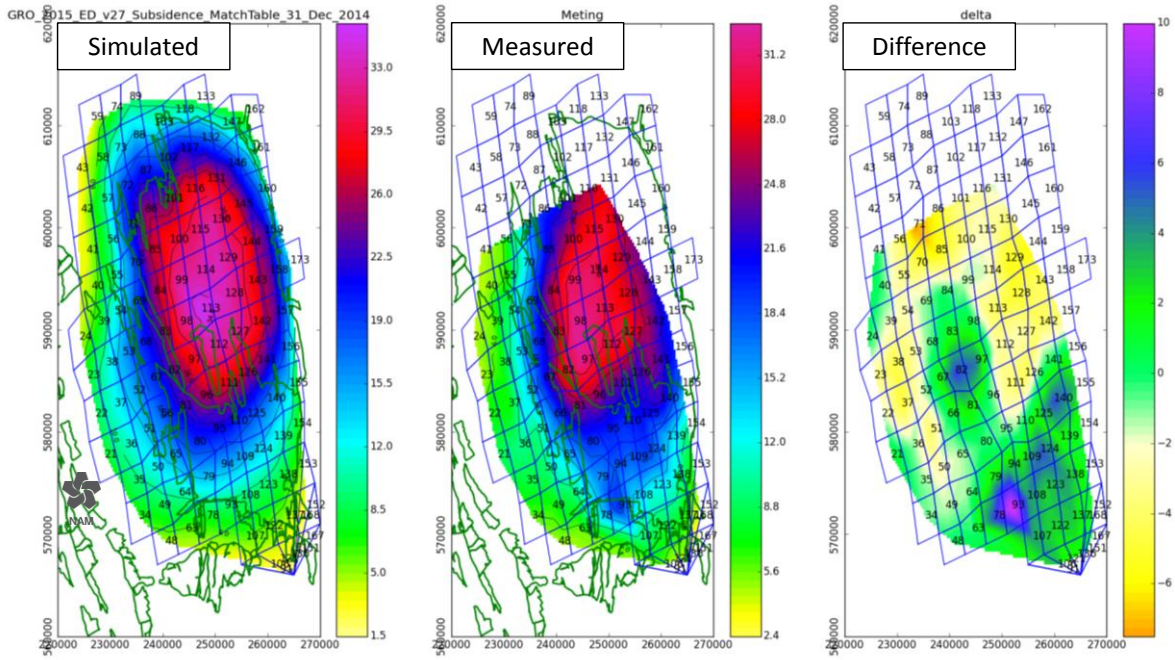

Figure 3.8 *History match quality on subsidence using the proxy in Mores (scale is in cm). The high difference area in the south is associated with salt recovery. The mismatch in the south of the field is due to the subsidence caused by salt mining, which is not captured by the model.*

Conclusion

The dynamic reservoir model of the Groningen field has been updated, extended and improved to provide better forecasts of the development of the pressure in the reservoir and the compaction of the reservoir.

Recommendations from previous model reviews have been incorporated together with newly acquired data. Furthermore, the model has been extended to also incorporate the aquifer areas adjacent to the field such that compaction can be evaluated over the entire model area.

Production System

Gas Production System of the Groningen field

The Groningen production system (Fig. 3.19) consists of a complex network of valves and pipelines connecting the production clusters with six production custody transfer stations (a.k.a. "overslagen"). At the production clusters, the gas is produced from the reservoir and treated (natural gas condensate, water and water vapour are removed). At the production custody transfer stations ("overslagen"), the gas is metered and delivered to the pipeline system of Gasunie Transport Services (GTS).

Each of the six overslagen preferentially services a dedicated market, as the capability of GTS to redistribute the gas outside the Groningen gas production system is limited. For instance, gas delivered at the Eemskanaal Overslag (EKLO) and the Sappemeer Overslag (SAPO) is primarily used to satisfy gas demand in the West of the Netherlands. Similarly, gas delivered at Oude Statenzijl Overslag (OSZO) is targeted for the northern German gas market.

The southern clusters are connected to a double ring pipeline system containing various valve arrangements allowing flexibility in operations. Three northern clusters (Leermens, 't Zandt and Bierum) are producing into this system through a dedicated pipeline system.

A number of additional operating constraints further complicate the operation of this system. These include:

- The gas needs to be delivered at the overslagen within a very narrow quality specification margin. However, gas produced from the Eemskanaal cluster has a composition and a calorific content which exceed the higher limit of the quality specification. It therefore needs to be mixed in the Groningen pipeline system with gas from other clusters to meet the market quality specifications.
- During the summer months (from 1st April to 1st October) the Underground Gas Storage (UGS) facility in Norg needs to be filled up again with Groningen gas. This facility is essential for maintaining capacity during winter. It is filled from the Sappemeer overslag through the dedicated NorGroN pipeline or the GTS gas network. For this purpose, the ring is split in two sections during the injection period, with a separate pressure regime for each section.
- For part of the year, some of the Groningen production clusters will not be available due to maintenance, testing, obsolescence replacement and other activities. Both the injection in the UGS for winter operations and the planned shutdowns for maintenance and other activities reduce the available capacity for the market. Other elements that can impact the available capacity/flexibility for GTS/GasTerra are: ambient temperature, GTS system pressure and local demand, unplanned unavailability of clusters, capacity and availability of the NAM pipeline system and the reserved volumes under regional caps.
- For calendar year 2015 and gas year 2015/2016, production caps have been imposed on four regions of the Groningen field, and for the total Groningen field production (see below).

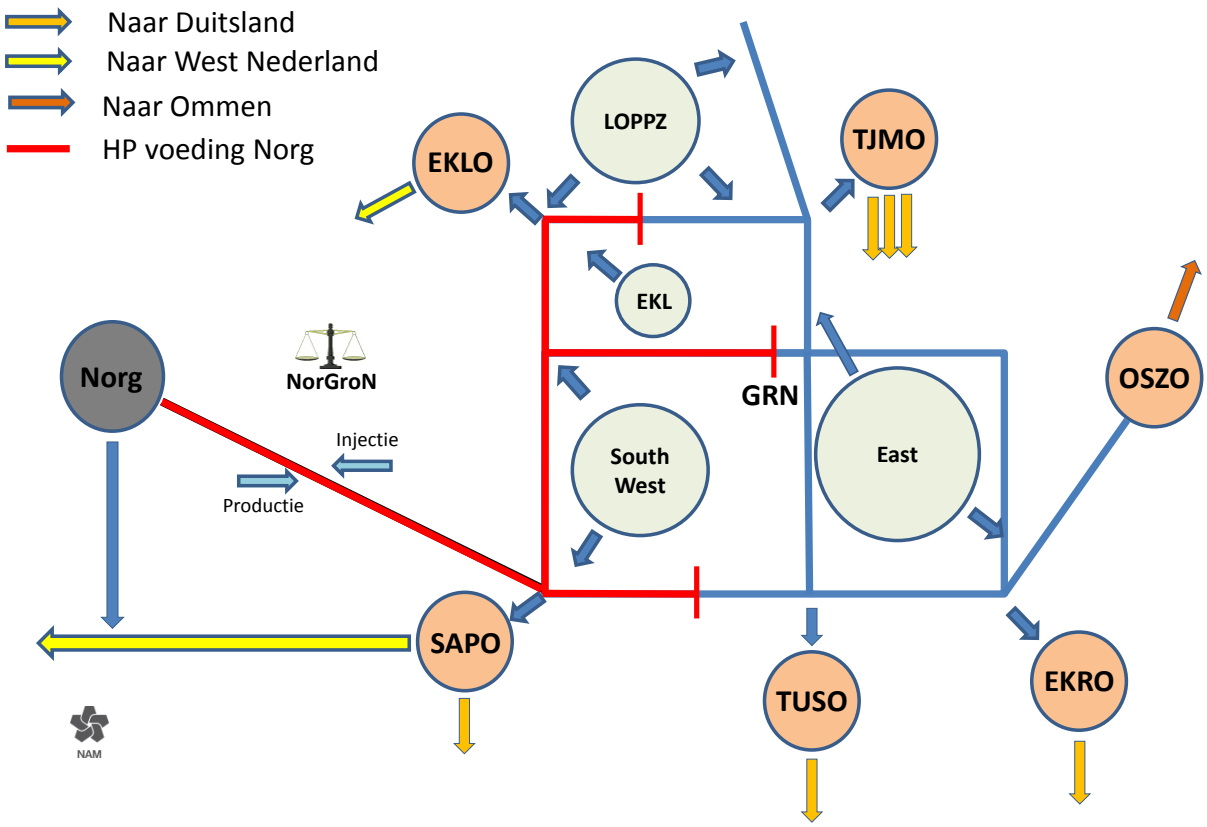

Figure 3.19 Schematic of the Groningen gas ring pipeline system as operated during the summer months with two pressure regimes.

Operating the Groningen gas field

At the time of conception of the production system, a large range of gas delivery conditions over the life of the field was anticipated to service a dedicated gas market with a highly variable seasonal demand. The production system is mainly tailored to achieving high production rates with high reliability in order to capture the additional sales opportunity in periods of peak demand. Such periods could occur during cold winter spells, in case of unplanned failure of other Groningen quality gas production facilities such as the Norg and Alkmaar UGS's, or during failure of nitrogen blending or gas distribution facilities of GTS.

Until 2012, the production strategy for the Groningen field was aimed at minimizing lateral pressure differences across the field by producing the clusters in the northern part of the field (the "Loppersum area") full year around, because these are accessing relatively large gas volumes. The clusters in the south of the field are draining relatively small gas volumes. These were produced mainly during the winter and closed-in or producing at low rates during the summer.

From early 2014 onwards, the production from the five clusters in the Loppersum area was limited to stand-by rates only. As a result, the Groningen production system is currently operated outside the operating envelope and conditions for which it was designed and built. NAM was forced to make changes to the Groningen system to also have flexibility at low production rates. An example change was the modification of the Loppersum clusters to stay in hot-standby mode at reduced gas production rates. In this context hot stand-by means maintaining the temperature of the facilities at

a minimum level that still allows for rapid ramp-up of production to increase the supply of gas when needed to meet demand due to unforeseen circumstances.

During winter periods, production capacity is also provided by the underground gas storage (UGS) facility near Norg. As planned before 2012, this facility has been upgraded in 2014 by drilling of three new wells, the maximum capacity to 76 mln Nm^3/day and the working volume was increased to 7 Bcm supported by the installation of a third injection compressor. The higher capacity of Norg now allows for reduction of the standby capacity from the Loppersum clusters.

Managing the production from the Groningen field

Although NAM ultimately decides how much gas can technically be produced from the Groningen field, the hourly production levels for the Groningen field are set in consultation with GasTerra in order to match its actual hourly sales and offtake. NAM reports the available gas capacity on an hourly basis to GasTerra, while GasTerra determines how much of that capacity is required to deliver the market demand. The gas delivery at the various overslagen is determined by NAM in consultation with GTS. Both the actual demand for Groningen gas and the mixing of hi-cal gas to Groningen gas (L-gas) specifications by GTS determine actual quantities from the Groningen field.

GasTerra manages the portfolio of customers and sets the hourly production level for the Groningen field based on nominations by NAM. NAM operates the clusters, the production system and the overslagen and produces the required gas from the reservoir. GTS manages the pressure in the distribution system and operates compression facilities in the gas delivery system, the mixing of nitrogen for the conversion of Hi-cal into pseudo Groningen gas (L-gas) and the Zuidwending underground gas storage (salt cavern).

Production caps

Since early 2014, the Minister of Economic Affairs has imposed annual production caps to constrain the yearly production of groups of clusters in the Groningen field to reduce the seismic hazard and risk caused by production-induced seismicity. Absolute numbers for the caps have changed in the period thereafter, but currently, the aggregated result of the consecutive ministerial decisions is as follows:

- Regional caps[2] (Figure 3.20):
    - LOPPZ[3] clusters: 3.0 Bcm per year
    - Eemskanaal cluster: 2.0 Bcm per year
    - South-West clusters: 9.9 Bcm per year
    - East clusters: 24.5 Bcm per year
- The same caps have also been set for gas-year 2015 (1-10-2015 to 30/9/2016)
- Total field production for the first half of 2015 has been capped at 16.5 Bcm
- Total field production for the full calendar year 2015 has been capped at 30 Bcm

In addition to the above, a provisional ruling was issued on April 14th 2015 by the Dutch Council of State (Raad van State), stating that gas production from the LOPPZ clusters is only allowed for

[2] All caps are in 100% WH N.m3
[3] LOPPZ = **L**eermens, **O**verschild, De **P**aauwen, Ten **P**ost and 't **Z**andt

security of supply. Because production clusters can only be ramped up quickly when they are at the operational temperature, some of the clusters will need to be kept on hot stand-by. The operationally required temperatures can be sustained with a production of 1.6 Bcm per year, which in normal circumstances defines the production from these clusters.

As a result, the Groningen production system is currently operated outside the operating envelope and conditions for which it was designed and built. The production cap imposed on the LOPPZ clusters caused an effective reduction of the Groningen field capacity by some 25%.

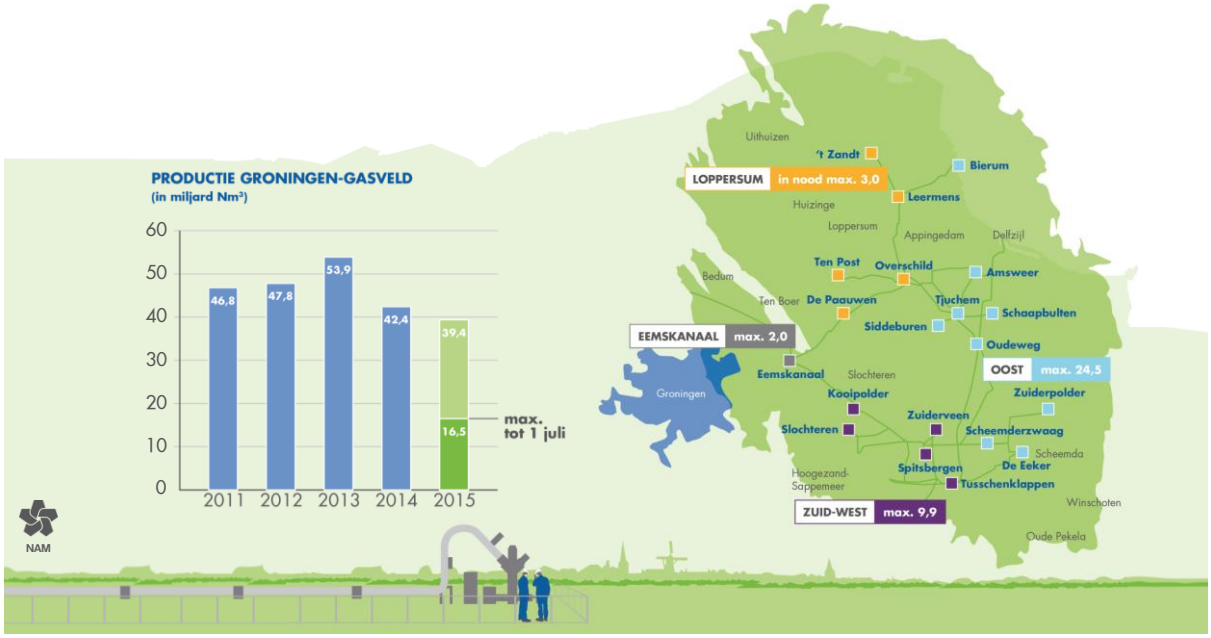

Figure 3.20 Grouping of the Groningen production clusters with production caps.

Groningen Field – Production clusters and Production Regions

Groningen Field – Hydrocarbon Column Map (Slochteren Fm)

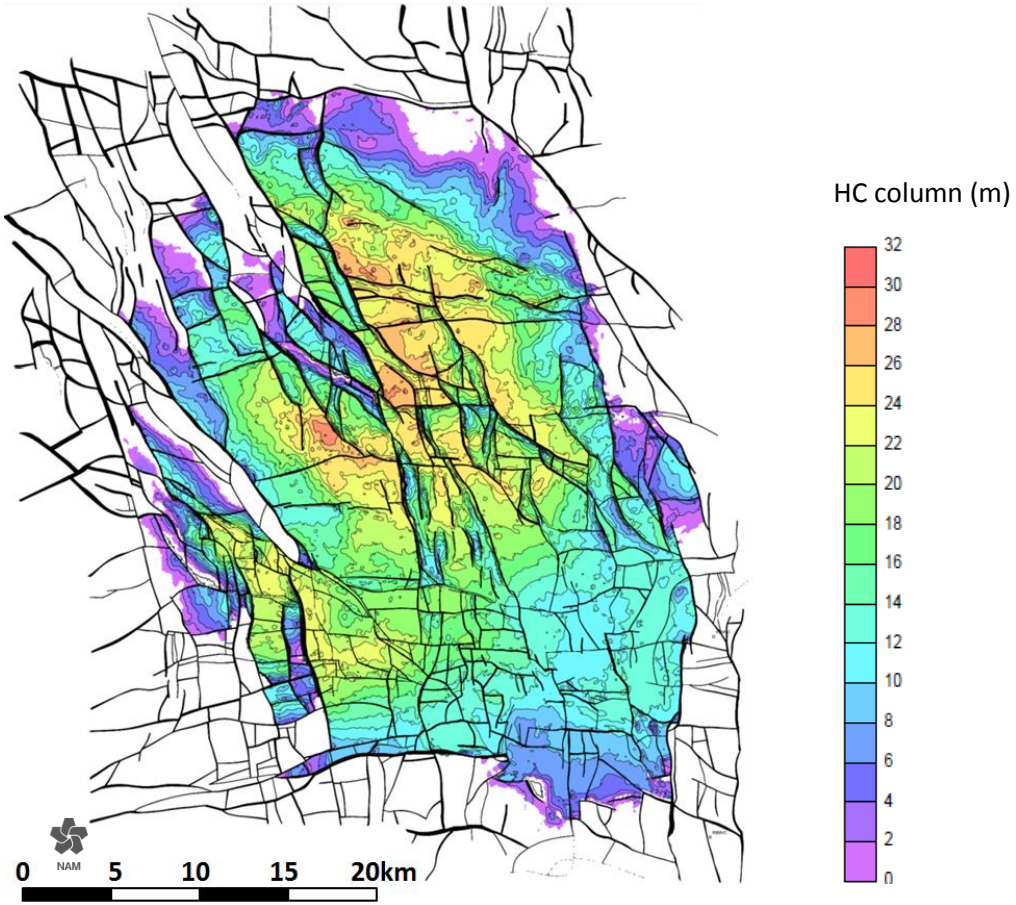

Figure 3.21: Production regions for the Groningen field, and Hydrocarbon column map. The constrained LOPPZ clusters are located in the most prolific area of the field (highest column thickness and lowest cluster density). The production cap imposed on the LOPPZ clusters caused an effective reduction of the Groningen field capacity by some 25%.

Production Scenarios

To be able to investigate the impact of production from the field on hazard and risk at different production levels, three production scenarios are evaluated. These scenarios have different production levels for the total field and extend the current production policy for the 5 clusters in the Loppersum area. Figure 3.22 depicts these scenarios. Ultimately, the Minister of Economic Affairs has the authority to impose the production caps on the gas production from the Groningen field.

The various production scenarios are briefly characterized in the following:

- 33 BCM

  This scenario assumes that the regional caps remain in place indefinitely, and that the current total field cap of 33 Bcm per year will also be extended.

- 27 BCM

  This scenario assumes that the regional caps remain in place indefinitely, and that the total field cap will be lowered to 27 Bcm per year as of 1/1/2016. Note that in this scenario there is insufficient Groningen quality gas to supply all households in a cold winter, even in a maximum conversion scenario, which is designed to maximize the use of non Groningen gas and minimize the volumes produced from Groningen field.

- 21 BCM

  This scenario assumes that the regional caps remain in place indefinitely, and that the total field cap will be lowered to 21Bcm per year as of 1/1/2016. Note that in this scenario there is insufficient Groningen quality gas to supply all households in all but the warmest winters, even in a maximum conversion scenario.

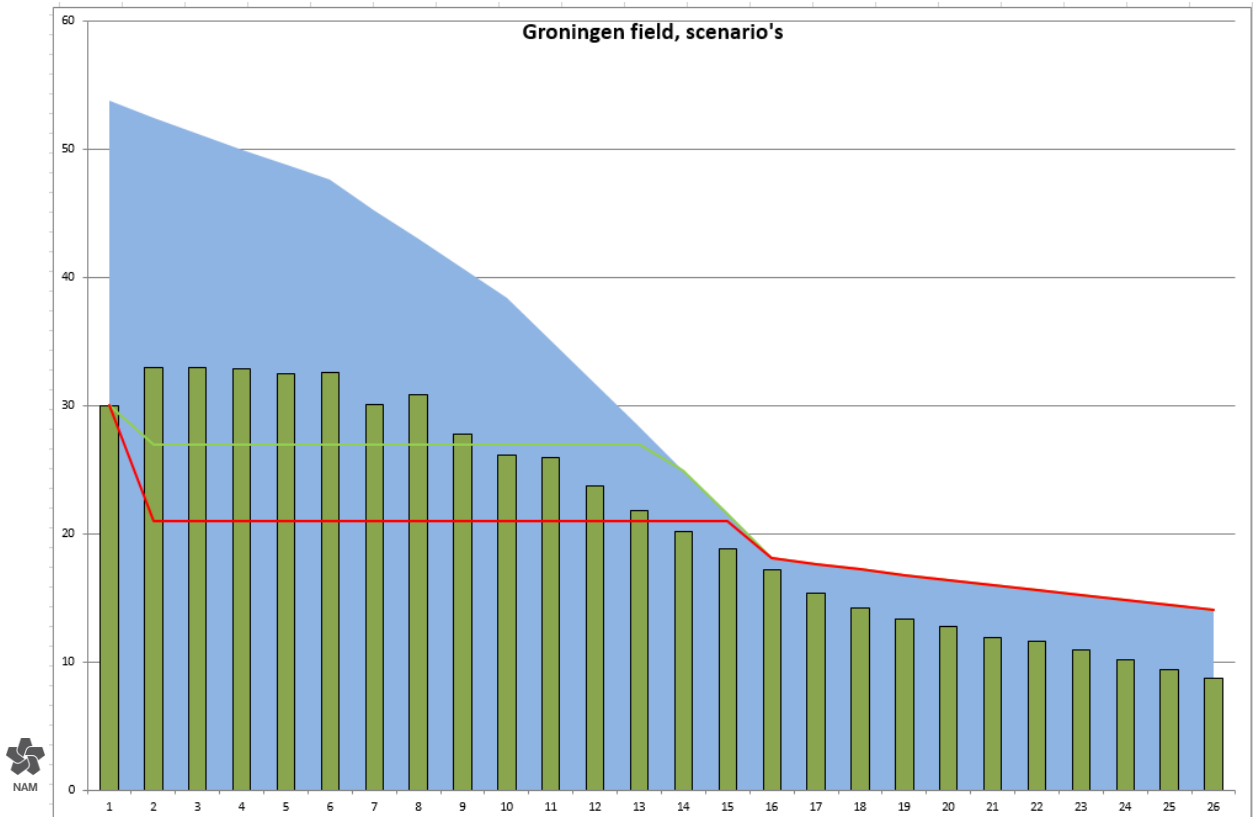

Figure 2.22 Production scenarios; base scenario 33 Bcm/yr (green bars), 27 Bcm/year (green line) and 21 Bcm/year (red line). Market for Groningen gas is indicated in blue.

Simulation results

It is not feasible to capture detailed operational aspects in the forecasting, so these were approximated in the production forecasting:

- Eemskanaal region

  Due to its higher Wobbe index, gas produced from the EKL cluster needs to be diluted with gas from the LOPPZ/SW clusters. For injection into Norg, less restrictive specifications are tolerated at the end of the injection season.

- Loppersum region

  Keeping the LOPPZ clusters available in a hot stand-by mode results in an annual production rate of approximately 1.6 Bcm/y.

- SouthWest region

  During summer, the Southwest clusters will mainly be used to fill the UGS Norg (7 Bcm), with a further 2.9 Bcm available under the regional cap of 9.9 Bcm.

- East region

  The East clusters will be used to produce the remainder of the allowed volumes under the total field cap.

Another important assumption is that the seasonal swing in gas demand will be modulated by UGS and the market (including conversion of high calorific gas to L-gas). It is assumed that the Groningen field will be produced on the basis of a relatively flat seasonal offtake profile, with some 15% higher rates in winter compared to summer, to reflect produ ction stops and higher ambient temperatures in summertime (Figure 3.23).

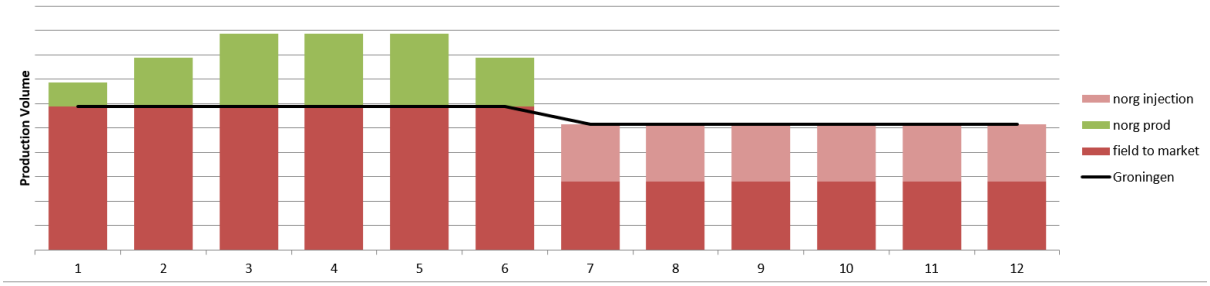

Figure 3.23 Schematic annual offtake profile

The reservoir model simulation results are given in Figure 3.24. It can be observed that, given the suite of operational constraints, the Southwest region will be the first region that will not be able to deliver its requested production plateau. With continued production, the local reservoir pressure declines, thus reducing the production capacity. The East region is ramped up to compensate for the difference, but once the Eastern region comes off plateau as well, the field can no longer produce up to the cap.

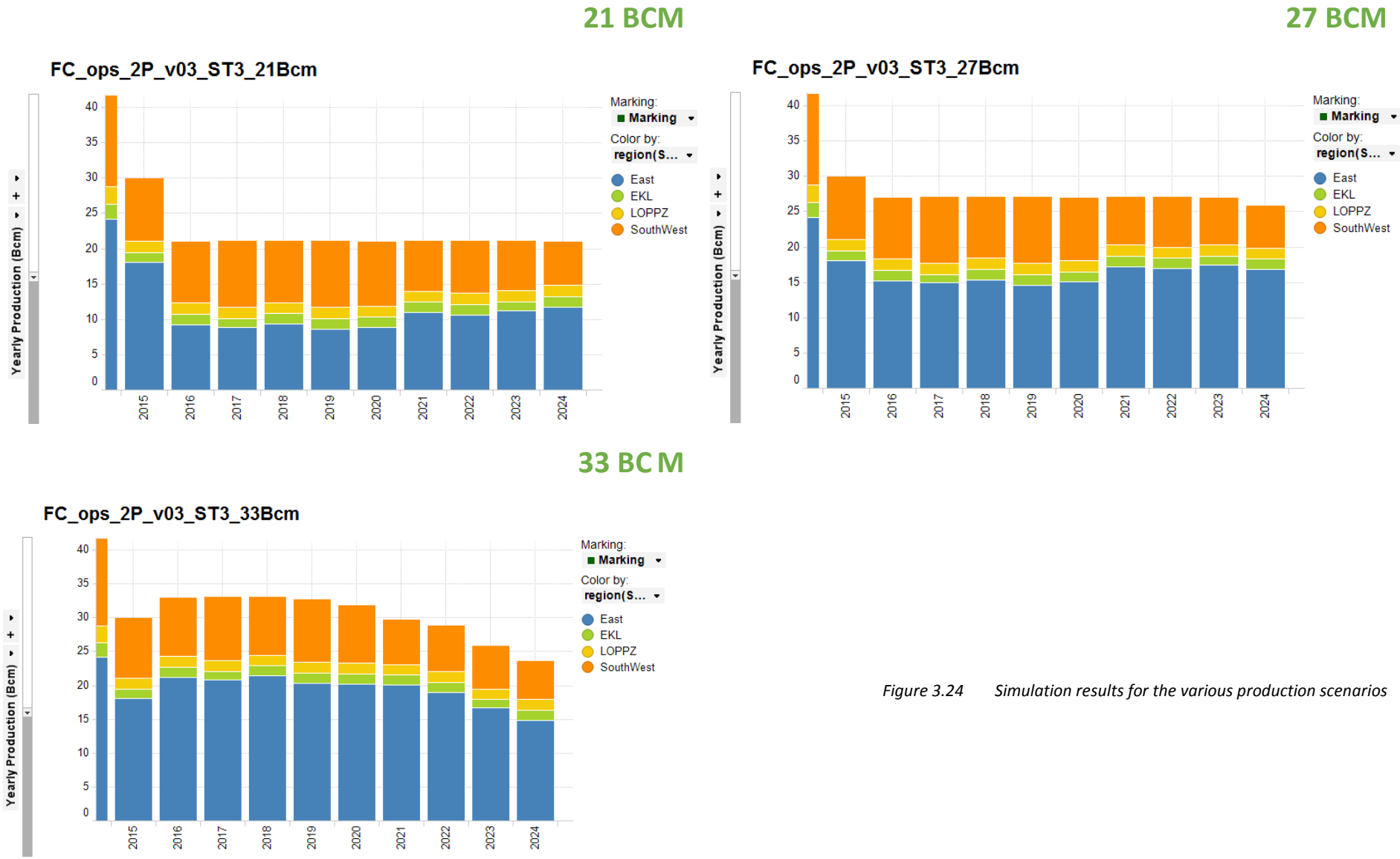

Figure 3.24 Simulation results for the various production scenarios

Rock Deformation - Compaction Modelling

Improvements Version 1 (Mid 2015)

- Inversion from subsidence by using optical leveling survey data up to 2008.

Improvements Version 2 (End 2015)

- Improved matching of aquifer depletion by history-matching for subsidence within Mores.
- Improved reservoir porosity model steered by seismic inversion results impacting compressibility estimation.
- Estimates of reservoir compaction by inversion from subsidence have been enhanced by incorporating additional optical leveling survey data from 2013. This has not led to a different view on the spatio-temporal progression of reservoir compaction. The additional 2013 data are in line with the assumption of constant rates of compaction per unit pressure decline
- A methodology has been developed for inversion to compaction using InSAR data, in which displacements in the line-of-sight to the satellite are modelled. Estimates of the spatial distribution of compaction in the reservoir obtained using optical leveling and InSAR are similar.
- For QA/QC purposes, an alternative workflow for inversion to reservoir compaction has been developed in which the amount of spatial smoothness is estimated through variance components. Cross-validation is not required in this alternative framework, and there is no non-negativity constraint. The results obtained are similar compared to the existing workflow which has led to increased confidence in the obtained results.

Outlook winningsplan 2016

- Extended inversion/modeling compaction grids (including lateral aquifers) will be used in the Hazard and Risk assessment.
- Evidence for the presence of anisotropy (horizontal/vertical subsidence) will be further investigated. Data from the Envisat satellite with an overlapping period of about 4 years with data from both descending and ascending orbit is available and may be suitable for this purpose.

Results

For the seismic hazard maps in the Winningsplan update 2013, three compaction models were used: bi-linear, time decay and isotach (Ref. 5). These models assume a relationship between compaction and porosity and produced local second order biased estimates of subsidence as evidenced by the spatio-temporal patterns in the residuals when compared to the levelling data. A direct inversion of the levelling data to compaction was identified as a useful alternative method to estimate the compaction grid of the Groningen field. It was demonstrated (Ref. 23 in May report) that it is indeed feasible to derive spatially smooth compaction estimates from the levelling on a course grid (2.5 X 2.5 km) using a homogeneous half space model with a Poisson's ratio of 0.25. Each block in the grid returns in this case a different compaction value. The study showed that a basic ('first-order') forward simulation model with constant rates of compaction per unit of pore pressure decline per reservoir grid block performed well in its ability to explain the variation in subsidence measurements. This linear relationship was used for a base case compaction scenario to forecast the seismic hazard in the near future (2016-2021).

In addition, both the time decay and RTCiM compaction models (Ref. 5) were used as separate sensitivity scenarios to reflect the compaction model uncertainty in the hazard calculations.

All compaction models use a homogenous half-space model to estimate subsidence from compaction and vice versa rather than the rigid-basement model that was used in the Winningsplan 2013 update.

The reservoir model was extended to include the lateral aquifers attached to the Groningen Gas field. New functionality in the Mores reservoir simulator allows for a fast forward calculation of the subsidence following the nucleus of strain approach. Possible depletion in the lateral aquifers was history matched against the available levelling data assuming a Cm-porosity relation as used in the Winningsplan 2013. The pressure grid that results from this first pass subsidence assessment in combination with the traditional history match for the gas field can be used for further geomechanical analysis and integrated with a spatially extended hazard and risk analysis, which will be included in the Groningen Winningsplan 2016

Linear compaction model (base case)

As a base case, the linear compaction–pressure drop relation inferred by inversion from the subsidence measurements for the different blocks was used to predict the compaction for the periods 1-1-2016 to 1-1-2018 (Figure 3.26), 1-1-2016 to 1-1-2021 (Figure 3.27), using forecasted reservoir pressure grids for the three alternative production scenarios described in the previous chapter. Figure 3.25 shows the cumulative compaction from the start of production to 1-1-2018 for the three production scenarios (33 BCM is the base case) using the linear compaction model. The impact of the production scenarios on cumulative compaction is limited because of the short additional time period (2 years) compared to the time the field has been producing already. This is especially the case in the area of highest compaction.

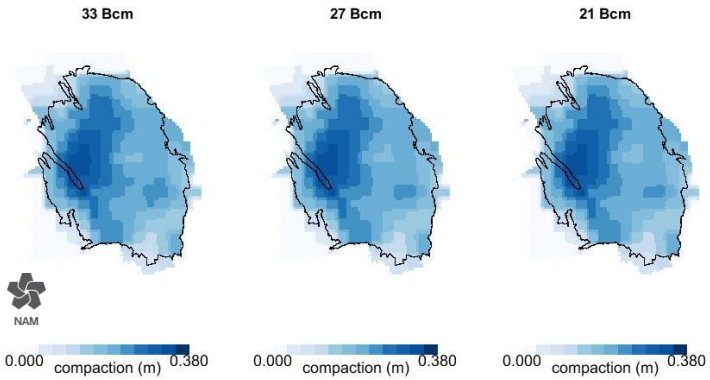

Figure 3.25 *Cumulative compaction from the start of production to 1-1-2018 for production scenarios based on the inversion of levelling data (linear compaction model).*

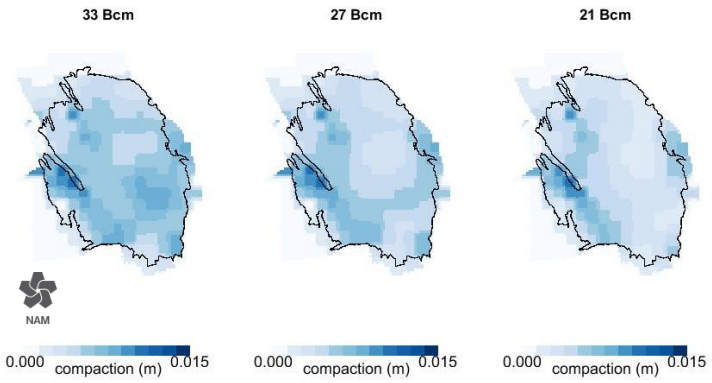

Figure 3.26 Compaction for the period 1-1-2016 to 1-1-2018 for three production scenarios using the linear compaction model

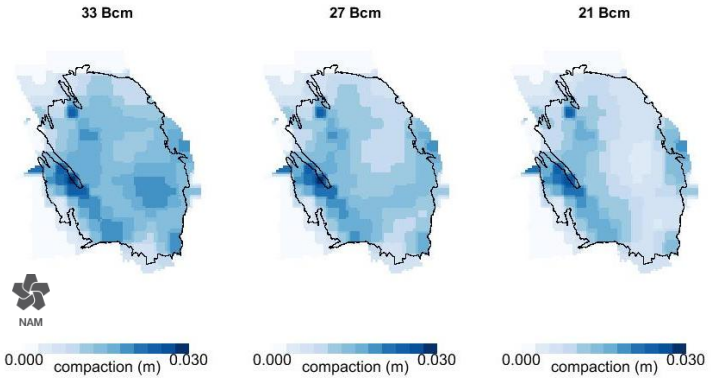

Figure3.27 Compaction for the period 1-1-2016 to 1-1-2021 for three produ ction scenarios using the linear compaction model

RTCiM / time decay compaction model

No changes with respect to the May report were made to the time-decay model. However, the procedure for matching the RTCiM to measurements was revised. The calibration/history match of this model to the measured subsidence data consists of several iterative steps:

- First an inversion to compaction using the levelling information for the period 1972-2013 was performed to obtain a spatial match for the compaction values. This inversion step can be carried out with or without using a Cm porosity relation as prior information. Using pressure and thickness information a Cm grid was derived with a grid spacing of 1x1 km^2 blocks.
- This Cm grid was used as an input to calibrate (over time) the RTCiM parameters (Cmref, Cma and b).
- With this first RTCiM model a spatial difference plot with the actual subsidence data is made. The difference values are used to derive a spatial correction grid. In a second iterative step,

this correction is applied to adjust the Cm grid, subsequently used as to estimate new values for the RTCiM parameters. These parameters are then used for the compaction calculations.

Figure 3.28 shows the compaction for the three alternative production scenarios (33 BCM is the base case) for the period 1-1-2016 to 1-1-2021 using the RTCiM model, calibrated to the subsidence data in the iterative procedure described above. The relatively high compaction values close to the western boundary of the field are caused by gas production from the neighbouring Bedum field.

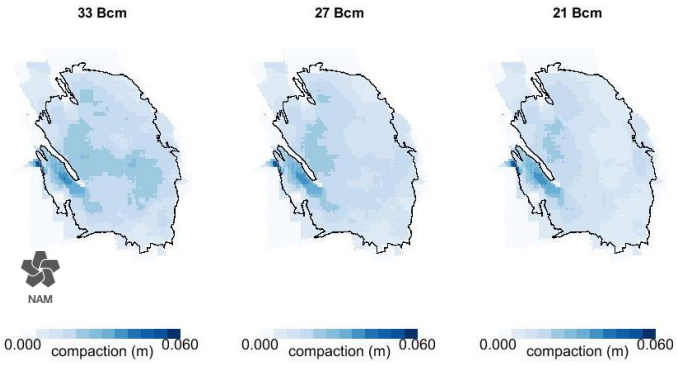

Figure3.28 Impact of the production scenarios on the compaction using the RTCiM for the period 1-1-2016 to 1-1-2021

To allow for a better comparison of the impact of the different compaction models on the compaction, we show the results for the base case scenario (33 BCM) for the period 1-1-2016 to 1-1-2021 in Figure 3.29. Differences between the base-case (linear) and time-decay results on the one hand, and the RTCiM results on the other hand are mainly caused by:

- Differences in the amount of smoothing that is applied (more smoothing / courser grid in base-case and time-decay, compared to RTCiM).
- Differences in the inversion workflow (e.g. for RTCiM another selection of subsidence measurements was used).

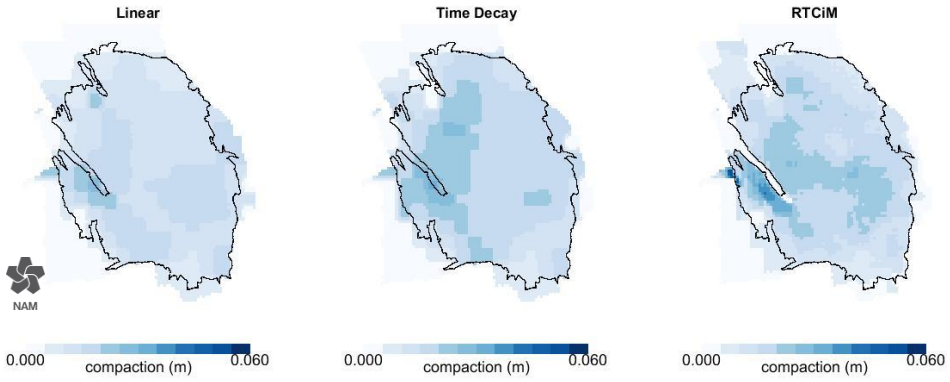

Figure 3.29 Compaction for the period 1-1-2016 to 1-1-2021 for the three compaction models (33 Bcm production scenario)

It was demonstrated in the Version 1 report (May 2015), that the epistemic uncertainties in the compaction model are small compared to some of the other uncertainties for the forward looking period of only 5 years. Therefore it was decided for this Version 2 report to only use the linear compaction model results in the hazard and risk calculations. This significantly reduced the number of branches in the logic tree (chapter 4) and reduced the computational effort accordingly.
For Version 3 (Winningsplan 2016) sensitivities to alternative compaction models will be re-evaluated and carried through the logic tree if required.

Seismological Model

The seismological model aims to predict the generation of earthquakes induced by gas production. In the Probabilistic Hazard and Risk Assessment (PHRA) workflow, the seismological model allows synthetic earthquake catalogues, detailing event locations, occurrence times and magnitudes, to be calculated given their joint probability distributions based on a model of the underlying geomechanical process. An important feature of seismicity in Groningen is that it is induced by gas production and therefore non-stationary.

When analyzing the KNMI catalogue of earthquakes and comparing the location and timing of earthquakes with the progression of compaction, there is a strong bias in the origin time and location of *ML* ≥ 1.5 events towards larger reservoir compaction. Figure 3.30 shows that 80% of these events occurred at a time and place when the reservoir compaction was at least 0.18 m. The location of the first observed *ML* ≥ 1.5 event in 1991 is within the region of greatest compaction. Over the following 20 years, the areal footprint of earthquake locations spreads mostly toward the south-east and approximately tracks a reservoir compaction contour as it extends away from the center of the field.

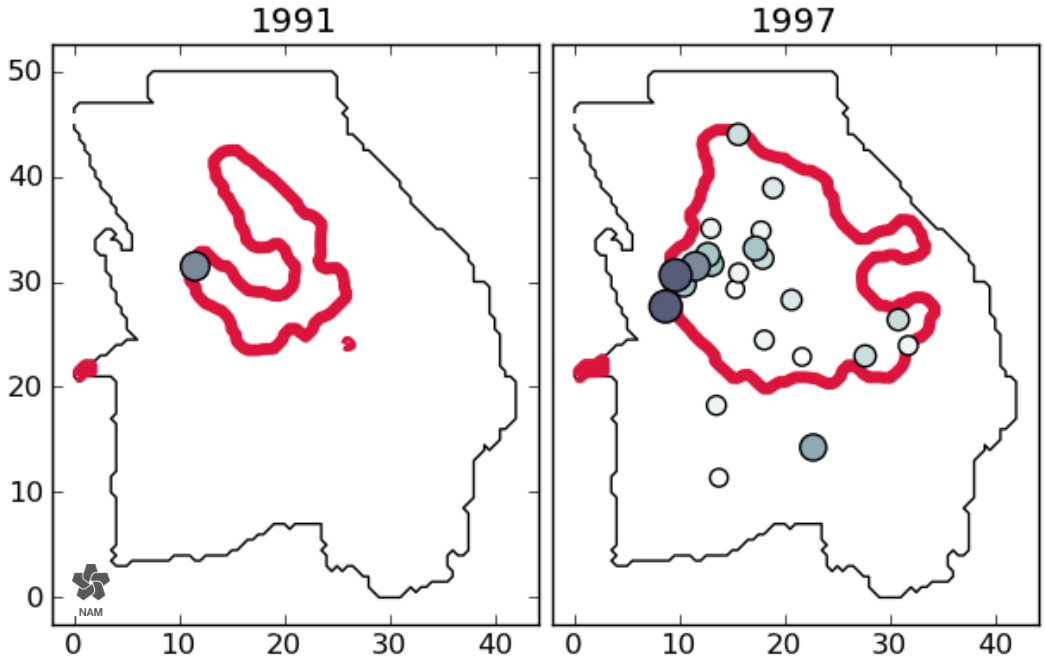

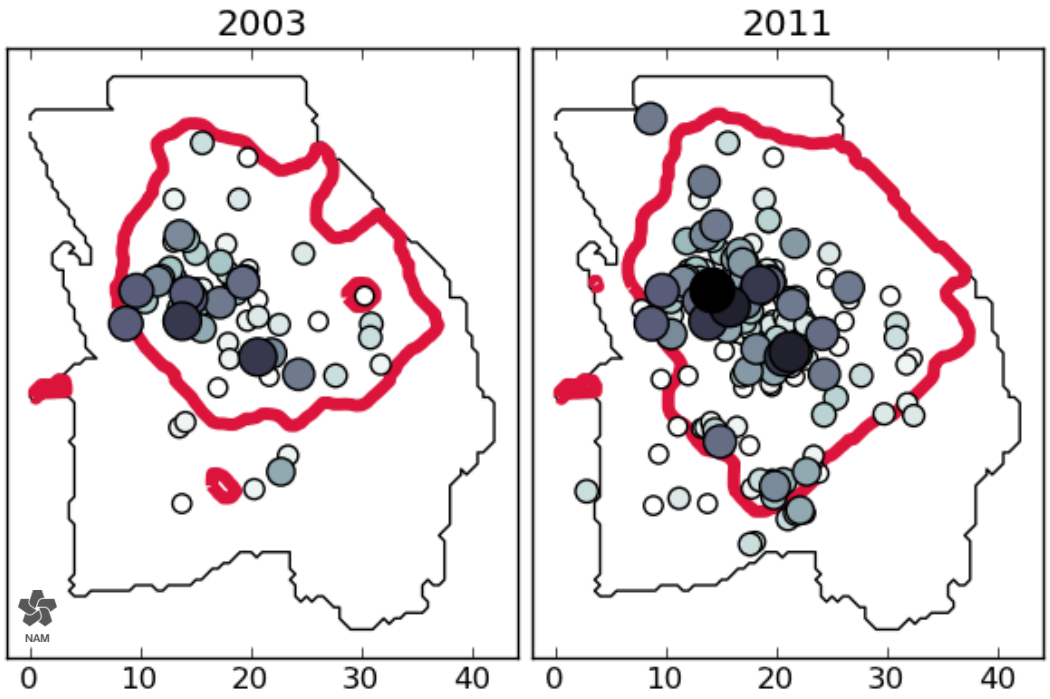

Figure 3.30 *The areal extent of M≥1.5 earthquake locations through time remains for the most part (80%) within the 0.18 m reservoir compaction contour (red line) according to the linear poroelastic reservoir compaction model.*

The time series of *ML* ≥ 1.5 events magnitudes, labeled according to the reservoir compaction at the time and location of each event (Figure 3.31), suggests there is no single threshold in compaction above which induced seismicity occurs but rather a much more continuous process where the likelihood of an event occurring increases according to the local reservoir compaction.

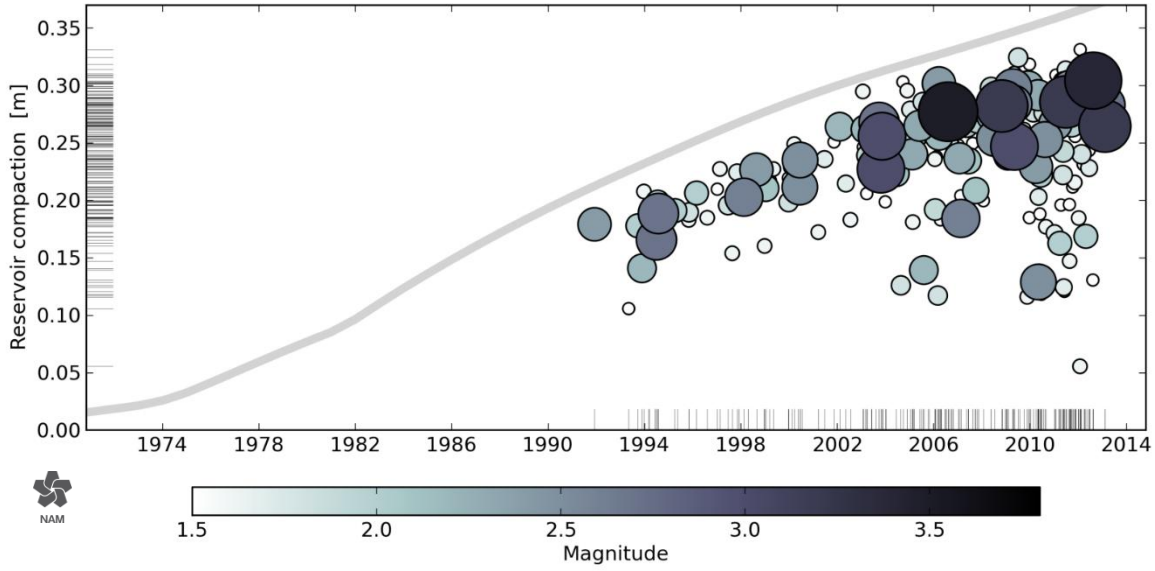

Figure 3.31 *Time series of ML ≥1.5 earthquake magnitudes versus reservoir compaction at the origin time and map location of each event.*

These observations of a strong correspondence between compaction and seismicity do not mean that faults do not play an important role in the generation of induced earthquakes. It simply means that there are many faults in the reservoir and that there are faults everywhere in the reservoir that

can accommodate a seismic rupture. Many of these faults will be too small to be identified in the seismic data. As described further down in this document the seismological model can be further improved when faults are taken into account.

Strain-partitioning and Event-rate models

In PHRAs for naturally occurring tectonic earthquakes, the seismological model usually comprises an identified seismically active region with assumed parameter values specifying the expected level of seismic activity. In the Groningen case, reservoir compaction has been identified as the geomechanical process inducing the seismicity. The seismological models have been built on this basis. For the 2013 Winningsplan submission, the seismological model used in the PSHA calculations was based on earlier work by Kostrov and McGarr, which linked the total seismic moment of a catalogue of events to the subsurface strains causing them. A strain partitioning factor was introduced to account for the observed division of strain into seismogenic and aseismic components.

An alternative to forecasting the total seismic moment according to strain is to forecast the occurrence rate of events above a certain magnitude according to strain. Models of both types (Strain Based Models and Event Rate Models) are seen in the literature and the choice between them is ultimately an empirical question: which type of model best fits the observed data? In the Groningen case, we see a more precise fit of the relationship between event rate and reservoir strain than we do for total seismic moment. Moreover, event rate based models can be naturally extended to incorporate after-shocks. This is particularly useful as it has been shown that spatial and temporal clustering of events needs to be accounted for in the Groningen earthquake catalogue. For these primary reasons, an Activity Rate model incorporating an Epidemic Type Aftershock Sequence (ETAS) model has been developed as the second generation seismological model. The performance of this model was further improved by also accounting for the influence of pre-existing fault offsets. A simple geometric argument can be used to show that the induced strain on a pre-existing vertical fault in a compacting reservoir is proportional to the product of fault offset and reservoir compaction. Generalising this simplified geometry it can be shown that replacing compaction in the initial version of the Activity Rate model with a strain-thickness attribute accounts for reservoir compaction and reservoir dip including fault offsets.

As well as accounting for the variation of seismicity with the process of reservoir level compaction, the seismological model must also account for the observed statistics of earthquakes magnitudes, in particular the relative abundance of large and small magnitude events described by the Gutenberg-Richter b-value. Consideration of the Groningen catalogue as a whole gives a b-value very close to the value of 1.0, generally found for earthquake populations elsewhere. If, however, the catalogue is subdivided into smaller subsets according to the strain-thickness attribute, then potentially significant systematic variations of the b-value with strain-thickness become apparent with b tending to smaller values at larger values of strain thickness.

Although a systematic variation of the b-value is seen, the error bounds on the values obtained are large due to the reduced number of events considered in each subset. For this reason a constant b-value close to 1.0 calculated for the catalogue as a whole is taken as the base case scenario with an alternative upper bound scenario determined by taking the b-value as a stochastic function of the strain-thickness. The lower bound scenario was taken as having the constant b-value used for the base-case but maximum likelihood values of the Activity Rate and ETAS model parameters rather than samples drawn from the joint multi-parameter distribution.

Seismic activity is in the first order determined by the total compaction of the reservoir. However, faults in the reservoir play an important role. As mentioned, the Activity Rate Model was extended to more explicitly take the presence of faults into account (Ref. 43). Figure 3.32 shows that the agreement between the observed and modelled seismic activity is improved if additional to compaction also the presence of faults is considered. The differences between the observed seismic density and the modelled seismic density are reduced if faults are explicitly taken into account.

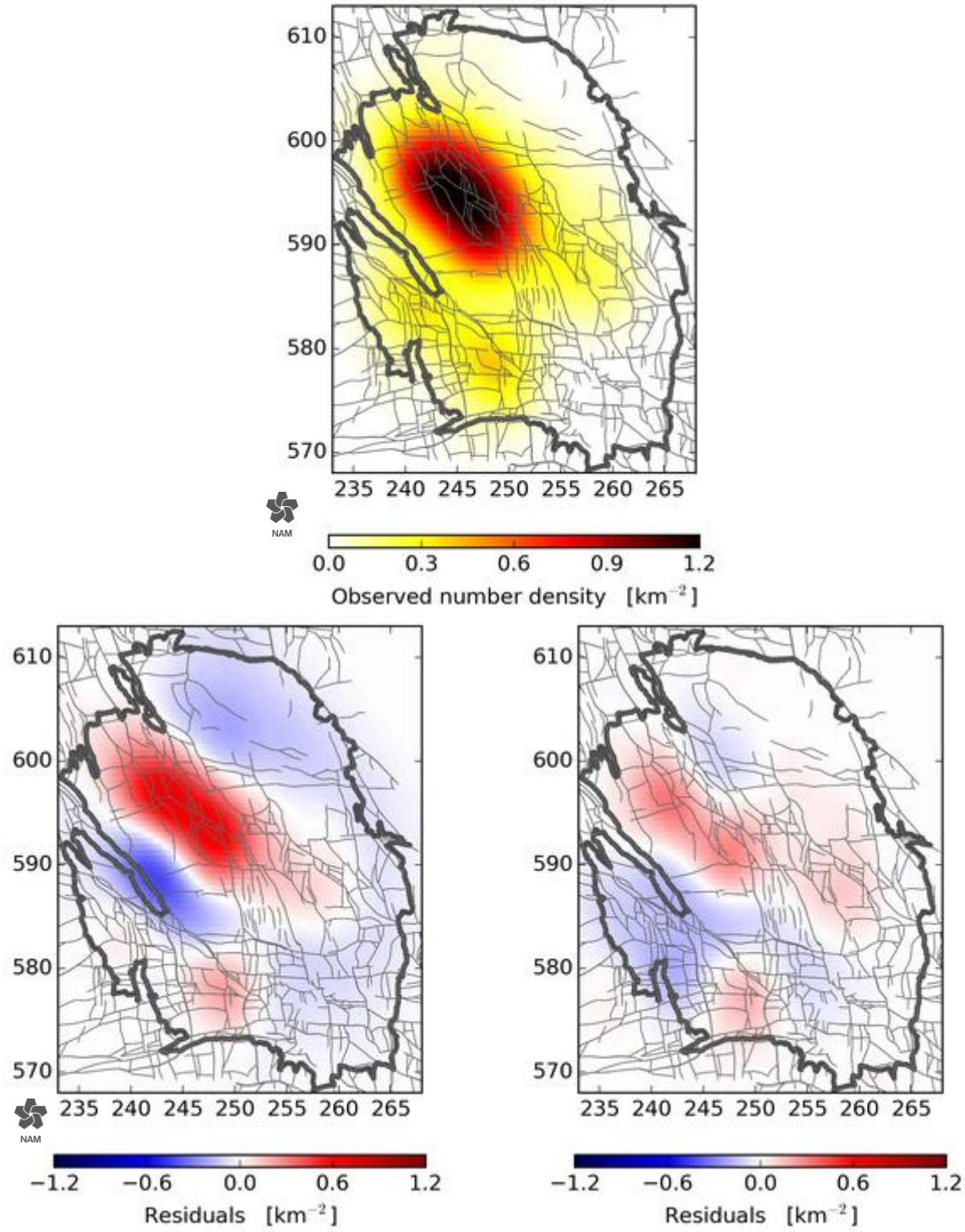

Figuur 3.32 Observed and simulated seismic event density. Upper image shows the observed seismic event density. Lower images show the difference between the modeled and observed seismic event density for the two

different versions of the activity rate model. Left result for the activity rate model based on compaction only and Right the impact when faults have also been taken into account.

Alternative Seismological Models

Geomechanical Model

In the Technical Addendum to the Winningsplan 2013 (Ref. 5), the geomechanical model was presented. The first version of this model includes a global model and two sub-models. The global model includes the entire Groningen field region but does not explicitly include faults. The pore pressure field is imposed and the model responds with deformations based on pore pressure changes and salt creep behaviour. The deformation of the reservoir rocks is modelled using porosity dependent elastic properties. Global model subsidence and predicted reservoir strains compare well with available data. The global model deformations are then used as boundary conditions to the sub-models, which have been developed to model regions of seismic activity in greater detail. The sub-models include detailed modelling of faults as contact surfaces, permitting slippage due to depletion-induced stress changes.

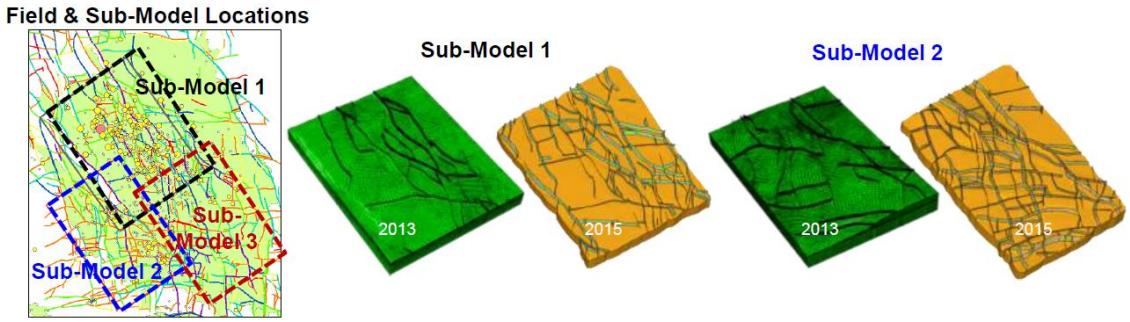

Figure 3.33 Large scale geomechanical model of the Groningen field. The additional complexity incorporated in this model since winningsplan 2013 in terms of faults and improved fault description with offsets is shown.

Update 2015

Since 2013, many additional faults have been included in the previous two sub-models, and a third additional sub-model has been developed. Further, the horizons have been modified at the fault interfaces to explicitly include fault offsets. The combination of the global and sub-models allows for the use of either compaction based metrics (global model) or fault-slip based metrics (sub-models) as the basis for a seismological model.

Currently, compaction from the global geomechanics model can be used as the basis of the seismological model. Rather than using a strain partitioning model, a direct correlation is made between the compaction (change in reservoir thickness) and the number of events (activity). This approach directly produces an activity map that can be read into a PSHA analysis. A variety of functional forms can represent the correlation between compaction (relative to a point in time (e.g. 1995)) and the total number of earthquakes. A maximum likelihood estimation is used to build a Poisson process model, which incorporates the spatial and temporal components for each individual observed earthquake. Quadratic, cubic or exponential forms all reasonably match the observed seismicity, with little difference in the predicted hazard for 2016-2021 between the cubic and the exponential forms. The use of the quadratic form reduces the hazard by 22%. The compaction and compaction derivative values are determined from a linear interpolation between the January 1 values calculated from the geomechanics model. To determine the activity for 2015, the compaction value at January 1, 2015 is used, and the derivative is a backward derivative considering the change from January 1, 2014 to January 1, 2015.

Future Development for 2016

It is planned to use a fault-slip based metric as an input for the seismological model. The advantage of this approach is that it incorporates the effect of fault orientation relative to the stress field in determining if a fault is likely to fail. By correlating the static geomechanics model to activity, rather than developing a strain partitioning model, it is suggested that the geomechanics model better predicts the nucleation of earthquakes (where faults are reaching failure) rather than the size of the resulting earthquake (since size will be controlled by dynamic effects which are not included in the model). Once a fault slips, either the slip moment (slip*area*shear modulus) or the dissipated fault energy (slip*area*shear stress) can be used as the geomechanical input. Qualitatively there is little difference between the slip and energy metrics because they are very well correlated over time. Fault slip occurs on discrete locations so a Gaussian kernel is used to distribute this slip over an area, resulting in a point-based area source that can be easily incorporated into the PSHA. This approach steps away from the idea that one particular fault is slipping (since not all faults are included in the model, there may be errors in seismic interpretation of faults, and some faults may not be visible in seismic and hence not mapped), instead allowing a fault in a general area the potential to be highly stressed and oriented for failure. Once a moment/energy map is generated, the same methods used to derive a compaction-based activity map can be used to derive a fault-slip based activity map (maximum likelihood estimation). The fault-based model can also be history matched by changing friction values on individual faults to better represent the historical seismicity.

Hazard Assessments for the Winningsplan 2013 and later updates, alternative seismological models were prepared.

Slider-block systems as a simple physical model of Groningen seismicity

There is an extensive literature on the statistical mechanics of failure (e.g. Pradhan, 2010), including the application of slider-block systems to natural seismicity (e.g. Rundle, 2003). The key aspect of these systems is that the evolution of failure, such as seismicity, is primarily governed by property fluctuations and not average values. In its simplest form a slider block system is a rectilinear array of rigid blocks, resting on rigid plate, connected to nearest neighbouring blocks and a second parallel rigid plate by elastic springs (Fig. 3.34). An essential feature of this system is that the initial stresses, failure stresses or stress drops during motion at the base of each block are not all identical, but rather at least one of these properties is drawn from a distribution. As one plate is increasingly displaced relative to the other, shear tractions increase at the base of each block. Once this traction equals the frictional resistance for one block it slides to reduce its basal shear stress whilst transferring stress to its neighbours via the connecting springs. This may trigger additional blocks to slides and this process repeats until a new equilibrium state is established (Fig. 3.35).

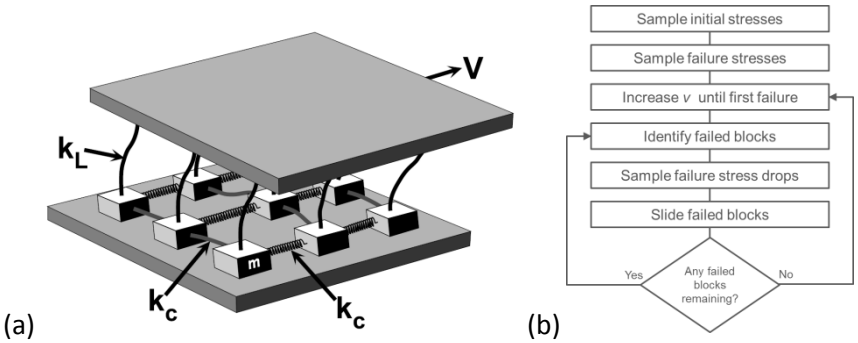

Figure 3.34 Schematic illustration of a simple slider-block model of seismicity on a single fault; adapted from Rundle (2003). (b) Example of simple physical rules that govern the evolution of a slider-block system.

For slider-block systems with a sufficiently large number of blocks the emergent phenomena possess many similarities to induced seismicity observed within the Groningen field, *e.g.*:

1. Earthquakes: Transient finite slip events
2. Event attributes: hypocenter, origin time, magnitude, rupture geometry
3. Power-law distribution of magnitudes
4. Maximum magnitude
5. Exponential-like increase in activity rates with displacement
6. Exponential-like increase in seismic moment rates with displacement
7. Recognizable *b*-values insensitive to initial conditions
8. Inverse power-law like decrease in *b*-values with displacement
9. Temporal aftershock triggering consistent with an inverse power-law
10. Spatial aftershock triggering consistent with an inverse power-law
11. Recognizable finite-rupture scaling with magnitude
12. Potential for slip triggering of basement faults

These statistical properties are reproducible despite the role of randomised sampling, but of course the exact location, timing and magnitude of each event differ from simulation to simulation. The particular statistical properties that emerge such as *b*-values, exponential trends and the maximum magnitude are critically sensitive to the choice of the ratio of spring constants (K_c/K_L) which represents the force interaction length-scale, the stress drop, and the spread of strength variations about its mean value. However, appropriate choices of these parameters do yield simulated seismicity trends that resemble the same trends observed in the induced Groningen seismicity.

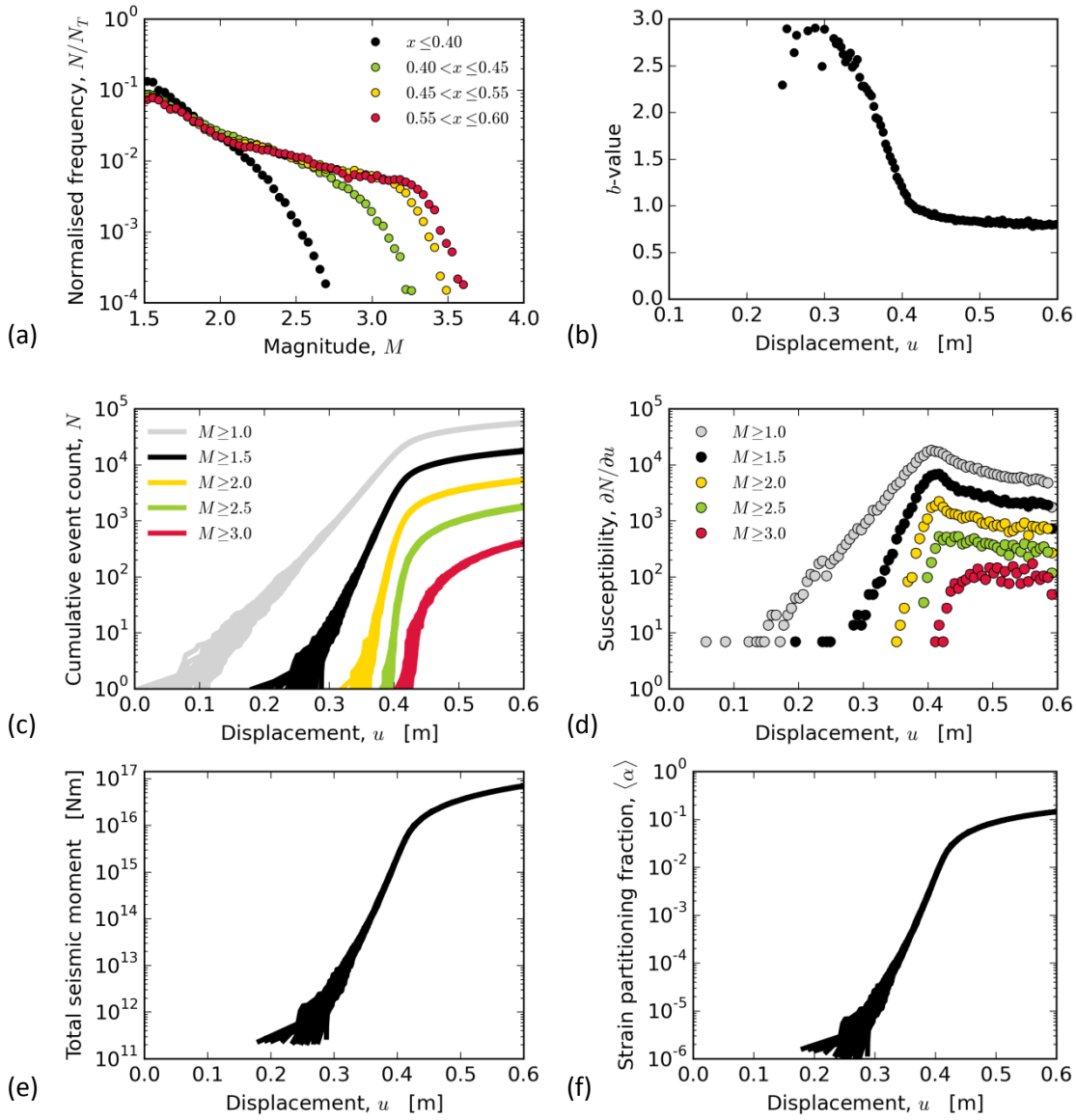

Figure 3.35 *Example results obtained from a simple slider-block system with a physical extent of 60 km by 600 m comprising 10^5 blocks each about 20 by 20 m in size. (a) Frequency-magnitude distribution of slip events as it evolves with increasing relative displacement, x, of the plates with an upper bound influenced by the finite size of the system. (b) The trend of decreasing b-values with increasing initial relative displacement of the plates, u, before reaching some steady-state value. (c, d) The cumulative event numbers and the rate of event numbers show an exponential-like increase with increasing relative displacement of the plates until reaching some steady-state. (e, f) The total seismic moment and fraction of the total strain accommodated by slip (strain partitioning fraction) show an initial exponential-like increase with increasing relative displacement of the plates.*

Maximum Magnitude

The earliest estimate for M_{max} in the Groningen field was 3.3, as determined by KNMI in 1995 (Fig. 2.4). This upper bound has since been exceeded by three earthquakes (in 2006, 2011 and 2012). A new estimate of 3.9 was proposed by van Eck et al. in 2006. This estimate was based on extrapolation of the exponential recurrence relationship, including one standard deviation of the measured distribution of residuals, and implemented by the relevant actors. Following the Huizinge earthquake on the 16th August 2012, this M_{max} is under evaluation again.

In the seismological models developed to date by NAM, the maximum magnitude considered in the hazard and risk calculations was M_{max} 6.5. This M_{max} value was estimated as: "*the maximum possible induced earthquake corresponding to the exceptional case of all induced strain being released in one single event at the end of production*" (Bourne et al., 2015). Disaggregation of preliminary hazard and risk estimates showed dominant contributions coming from considerably smaller earthquakes, which led NAM to treat the results as being insensitive to the choice of the limiting upper bound on magnitude.

In the more recent PSHA calculations performed to generate the seismic zonation map required for the NPR 9998 seismic design code for Groningen, KNMI employed a single M_{max} value of 5.0. A report by TNO prepared for the NEN (Ref. 33) proposed alternative values for M_{max}, the largest of which was 5.0, assuming a limiting value of 0.1 for the strain partitioning factor. More recently, reports have been issued suggesting TNO has reduced its estimate of M_{max} to 4.5.

The key point is that it is standard practice in probabilistic seismic hazard and risk assessment to acknowledge the epistemic uncertainty in the estimation of the largest earthquake (of M_{max}) that could occur. NAM has decided to follow this precedent from global best practice by including a logic-tree node for M_{max} and assigning a distribution of weighted values of moment magnitude that could represent the effective upper limit for induced earthquakes in the Groningen field.

The range of two full magnitude units in the unique estimates of M_{max} currently being used in probabilistic seismic hazard assessments for Groningen represents a clear divergence of interpretations. This divergence is accentuated by the use of single estimates for this parameter rather than distributions to capture the epistemic uncertainty that is inevitably associated with the estimation of M_{max}. The response of NAM is two-fold: firstly, we have used a distribution of M_{max} estimates to reflect the current range of uncertainty, as discussed in the next section. The second step, discussed thereafter, is to convene an independent specialist panel specifically to address the issue of M_{max} estimation for Groningen.

In view of the considerable uncertainty that is clearly associated with the assessment of the M_{max} value for the Groningen field, a broad continuous distribution on this parameter is deployed in the short-term. The existing estimate of M 6.5 is taken as the upper bound for the distribution of M_{max}, since within the framework of induced earthquakes, it does represent a limiting value indeed. To be conservative for the hazard assessment, an initial lower limit of M 5 has been adopted. The preliminary distribution on M_{max} is uniform between a lower bound of M 5.0 and an upper bound of M 6.5.

Improvements Version 1 (May 2015)

- Seismological models for V1
  - Base case: Extended Activity Rate, ETAS, parameter distributions, constant b-value
  - Upper bound: As base case except *b*-value is a stochastic function of strain thickness
  - Lower bound: As base case except maximum likelihood parameter estimates

Improvements Version 2 (November 2015)

- Developments for V2
  - Assessed evidence for any significant changes in *b*-value
  - Assessed model performance following production changes
  - Established a Bayesian framework for ranking model performance

- Investigated potential influence of finite ruptures on mapped faults
- Used data available from the upgraded monitoring network

Improvements for Winningsplan 2016 (Mid 2016)

- Consideration is given to M_{max}
- Alternative seismological models (e.g. slider block) will be developed to gain additional insight.

Ground Motion Prediction

Ground Motion Prediction is essential in order to understand how an earthquake, which often takes place at a depth of several kilometers, is felt at the surface and impacts the buildings that are built on that surface.

The main innovation of the Version 2 Ground Motion prediction methodology, compared to the Version 1 used in the Hazard and Risk Assessment of May 2015, is the incorporation of local site response, capturing the effect of the shallow sub-surface and soils through spatially-varying non-linear site amplification functions. Detailed data from the complete rock and soil package above the gas fields was needed as input into the Ground Motion Prediction methodology. As a result, the new Ground Motion Prediction methodology is tailored to the Groningen field area circumstances and not a generic methodology. This also means that the new GMP methodology cannot, without modification, be applied to others areas.

The Ground Motion Prediction methodology is important for the next link in the causality chain from production to risk; building fragility and response. The methodology allows for prediction of Peak Ground Acceleration, Ground Motion significant duration ($D_{S5\text{-}75}$) and spectral acceleration for a range to periods as input into building response assessments for a range of different typologies. Spectral accelerations are predicted for 16 periods ranging from 0.1 sec to 5 seconds to cover all building typologies from single story houses with a response period in the range of 0.2 seconds to high rise buildings with a response period of several seconds.

Additionally, the methodology provides input into risk assessments for a range of other infra-structure and industrial objects like levees.

Availability Ground Acceleration Data

The extended geophone network with accelerometers installed at some 70 locations has led to an increase in the available earthquake data, with denser sampling of the ground-motion field during recent earthquakes. At the time of the preparation of Winningsplan 2013, relatively few earthquake acceleration records were available for the Groningen field area and therefore little data was available on which to base a ground motion prediction methodology. This was caused by the relatively low number of earthquakes causing measurable ground accelerations and the relatively low number of accelerometers placed over the field, recording these earthquake accelerations. Although the number of earthquakes with significant accelerations measured at surface only increased from 8 to 16 from Winningsplan 2013 to this assessment, the number of recordings of these earthquakes increased from 40 to 146. This is mainly due to the expansion in 2013 of the KNMI permanent accelerograph network to 18 instruments plus the increased number of recording sites as the first geophone sites equipped with accelerometers installed as part of the KNMI network extension have now been taken into operation. As per end-October, of the 70 additional geophone stations with accelerometers, 58 stream their data directly to the KNMI.

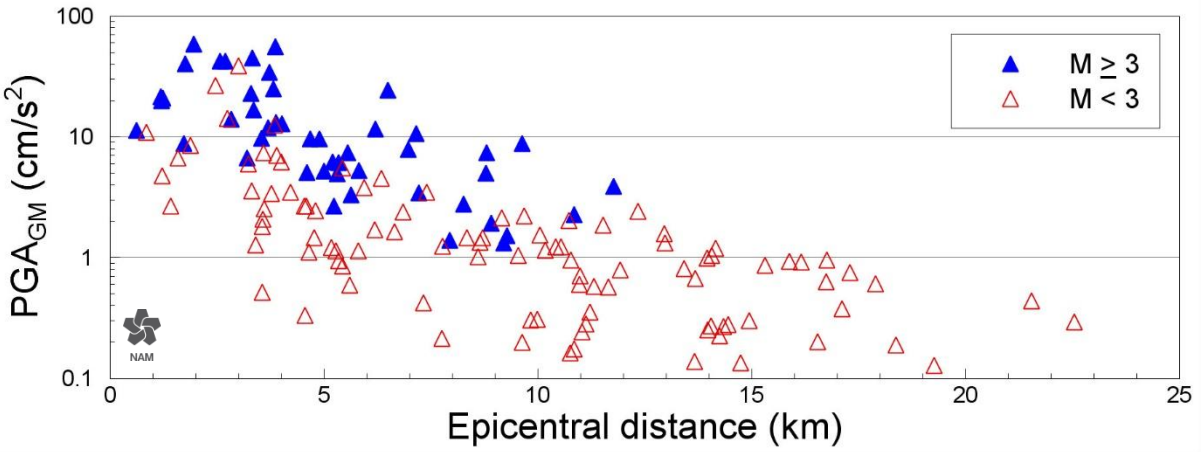

Figure 3.36. Geometric mean values of horizontal PGA plotted against epicentral distance. General trends of increasing acceleration with increasing magnitude and decreasing distance can be observed, as would be expected. A noteworthy observation is that less than 30 records (i.e., about 20% of the dataset) have geometric mean PGA values greater than 0.01g.

The acceleration records currently available in the Groningen area are for low magnitude earthquakes (M≤3.6), which may cause damage to buildings, but have proven to be too small to cause buildings to collapse – even though building inspections have detected some houses to be in a bad state due to loss of structural capacity for various reasons. For the hazard and risk assessment, the ground motion forecasts for larger magnitude earthquakes are important. To achieve this, the available data needs to be extrapolated to larger magnitude earthquakes. Within the available time for Winningsplan 2013, a model derived from recordings of tectonic earthquakes in southern Europe was used. Because equations were used that were intended for much stronger tectonic earthquakes, the hazard associated with larger magnitude earthquakes was (in hindsight) overstated in the first pass in the Winningsplan 2013 (Ref. 5; Chapter 7). The latest studies (Ref. 25) now show that for an earthquake of a given magnitude the ground accelerations are smaller at short periods (e.g. PGA).

Properties of the overburden (s-wave velocity and density)

To be able to predict ground motion at surface resulting from an earthquake originating from the Rotliegend reservoir located at 3 km depth, knowledge of the full rock and soil column from the surface down to the reservoir section and lower is required (Fig. 3.36).

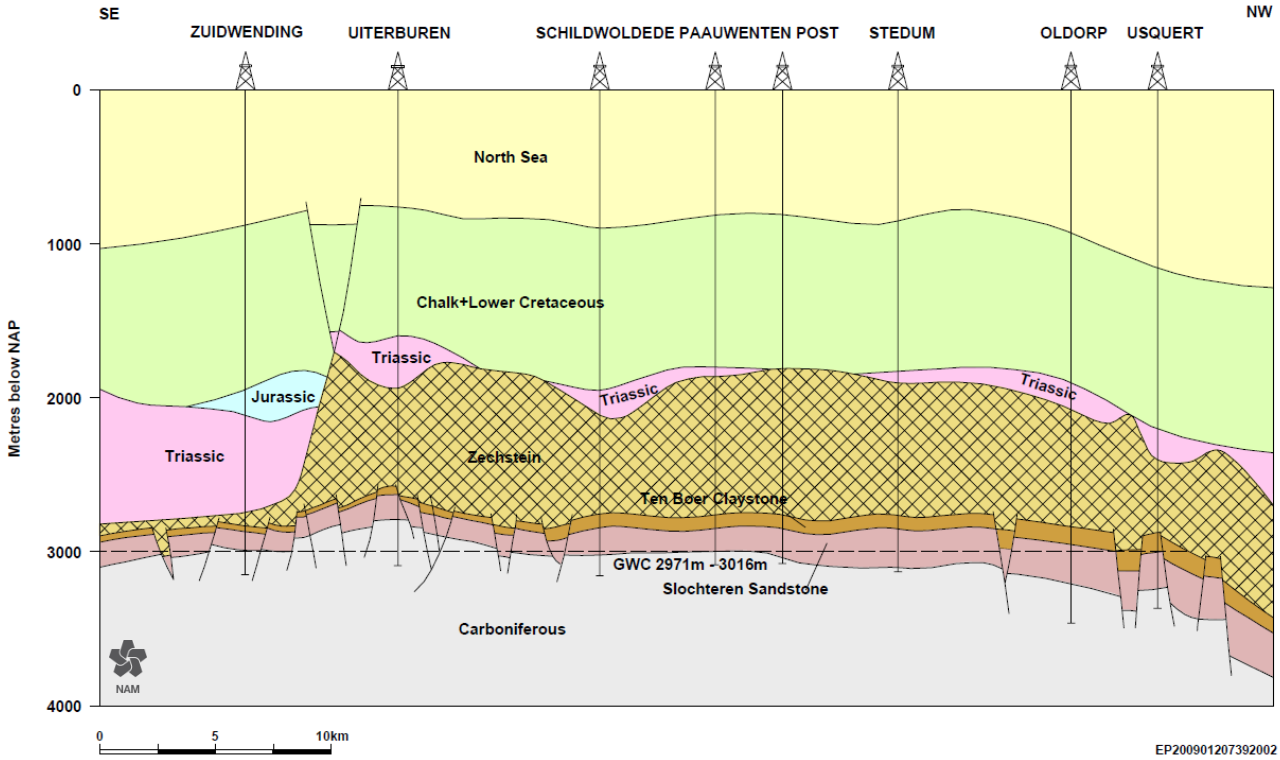

Figure 3.37 Simplified geological profile of the Groningen field. The thick Zechstein salt layers above the reservoir plays an important role in the transmission of seismic energy from the reservoir depth to the surface.

Rock property data, mainly density, P-wave velocity and S-wave velocity, were collected for different depths using different methods:

- For the deeper section from below the reservoir up to some 60 m depth from surface the seismic data obtained during the 1980s supplemented by more recent well logging data was used. This includes density and sonic data (P- and S-wave velocity) obtained over the full well length in the most recently drilled three wells (BRW-5, ZRP-2 and ZRP-3A).
- The original seismic survey acquired in the 1980s was reprocessed and re-imaged using new research techniques to also obtain a detailed geological image of the shallow sub-surface. This technique improved the model over the depth range from 300 to 100 m depth.
- Well logs were obtained in 70 newly drilled wells of the geophone network. These wells are 200 m deep and provided log data over this depth range.
- Geophysical measurements of the response of the shallow subsurface and soil layers were carried out near the accelerometers that have been recording since the mid-1990s.
- A detailed geological model of the shallow sub-surface and soils was prepared. Main data source was the DINO and GEOTOP databases of TNO-NITG. These data were supplemented by additional data from private parties acquired through Fugro and Wietsema. An introduction into the geology of the shallow underground of the Pleistocene was prepared (Ref. 27).

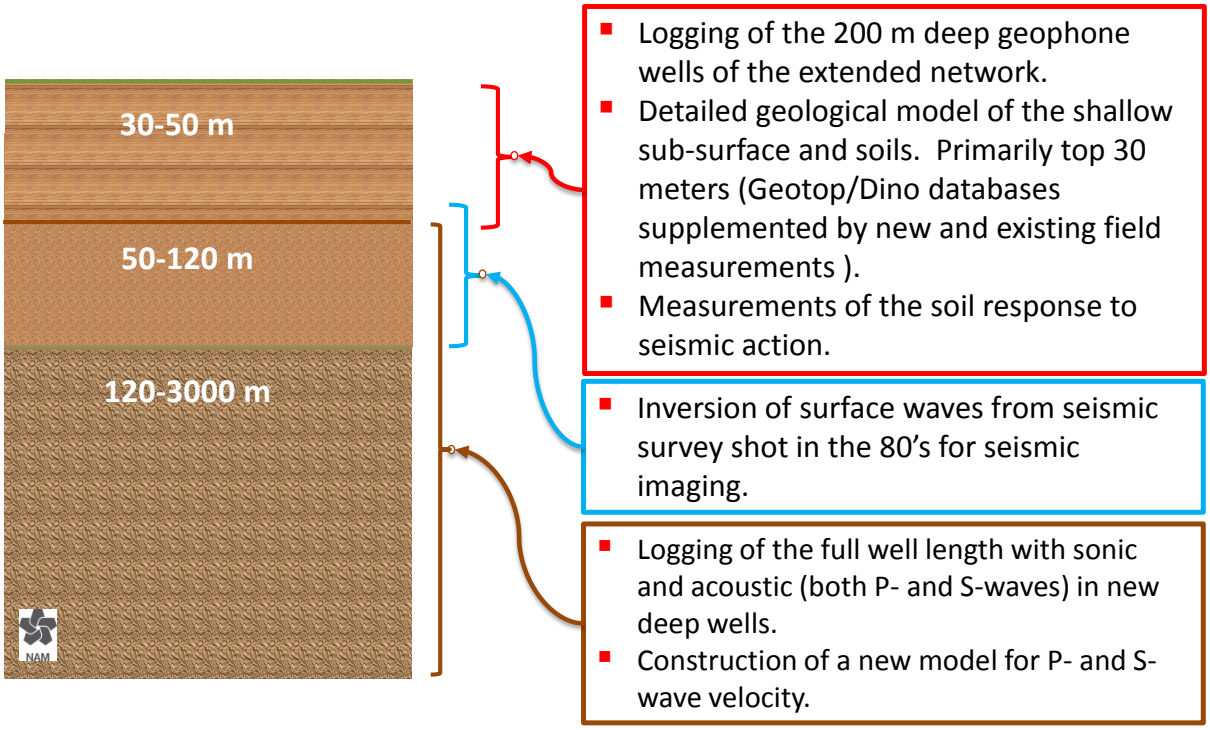

Figure 3.38 *Rock column from the seismically active reservoir section to the surface (overburden), with the data gathering to improve our understanding of the progression of the seismic energy indicated in the boxes to the right.*

Initiation in the Reservoir (Rotliegend Formation)

There is strong evidence that the earthquakes in Groningen originate in the Rotliegend reservoir section. Especially the data obtained from the geophones installed in the deep seismic observations wells in the Loppersum area support this. In the current model it is still assumed that the earthquakes originate from a point source, which means the size of the earthquake rupture is small compared to other length dimensions like the depth of the hypocentre. A sensitivity study showed this is a conservative assumption for the calculation of local personal risk and group risk.

Propagation to the Near Surface (through Zechstein to Base Upper North Sea Formation)

Based on available seismic data from the surveys done in the 1980s, and supplemented by the density, P- and S-wave logs from the three new wells (Fig. 3.39), the model of the rock above and below the reservoir was updated. Figure 3.39 shows the P-wave velocity model and the different geological formations. Using this model, the spreading of the seismic energy as the earthquake wave progresses through the hard formations above the Rotliegend formation was modelled in detail. A snapshot of the simulated wavefield propagation is shown in Figure 3.40, with the seismic velocity structure in the background. The geologic layering in this deeper part of the Groningen subsurface has several interfaces which have a significant impact on the spreading of the seismic energy as the waves travel upwards. Major interfaces such as those between the Rotliegend reservoir and the high-velocity Zechstein salt or the even higher velocity Zechstein anhydrites divide the wave energy through reflection and refraction. Other key geological interfaces which further redistribute wave energy through reflection include the base of the Chalk and the base of the Lower North Sea Formation.

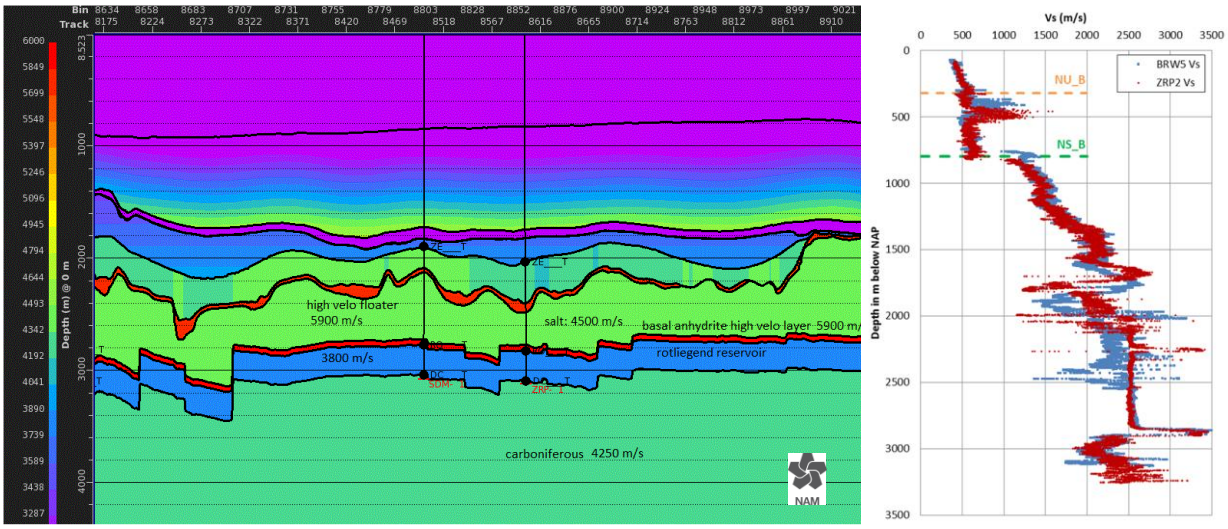

Figure 3.39 *Left: P-wave model based on PSDM, DCAT and sonic logs S-wave model based on P – S sonic log relations per litho-stratigraphic unit. Figure 3.39 Right: Shear-wave velocity profiles from two deep borehole logs, indicating the location of the base of both the North Sea Supergroup Formation (NS_B) and the Upper North Sea Formation (NU_B) formations. The base of the Upper North Sea Formation NU_B horizon is seen as the interface between the hard rock and the softer and soil formations.*

The progression of the seismic waves through the deeper formations is calculated up to the base of the Upper North Sea Formation (NU_B). This is across the field located at some 300 - 350 m depth. From this reference horizon upwards spatially-varying non-linear site amplification functions are used to estimate the ground motion at surface.

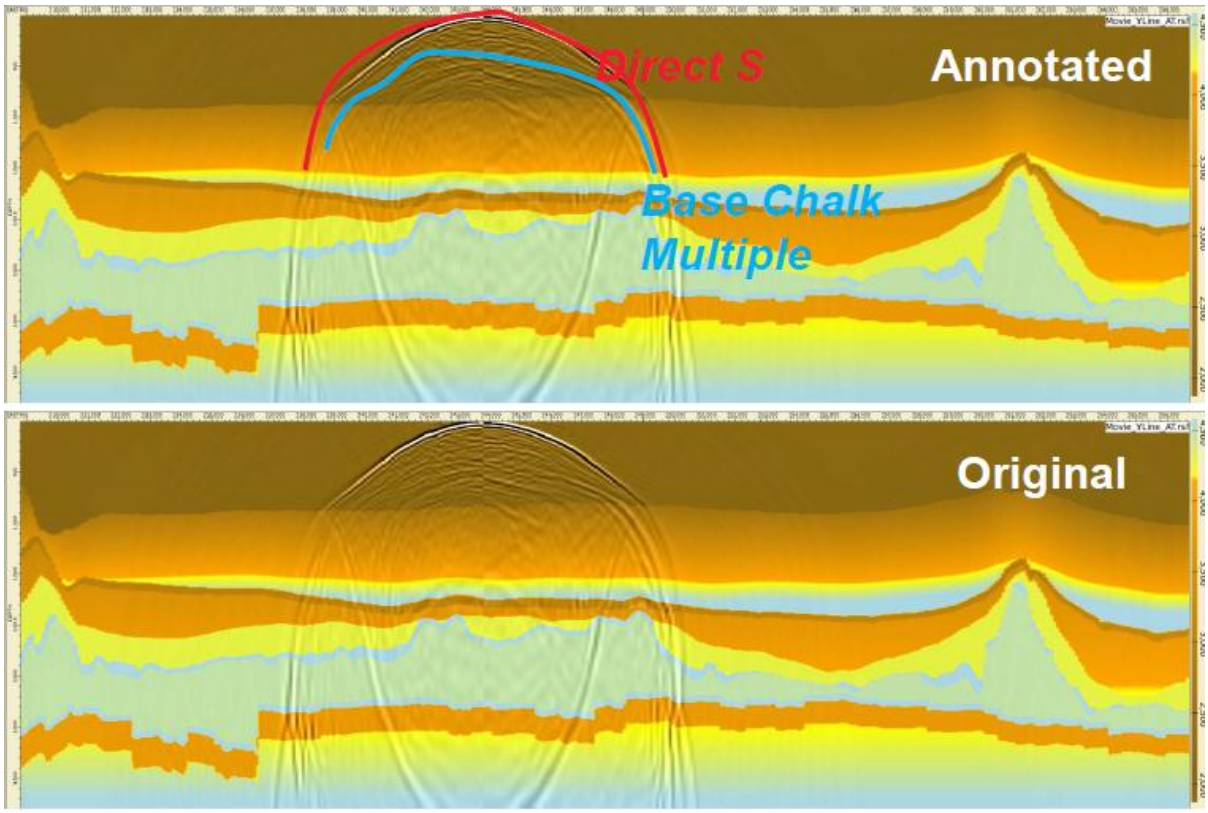

Figure 3.40 *Image of the modelling of the progression of the seismic waves from the rupture area in the reservoir to the surface. This modelling does not include the effects of the approximately 350 m deep soil layer. The snapshot was taken 2.7 seconds after the rupture took place, when the S-waves reaches the surface.*

While small-scale spatial variations in wave energy reaching the near surface are shown by elastic wave propagation modelling, a field-wide systematic reduction in wave energy has been independently predicted by two separate full elastic 3D wavefield modelling codes (Shell and ExxonMobil). This deviation is relative to the spherical 1/R-type spreading typical for a formation with homogenous and isotropic rock properties.

Wavefield analysis has shown that the primary source of the distance-dependent amplitude reduction is refraction of the up-going direct shear wave off the base of the Zechstein salt and anhydrites. The reduction does not depend on the continuous presence of these layers because of the many other strong velocity inversions in the Groningen stratigraphy. The reduction is robust to event location and source orientation, and is therefore incorporated as two distance-dependent terms (corresponding to 0-6.3 km and 6.3-11.6 km from epicenter) in the V2 GMPE. This phase of wave propagation, between the source and the near surface, is assumed to be linear, so this distance-dependent reduction in wave energy reaching the near surface is one aspect of the updated GMPE which is independent of event magnitude.

The earthquakes in the Groningen ground-motion database have a limited magnitude range —with an upper limit of M 3.6. A key challenge in developing the GMPEs for the hazard and risk model is the extrapolation to the largest magnitude currently considered, i.e. M 6.5. As for the V1 GMPEs, this extrapolation is performed using point-source simulations based on seismological theory. In order to perform these simulations, estimates of the source, path and site parameters that define the Fourier amplitude spectra (FAS) of the motion are required. In reference 46 the method for the inversion of the FAS of the Groningen ground-motion recordings to obtain estimates of these source, path and site parameter is explained. These results were used with appropriate uncertainty ranges to extend the Ground Motion Prediction methodology to larger magnitudes. To reflect the uncertainty in the resulting Spectral Acceleration predicted using Ground Motion Prediction methodology, a lower, central and upper model were prepared, straddling the uncertainty range. Figure 3.41 shows the Spectral Acceleration at 0.01 s, which is of importance for 1 and 2 storey buildings.

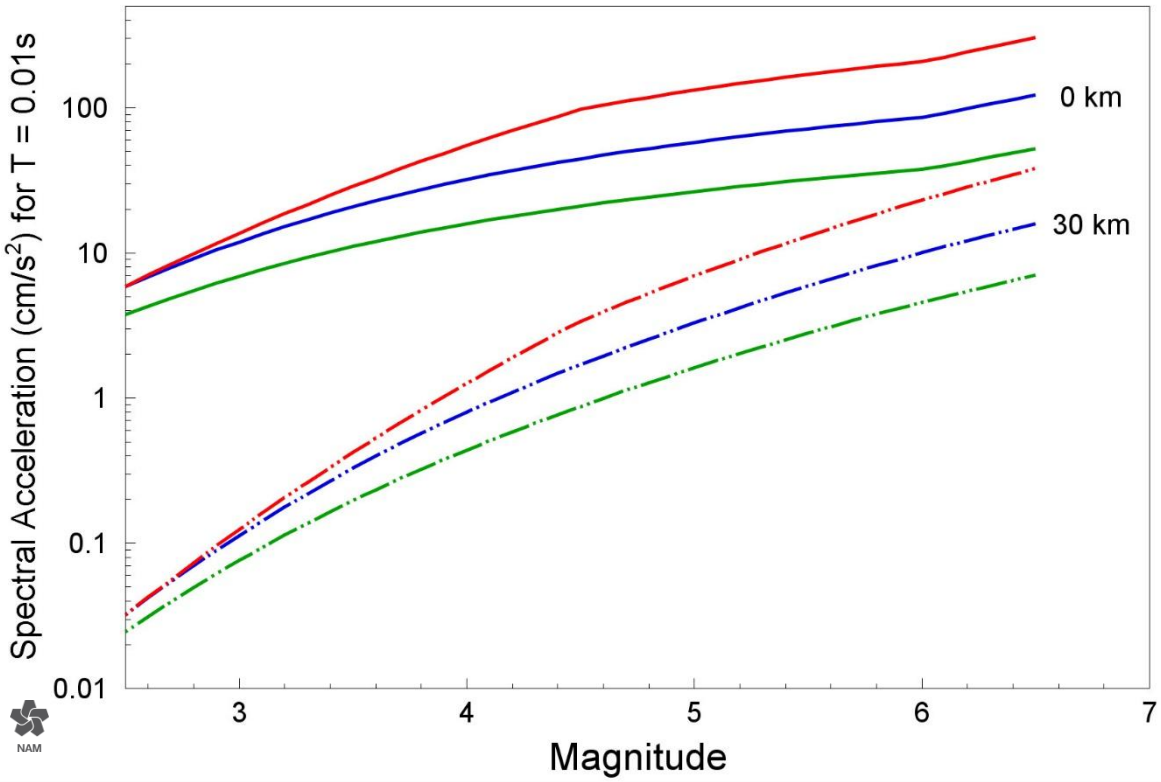

Figure 3.41. Spectral accelerations at 0.01 s from point-source stochastic simulations for lower (green), central (blue) and upper (red) models at epicentral distances of 0 and 30 km as a function of magnitude

Propagation to the Surface (from Base North Sea Formation to Surface)

A model of the shallow subsurface and soil was prepared by Deltares based on the GEOTOP model of TNO-NITG supplemented by additional data obtained from private owners through Wiertsema and Fugro (Ref.27). This model assigns a lithostratigraphical unit and a lithological class to each voxel (small volume of rock in the model) in the Groningen area. This is required as V_S depends on both stratigraphy (i.e. formation, for instance Naaldwijk Formation) and lithology (i.e. sand, peat or clay). A description of the formations in the shallow Pleistocene geology of Groningen can be found in reference 26. Values of shear wave velocity (V_s) are assigned to geological formations present in the area of interest from published values of measured V_S in the Netherlands. In some cases, this assignment can be extended to lithological classes. Additionally, there are 60 seismic cone penetration tests (SCPTs) in the Groningen region that allow for determination of representative V_S values that are specific to this region. The SCPTs typically reach to a depth of approximately 30 m below the surface.

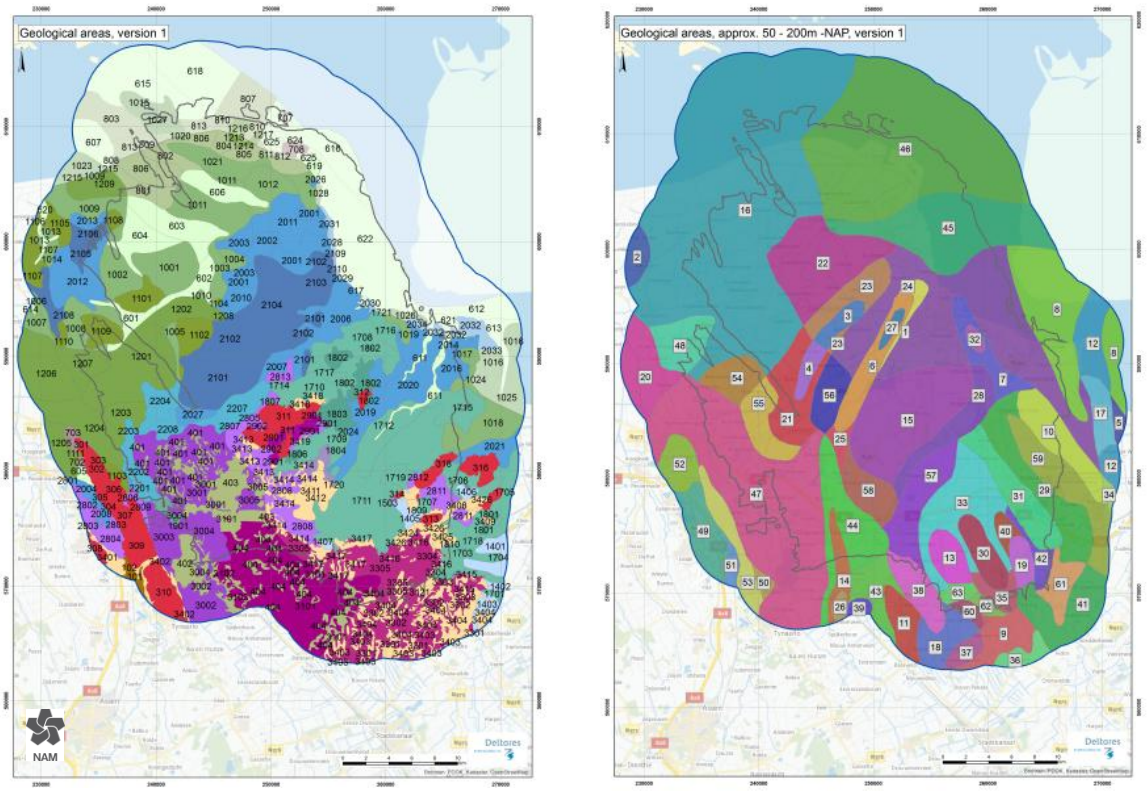

Figure 3.42 *Left Surface to 50 m-NAP Map for entire field 225 geological areas sorted by profile type*

Right: 50 to 200 m-NAP Wider range for overlap with shallower part from top Peelo when shallower than 50 m-NAP and to at least base of Peelo when deeper than 200 m-NAP. This is for 3 geological areas, max depth is 235 m. Based on DGM, REGIS II, DINO, new borehole logs (15), geological expertise X-Y: map of geological areas Z: scenarios Wider range than 50 – 200 m-NAP < 50 m-NAP start at Peelo > 200 m-NAP when base of Peelo is deeper (max 235 m-NAP)

To extend the model deeper towards the reference level of the Base Upper North Sea, use was made of the large seismic survey campaigns conducted by NAM/Shell around 1988 to obtain a clear image of the deep gas reservoir. Legacy datasets were reinterpreted to extend the V_s distributions to depths beyond those measured by the SCPT. Using the at the time of acquisition unwanted surface waves (ground roll data) both Vp and Vs were derived using the Modal Elastic Inversion method (MEIDAS). Because of the acquisition setup, which tried to reduce ground roll, and the frequencies present in the data, the depth range for which the near surface model obtained from the MEIDAS inversions is considered to be reliable from approximately 30 to 120 m below the surface (Figure 3.42).

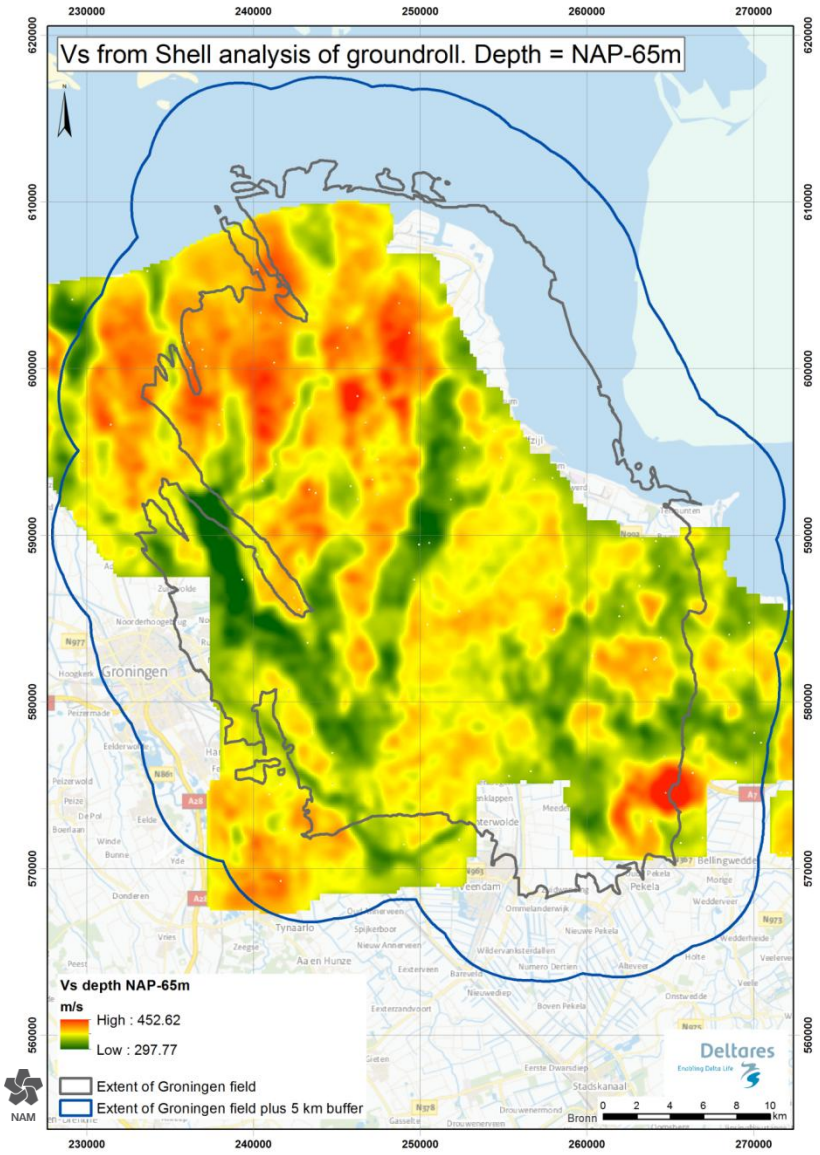

Figure 3.43 *The V_S model from the inversion of the ground roll yielded depth slices of V_S at 10 m depth intervals. This figure shows a depth slice at NAP-65 m through the MEIDAS V_S model.*

Overlapping with and extending below depth range covered by the Model of the shallow Pleistocene geology and the MEIDAS model, the model based on the active seismic acquisition in the 1980s is used to reach the reference level of the Base Upper North Sea (fig. 3.38).

Based on this detailed description of the shallow geology, zone amplification factors were derived that define the change in amplitudes of the waves as they travel from the NU_B horizon to the ground surface (Figure 3.44).

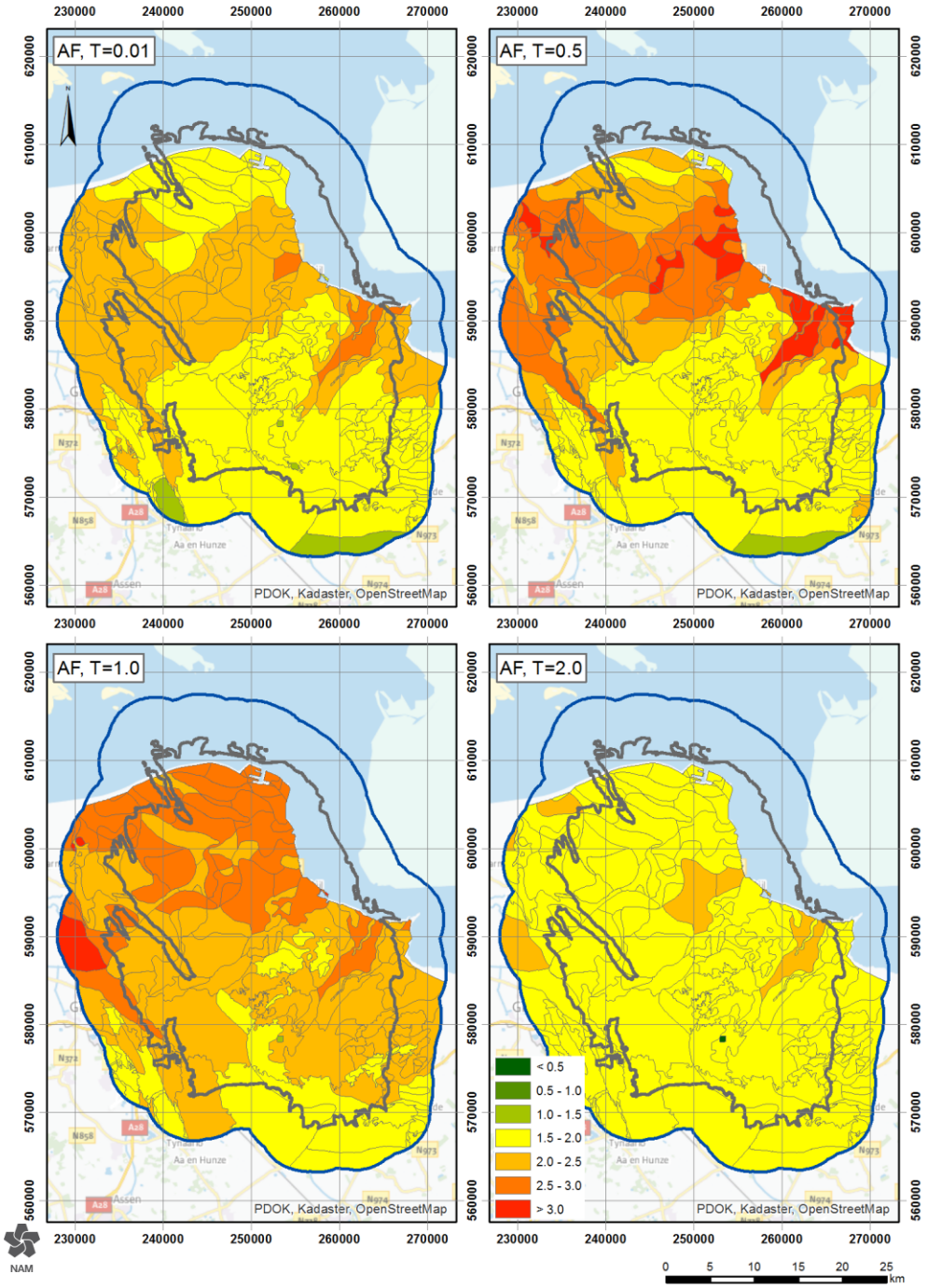

Figure 3.44 *Amplification factors (AF) for the Groningen region for a scenario with M 4.0 and R_{epi} 50 km. AF for four periods are shown.*

For the Groningen profiles, the nonlinearity of the soil properties with larger excitations implies a reduction in AF for shorter periods but an increase in the AFs at longer periods. This increase is expected as the resonant period of the sites shifts to longer periods as the soil softens (Figure 3.45).

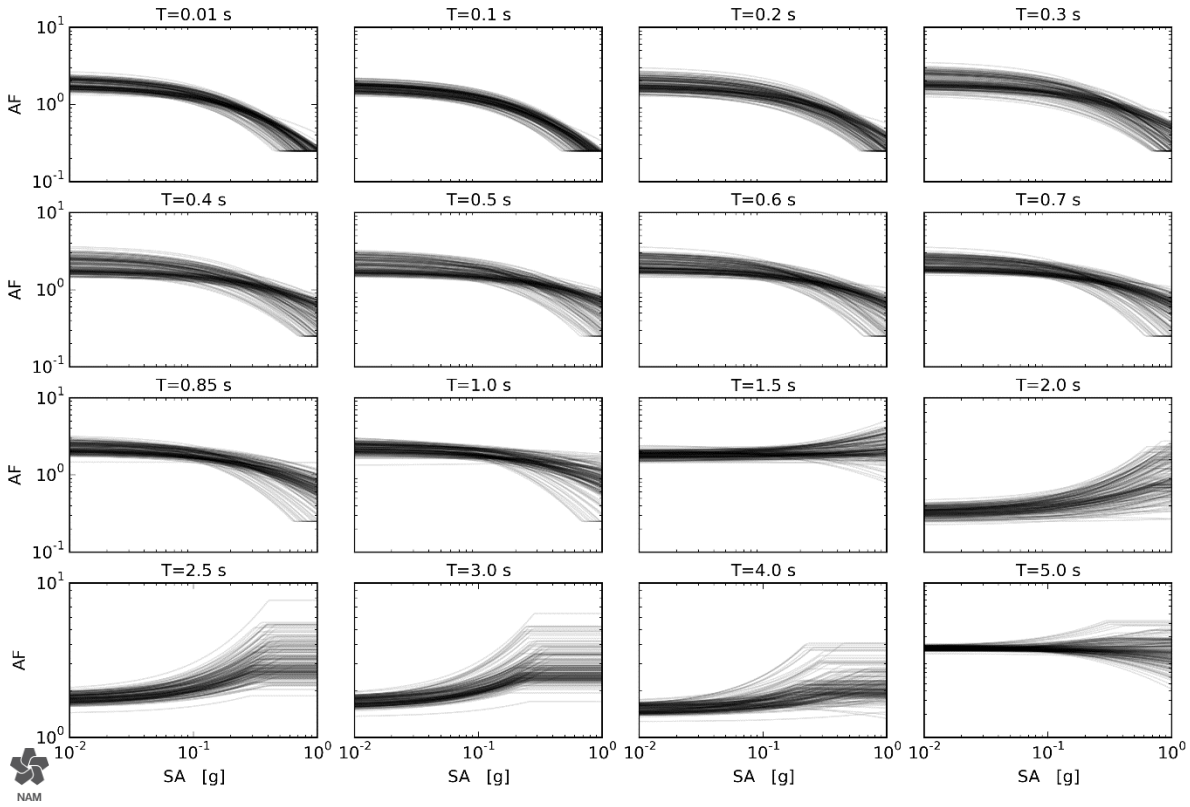

Figure 3.45 Non-linear site amplification factors (ratios of acceleration at the ground surface to acceleration at the NU_B horizon) for spectral accelerations at 16 oscillator periods

These three steps allow prediction of the transmission of seismic energy from the reservoir to the surface and estimation Ground Motion resulting from an earthquake. Every step in the Ground Motion prediction methodology is supported by evidence collected in the Groningen area and bespoke models based on this evidence.

As well as predicting the median (or best estimate) values of the ground-motion amplitudes, the model also characterises the variability (or apparent randomness) in the predictions. These are represented by Gaussian or normal distributions of residuals, which are characterised by their standard deviation (sigma). The sigmas capture the earthquake-to-earthquake variability and the spatial variability of the ground motions at the NU_B horizon, as well as the variability of the site amplification factors within each of the 167 zones into which the field has been divided for the purposes of modelling the ground shaking.

The likelihood of collapse of certain structures—particularly unreinforced masonry that demonstrates reduced strength and stiffness under cyclic loading—is a function of both the acceleration of the motion and the duration of the shaking. In order to capture the influence of the duration on the estimation of risk in the Groningen field, a GMPE for the prediction of duration was also derived and a framework developed for the joint prediction of spectral acceleration and duration.

Improvements for Version 2 (End 2015)

Since the Hazard Assessment of Winningsplan 2013, the Ground Motion Prediction Methodology has been continuously improved adding new features with each subsequent update. The table below gives an overview of the added features over the development phases:

GMPE Feature	Hazard Assessment Winningsplan 2013	Intermediary Hazard and Risk Assessment May 2015	Intermediary Hazard and Risk Assessment November 2015
Predicted parameters	PGA, PGV	Sa(T) for 5 periods	Sa(T) for 16 periods
Sigma model (variability)	Akkar *et al*. (2014a)	Groningen-specific	Groningen-specific
Epistemic uncertainty	Single model	Three alternatives	Three alternatives
Site classification	V_{S30} = 200 m/s across the field	Field-wide constant	Zonation based on amplification factors
Site amplification	Akkar *et al*. (2014a)	Network average, linear extrapolation	Groningen-specific, non-linear soil response
Components	Horizontal geometric mean	Horizontal geometric mean	Horizontal geometric mean and arbitrary components, the latter accounting for the component-to-component ratios (polarisation)
Duration model	n/a	Adopted model from California	Adjusted new global model to Groningen conditions

Table 1.1. Key features of the three phases of Groningen GMPE development

Improvements for Winningsplan 2016 (Mid 2016)

The current ground-motion model will be refined using an expanded database of ground-motion recordings for the field, especially taking advantage of the large number of records becoming available from the newly-installed networks.

Recognising the need to have reliably measured shear-wave velocity profiles at the recording stations, NAM commissioned Deltares to conduct *in situ* measurements at the locations of the KNMI accelerometer stations with a view to extending these subsequently to the new accelerometers being co-located with the 200-m geophone boreholes.

The campaign of *in situ* measurements envisaged applying a wide range of techniques at the first few stations in order to select those most suitable for general application across the networks. The multiple measurement approach was also designed to provide insight into the inherent uncertainty in the resulting V_S profiles and, to some extent, the degree of lateral heterogeneity at each site. The techniques envisaged included seismic CPT (with differing offsets), active MASW (with multiple sources), passive MASW, cross-hole measurements and PS suspension logging. Some of the borehole measurements, particularly the PS suspension logging, proved challenging in the Groningen ground conditions, but extensive measurements using seismic CPT and both active and passive MASW have been conducted at all of the 18 KNMI accelerograph stations. These measured Vs profiles will now replace the inferred profiles from the GEOTOP model and look-up tables, allowing more reliable deconvolution of the surface recordings to the NU_B horizon. For the site response modelling, the new measurements will enable a refinement of the empirical relationships used to define the look-up tables through which dynamic soil properties are assigned. Additionally, laboratory experiments are planned to better determine the stiffness and damping characteristics of the peat deposits in the Groningen field so that their influence on the site response can be more accurately modelled.

4 Hazard

Hazard Metric

Different metrics have been proposed to describe the hazard resulting from seismic activity. Most commonly used are the peak ground velocity (PGV) and peak ground acceleration (PGA). Because PGA is required to model the response of buildings, it was chosen as the most appropriate hazard metric for this hazard assessment. When extending the assessment to encompass risk, spectral acceleration (SA) will be used – this is a generalisation of the PGA concept which takes account of the response frequency of the building being considered. Figure 4.1 shows the measured acceleration near the epicentre during the Huizinge earthquake of 16th August 2012. Apart from the peak values also the duration of the event is important for the hazard.

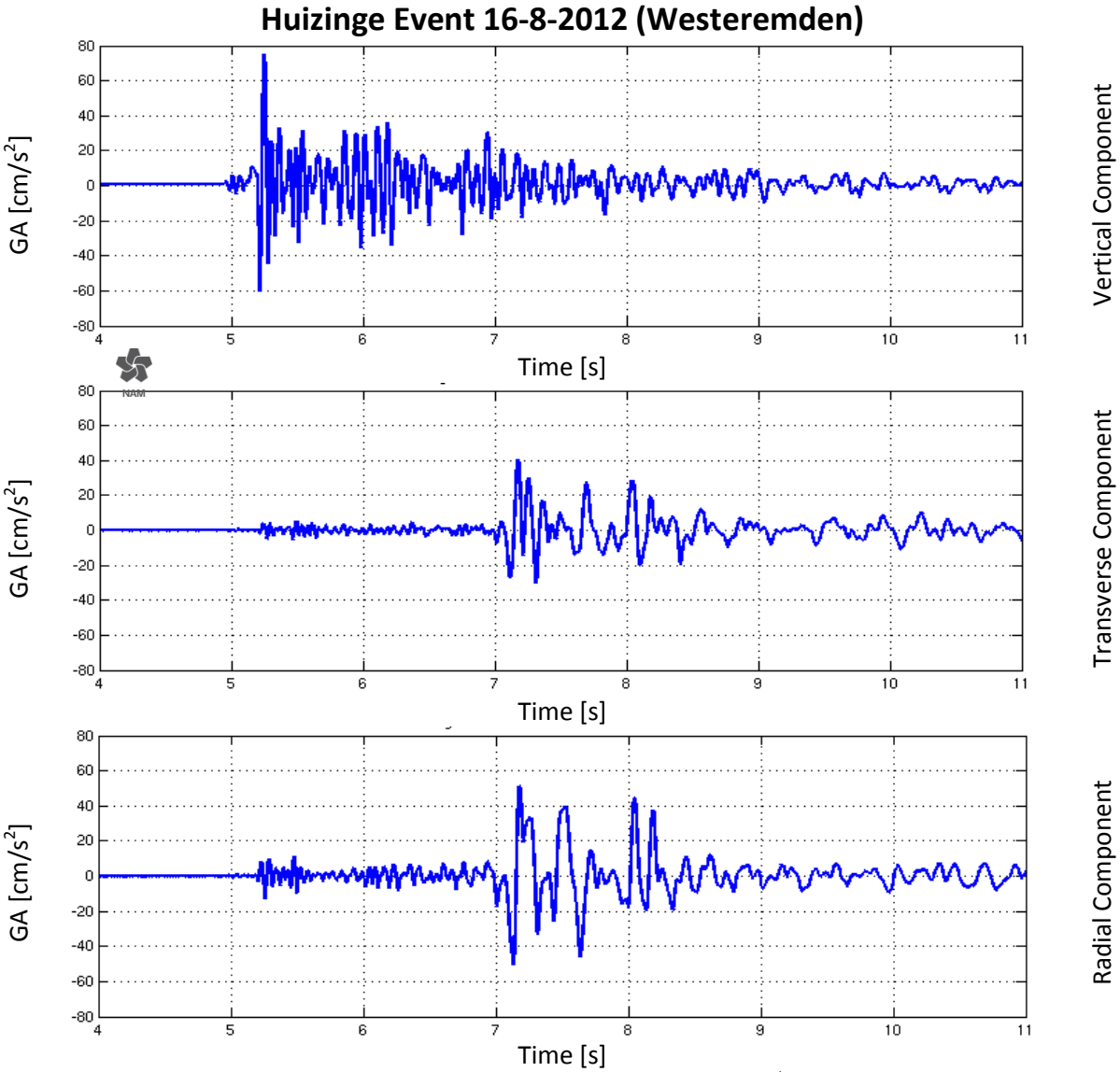

Figure 4.1 *Accelerogram of the earthquake near Huizinge recorded at the 16th August 2012 by the accelerometer located near Westeremden.*

Peak Ground Acceleration

For the probabilistic description of the ground accelerations (PGA, or generalised to Peak Spectral Acceleration, PSA) a hazard map is used. On this map for each location the acceleration is plotted that could, with a prescribed annualised probability of exceedance (exceedance level), over a

prescribed period. Hazard levels are shown using a gradual colour scale, with sometimes contours of equal hazard, i.e. PGA, added for convenience at certain intervals.

The construction of the hazard maps shown in this section requires clarification. The hazard maps shown in the section were constructed according to the following procedure. Each location in the Groningen field during the 5-year analysis period is subjected to ground motion accelerations resulting from induced earthquakes. At some locations, e.g. near Loppersum, the chance of exceeding a given peak ground acceleration threshold is higher than at the periphery of the field. Equally, at any one location, the chance of exceeding some value of peak ground acceleration decreases with increasing peak ground acceleration. A generic example of a set of hazard curves is shown for a number of locations in figure 4.2. Each declining line indicates the hazard curve for a single location in the field.

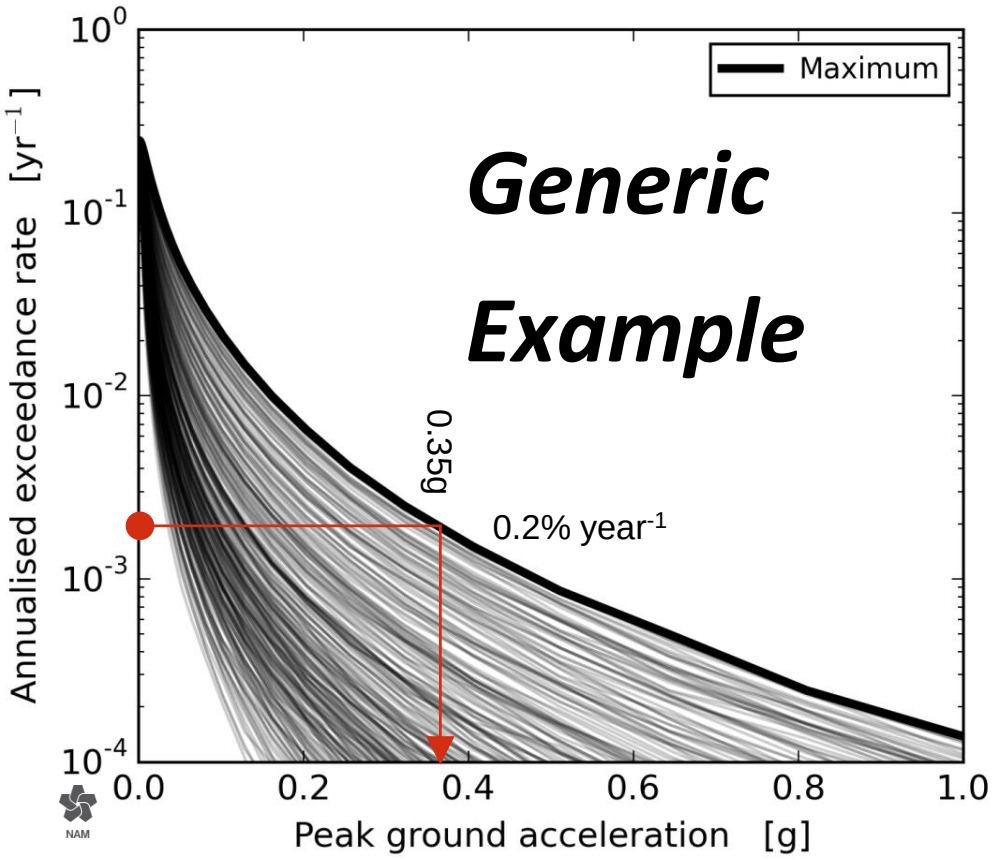

Figure 4.2 *A generic example of a set of hazard curves showing average annual exceedance rate for peak ground acceleration at different locations in the field. Each line corresponds to a location in the field. The bold line indicates the maximum PGA anywhere within the field for a given exceedance level (bounding envelope). In this generic example, the red line indicates that for an exceedance level of 0.2%/year the highest PGA in the field is 0.35g.*

To prepare a hazard map, an exceedance level needs to be chosen. This is not a purely technical choice. However, inspired by Eurocode 8[4], part of the current technical standards for structural

[4] The Eurocodes are the current technical standards for structural design in Europe, and it is now compulsory for the 28 countries in the Eurocode zone to adopt these. Eurocode 8 specifically deals with earthquake-resistant design of structures (CEN, 2006). Each country adopting Eurocode 8 must develop a National Annex to indicate how the code is implemented; the National Annex for the Netherlands is being developed. Eurocode 8 uses a standard practice to represent seismic hazard via PGA maps associated with ground motions having a 10% probability of exceedance during 50 years, equivalent to 0.2%/year for a stationary process, or a return period of 475-years.

design in Europe, it has become practice to prepare hazard maps for an exceedance level of 0.2%/year. This same exceedance level is also used by KNMI for their hazard maps and is equivalent to a 475-year return period for stationary seismicity.

Hazard maps can be made for different production scenarios. The hazard maps are shown with a topographical background. For the most important hazard maps a more detailed topographical background will be used (Figure 4.3). This allows for quick orientation of the hazard map.

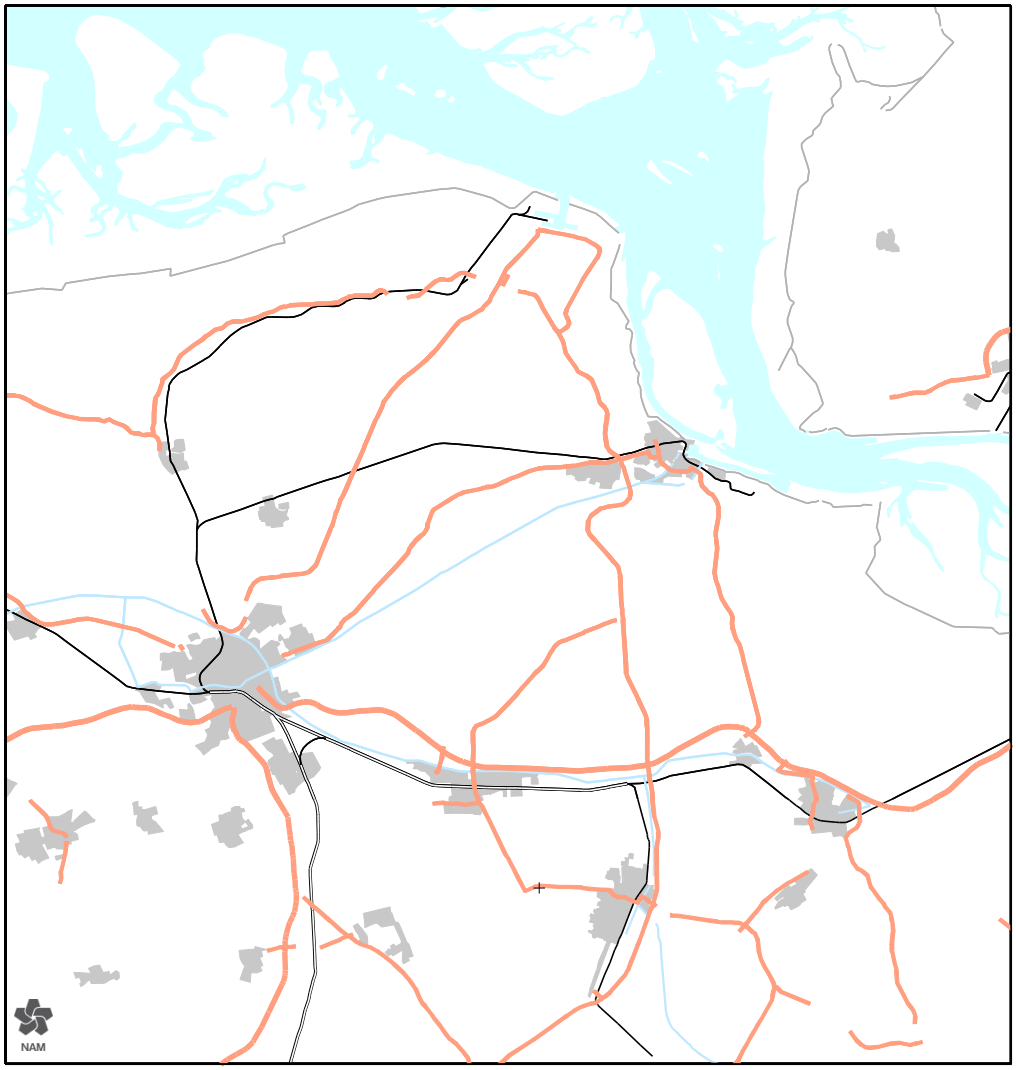

Figure 4.3 *Detailed topographical background with city limits (grey area), main roads (red lines), dikes (grey lines), the Waddenzee and Eems estuary (blue area), railways (black lines) and waterways indicated (blue lines).*

For the hazard maps shown as sensitivities, a simplified topographical background will be used (Figure 4.4).

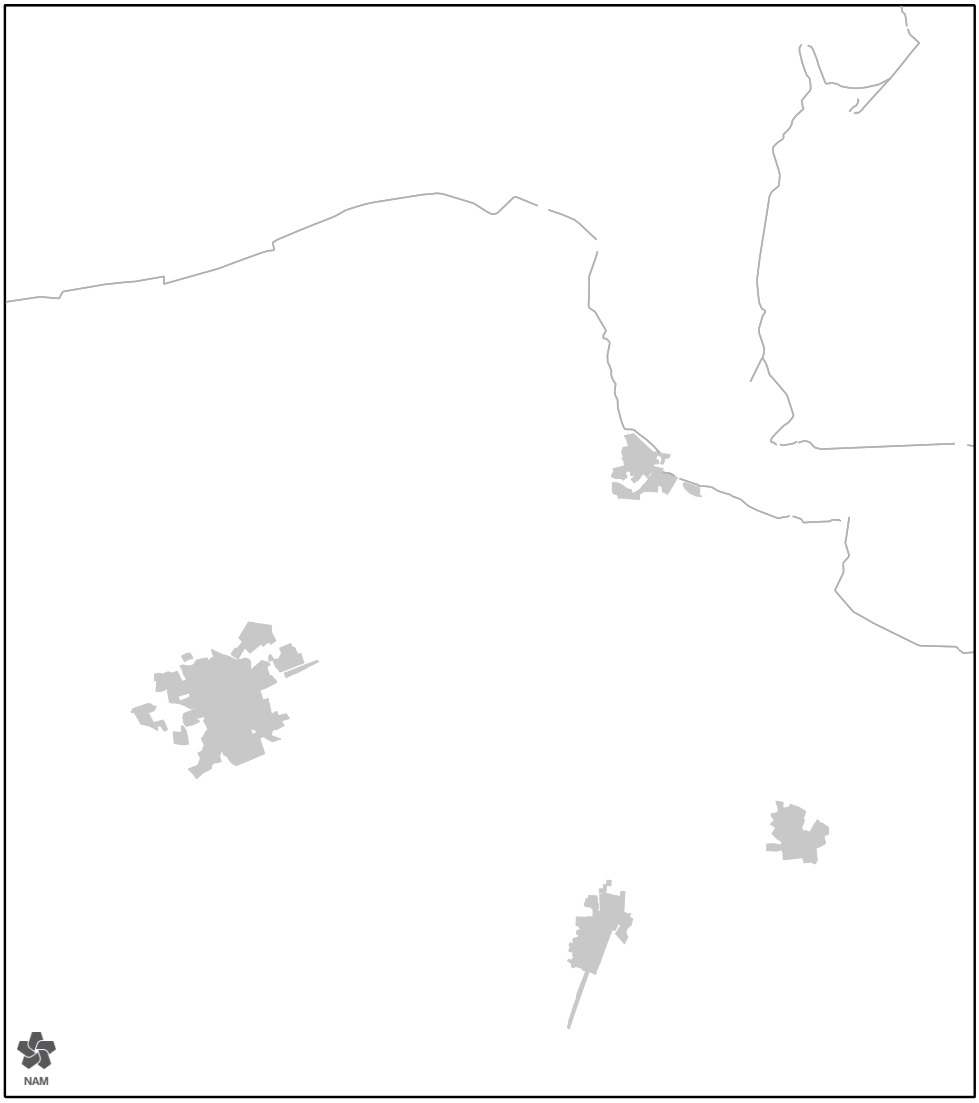

Figure 4.4 *Simplified topographical back ground with city limits of main urban centres (grey areas) and coast line (grey lines) indicated.*

Probabilistic Hazard Assessment

Seismic Event Rate and Moment release with time

Starting at the first step of the causal chain, from gas production via the resulting compaction, seismicity can be assessed. Seismicity is interpreted in this context as the event rate density of earthquakes larger than M ≥ 1.5. This minimum earthquake magnitude of M = 1.5 corresponds to the minimum magnitude of an earthquake which the historically installed geophone network is able to record without fail (independent of its hypocentre or day/night timing). Earthquakes with smaller magnitude could potentially have occurred unnoticed, because the signal could not be distinguished from the background noise.

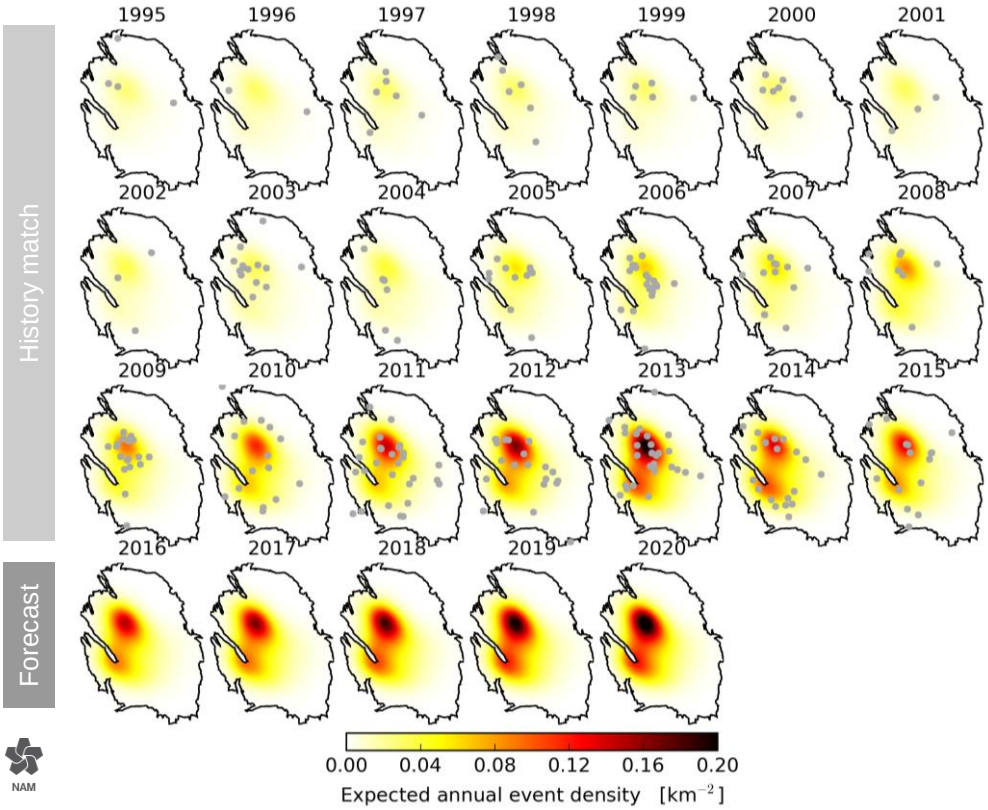

Figure 4.5 Annual M ≥ 1.5 event density maps for a production plan based on 33 bcm/year.

Figure 4.5 shows the recorded seismicity since 1995 and the expected event density maps for the period from 2016 to 2020, according to the base case production scenario (33 bcm/annum, with the regional production caps maintained). Expected event density maps for the period from 2016 to 2020 for all three production scenarios are shown in figure 4.6.

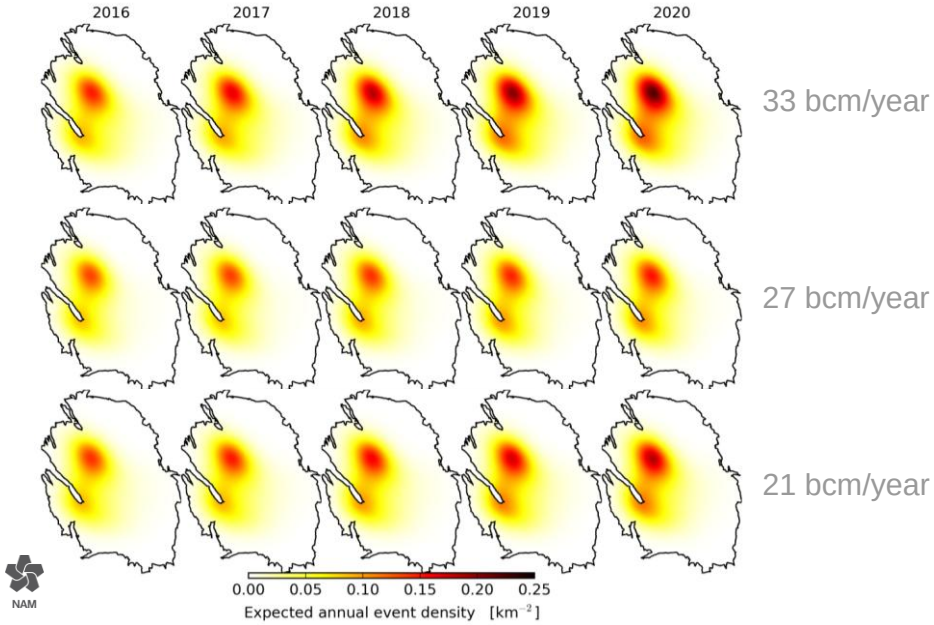

Figure 4.6 *Annual M ≥ 1.5 event density maps for different production scenarios. Annual production rates have been indicated to the right.*

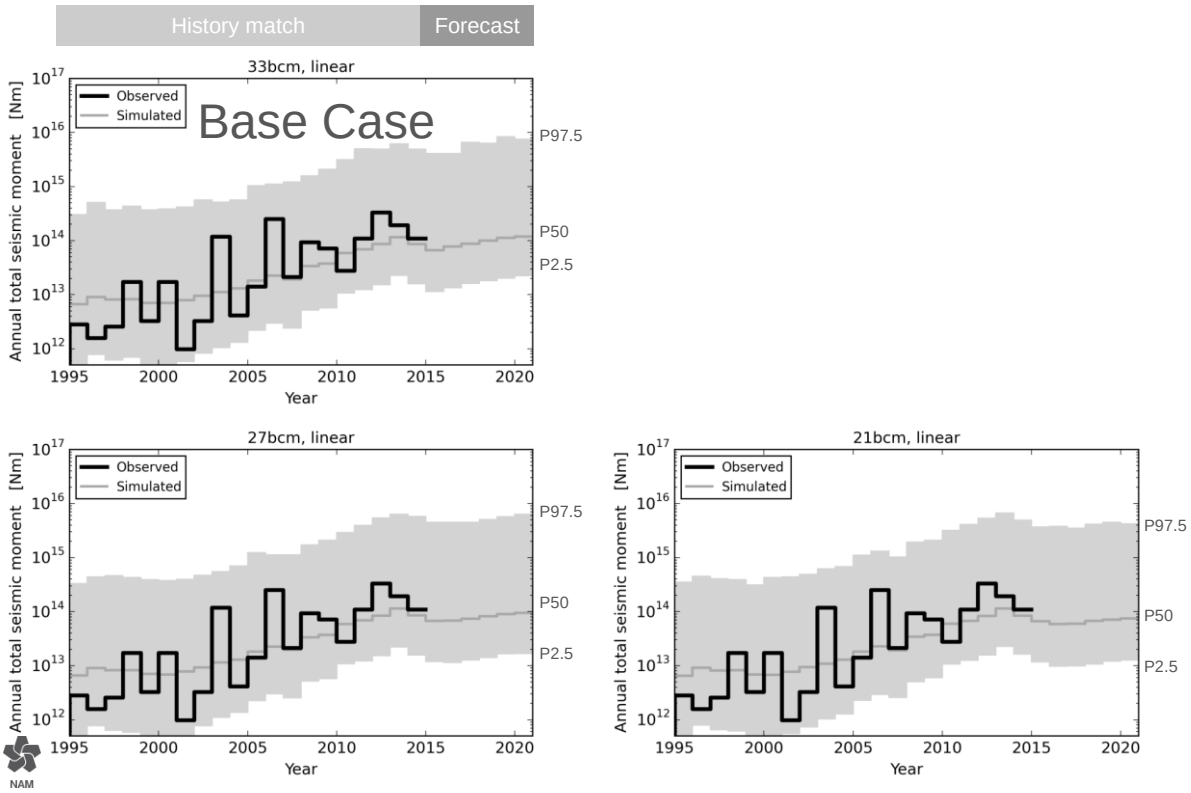

Figure 4.7 *Total annual seismic moment time series including aftershocks.*

The development of the annual total seismic moment released by these seismic events over time is shown in figure 4.7. Over the period from 1995 to 2015, the results of the Monte Carlo simulation and the observed annual total seismic moments are shown. The observed annual total seismic moment fluctuates around the median values of the simulated annual total seismic moments remaining within the grey uncertainty band (the 95% confidence interval), indicating the model is well calibrated. For the period 2016 to 2021, the forecasted annual total seismic moments and their

confidence intervals are indicated. For all three production scenarios, the median annual total seismic moment is forecast to remain in the same range as the actual seismic moment in the period 2012 – 2015.

Ground Acceleration incorporating Site Effects

The effects of the local shallow subsurface and soils on ground acceleration can be incorporated by subdividing the Groningen field area in smaller areas, based on the observed variability in subsurface composition.

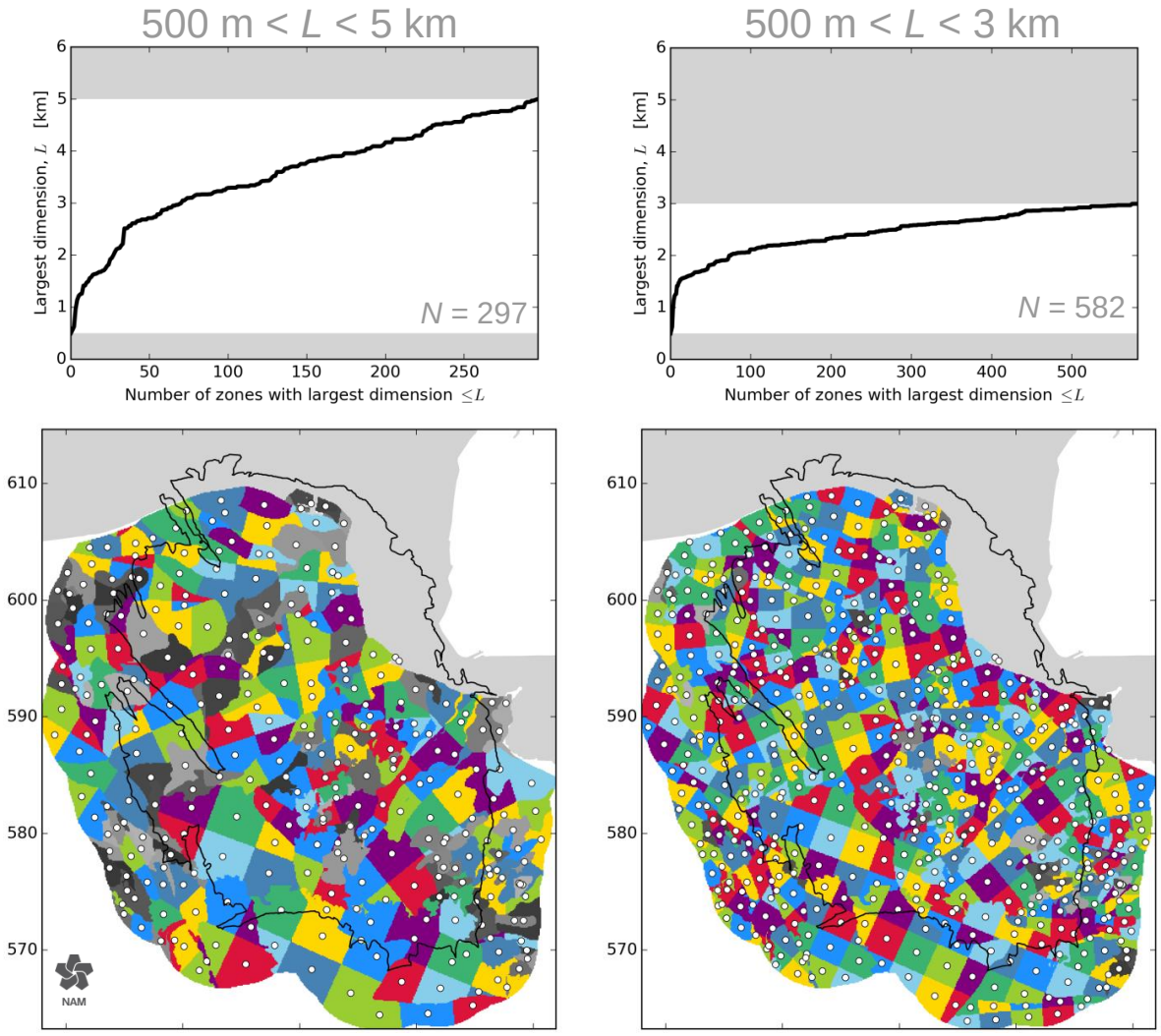

Figure 4.8 *Zonation of the near-surface amplification of ground motion is represented by an irregular grid to honour the mapped geological boundaries: Left zonation with 300 zones. Right zonation with 500 zones. Note that colours do not represent any geological property but are randomly assigned to illustrate the topology of the grid.*

Irregularly shaped zones were chosen to represent the complex local geological features in the shallow subsurface such as channel infills and peat areas, as realistically as possible. This causes an additional computational challenge, but leads to an improved result. Figure 4.8 shows different zonation options. A sensitivity analysis comparing the results from using the two zonation schemes motivated the use of the zonation scheme with some 300 different soil response areas.

Previous simulations of the acceleration caused by a single earthquake resulted in concentric PGA contours. In the current update of the hazard assessment, the effect of the soft soils is visible in the PSA map for a spectral period of 0.3s.

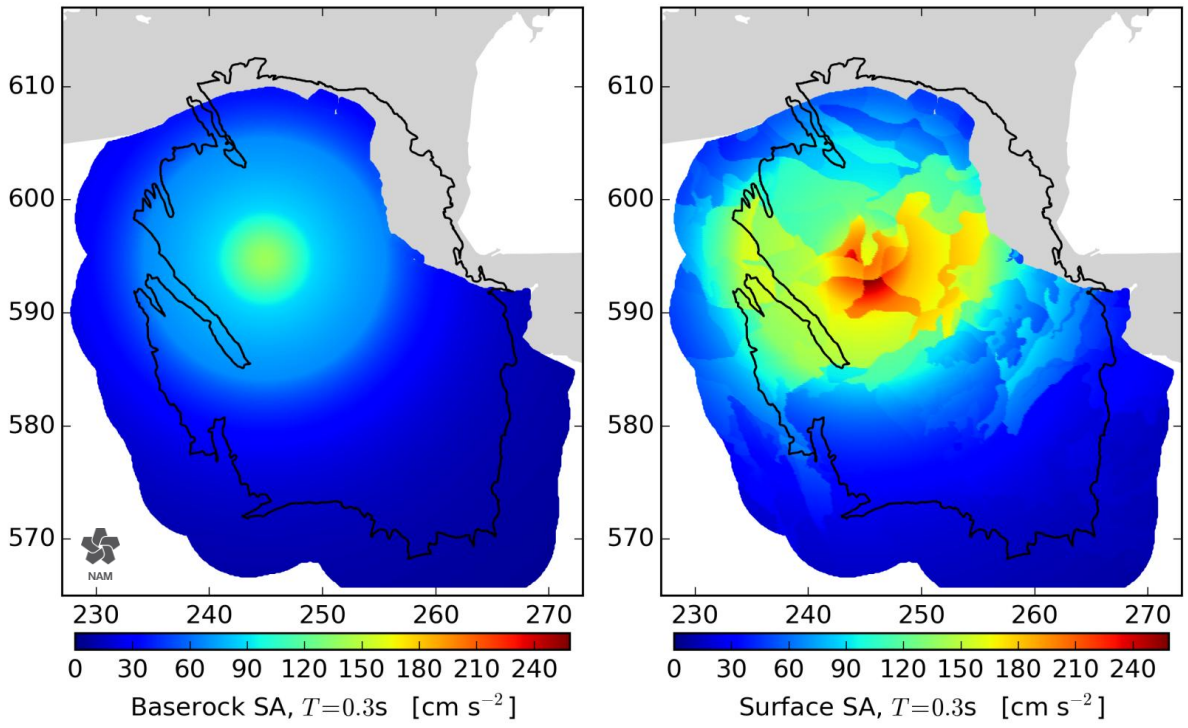

Figure 4.9 Ground motion spectral acceleration (SA) prediction. Example for M = 5

This effect is most clearly shown by comparing the PSA map at the base rock interface (Base Upper North Sea; NU-B) with the PSA map at surface. Figure 4.9 shows on the left the concentric pattern of the PSA at the Base Upper North Sea at some 350 m depth. The right-hand map shows the PSA at surface with the irregular imprint of the local soils, and the highest simulated PSA away from the earthquake epicentre.

Hazard Assessment

The impact of lateral heterogeneity in composition of the shallow subsurface is less apparent when the effects of the multiple earthquakes in the evaluation period (2016-2012) are combined in a single hazard map. Figure 4.10 shows the update of the hazard map of November 2015. This map is the outcome of the mean of the full logic tree (Ref. 5).

A comparison of the hazard map from the Hazard Assessment issued in May 2015 and the latest hazard map of November 2015 is shown in Figure 4.11. The maps in this comparison were prepared for the base case production scenario of 33 Bcm/annum. On the left the hazard map of May 2015. At the top right the new Ground Motion Prediction Method is used to show the impact of the heterogeneous soil. The mean hazard map for the full logic tree is shown at the bottom right.

These new hazard maps are also shown as an overlay on the surface topography in Figure 4.15 (Mean over the full logic tree). For the period 2016-2021, the maximum PGA at a 0.2% year^{-1} chance of exceedance (using the full logic tree) is smaller than 0.27 g.

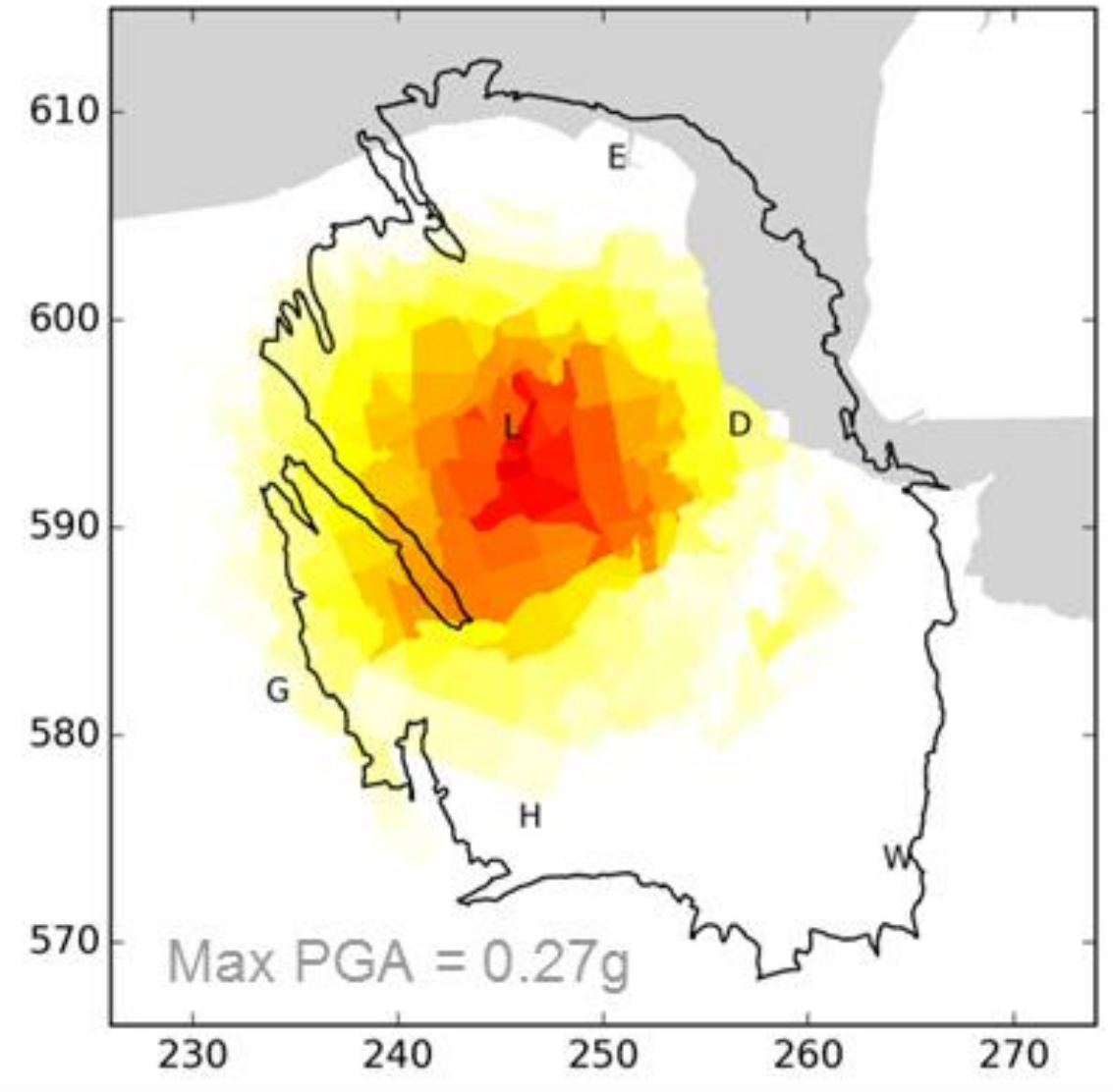

Max PGA = 0.27g
2016/1 – 2021/1

Figure 4.10 *PGA hazard maps Period: 2016 – 2021, Production: 33 bcm/year, Compaction: Inversion, Activity* Rate Model: Version V2, 3.5≤M≤6.5, Metric: 0.2% year^{-1} chance of exceedance (10% chance in 50 years). *M*ean hazard from logic tree.

GMPE V1 (Mean)
May 2015

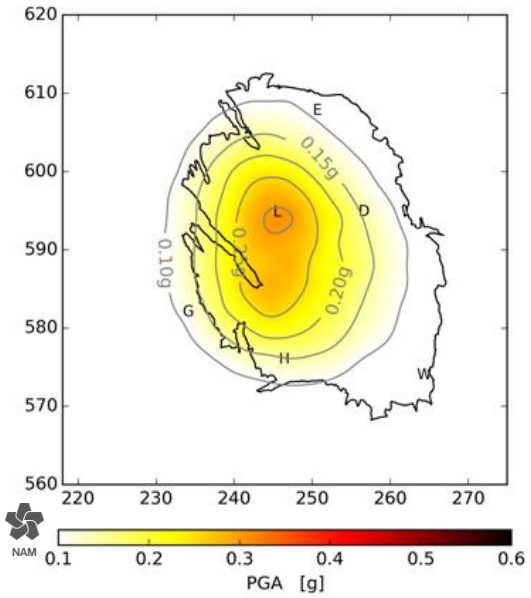

Max PGA = 0.31g
2016/7 – 2021/7

GMPE V2 (Mean)
November 2015

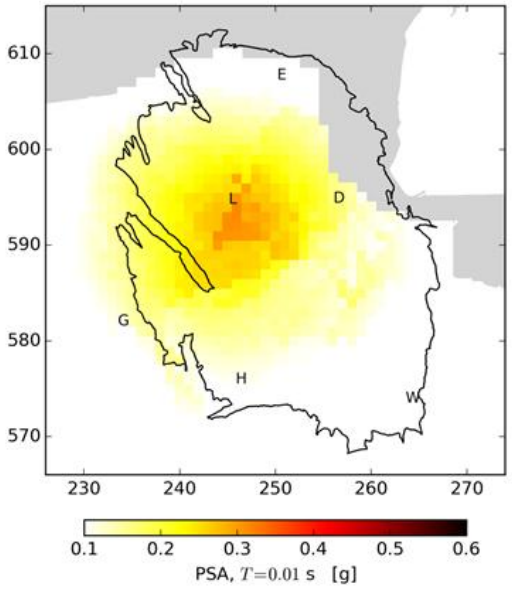

Max PGA = 0.316g
2016/1 – 2021/1

Logic tree V2 (Mean)
November 2015
Complete Assessment

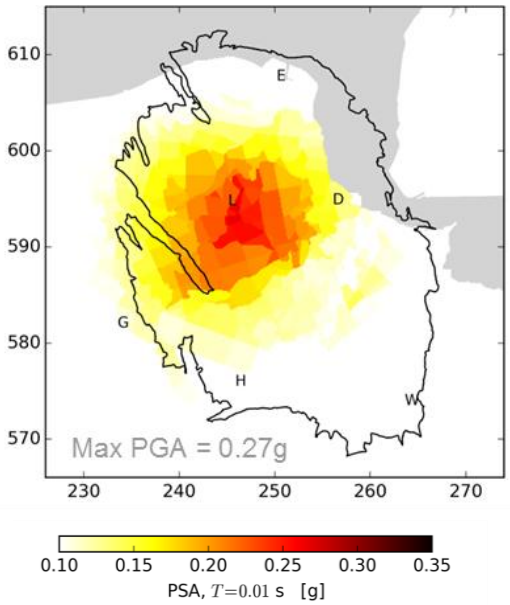

Max PGA = 0.27g
2016/1 – 2021/1

Figure 4.11 *PGA hazard maps Period: 2016 – 2021, Production: 33 bcm/year, Compaction: Inversion, Activity* Rate Model: Version V2, 3.5≤M≤6.5, Metric: 0.2% year^{-1} chance of exceedance (10% chance in 50 years). Three Hazard Maps are shown: Top Left: GMPE Model: Version V1 (Mean), Top Right: GMPE Model: Version V2 (Mean) and Lower Right: mean hazard from logic tree. For the update of November 2015 spectral acceleration at short period (T=0.01S is shown as this represents maximum PGA.

The question which earthquakes have the largest impact on the hazard assessment was studied through a disaggregation of the hazard. Two disaggregations are shown; one for the hazard in the Loppersum area (Fig 4.12) and one for the city of Groningen (Fig. 4.13).

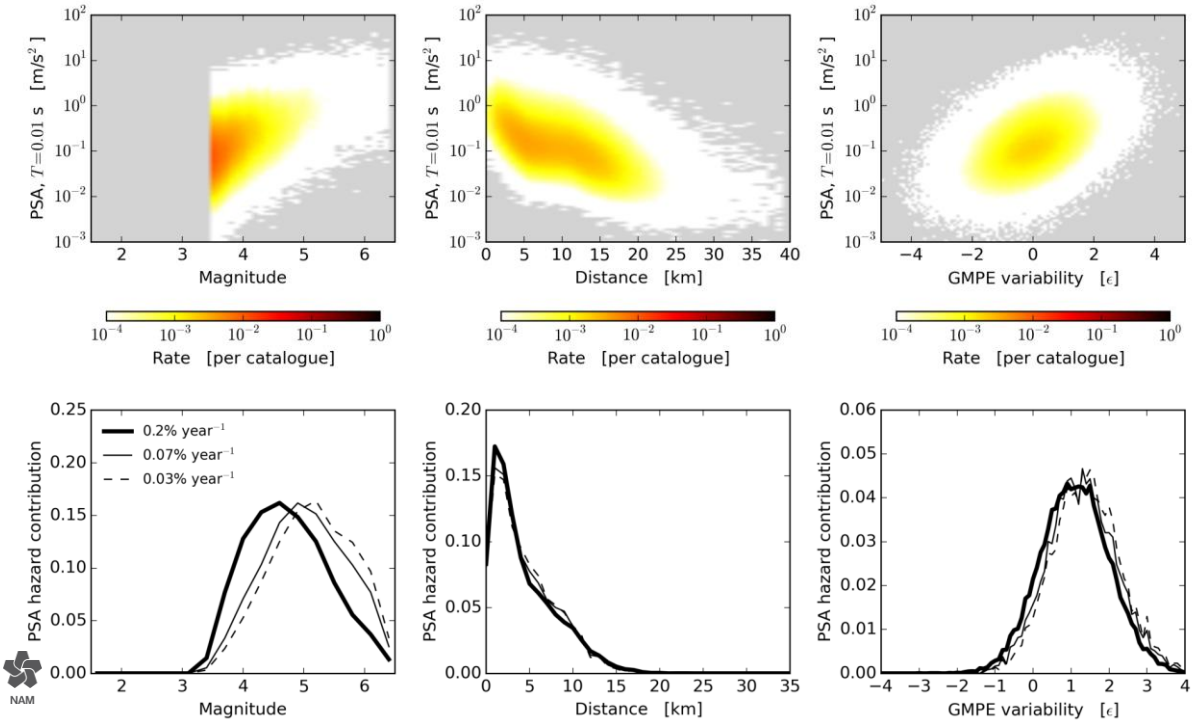

Figure 4.12 PGA hazard disaggregation (1) Period: 2016/1 – 2021/1, Production: 33 bcm/year, Compaction: Inversion, Activity Rate: V2, 3.5≤M≤6.5, GMPE: V2 (Mea n) Location: Loppersum.

The disaggregation of the hazard for the Loppersum area shows that the largest contribution to the hazard is from earthquakes within the Loppersum area (small distance of less than 5 km away with a magnitude ranging from 4 to 5). In contrast the largest contribution to the hazard in the Groningen city is from earthquakes with an epicenter approximately 10 km away from the city (towards the Loppersum area). To cause significant ground acceleration in the city of Groningen, these earthquakes located further away need to have a larger magnitude to cause similar ground motions.

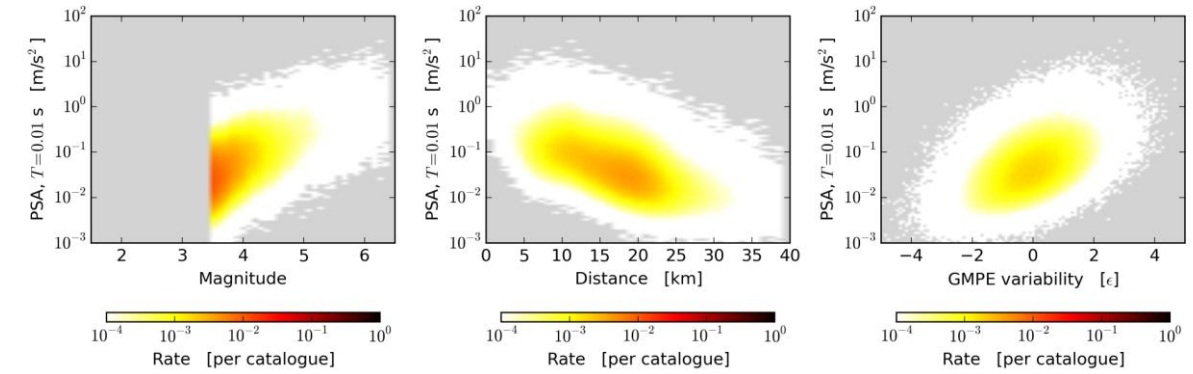

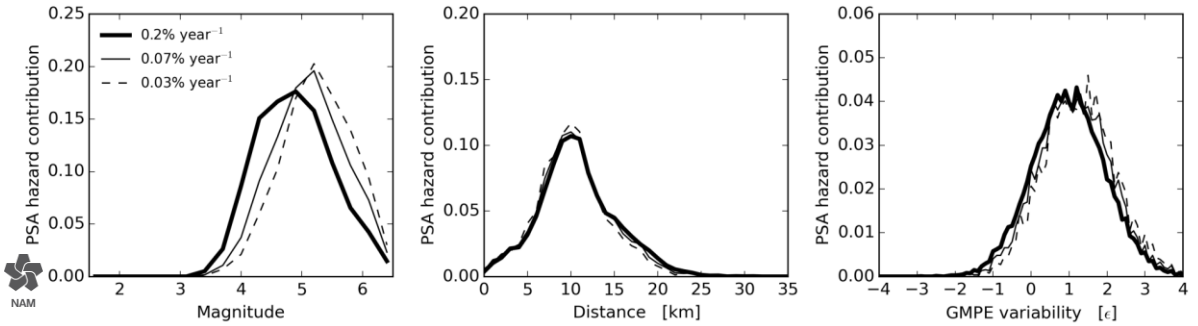

Figure 4.13 *PGA hazard disaggregation (1) Period: 2016/1 – 2021/1, Production: 33 bcm/year, Compaction: Inversion, Activity Rate: V2, 3.5≤M≤6.5, GMPE: V2 (Mean) Location: City of Groningen. The ε refers to the local GMPE variability.*

Sites with poor site response (ε≥0) contribute most to the hazard for the Loppersum area and the city of Groningen, with the largest contribution for ε=1.

Sensitivity of the Hazard Assessment to Production

Hazard maps have been prepared for all three production scenarios for the period from 1/1/2016 to 1/1/2021 (Figure 4.14). These maps show that for an 18% reduction in production (from 33 to 27 bcm/year), the maximum PGA hazard is reduced by 4%. For a 36% reduction in production (from 33 to 21 bcm/year) the reduction in the maximum PGA hazard is 18%.

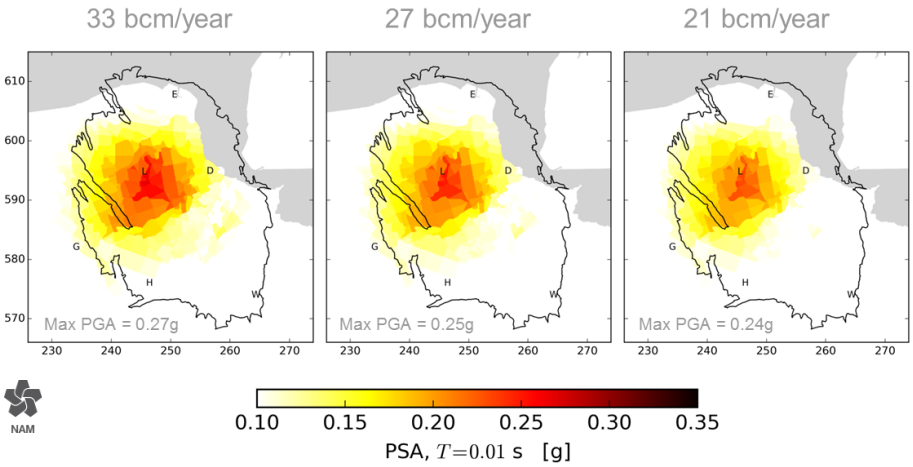

Figure 4.14 *Mean PGA hazard sensitivity to production rates. Period: 2016/1 – 2021/1, Production scenarios: 33, 27, 21 bcm/year, Compaction: Inversion-linear, Seismological model: V2, M≥3.5, GMPE: V2 Metric: 0.2% year^{-1} chance of exceedance (equivalent to 10% chance in 50 years)*

Hazard Summary

The soil effects have been incorporated in the Hazard Assessment providing an improved site specific hazard indication. Hazard Assessment over 5 year period 2016 to 2021 shows a maximum PGA≤0.27*g* for mean (based on logic tree) and an exceeedance probability of 0.2%/annum.

Hazard sensitivity to production:

- A 18% reduction of production from 33 Bcm/annum to 27 Bcm/annum reduces the maximum PGA by 4%.
- A 36% reduction of production from 33 Bcm/annum to 21 Bcm/annum reduces the maximum PGA by 18%.

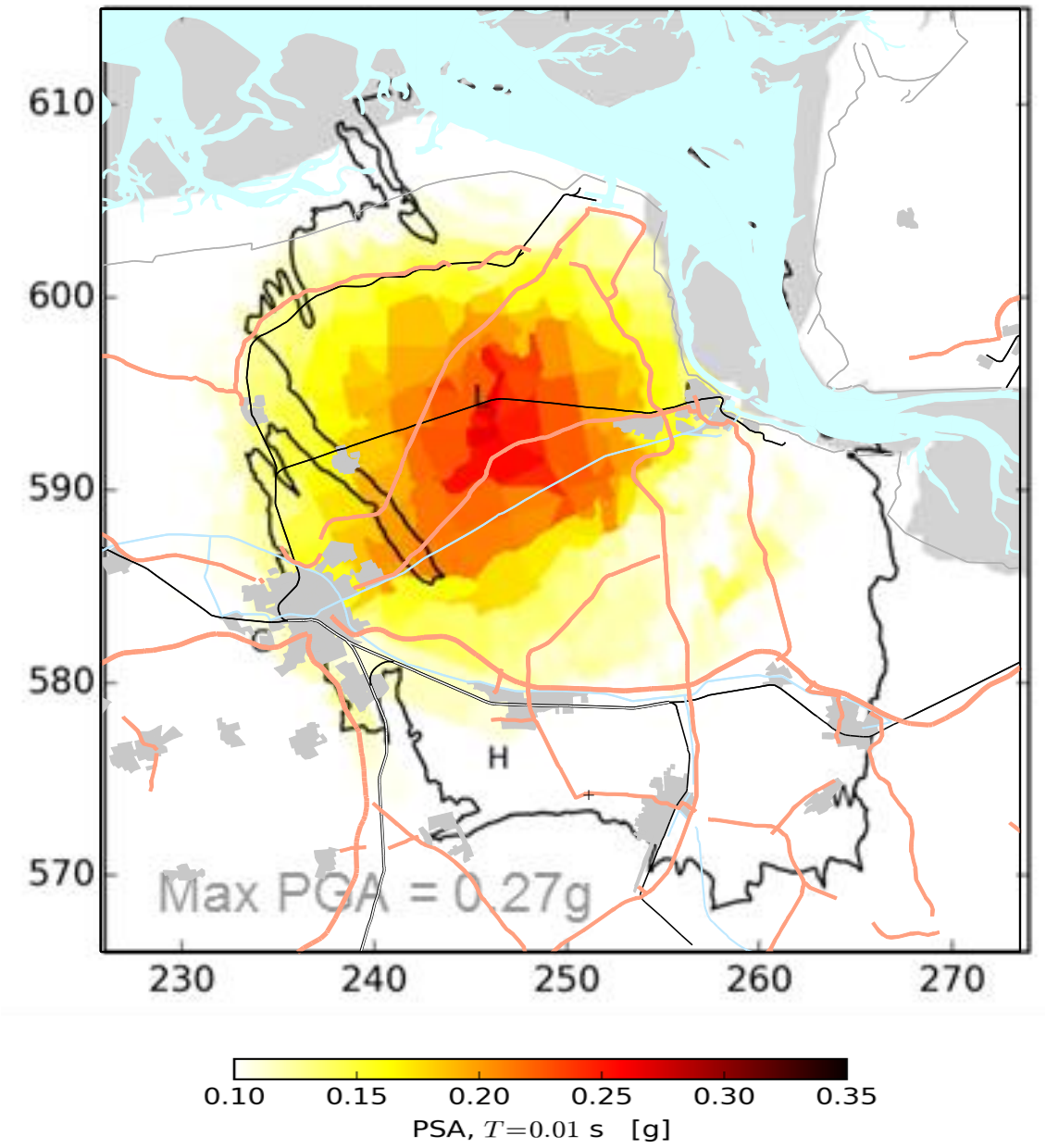

Figure 4.15 PGA hazard maps Period: 2016 – 2021, Production: 33 bcm/year, Compaction: Inversion, Activity Rate: V2.

5 From Hazard to Risk

For the assessment of risk due to induced earthquakes, the resilience of buildings to seismic action needs to be understood, since it is damage to buildings and infrastructure that impacts financial loss and building collapse that impacts people's safety (in case of injuries or fatalities). Buildings in the area were constructed throughout the 20th and 21st century without anticipating earthquake induced loads. NAM therefore had to investigate the level of resilience to seismic action (or in other words the fragility) of the buildings in Groningen. Most knowledge of the response of buildings to seismic action stems from buildings located in regions with known tectonic seismic activity. Buildings in those areas have been constructed with seismicity in mind, either due to an enforced building code or existing building construction practises. In order to assess seismic risk in the Groningen gas field region, two inputs are needed: the exposure of buildings and people to earthquakes, and the fragility of those buildings. The fragility assessment was based, as much as possible, on actual measurements and experiments on materials and buildings practices typical for the Groningen region.

To gather insight into and knowledge of the buildings in the Groningen field area and their response to seismic agitation, NAM initiated the following programs:

- Extensive network of building sensors installed in basements of over 300 public buildings and private houses.

Figure 5.1 Installation of a building sensor at the basement of a building.

- Program of experimental testing and modelling of building materials used in the construction of buildings in the Groningen field area. This program covers the measurement properties of older and more modern building materials, both in the laboratory and in-situ in local houses. Several laboratories cooperated to execute this program; EUcentre in Pavia, Delft University of Technology, Eindhoven University of Technology and ARUP.
- Testing of small wall assemblies (wallets) and other building elements like cavity walls and piers.
- Testing of full scale buildings typical for the Groningen field area. Especially, the shake-table tests of full scale buildings at EUcentre provide valuable information and insight. The first shake-table test was executed in September 2015 on a terraced house, built to 1970s design specifications.

The results of these tests and experiments have been shared with the NEN-NPR committee.

The main new features of the Risk Assessment incorporated since the previous assessment of 15th May 2015 are:

- Fragility curves based on an experimental program into the strength of building materials, building elements (like walls etc.,) and a test of a full scale detached house on a shake-table.
-

Monitoring Network for Building Damage

In addition to the accelerometers at the 70 geophone stations, NAM has also installed accelerometers in the foundations of buildings in the Groningen area. Initially some 200 buildings were selected. Around 20 of these were public buildings like town halls of municipalities. During 2015, additional accelerometers have been placed by TNO and currently the number of sensors installed exceeds 300. .

This accelerometer network will be used to study the relationship between ground acceleration and building damage and the effectiveness of damage repairs.

Building Selection

Through www.namplatform.nl owners could request to have a sensor installed in their building. A selection of buildings was made using the following criteria:

1. Area criteria to
    a. Achieve a good coverage of the seismically active area.
    b. High likelihood of measuring the highest accelerations based on the hazard map
    c. Proximity to geophone stations
    d. Distribution to cover different soil conditions
2. Building criteria:
    a. Achieve a good coverage of the building typologies
    b. Cover different foundations (piles versus no piles)

During the registration additional data on the buildings was collected, also on the status of the building.

Building Sensors

The vibration measurement system consists of a tri-axial vibration sensor and a central unit. The central unit is for signal conditioning (sensor conditioning, filtering) and transfer of the data to the TNO remote data centre. Based on detailed specifications, NAM has selected GeoSig as the supplier for the vibration measurement systems. Their system consists of a separate recorder and sensor (Figure 5.2) with the following specifications:

- Recorder: GMSplus Measuring System
- Sensor: AC-73 Force Balance Accelerometer

Figure 5.2 Vibration monitoring system – recorder (left) and sensor (right)

Vibration is sampled continuously at 250Hz and stored in an internal buffer. When vibration exceeds a certain threshold level (set at velocity of 1 mm/s[5]) the Data Centre is notified by sending the time of triggering. At that time logging of the event starts with a pre-trigger duration of 10 seconds. After collecting data for 20 seconds (at 250 Hz) the time traces (one per channel) are instantaneously sent to the data centre (Fig. 5.3). In addition to the communication of measurements during the events, the vibration measurement system also sends a regular 'heartbeat' containing the peak vibration velocity and acceleration over the last minute. Examples of the heartbeat signal and a recording of a seismic events are shown in figures 5.4 and 5.5.

[5] The trigger level of 1 mm/s is in the order of the strictest limits of the SBR directive () for vibration damage. Other vibration sources like traffic may cause such, or higher, levels. These levels tend not to occur often but when they do, they may be relevant.

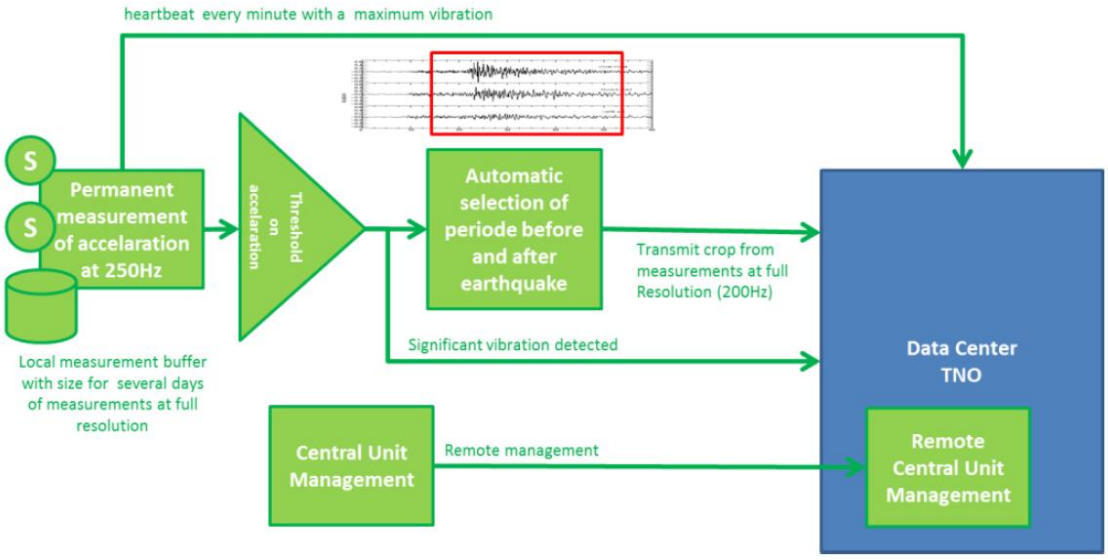

Figure 5.3 *The sensors send their data event based when the vibration level exceeds a certain threshold and send a regular (every minute) heartbeat signal with a maximum vibration.*

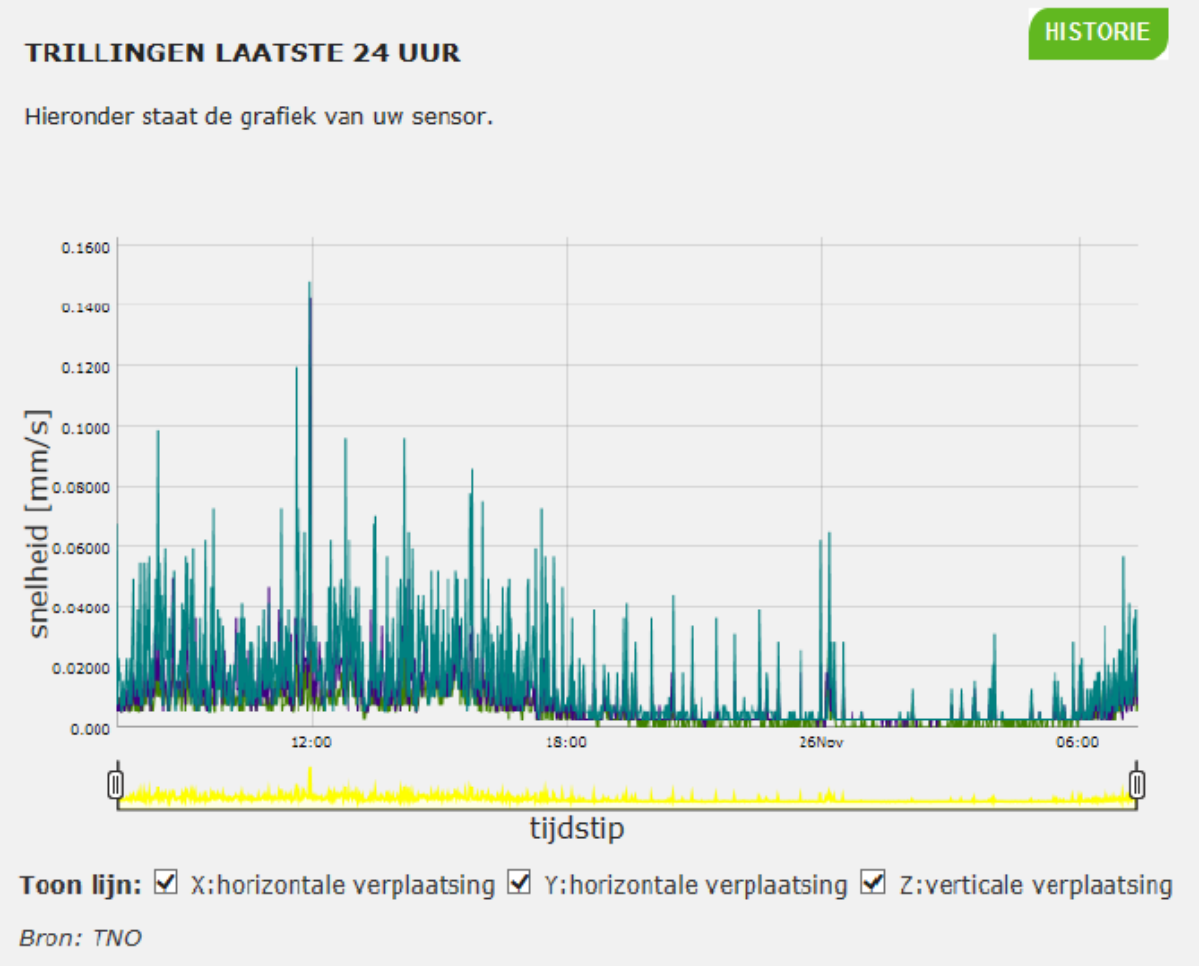

Figure 5.4 *Example of a graph with results of heartbeat measurement*

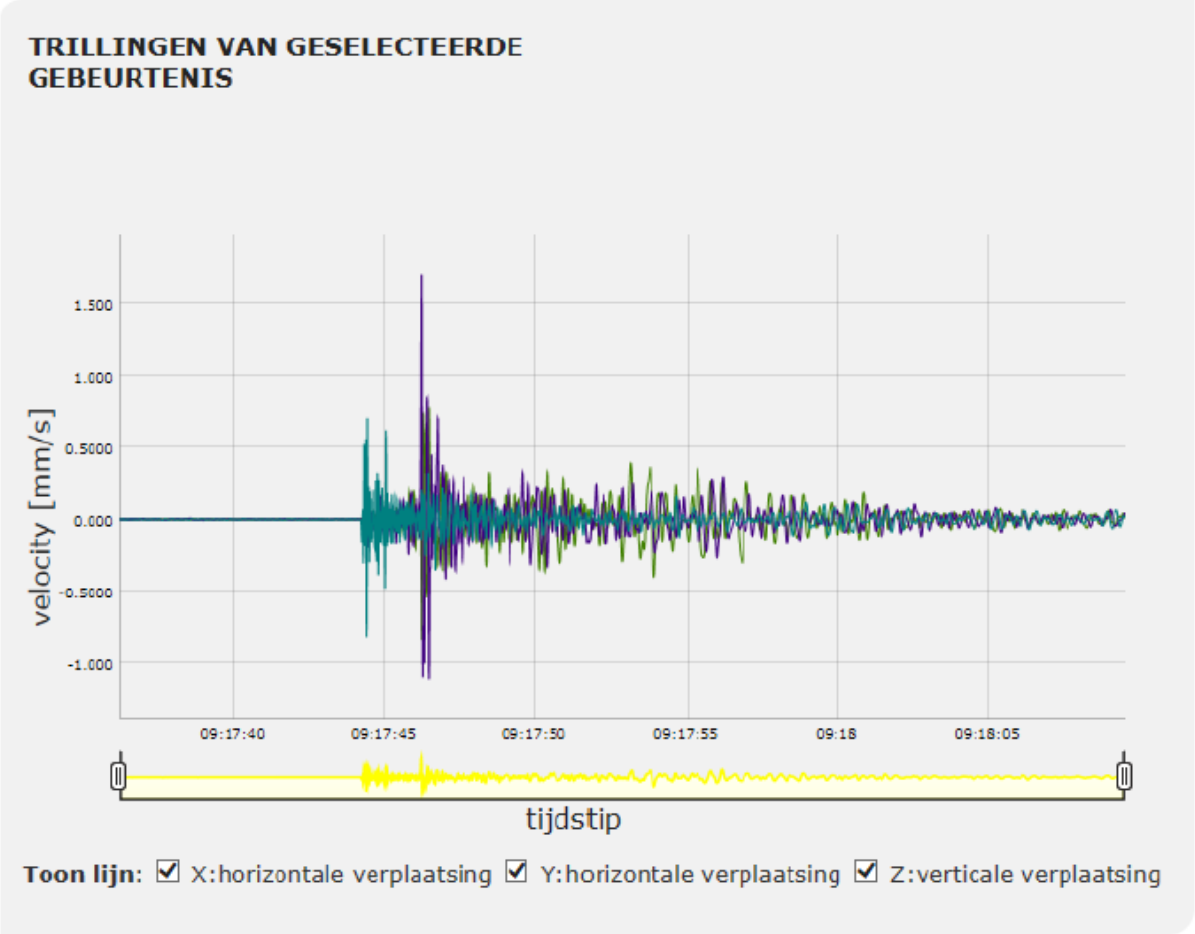

Figure 5.5 Example of a graph with results of an event

Building Inspections

To improve the understanding of the vulnerability of the buildings in the Groningen field area for damage caused by earthquake vibrations, regular building damage inspections are carried out. As part of the sensor installation, an initial inspection of damage on the outside of the building (e.g. cracks in exterior walls) is carried out. During this initial inspection, any characteristic properties of the building are logged that may be relevant for damage analysis at a later stage. After each significant earthquake a repeat inspection is carried out to establish potential additional damage caused by the earthquake.

The nature and degree of that damage is then classified in a damage category that is, in turn, related to the vibration. By plotting the measurements of all the buildings in the monitoring network against the vibration velocity, relationships can be established between the two.

Data Transmission and Communication

The total monitoring network consists of the building sensors and the TNO Vibration Data Centre, which collects and handles the measured data. Data is securely transferred from the building to this Vibration Data Centre using the own internet connection of the building.

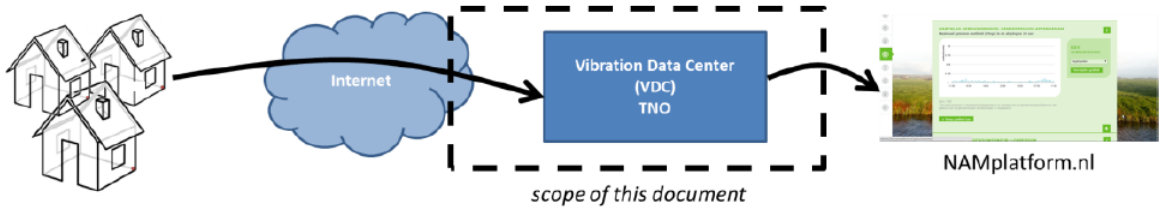

Figure 5.6 Measurements are securely transferred by making use of the household internet connection

At the Vibration Data Centre the data is analysed and sent through to NAM, where it is published at the website www.namplatform.nl. There are limitations to the level of detail at which the vibration data can be shared publicly, relating to the privacy of the house owners

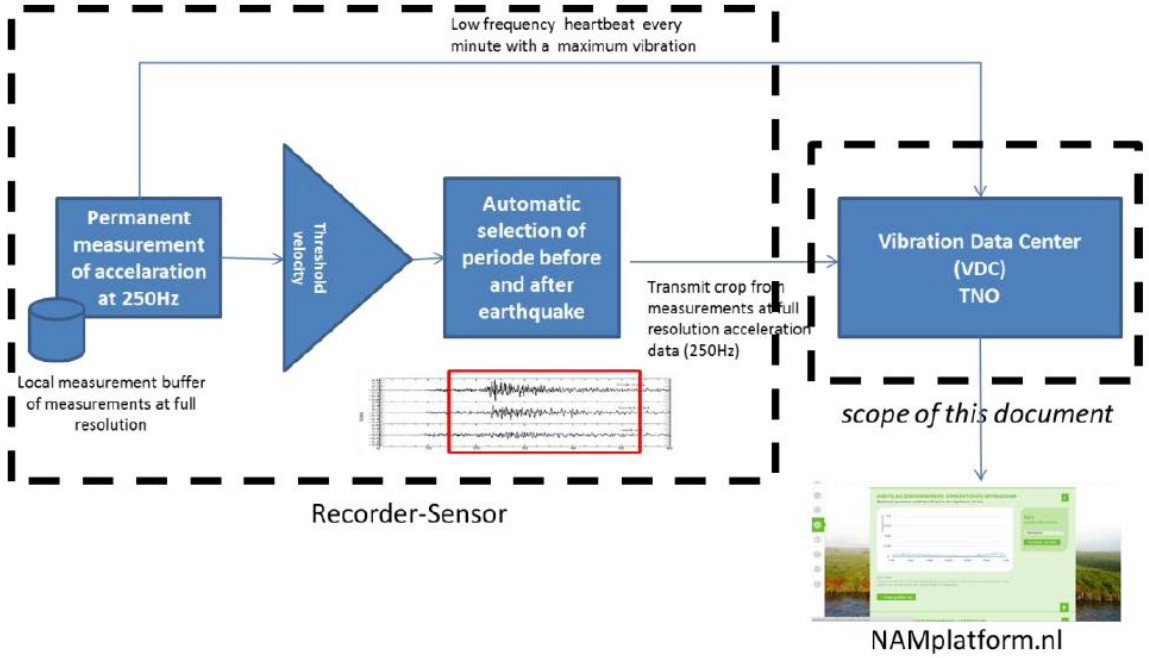

Figure 5.7 Data transfer from vibration monitoring system to Vibration Data Center (VDC)

Development and Calibration of Building Fragility

Overview of program for developing v2 fragility functions

To be able to assess the fragility of the complete building stock in the region, all buildings in the area were categorised into 65 different typologies, each typology having a specific resistance to earthquake-induced accelerations and specific usage and occupancy characteristics. Fragility curves for input to risk assessments are developed considering the building materials and practices specific for the Groningen area over the past decades and centuries.

Many of the residential buildings in the Groningen area were built using unreinforced masonry. This is a highly heterogeneous material, so these buildings were given significant attention in the Study and Data Acquisition Plan and a special work program was prepared for them. Therefore, the research into building typologies is split into masonry buildings and non-masonry buildings. The latter category includes reinforced concrete, steel and timber constructions.

Figure 5.8 Examples of some of the typical unreinforced masonry building typologies found in the Groningen region

Modelling of masonry buildings requires in-depth knowledge of the material properties manufactured and used locally, and the possibility to capture these properties faithfully in numerical models. Therefore the program to assess the fragility of masonry buildings has started with (1) a program to measure these properties through in-situ and laboratory tests, and (2) a program to validate the numerical methods by assessing the response of masonry buildings to ground shaking.

For non-masonry buildings, it has already been possible to model a large number of real buildings from the region, as reinforced concrete, steel and timber are more readily modelled with existing software that has been validated against available experimental tests from around the world [Mosayk, 2014 and 2015a]. However, to increase confidence in the response of the specific connections of pre-cast reinforced concrete buildings in Groningen, a set of laboratory tests on pre-cast connections has also been undertaken.

Following the development of numerical models and subsequent calibration through in-situ and laboratory testing on materials, connections, structural components and even a full-scale building, fragility curves that are specific to the buildings in the Groningen field area were developed. These curves provide an estimate of the probability of structural failure, given a specific level of ground shaking, and include the variability between buildings (due to different geometrical and material properties, which can be accounted for in the numerical models) and between the ground shaking characteristics of earthquakes with the same magnitude.

Calibrating numerical models with data from the field

A number of tests on masonry houses were carried out in-situ, i.e. inside the masonry buildings in the Groningen region (EUCentre et al, 2015). Geophone tests to characterise the frequency characteristics of the buildings were used to compare with the mode shapes and frequencies of vibration obtained from the numerical models of these buildings.

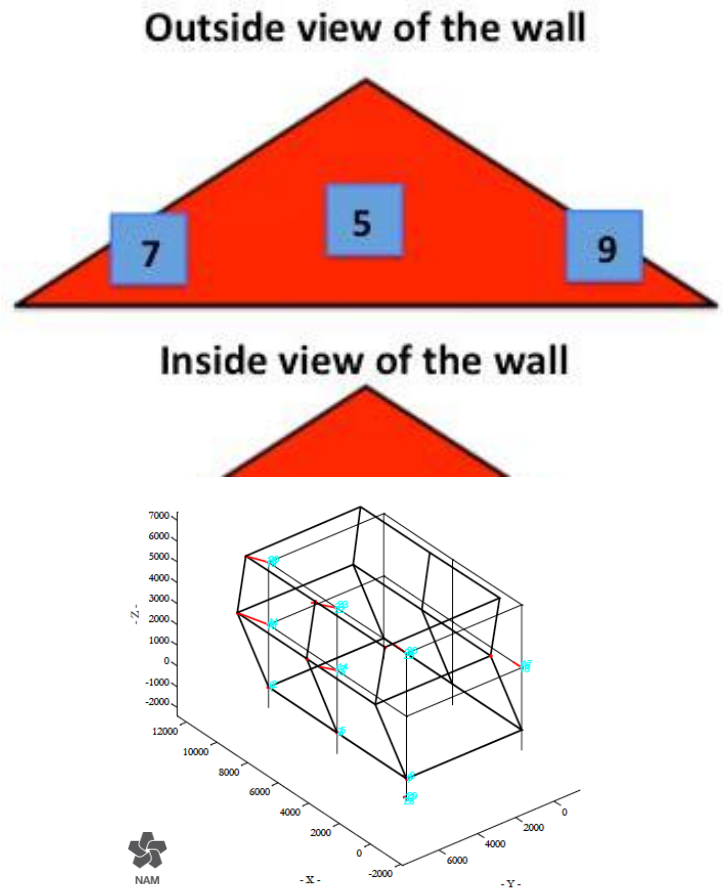

Figure 5.9 Geophones applied to a terraced masonry house to measure its frequency characteristics (EUCentre et al., 2015).

Various tests on the walls provide insight into the material properties of masonry - combining bricks of either calcium silicate or clay with the mortar that binds them together - which can then be used as input to the numerical software.

Figure 5.10 In-situ material tests on walls inside masonry houses (EUCentre et al., 2015).

Calibrating numerical models with data from the laboratory

For further calibration and testing of the numerical methods used to predict the response of masonry to ground shaking, sets of solid and cavity walls were constructed by Groningen masons and tested within laboratories in the Netherlands and Italy (EUCentre et al., 2015b).

These walls have been tested both in-plane and out-of-plane, and a number of modelling teams have attempted to predict the response of the tests (in terms of strength and stiffness of the walls, displacements at which failure occurs, crack patterns etc.) using various numerical software packages (ARUP et al., 2015). The lessons learned from the tests were then used to improve the modelling capabilities.

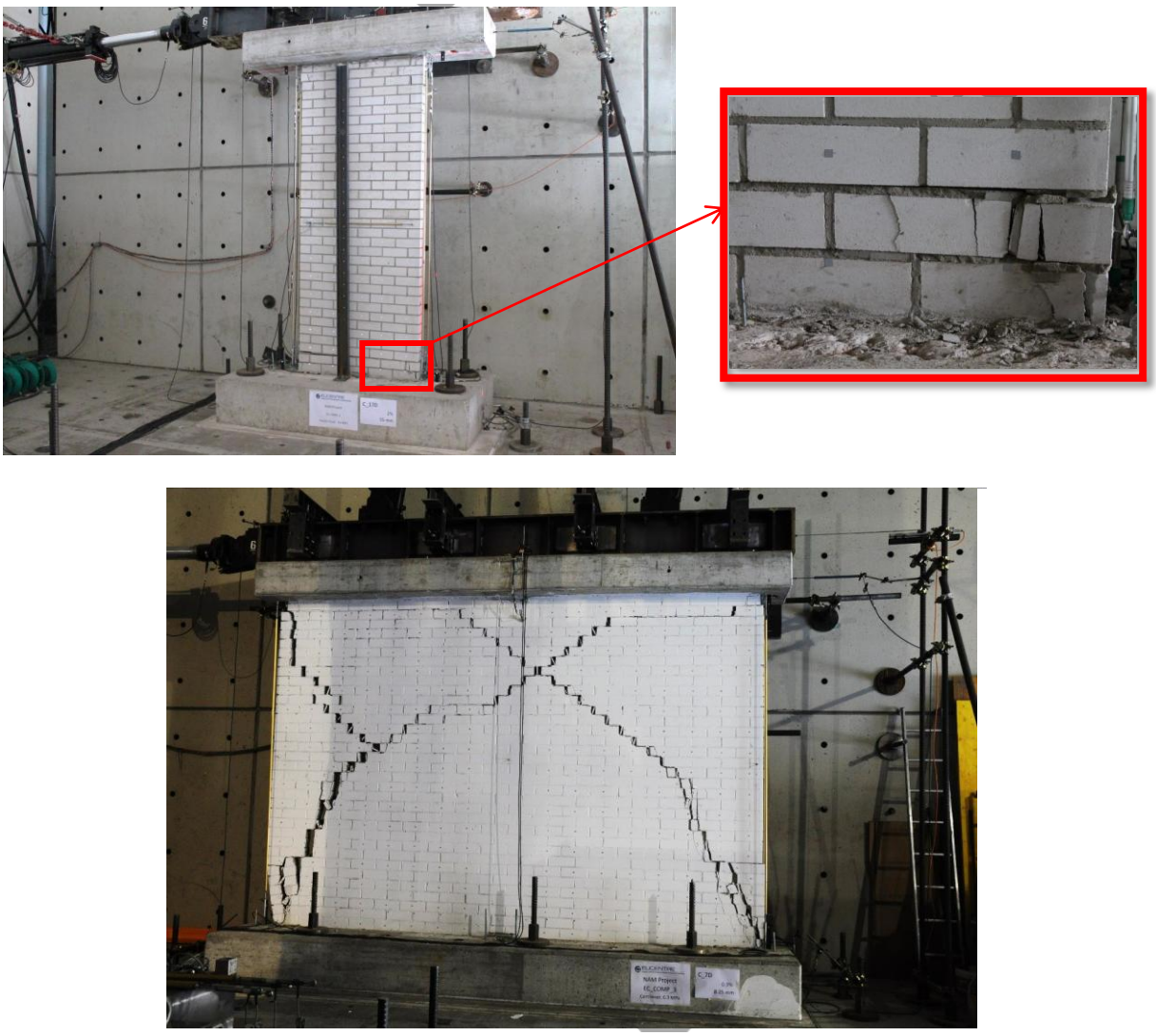

Figure 5.11 Masonry walls constructed by Groningen masons and tested in laboratories (EUCentre et al., 2015).

So far, the in-plane tests of slender walls have highlighted an important characteristic of the calcium silicate brick walls, which prove to have a much higher capability to dissipate energy than expected (modifications to the numerical models are currently being undertaken to address these differences). With regards to squat walls, comparisons with test results have indicated that current models are readily simulating the actual response of these masonry components as shown in the figure below.

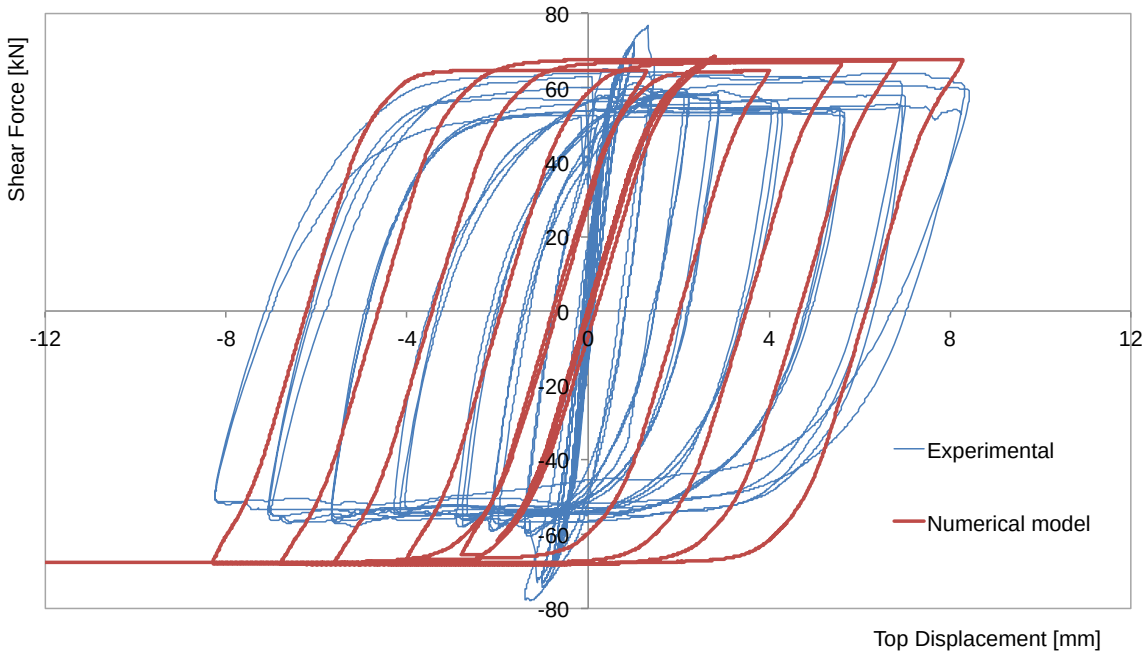

Figure 5.12 Example comparison of experimental in-plane response of calcium silicate wall and predictions by one of the modelling teams.

The results of the out-of-plane (OOP) tests on solid and cavity walls (with different numbers of ties) have also been compared with numerical models, which have also been seen to accurately predict the experimental results, as shown below.

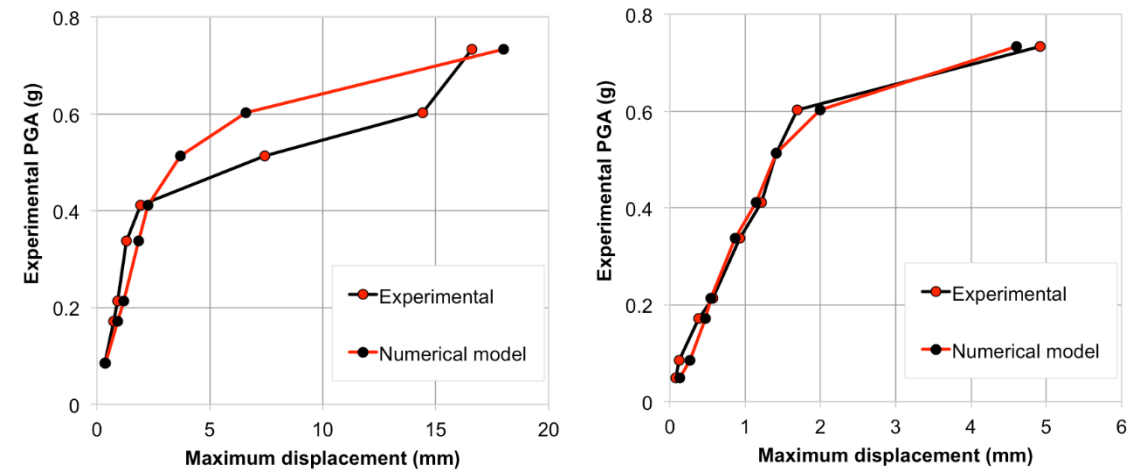

Figure 5.13 Comparisons of the predicted dynamic out-of-plane response of walls with the experimental results

A full-scale model of a terraced house (with one unit) was constructed on a shaking table by Groningen masons using local and historical materials and construction practice. This type of house was chosen as it is the most prevalent in the area. This structure has been tested by applying accelerations to the base of the structure, as would be the case during a real earthquake (EUCentre, 2015a). The accelerations have been scaled to values much higher than those that have already been experienced in the Groningen field, so that comprehensive calibration of the numerical models can be undertaken (examples of the latter are shown below). As per scientific practise the tests were stopped before collapse of the structure, in order to prevent damage to the testing facilities.

Figure 5.14 Full-scale terraced house building on the shaking table

Finally, it is noted that not only masonry structures, but also precast reinforced concrete wall panels (and their connections) were tested in the laboratory (EUCentre, 2015c), to obtain data required to calibrate numerical models. The building was subjected to several earthquakes of increasing magnitude (largest PVA was 0.34g). After each earthquake the house was visually inspected for damage and subjected to small vibrations to establish the stiffness and detect (accumulated) structural damage.

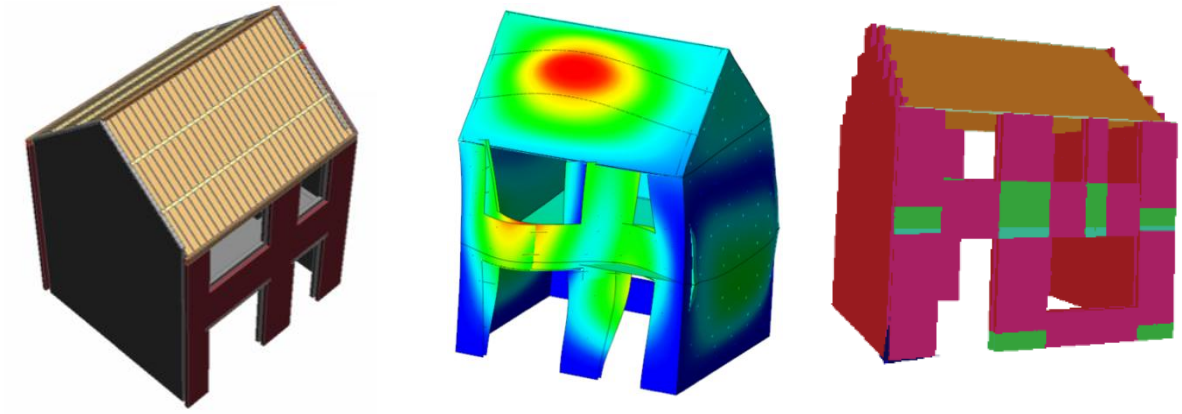

Figure 5.15. Numerical models (developed by Arup, TU Delft, Eucentre) of full-scale terraced house building tested on the shaking table

Development of v2 fragility functions

The shaking table tests provide useful data for calibrating the numerical models of masonry buildings, which can then be subjected to earthquake accelerograms with different characteristics in terms of magnitude, duration, and site amplification. Also, the models can account for the varying geometrical and material properties that are found within the actual building stock in the region, thus allowing fragility curves that are specific to the building in stock in Groningen to be developed.

Version 0 and 1 fragility functions (Crowley and Grant, 2014 and Crowley et al., 2015) were both based on nonlinear static procedures, as they needed to be developed in short timeframes, whilst the ground motion and structural modelling activities were still being developed. Instead, a move towards implementing a nonlinear dynamic procedure of equivalent single-degree-of-freedom (SDOF) (MOZAYK, 2015b) systems has been carried out for the v2 fragility functions (Crowley et al., 2015).

The first step was to calibrate hysteretic models and develop backbone capacity curves for each structural typology using the results of the calibrated numerical models of full structures, as discussed above.

In addition, the effects of soil-structure interaction (i.e. foundation-soil flexibility and damping) were also accounted for by adding springs and dashpot dampers at the base of the SDOFs, to represent the presence of either shallow foundations or piles on the different soils found within the Groningen field [Deltares, 2015].

Records that uniformly covered a range of ground shaking intensities (arising from a range of earthquake magnitudes, distances and durations expected in the Groningen field) have been identified for the nonlinear dynamic analyses, and the displacement response of each structural typology to these records has been estimated (see figure below). From this cloud of data, it is then possible to obtain the parameters that describe the fragility functions, again for each structural typology.

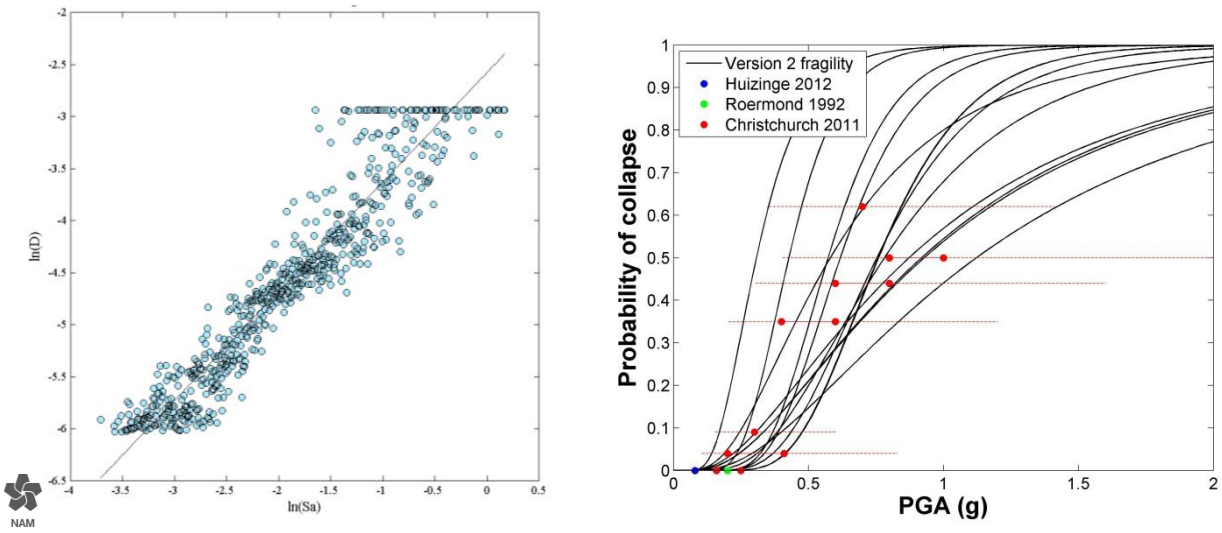

Figure 5.16 *Results of nonlinear dynamic analyses and resulting fragility functions (the latter are herein defined in terms of PGA simply for the purpose of facilitating comparison with damage data from past earthquakes that have hit buildings with characteristics similar to those in Groningen)*

Finally, history and consistency checks are carried out, comparing damage estimates obtained with the derived analytical fragility functions against the actual damage observed in past earthquakes that have hit buildings with characteristics similar to those in Groningen (including past events in the Groningen region itself).

Future plans for further calibration of fragility functions

Both the in-situ and laboratory experimental campaigns will be continued over the next months/years, and this will naturally provide opportunities for further verification and calibration of the numerical models used to develop fragility functions, as described above. A push-over test of a

simplified full scale building is planned for November 2015 at Delft University and a further shake-table test for April 2016 at EUcentre in Pavia.

Improvements for Version 2 (November 2015)

Feature	V0	V1 May 2015	V2 Nov 2015
Number of Building Typologies	94	65	56
Foundation Types	-	-	√
Soil-Foundation-Structure Interaction	-	-	√
Methodology	SDOF Non-linear Static	SDOF Non-linear Static	SDOF Non-linear Static
Intensity Measure	PGA	Spectral Acceleration (Sa) at 5 periods	Sa at 16 periods and 5–75% significant duration
Capacity of Structures	Weakest direction of URM, no out-of-plane (OOP)	Weakest direction of URM, OOP model not used in risk	Transverse and Longitudinal directions and OOP
Experimental Calibration of Analytical Models	-	-	Based on URM component tests (in-plane and OOP) shake-table test, in-situ material tests and pre-cast connection tests.

Improvements for Winningsplan 2016 (Mid 2016)

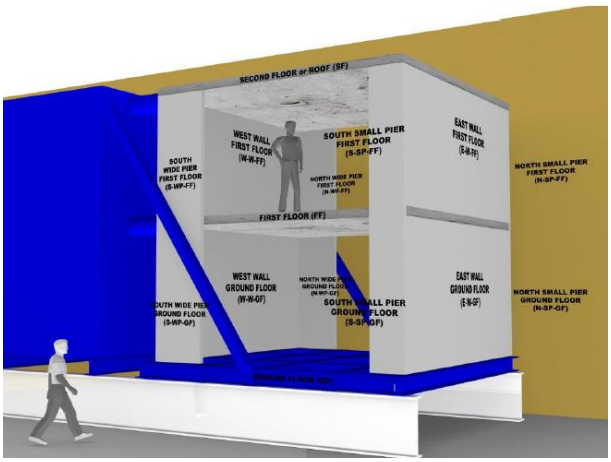

Falling Objects Risk Assessment

Introduction

The main component of NAM's Hazard and Risk assessment addresses the risk to people from the failure (collapse) of structural elements of buildings. However, it is also recognised that non-structural elements, such as chimneys, gables or parapets can fail and fall to the ground during earthquakes and cause a potential risk to people. The characteristics of falling object risk are different in nature to collapse risk. Global earthquake experience indicates that non-structural elements tend to fail at lower levels of ground motion than that which causes building collapse. On the other hand, the likelihood of fatality given failure is lower for falling objects compared to collapse, due to the relative size of the objects and since the objects mainly fall into the area outside of buildings where people are less likely to be present. Taking these factors into account, it is considered important to assess falling object risk for Groningen earthquakes.

A falling objects risk assessment is being developed for NAM by risk management consultancy TTAC Ltd and ARUP. The objectives of this risk assessment are:

1. To improve prioritisation of the structural upgrading program by providing guidance on the areas/objects which represent the highest risk (in relative terms)
2. To provide an indicative assessment of the absolute risk for different types of falling objects, to help develop a practical approach to manage the risk (defining for which objects the risk needs to be mitigated), and to give an indication of the overall falling object structural upgrading scope that may ultimately be required.

The risk assessment is not intended to provide a definitive assessment of the risk for specific objects, which first requires a site visit and detailed inspection of the object.

At the time of writing, a first version of the falling objects risk assessment has been developed, and review of the results is ongoing. This report provides an overview of the assessment methodology and preliminary conclusions. A more detailed description of the methodology and results will be published around year-end 2015.

Risk Assessment Methodology

The methodology for the falling objects risk assessment (summarised in figure 5.17) is based upon a similar approach used for the assessment of earthquake related rockfall risk in Christchurch, New Zealand, which has been peer reviewed and is being used for government decision making.

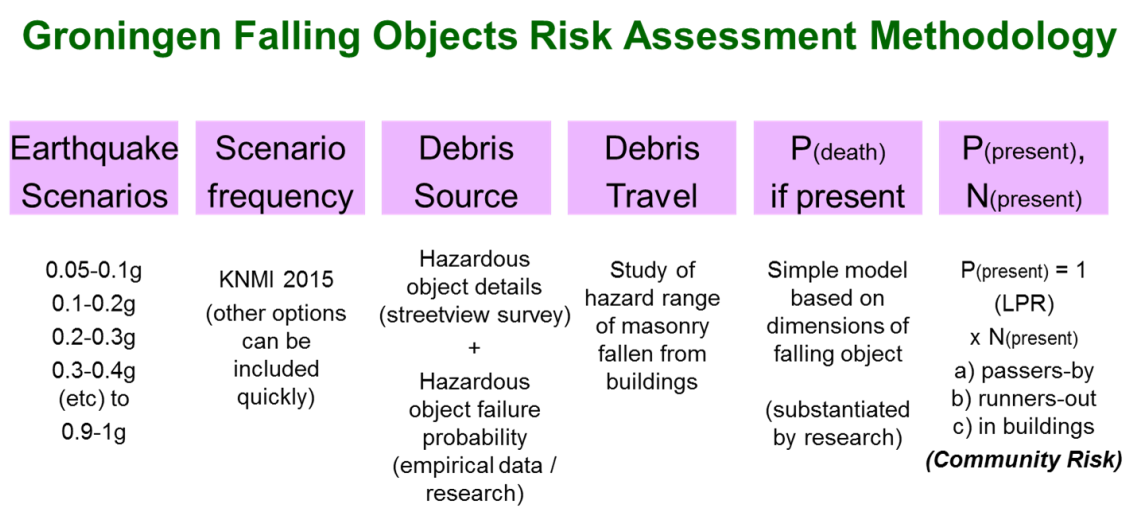

Figure 5.17 Overview of the methodology of the Groningen falling objects risk assessment

The risk assessment methodology is now described, step by step:

The first step is to define a set of earthquake "scenarios" which in combination represent the totality of all possible earthquakes. The scenarios are defined in terms of bands of PGA. Empirical data indicates a reasonable correlation between PGA and the probability of failure of non-structural elements.

Next, the frequency of each PGA band is estimated using probabilistic seismic hazard analysis (PSHA), which gives an indication of the frequency of exceedance of PGA levels for a given location. Based on schedule and availability, the risk assessment currently uses the KNMI October 2015 model, however the assessment has the flexibility to use other PSHA models if/when deemed appropriate. The consequences of earthquakes within each PGA band are then estimated, typically based on the mid-point of the band.

Estimation of earthquake consequences starts by characterising what non-structural objects have the potential to fail and fall from buildings (i.e. what "falling hazards" exist), and with what probability:

- To characterise the number and type of falling hazards in the Groningen area, a survey has been conducted in summer/autumn 2015 using Google streetview. This followed successful pilots in Bedum and Groningen city (Groningen city was included in the pilot program, due to its special character with high building density, prior to confirmation that the city needs to be included in this program.), where it was determined that using Google street view was a good method for quickly surveying a large number of buildings for falling hazards, and with a level of accuracy fit for purpose for this risk assessment (clearly a definitive survey for a specific building can only be carried out via a site visit). The survey was prioritised such that municipalities judged likely to have the highest falling object risks were surveyed first. In practice, this meant prioritising municipalities in areas with the highest PGA, and/or with urban areas with busy streets. The municipalities surveyed to date have been listed in figure 5.18 (some 100,000 buildings), and are judged to represent the majority of the falling object risk in the region. Objects in the

remaining municipalities not yet surveyed are judged to represent a relatively low level of risk.

- The probability that non-structural objects will fail and fall from buildings is based on empirical data from more than 20 worldwide earthquakes where reasonable data was available on the building damage and ground motions, and where the building stock was as similar as possible to the North European style masonry buildings found in the Groningen area. The data set includes earthquakes from Europe (including Liege 1983, Roermond 1992 and Roswinkel 1997), New Zealand, Australia, and California. The data set is used to estimate the probability of "failure" (defined as any part of the object falling to the ground) and the proportion of the object falling to the ground given failure, which tends to be greater at higher levels of PGA.

List of Municipalities surveyed to date for falling hazards (in alphabetical order)	
Appingedam	Loppersum
Bedum	Menterwolde
Delfzijl	Oldambt
Eemsmond	Slochteren
Groningen	Ten Boer
Haren	Veendam
Hoogezand - Sappemeer	Winsum

Figure 5.18. Municipalities surveyed to data using Google street view.

Next, the travel path of the debris from the object needs to be considered i.e. the at-risk area needs to be defined. This risk assessment considers both the possibility of objects falling in the area outside of buildings, and falling through the roof into a building. In the latter case, the at-risk area is defined as the entire area inside the building. For outside of buildings, the at-risk area is defined as up to 5 meters from the building façade, based on extensive research into falling masonry objects, which indicated that nearly 100% of people injured by these objects were within 5 meters of the building.

The next step is to estimate the probability of fatality for a given object falling to the ground. A simple geometric model is used to estimate the likelihood of a single person in the at-risk area being struck by the falling object (taking into account the size of the object relative to the size of the at-risk area). A simple assumption is then made that if the person is struck on the head by the object the probability of fatality is 100%. Based on research, this is a very good approximation for larger objects, while it introduces a degree of conservatism (overestimate of risk) for smaller objects.

The steps described so far allow the calculation of Local Personal Risk (LPR, see Risk Metrics section of the report for definition), by summing the risk contribution of each PGA band. However, the metric judged most appropriate to measure risk for falling objects is Community Risk, which is calculated by multiplying LPR by the average number of people present in the at-risk area. There are 3 falling object risk scenarios considered in this assessment, each requiring a different method to estimate the average number of people present:

1. Object falls through roof and impacts people inside the building
2. Object above door falls and impacts building occupants running outside of the building
3. Object falls outside building and impacts passers-by

The first two cases involve risk to residents of the building. The population data used to estimate the average number of people present inside buildings is described in the exposure database section of the report. In the 2nd scenario, assumptions have to be made regarding the likelihood of people attempting to run outside during an earthquake and being in the at-risk area beneath the door when debris falls. These assumptions are subject to significant uncertainty, although data from the Liege earthquake in 1983 provides some guidance. In the 3rd case, to estimate the number of passers-by (and therefore number of people on average in the at-risk area), "footfall" data has been obtained for some of the busiest streets in the area (primarily in Groningen city) from the research company Locatus. Streets where footfall data is not available were categorized during the Google streetview survey based on the type of street and local features likely to affect pedestrian traffic, and then footfall estimates were made for each of these categories using the Locatus data as a starting point.

Finally, the overall Community Risk for a hazardous object is calculated by summing the consequences of all PGA bands.

Preliminary Conclusions

Review of the results from the first version of the falling objects risk assessment is ongoing, and full results will be published in a detailed report around year-end 2015. In the meantime, the following preliminary conclusions can be made from the risk assessment:

- Based on the survey results to date, a total of ~110,000 potential falling hazards have been identified in ~150,000 buildings surveyed. Chimneys, parapets and gables account for ~75% of the hazards identified, with the remainder covering a variety of different types of objects.
- Masonry objects are assessed to present a higher level of risk than other types of objects, owing to their size/weight and fragility. Empirical data indicates that older masonry objects (particularly pre-WW1) are significantly more fragile than modern masonry objects.
- The location of the falling hazard relative to people is a very important factor in determining the level of risk. For objects above busy streets and doors or where the object has the potential to fall through the roof of a neighbouring building, the Community Risk tends to be 2-4 orders of magnitude higher than for the same objects above quiet streets or gardens.
- Based on the preliminary falling objects risk assessment, utilising the October 2015 KNMI PSHA, the following conclusions can be made about the prioritisation and overall structural upgrading scope for falling objects:
  - The risk assessment results generally support the current NAM structural upgrading prioritisation guidelines. Objects assessed to have higher levels of Community Risk are those that are more fragile, in areas of higher PGA, and are located above doors, busy streets, or have the potential to fall through the roof of a building. Driven by these factors, several hundred objects have been identified with Community Risk >10^{-5}, and these results will be used to help prioritise the program of building inspections.
  - Work is ongoing to define how the Individual Risk norm (10^{-5} probability of fatality per year, as recommended by Commissie Meijdam) should be applied for falling objects, and this will

ultimately determine the total falling object scope in the structural upgrading program. Based on the options available for applying the norm, the total scope is estimated to be no more than a few thousand objects, and execution of this scope is judged to be achievable within a period of 5 years.

Exposure

Exposure Database

The exposure database combines a number of existing public and proprietary datasets containing information related to the buildings and population within the affected area, with proper care to privacy regulations. The area currently extends 5 km (in all directions) from the boundary of the Groningen gas field. The datasets include:

- Basisregistratie Adressen en Gebouwen (BAG)
- AHN Actueel Hoogtebestand Nederland (Heights of buildings)
- DataLand address usage data
- CBS StatLine - Inhabitants per hectare 2014/ Education per municipality 2014/2015/ Time use data
- LISA – Landelijk Administratiesysteem Arbeidsplaatsen/ Number of jobs per category per postcode

Merging all this data into a single Geographical Information System (GIS) allows for the identification of the coordinates of each individual property (some 250,000, of which over 150,000 are regularly occupied by people) within the region and an estimate of the occupancy of each property during day and night. The database identifies individual buildings, an apartment complex is one building, but may contain several hundred addresses. By combining different datasets, the buildings are grouped into categories.

The most important characteristic for the seismic response of a building is the construction material of walls, frames and floors and the construction type of the building, the “resistive system”. This can be unreinforced masonry (URM), steel (S), reinforced concrete (RC), or wood (W). A total of 56 different building categories have been identified (Fig. 5.19). Unfortunately there is no database with construction material information for each property nor information about the foundation. Therefore this needs to be pieced together (inferred) from available data like age, usage, location and the assigned initial category as described before. This piecing together is done using inference rules defined with the help of structural engineers with many years of experience in the region, who have provided information on the local Groningen construction practices over the last century. The result of this analysis is that an individual building is assigned a probability that it belongs to a certain building typology. The sum of all the probabilities for each unique building is unity but may consist of probabilities for several building classes.

For example:

DataLand usage label “Residential” and adjacency label “semi-detached” obtained through GIS analysis of Kadaster combined with height data from AHN determines this building is a 2 story semi-detached house (and the neighbouring house seems to be a set of 3 apartments). After this first step it is fairly certain that this building is a semi-detached house but whether it has cavity walls or solid walls, wooden or concrete floors is unknown and will depend on location and age of the building and requires inference rules to be applied. Inference rules lead to a probability that the building belongs to a certain typology. For example a 40% probability of a semi-detached house with cavity walls and concrete floors, 30% semi-detached house with cavity walls and wooden floors, and 30% probability semi-detached house with solid walls and wooden floors. There are more than 250.000 buildings in the database and careful inspection inside a building is often required to get the information necessary to reliably assign the building typology. It will take time to make the database more accurate, but efforts are on-going to collect additional information from damage claims and screening reports. If home-owners and business-owners could be engaged in the process of gathering building data, the accuracy of the building database could be further increased.

Buildings in Groningen Area

No.	Use category	Material	Sub-typology	Description of lateral load resisting system	Modifier
1	Residential Detached (RESD)	URM	A	Detached house - timber diaphragms, solid walls	
2			B	Detached house - timber diaphragms, cavity walls	
3			C	Detached house - RC diaphragms, cavity walls	
4			D	Labourer's cottage - timber diaphragms, solid walls, particular shape	
5			E	Mansion - timber diaphragms, solid walls - 1+attic storeys, mansard roof	
6			F	Large URM villa - timber diaphragms, solid walls - ≥ 2+attic storeys	
7		W	A	Timber or steel frame, timber shear panels	
8	Residential semi-detached (RESS)	URM	A	Semi-detached house - timber diaphragms, solid walls	
9			B	Semi-detached house - timber diaphragms, cavity walls	
10			C	Semi-detached house - RC diaphragms, cavity walls	
11		W	A	Timber or steel frame, timber shear panels	
12	Residential terraced (REST)	URM	A	Timber floors, solid party walls, solid gable/façade walls	
13			B	Timber floors, solid party walls, cavity gable/façade walls	
14			C	Concrete floors, solid party walls, cavity gable/façade walls	
15			D	Concrete floors, cavity party walls, cavity gable/façade walls	
16			E	Mixed floors (timber ground/concrete first/timber attic), solid party walls, cavity gable/façade walls	
17			F	Nehobo or Mixed floors (timber ground/concrete first/timber attic), cavity party walls, cavity gable/façade walls	
18		RC	A	Cast-in-place (CIP) tunnelgietbouw or CIP gable/façade walls with hollow block slab (unreinforced walls may be present)	
19			B	Precast floors, Precast party/gable walls, precast walls long direction	
20	Residential apartment (RESA)	URM	A	Clay brick walls	
21			B	Calcium silicate walls	
22		RC	A	Cast-in-place (CIP) tunnelgietbouw or CIP structural walls (predominantly in one direction) with hollow block slab (unreinforced walls may be present)	≤ 4 storeys
23			A	Cast-in-place (CIP) tunnelgietbouw or CIP structural walls (predominantly in one direction) with hollow block slab (unreinforced walls may be present)	> 4 storeys
24			B	Precast structural walls	≤ 4 storeys
25			B	Precast structural walls	> 4 storeys
26	Mixed residential / commercial apartment (RECA)	URM	A	Solid walls, timber diaphragms, reduced walls at ground floor replaced with steel frame or precast columns	
27			B	Structural URM walls (predominantly calcium silicate), reduced walls at ground floor replaced with steel frame or precast columns	
28		RC	A	Cast-in-place (CIP) tunnelgietbouw or CIP structural walls (predominantly in one direction) with hollow block slab (unreinforced walls may be present), reduced walls at ground floor, replaced by RC frame	≤ 4 storeys
29			A	Cast-in-place (CIP) tunnelgietbouw or CIP structural walls (predominantly in one direction) with hollow block slab (unreinforced walls may be present), reduced walls at ground floor, replaced by RC frame	> 4 storeys
30			B	Precast structural walls with reduced walls at ground floor, replaced by precast columns	≤ 4 storeys
31			B	Precast structural walls with reduced walls at ground floor, replaced by precast columns	> 4 storeys
32	Agricultural, industrial and large commercial (AIC)	S	A	Steel braced frame (w/ and w/out basement)	
33			B	Steel portal frame one direction, braced frame in other (w/ and w/out basement)	
34			C	Steel or precast columns with concrete beams and hollowcore slab, w/ steel stability bracing	
35		W	A	Wooden trussed roof with URM façade walls (which may become bearing)	
36			B1	Glulam portal frame, steel braces in other direction	
37			B2	Glulam portal frame, URM wall in other direction	
38		URM	A	URM soild or cavity wall, steel or timber roof (may feature precast gravity system)	
39		RC	A	Cast-in-place (CIP) reinforced concrete (RC) portal frame	
40			B1	Precast RC portal frame (grouted dowels)	
41			B2	Precast RC structural walls	
42	Commercial (other) (COMO)	URM	A	Clay brick walls	
43			B	Calcium silicate walls	
44		RC	A1	Cast-in-place (CIP) reinforced concrete (RC) core walls	≤ 4 storeys
45			A1	Cast-in-place (CIP) reinforced concrete (RC) core walls	> 4 storeys
46			A2	Cast-in-place (CIP) RC moment frame	≤ 4 storeys
47			A2	Cast-in-place (CIP) RC moment frame	> 4 storeys
48			B	Precast RC walls	≤ 4 storeys
49			B	Precast RC walls	> 4 storeys
50		S	A	Steel braced frame	≤ 4 storeys
51			A	Steel braced frame	> 4 storeys
52			B	Steel moment frame	≤ 4 storeys
53			B	Steel moment frame	> 4 storeys
54	Schools				
55	Churches				
56	Hospitals				

Table 5.19 Building typologies in the v2 exposure model

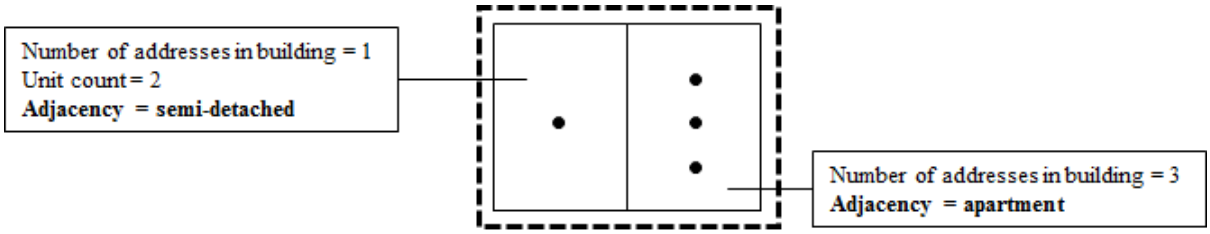

Figure 5.20 Adjacency Analysis

Figure 5.21 ANH height data, to help evaluate number of stories, it also shows some of the problems that may arise.

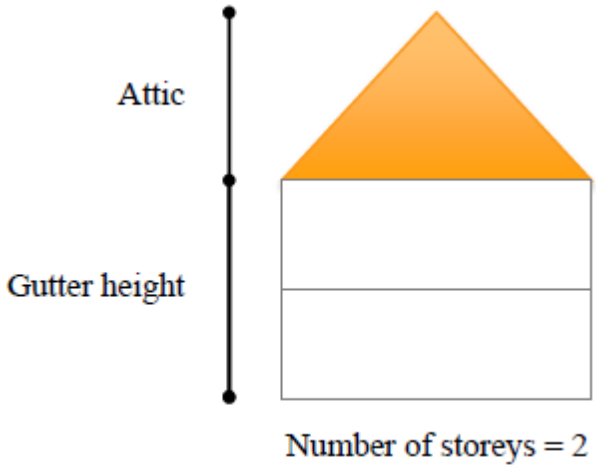

Figure 5.22 ANH data on height

5.23 shows the frequency distribution of buildings of each building typology, and average day/night occupants within each typology. There are over 150,000 regularly populated buildings in the exposure database, and over 90% of the buildings are constructed in unreinforced masonry (URM). Figure 5.25 shows the most predominant URM building typology is well distributed across the region, with higher density in many of the villages. However, despite the abundance of masonry buildings, it can be seen from Figure 5.23 that a large proportion of the population live and work in higher rise reinforced concrete buildings, though Figure 5.24 shows that they are mainly concentrated in the city of Groningen.

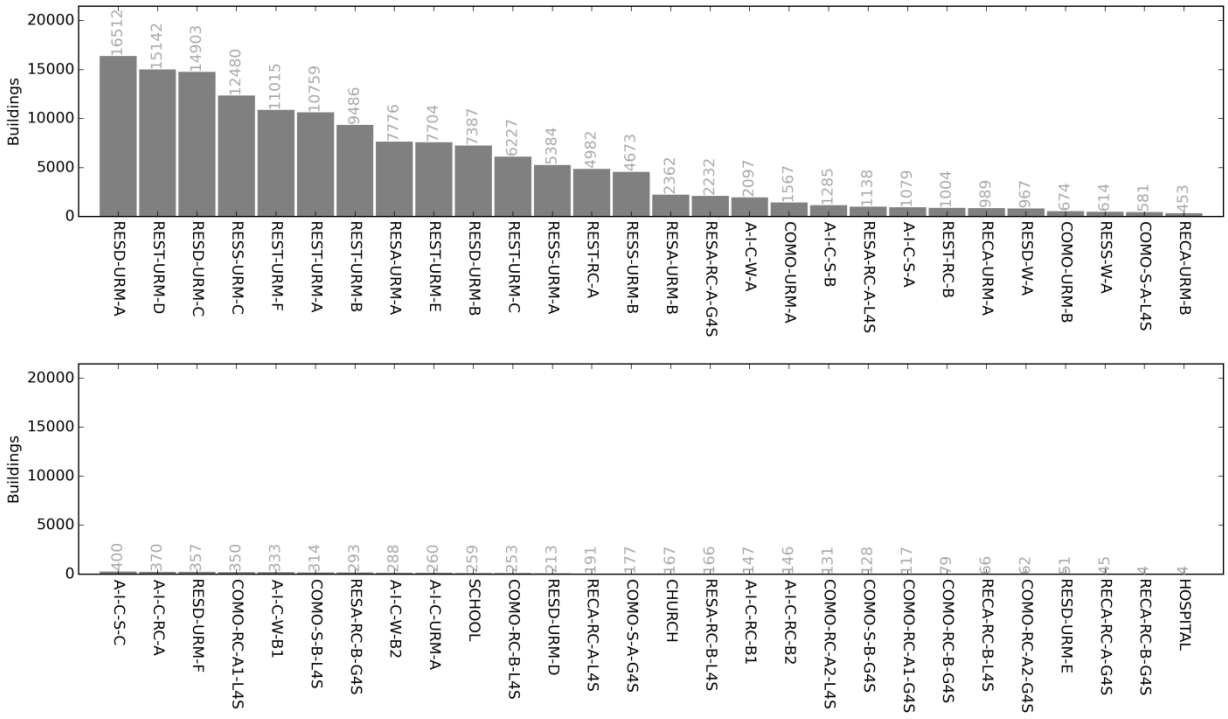

(a)

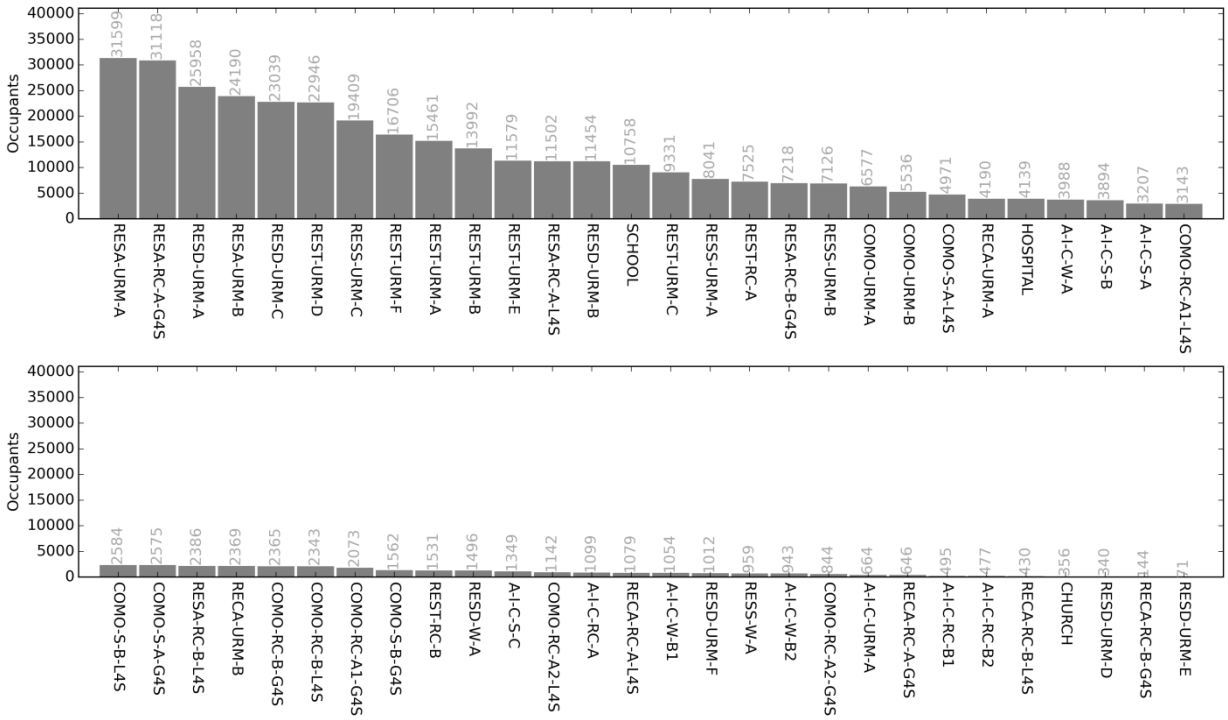

(b)

Figure 5.23 The frequency distribution of (a) buildings and (b) occupants within each building typology.

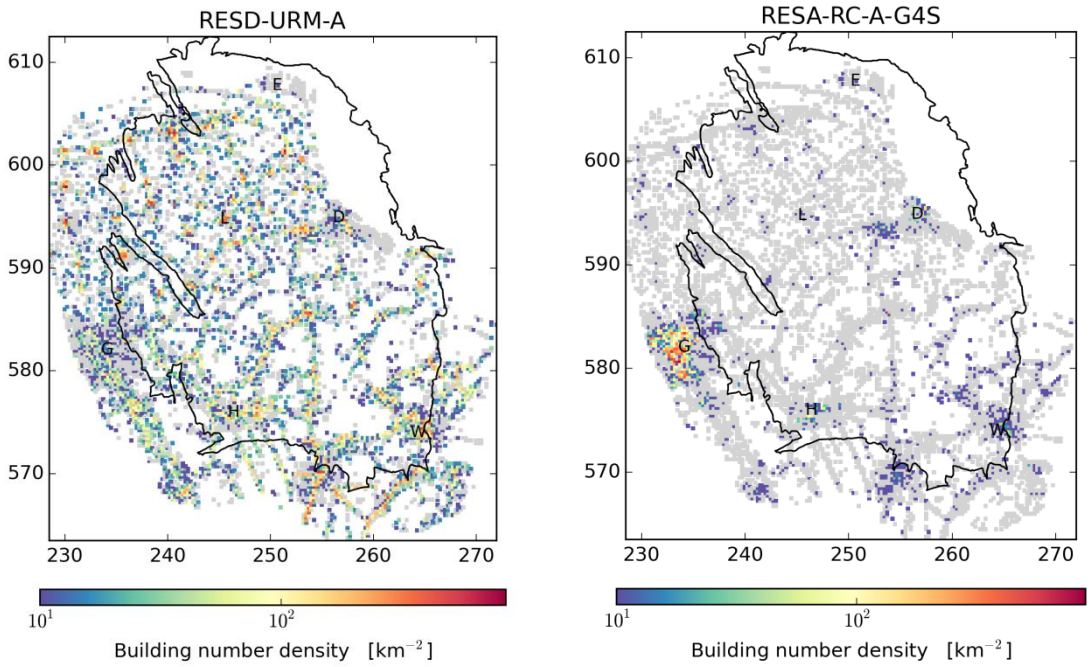

Figure 5.25 *Maps showing the building number density of two building typologies (RESD-URM-A and RESA-RC-A-G4S) on a regular 250 x 250 m grid. They grey cells denote areas where buildings of other typologies are located. The letters 'D', 'E', 'H', 'L', 'W' denote the place names Delfzijl, Eemshaven, Hoogezand, Loppersum and Winschoten respectively, and the black line denotes the outline of the field.*

Using a number of data sets (CBS, LISA, DATALAND) this database provides an estimate of the number of occupants per building during day and night. It also contains an estimate of the number of people outside, and close to a building. To analyse the risk to people from objects that might fall off a building during an earthquake (like a chimney) it is important to know the chance that someone will be in a location where they might be hit by a falling object. This "falling objects" risk model is described elsewhere in this report. The number of people outside and close to a building consists of an estimate of pedestrians walking past the building and an estimate of a percentage of the occupants of a building that could run outside in the event of an earthquake and be in the location where they might be hit by a falling object.

Building Occupancy

The occupancy has been analysed for many types of occupants: factory workers, government workers, office workers, teachers, nurses, patients, inmates, hotel guests, holiday home occupants, visitors to theatre/bar/sport facility or museum, church or mosque visitors, inhabitants of care homes, pupils in primary and secondary schools and university students. An analysis of time use data has provided estimates of the amount of time that people spend inside different buildings and footfall data has been used to estimate the people walking past buildings close to the street.

Using CBS StatLine data on inhabitants per hectare, the inhabitants are evenly distributed over the residential properties in a particular postal code and with the time use information the percentage of inhabitants at home during day/night can be estimated.

The exposure database version 2 has several improvements over previous versions, including updated datasets, new analysis methods to improve the accuracy of the assigned building typologies, and the inclusion of inference rules to assign the type of foundation. To estimate the occupancy of buildings, the V1 exposure database contained 2013 data from a company called BridGIS. This company no longer exists. To update this information NAM used the latest available

information from CBS and several other sources, listed above, to estimate the occupancy of buildings taking into account both residents and workers, such as nurses and doctors, but also an estimate of patients (through available data on number of hospital beds), teachers as well as estimates of pupils (through education data), and staff working at the prison as well as the prisoners. The current estimates of population were generated in a transparent manner and tuning the results to be accurate in the places where accuracy is most required is now possible.

The accuracy of the exposure model is being measured by comparisons with ground-truth data from 40,000 damage claims (non-privacy related data), 15,000 rapid visual screening reports, and 1,500 extended screening reports. In addition to continuing to test the accuracy of the exposure model using all available ground truth data, in particular with regards to the building typology and foundation type inference rules, future developments are expected to also focus on incorporating the data that is currently being collected on chimneys, parapets, gable walls and other falling objects.

Consequence Modelling

Given that all of the currently calculated risk metrics focus on loss of life (see Section 8), a model is needed to predict the probability of loss of life given different levels of ground shaking.

Methodologies for estimating fatalities from earthquakes range from those that directly attempt to predict the number of deaths from the magnitude of the earthquake (e.g. Samardjieva and Badal, 2002) or a level of ground shaking such as macroseismic intensity (e.g. Jaiswal et al., 2009), to those that propose ratios between the mean number of deaths (or injured persons) and the number of people exposed to a building with a given level of damage, so-called mean fatality ratios (e.g. Coburn and Spence 2002).

The latter approach has been selected for the Groningen risk model, given that it has been observed in past earthquakes that the number of earthquake shaking fatalities is clearly related to the number of buildings that fully or partially collapse (e.g. Alexander, 1996). Furthermore, by estimating the fatality risk for different typologies of buildings, it will be possible to guide the strengthening efforts that are currently being applied to the buildings in the region.

The volume of a structure that collapses will influence the number of people within the building that are affected (Seligson, 2008; Spence and So, 2009; So and Pomonis, 2012). So (2015) has shown (Figure 5.26) that mean fatality ratios are directly correlated with volume loss in collapsed buildings (defined by Okada (1996) as the "*void index, or volume loss of survival space, given by volume of debris (Vd) divided by the space capacity (Vc, which is the volume given by 2 metres height from floor level)*" – see Figure 5.20). Furthermore, Figure 1 shows that for a given volume loss, the main construction material can further influence the fatality ratio.

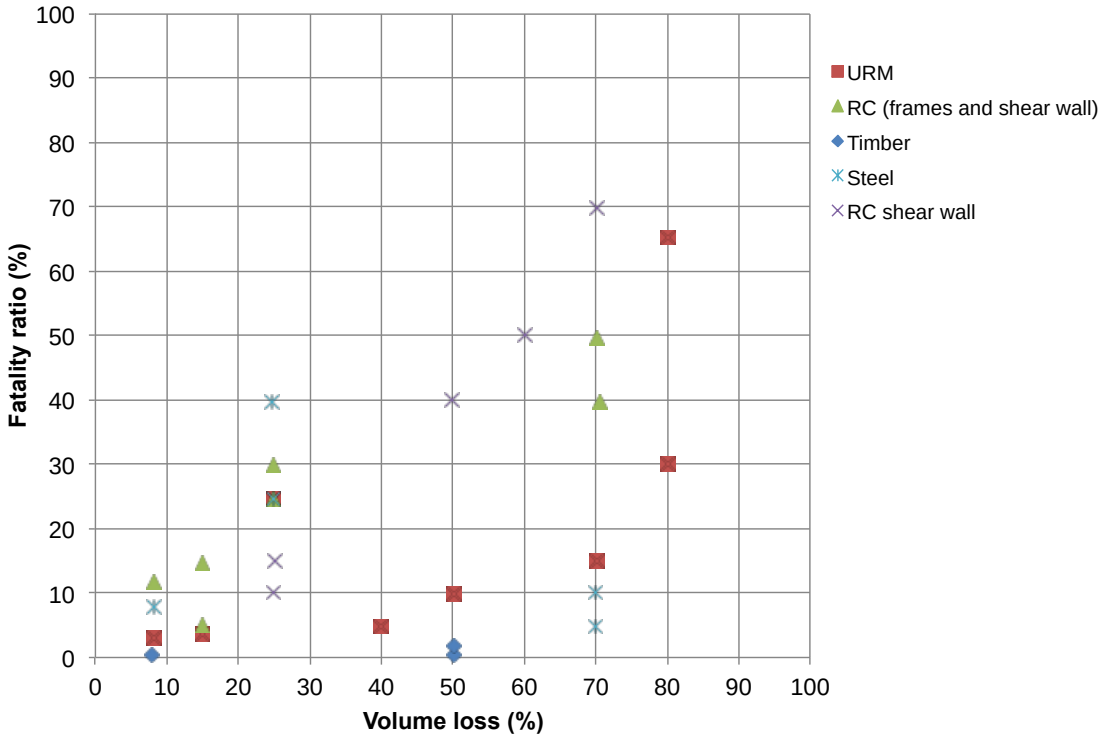

Figure 5.26. Relationship between fatality ratios and volume loss (So, 2015)

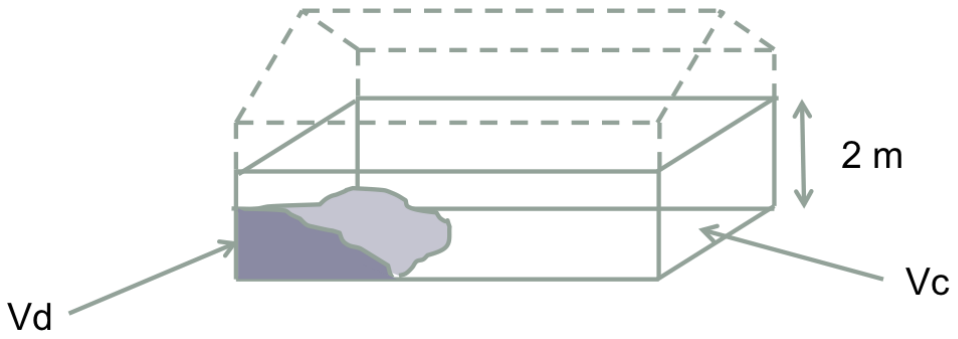

Figure 5.27. Illustration of volume loss (adapted from Okada, 1996)

Despite the observed differences in collapsed volumes in buildings that have collapsed in earthquakes, these buildings are generally defined as having the same "damage state" in post-earthquake reconnaissance missions (see Figure 5.28). Instead, different modes of collapse (so-called collapse mechanisms) may have occurred in these "collapsed" structures, leading to very different volume losses. This is one of the drawbacks in using such empirical data to derive fragility functions which are then used to estimate fatalities, and, as discussed further below, this can be overcome by using analytical models that allow different collapse mechanisms and associated volumes to be estimated.

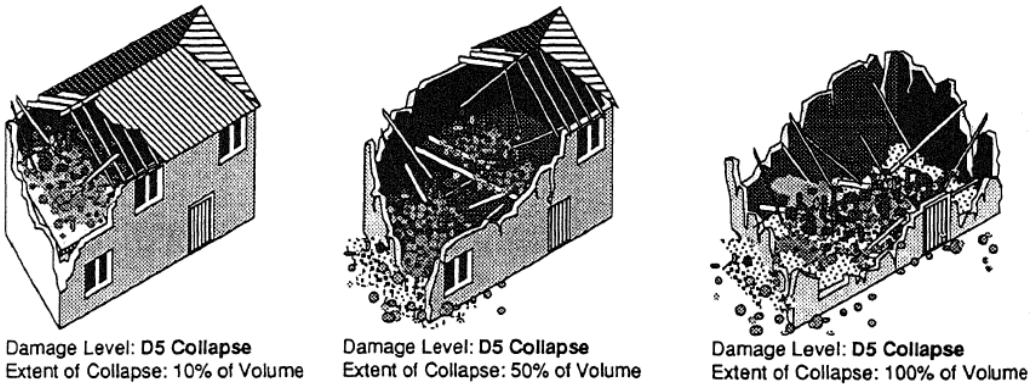

Figure 5.28. Varying volumetric reduction of a building defined as having a "collapse" damage level (from Coburn et al., 1992)

The collapse mechanism thus plays an important role in the estimation of casualties. A study by So et al. (2015) of 458 photos of collapsed and partially collapsed buildings in 47 different earthquake events from all over the world (Figure 5.29) further enforces this message: different collapse mechanisms do indeed lead to different volume losses. As there is no collapse data available from earthquakes in the Netherlands, data from earthquakes elsewhere is used. A similar study was also carried out for the debris falling outside of the building, to understand the risk to people outside of buildings, and again collapse mechanisms and area of debris were seen to be correlated (Baker et al., 2015). There are a number of limitations to the direct use of the data given in Figure 5.29, which include the fact that only some sides of the building can be observed in photos, the volume loss inside the building cannot always be seen, the data can be from buildings which have very different construction practices to those in Groningen and from earthquakes of much larger magnitude and duration.

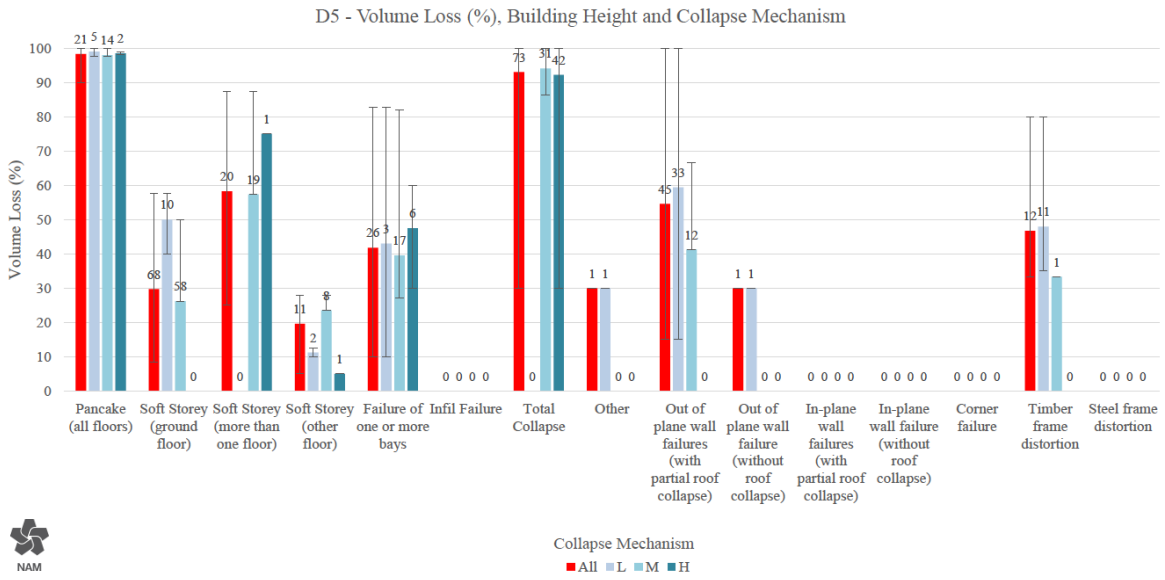

Figure 5.29 Distribution of volume loss by collapse mechanism and height for collapsed buildings based on observations (So et al., 2015)

As discussed previously, an analytical approach (calibrated using experimental evidence) has been adopted for the development of collapse fragility functions in the Groningen risk model. These advanced numerical models can also provide insights into the way in which structures with different characteristics collapse (see Figure 5.30), and the volume loss that would thus be expected. However, empirical evidence from past events with similar characteristics (in terms of seismicity and building typologies) should also be used to support the results from these numerical models (e.g. Figure 5.30b and 5.30c).

(a) (b) (c)

Figure 5.30. (a) Advanced numerical models for collapse modelling and comparisons with empirical evidence from (b) 2011 Christchurch earthquake and (c) 1989 Loma Prieta earthquake

This area of the risk model will receive significant attention in the run up to the Winningsplan 2016, with a number of nonlinear dynamic analyses of advanced numerical models being carried out for different structural typologies, in order to better understand the different collapse mechanisms that can be formed under different shaking scenarios. Further effort will also be placed on collecting empirical evidence from events with similar magnitudes and building conditions to those found in Groningen.

6 Probabilistic Risk Assessment

Risk Metrics

The results from the probabilistic hazard and risk analysis (PHRA) are primarily summarised via risk metrics which are related to the annualised probability of fatality for an individual person or for groups of people, taken as an average across the forecast period of the PHRA. These primary risk metrics - "Inside Local Personal Risk", "Community Risk, and "Number of People at Risk" – are defined below.

When measuring risk, it is important to select a risk metric that is appropriate given the purpose of the risk measurement. However, in many cases there is more than one option available as to which metric to use. An advisory committee, Commissie Meijdam, was established in early 2015 to advise on risk policy related to Groningen earthquakes, including the selection of risk metrics (Ref. 37). As of November 2015, discussion (led by Commissie Meijdam) amongst key stakeholders and risk experts on the choice of risk metrics is ongoing. The selection of risk metrics for this PHRA is based upon judgment on which metrics are most suitable for each purpose, and reflects stakeholder discussion and advice published by Commissie Meijdam to date (due to the timing of the 2nd Commissie Meijdam advice (Ref. 76), it could not be fully reviewed and incorporated into this PHRA). However, it is recognised that alternative options are available, and the choice of metrics may change for future versions of the PHRA taking into account the final advice from Commissie Meijdam, expected by year-end 2015.

Inside Local Personal Risk

"Local Personal Risk" (LPR) is generally defined as the annual probability of fatality for a fictional person, who is continuously present without protection at a specific at-risk location. For Groningen earthquakes, LPR is defined as follows: *"the probability of death of a fictional person who is permanently in or near a building"* (Ref.35). "Inside LPR" (ILPR) focuses on the risk to people inside of building, and assumes that the fictional person is present inside the building 100% of the time, and the location of the person is uniformly and randomly distributed inside the building i.e. if 10% of the building collapses there is a 10% probability that the fictional person will be in the collapsed part of the building. Note that individual risk metrics that account for the proportion of time a building is actually occupied will yield a lower calculated risk than ILPR (particularly for buildings occupied a small proportion of the time). In this PHRA, the mean value of the ILPR is the primary metric used to compare against the 10^{-5} individual risk norm (as recommended by Commissie Meijdam, which requires the fatality risk for a person inside a building to be less than 10^{-5} per year).

Whereas ILPR is normally calculated for a specific building, it can also be averaged across a number of buildings within a geographical area, such as within a map grid cell. In this report, the averaging of ILPR uses weighting based on the estimated day/night population of each building.

Community Risk

Community Risk (CR) is the annualised rate of fatalities for a specified risk, with units of fatalities per year. CR is calculated by multiplying the LPR for a specified risk by the average number of people present in the at-risk area. Inside a building, the at-risk area is defined as the entire area inside the building, and CR is calculated by multiplying LPR by average number of building occupants (taking into account the proportion of time that the building is occupied). Outside of buildings, the at-risk area is defined as the area up to 5m from the building façade (based on empirical evidence of masonry falling from buildings), and CR is calculated by multiplying the LPR for this at-risk area by

the average number of people in the at-risk area. The method for calculating CR for the area outside of buildings is further described in the falling objects section of the report.

CR is used in this PHRA for two purposes:

1. To measure the risk to people outside of buildings from falling objects. CR is considered a superior metric for this purpose rather than LPR because it considers the likelihood that people will be present, which is highly variable for the area outside of buildings. For example, the average number of people present on a busy shopping street will be many orders of magnitude higher than those present in a garden.
2. To prioritise buildings/objects for upgrading within the structural upgrading program. CR (rather than LPR) is considered to be the most suitable metric, because it allows a reasonable comparison to be made between collapse risks for different types of buildings and falling object risks, with different average occupancies inside buildings and beneath the potential falling objects.

Number of People at Risk

The number of people at risk is used in this PHRA as an aggregate risk metric, with the purpose of determining the overall scale of the risk from Groningen earthquakes, and to assess the feasibility and options for the mix of measures available for mitigating of the risk to comply with the set norms (acceptable level in an acceptable timeframe).

In this PHRA, the number of people at risk is shown for ILPR, and is presented as a cumulative distribution (of people versus risk level). An ILPR distribution is also presented based on the number of buildings (rather than people), which can be easily compared to the structural upgrading scope.

Industry and Infrastructure

NAM is in active discussion with industry and infrastructure owners regarding the assessment of risk associated with induced earthquakes. Industry and infrastructure owners, as competent parties working under their respective set of (external) safety regulations, develop, with NAM input on the hazard side, their own risk assessment and strengthening requirements.

Industry

The Ministry of Economic Affairs has requested Deltares to, in conjunction with TNO, coordinate, guide, and review studies into the effect of induced earthquakes on industrial constructions (buildings, systems, installations). These studies are initiated by the industry parties, conducted by a number of (prequalified) engineering consultants, and paid for by NAM. In the absence of a local annex to Eurocode 8, Deltares has developed guidelines for the assessment of the risk, which are contained in the "Handreiking", of which version 4 has recently been issued. The Handreiking covers aspects such as hazard, subsurface / soil response and methods and techniques to be used to assess the strength / resistance of the constructions.

The studies have a two-phase approach. Phase 1 studies concern the qualitative assessment of the risk using conservative methods and result in a ranked list of constructions with the largest risk associated with failure due to the earthquake hazard. In case the calculated risk isn't deemed acceptable, the relevant, most critical constructions will be assessed in phase 2 studies, using advanced assessment methodologies, such as finite element modelling. Phase 2 studies also comprise identification and assessment of risk mitigation measures, potentially required to reduce the risk to acceptable levels, and, where relevant, a sensitivity analysis to the existing QRA.

At the end of September 2015, more than 30 study grants had been approved, the vast majority phase 1 studies. In terms of study progress, the current status is as follows:

Priority	#	Phase	Not started	PvA	40%	60%	80%	Completed
4, 5[6]	**6**	1	-	-		2		3
3	**8**	1	2	3			3	
2	**15**	1	6	1	1	2	3	2
1	**6**	1	2	4				

Table 6.1 Phase 1 study overview

Priority	#	Phase	Not started	PvA	40%	60%	80%	Completed
4, 5[5]	**6**	2	2	1		3		
3	**8**	2	6	2				
2	**15**	2	14	1				
1	**6**	2	6					

Table 6.2 Phase 2 study overview

[6] The status for priority 4 and 5 takes into account that three companies (NAM and two AkzoNobel companies), have conducted their own risk-assessment studies, predating the establishment of the Handreiking. These companies are currently updating their assessment in accordance with the latest version of the Handreiking, with an expected completion in (early) 2016.

The priority number is based on a study by Deltares (Ref. 40). Priorities have been assigned based on public data, with priority 5 as the highest priority and priority 1 as the lowest priority.

The expectation is that by end 2015, all BRZO companies in the 0.1g contour will have their "Plan van Aanpak" (action plan) for the phase 1 studies approved, and all priority 4&5 companies on the Chemiepark Delfzijl will have completed the phase 1 studies. It is anticipated that phase 2 studies for priority 4 & 5 companies on the Chemiepark Delfzijl will be completed early 2016 for the other priority 4 & 5 companies in the first half of 2016.

There are no formal guidelines how to incorporate the earthquake risk in the QRA methodology. This issue is addressed in a QRA pilot study for two AkzoNobel installations on the Chemiepark Delfzijl, under guidance of a steering committee with, amongst others, representatives from IenM, RIVM, Deltares, TNO, and EZ. The pilot is based on the method to include the seismic risks in the existing QRA of the facility in accordance with the Handreiking., The inclusion of seismic events in the facility QRA is, however, still subject to discussion/agreement by the policy makers of the various ministries. It is expected that the Government will issue a formal policy on the inclusion of seismic events in the facility QRA in the course of 2016. The QRA pilot is expected to be completed in early 2016.

Liquefaction is the predominant failure mechanism identified in many phase 1 reports. Given the high level of uncertainty associated with the liquefaction assessment, Deltares is planning on a dedicated liquefaction assessment for the Chemiapark Delfzijl and Eemshaven locations, including additional soil measurements.

Given the state of the phase 2 assessments, it would be premature to draw conclusions in regard of the risk arising out of the earthquake impact on industrial installations. This is supported by early indications from the detailed (phase II) analysis, indicating that the investigated industrial installations appear to be more robust and more resistant under seismic loadings than simple, qualitative assessments made under phase I, indicate. Conclusions can be expected in the course of 2016, following completion phase 2 studies of the highest priority installations.

A monitoring program is being implemented on the Chemiepark Delfzijl, comprising the installation of various seismic sensors in industrial buildings and installations, the signals of which will feed into the relevant process control domains, enabling for manual / automatic interventions in the process controls based on observed seismic impact.

Infrastructure

The Ministry of Economic Affairs has requested Deltares to provide an initial, high-level, assessment of the risk of induced earthquakes on the critical infrastructure in Groningen, such as levees, quays, advanced structures (locks, dams, etc., "kunstwerk"), and the high-voltage electricity grid. The study also comprised a liquefaction study.

The study identified 43 km primary levees and 75 km secondary levees that potentially require strengthening[7] and recommended further study as well as the development of norms and a formal assessment framework in order to establish the more definite strengthening requirements.

It was further recommended to prioritize the strengthening of regional levees in the centre of the risk area, and the further assess the risk using additional data (to be collected) and advanced methods, potentially leading to a reduction in the required strengthening measures.

[7] Lengths derived under the assumption that the levees meet current norms

The study of a selected number of representative and critical advanced water defense structures (locks, dams, etc) did not identify any immediately required strengthening requirements. However it was recommended, as with levees, to do further study on all critical advanced water defense structures and to develop norms as well as a formal assessment framework.

The study of the high-voltage transmission grid identified a limited number of critical structures that may be considered for strengthening, as well as areas for further study. Due to the redundancy of the grid (n-1 design) the potential impact of failure due to an earthquake was considered limited.

Gasunie, the operator of the high-pressure natural gas transmission grid has performed its own risk assessment studies and implemented a number of strengthening measures.

NZV infrastructure

Based on the afore-mentioned Deltares report, Waterschap Noorderzijlvest (regional water Board), NZV, accelerated a number of planned strengthening measures[8], in particular the strengthening of the regional levee at the north side of the Eemskanaal at Garmerwolde (in execution) and the sea levee Delfzijl – Eemshaven (preparations in progress, tender award planned for 2016).

To establish the necessity and scope for strengthening measures for the Delfzijl – Eemshaven sea levee, Deltares, at the request of NZV, has embarked on advanced impact assessment studies and on the development of an earthquake impact assessment framework. The studies include a site-specific hazard assessment to which NAM contributes.

Rijkswaterstaat infrastructure

Rijkswaterstaat (RWS) has embarked on earthquake impact assessment studies for the Zuidelijke Ringweg Groningen. NAM is in discussion with RWS on the necessity and scope for strengthening measures. Based on the studies to date it is not clear whether strengthening measures are required. The strengthening scope, if any, is expected to be limited. A formal earthquake risk assessment framework, has yet to be developed.

[8] These planned strengthening measures were necessitated by the implementation of new norms (WTI2017)

Probabilistic Risk Assessment of Building Collapse

In this section an assessment is presented of the risk associated with the collapse of buildings. While the Hazard Assessments issued by NAM have all been fully probabilistic since the Winningsplan of November 2013, the initial risk assessments were scenario based. In May 2015, NAM issued for the first time a fully probabilistic hazard and risk assessment (PHRA). At that time risk results were qualitative only, as these had not yet been fully calibrated to sufficient data obtained for the site-specific conditions of the Groningen field.

For this interim update of the hazard and risk assessment, a large amount of additional new data has been collected from the Groningen field area. This primarily comprises new data for soil and building types within the Groningen area. As a consequence, this assessment provides, for the first time, a quantified appraisal of the seismic risk.

Inside Local Personal Risk (ILPR)

With knowledge of the presence of people in these buildings, the number of people exceeding an Inside Local Personal Risk (ILPR) can be estimated. The solid black line in figure 6.1 shows the number of people exposed to a certain level of local personal risk. During this 5-year period, there are no buildings where the occupants are exposed to a mean local personal risk larger than 10^{-4}/year. Occupants of some 5,000 buildings are exposed to a mean local personal risk exceeding 10^{-5}/year. As risk is in this context is often plotted as a logarithmic quantity, the mean log local personal risk is also shown. This is close to both the P50 and most likely values. The shaded grey areas indicate the norm set by the Committee Meijdam.

An assessment has also been made of the probability that a single earthquake event in the period 2016 to 2021 will result in at least 1, 10 or 50 fatalities. This is preliminary estimate for inside group risk curve. These estimates were made for the most-likely scenario in the logic tree, assuming a gas production rate of 33 bcm/year and without implementation of the structural upgrading program. Based on the current models, the probability of one or more fatalities as a consequence of a single earthquake is estimated to be less than 1.5 %/annum. Similarly, the probability of the occurrence of 10 or more fatalities as a consequence of a single earthquake is estimated to be less than 0.2 %/annum and of 50 fatalities as a consequence of a single earthquake, less than 0.015 %/annum. With implementation of the structural program these estimates will reduce.

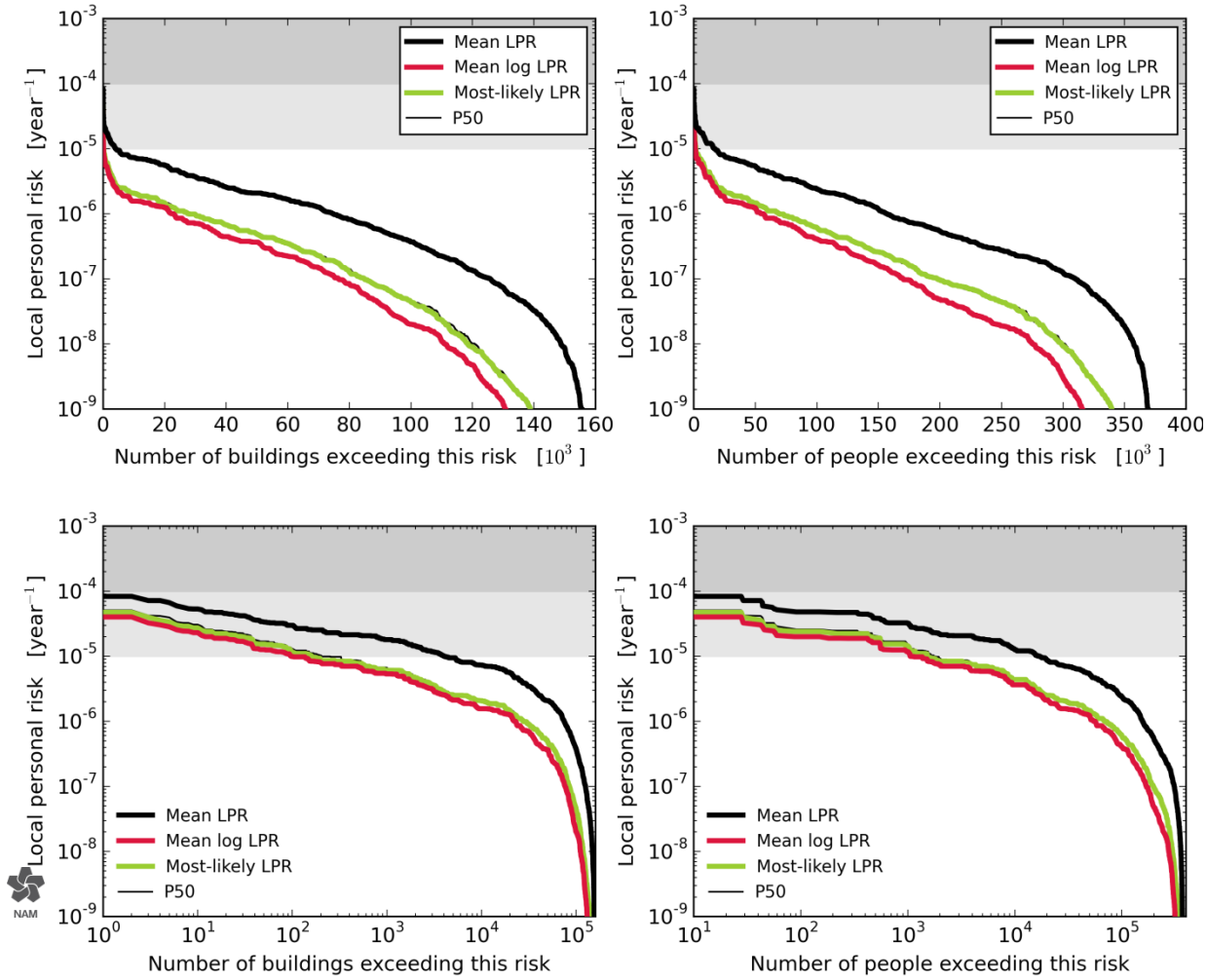

Figure 6.1 *Number of buildings and people exceeding a given inside local personal risk shown on (top) a linear scale for the overall view and (bottom) a log scale to accentuate the lower end of the building count. These figures are for the 33 bcm/year production scenario and the 2016-2021 assessment period. The grey areas indicate the norm advised by the Committee Meijdam.*

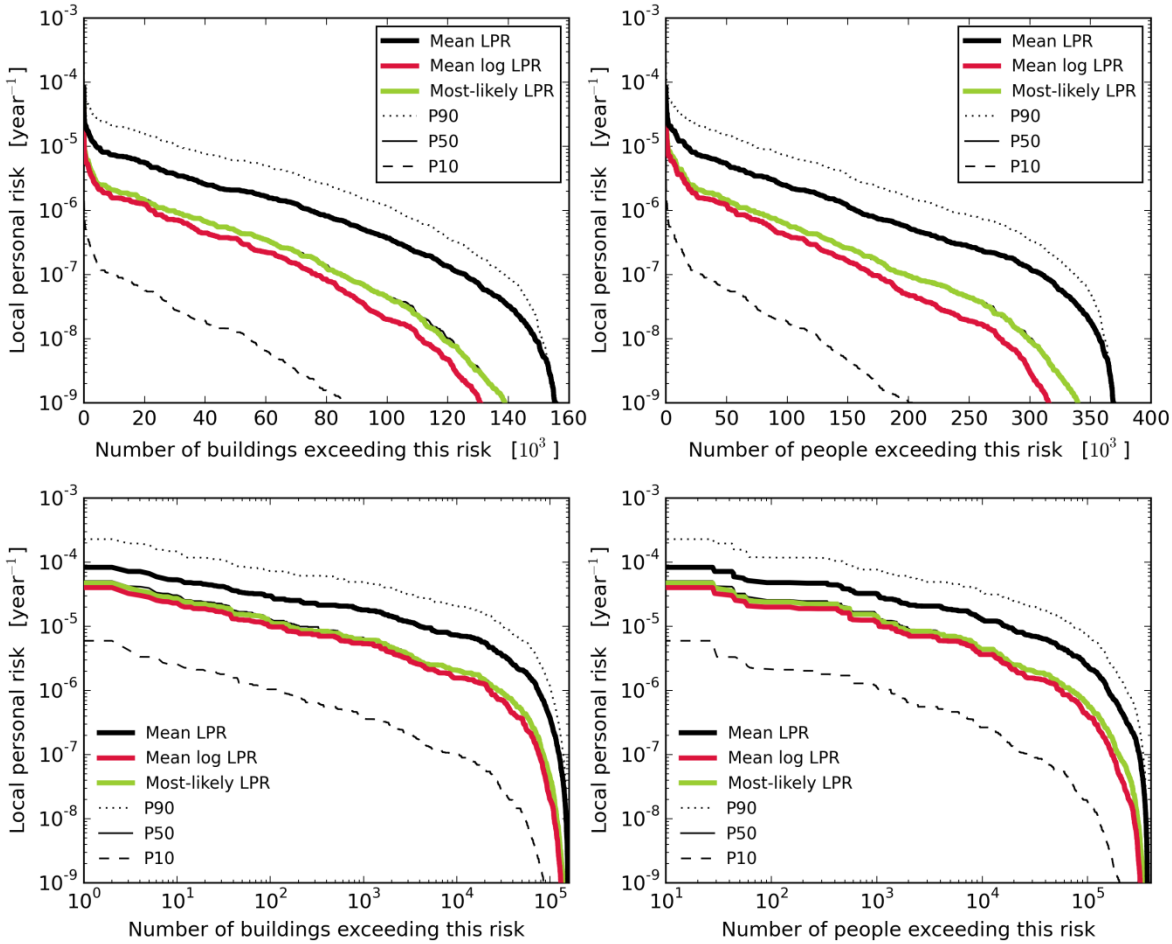

Figure 6.2 *Number of buildings and people exceeding a given inside local personal risk shown on (top) a linear scale for the overall view and (bottom) a log scale to accentuate the lower end of the building count. These figures are for the 33 bcm/year production scenario and the 2016-2021 assessment period.*

The distribution of buildings with mean I LPR> 10^{-5}/annum over the different building typologies is shown in Figure 6.2. These estimates of buildings and people exposed to risk are aggregates over the total Groningen gas field area. Figure 6.3 shows a distribution map for the base-case ILPR for each building typology.

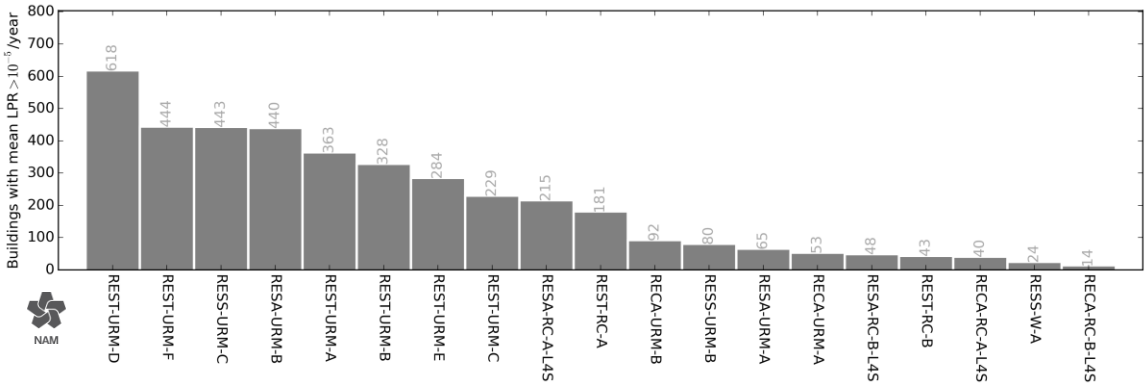

Figure 6.3 *Buildings with mean inside LPR> 10^{-5}/year according to building typology for 2016 to 2021.*

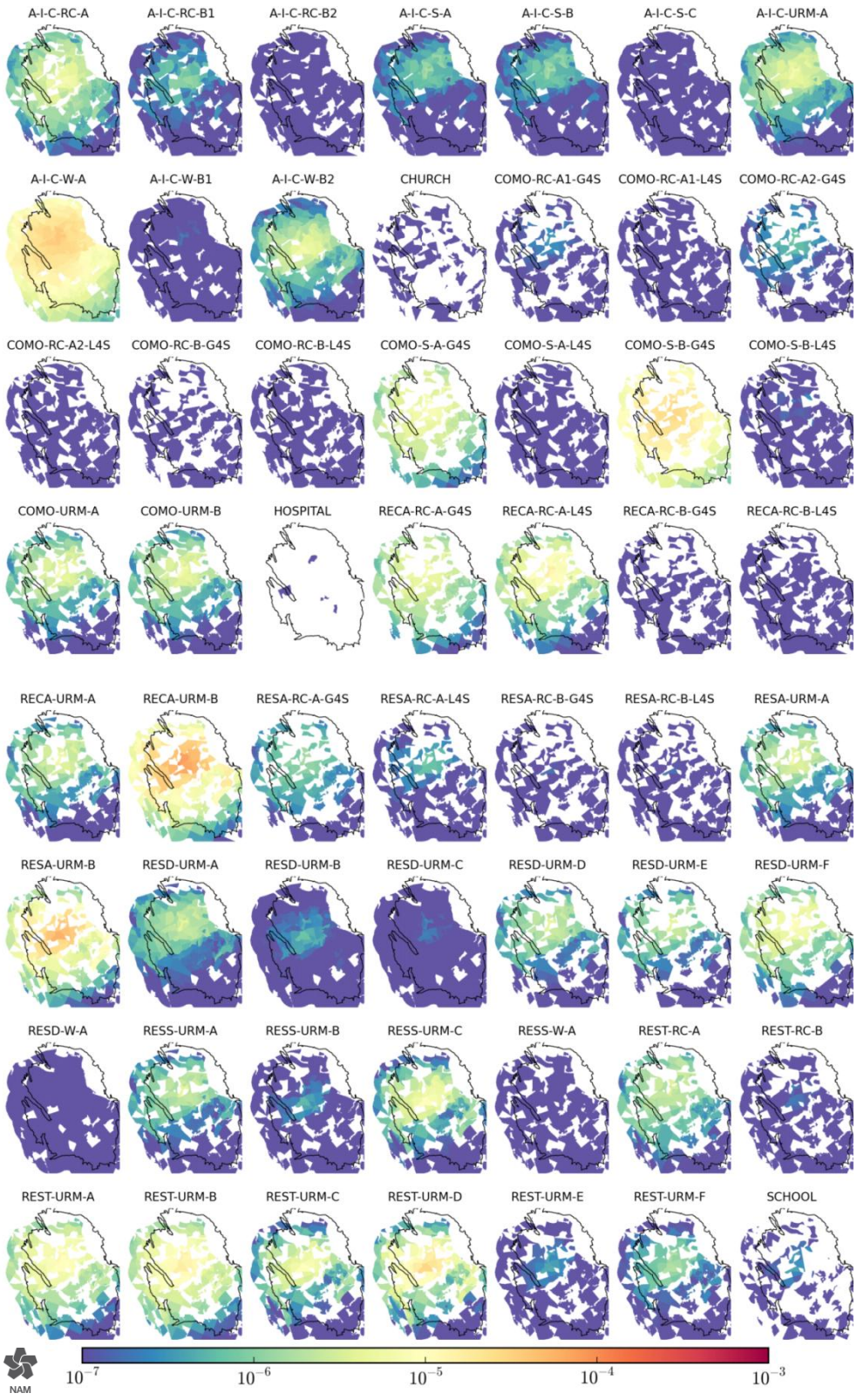

Inside Local Personal Risk [/year]

Figure 6.4 *Maps of inside local personal risk according to building typology under the base-case risk assessment from 2016 to 2021.*

These maps show that the risk is primarily concentrated in residential apartment buildings of unreinforced masonry with silica-calcium load bearing walls (type B) in the Loppersum area

(typology RESA-URM-B) and similar buildings with a mixed residential commercial use, often with a large open area shop at the ground floor (RECA-URM-B). Large agricultural/industrial/commercial buildings (warehouses) with wooden truss roofs and URM walls (typology A-I-C-W-A) and Commercial steel frame buildings without a moment frame (typology COMO-S-B-G4S) located in the Loppersum area also have a higher inside local personal risk.

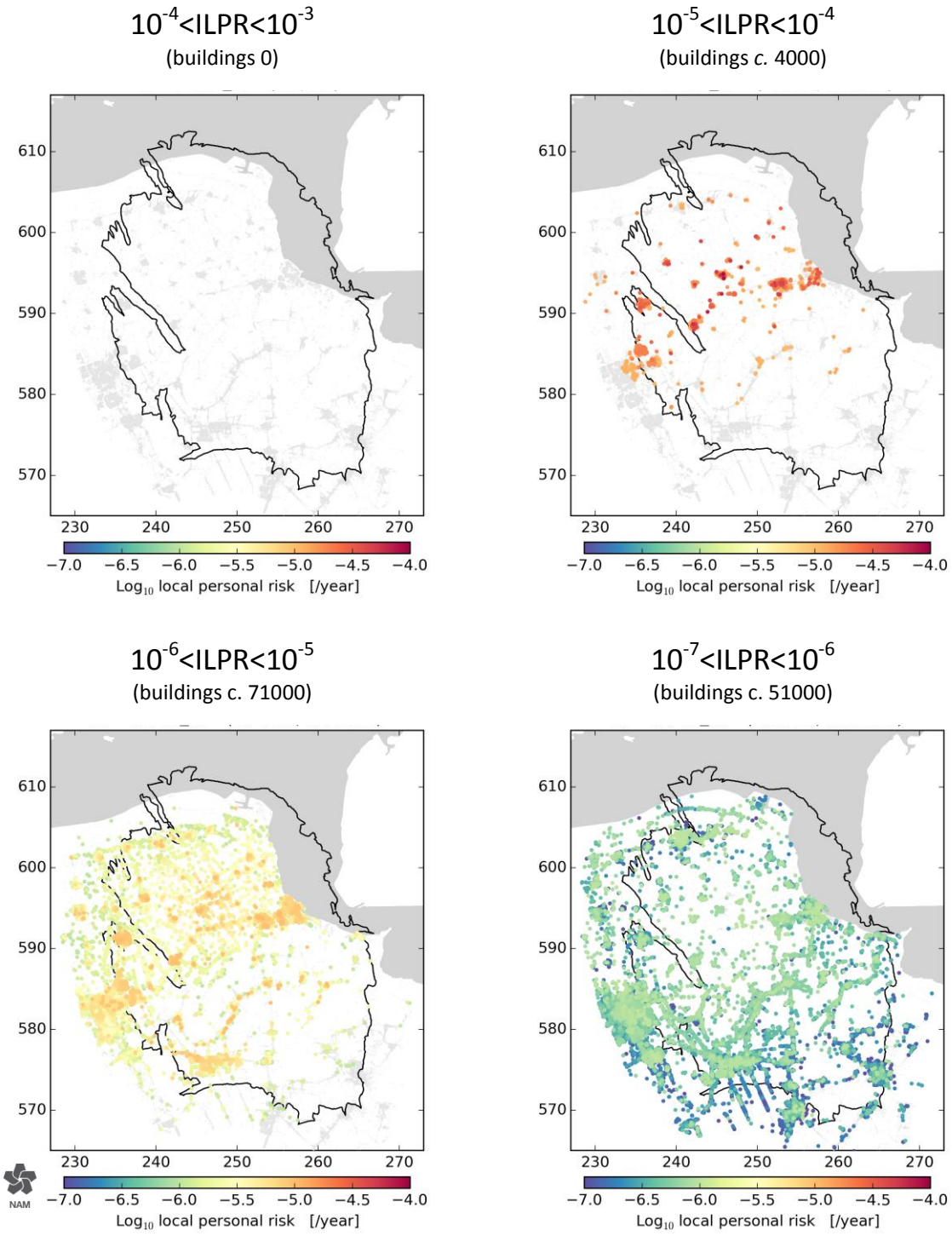

Figure 6.5 *Mean inside local personal risk, ILPR for every individual building within four equal risk bands from 10^{-7} to 10^{-4}/year for the 5-year assessment period 2016 to 2021 under the 33 bcm production scenario without structural upgrading.*

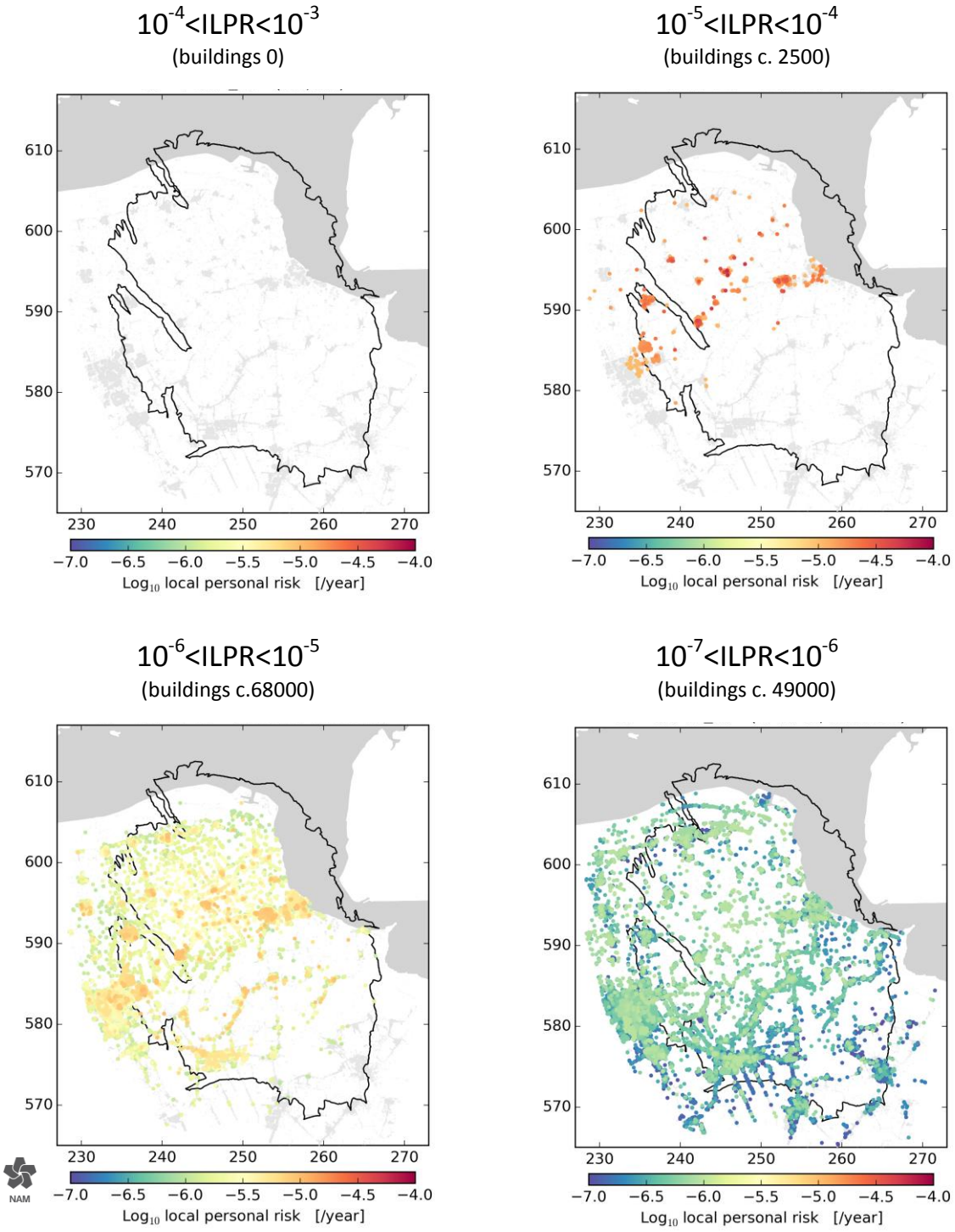

Figure 6.6 *Mean inside local personal risk, ILPR for every individual building within four equal risk bands from 10^{-7} to 10^{-4}/year for the 5-year assessment period 2016 to 2021 under the 21 bcm production scenario. As Figure 6.8, except for the 21 bcm production scenario without structural upgrading.*

The spatial distribution of buildings within given ranges of ILPR is shown in figure 6.5 for a production scenario of 33 Bcm/annum and in figure 6.6 for a production scenario of 21 Bcm/annum. When comparing these numbers with the norms advised by the committee Meijdam, the relevant map is upper right hand map, which shows that about 4,000 buildings need to be structurally upgraded in the 33 Bcm/annum production scenario. Some 2.5% of the total population living in the Groningen field area are living in these buildings.

Disaggregation of Inside Local Personal Risk (ILPR)

A disaggregation of contributions to the base-case ILPR was performed for magnitude, distance from the epicentre, the ground motion variability measure ε, and spectral acceleration causing building collapse. Figure 6.7 shows the results for the residential apartment buildings of unreinforced masonry with silica-calcium load bearing walls (type B) in the Loppersum area (typology RESA-URM-B).

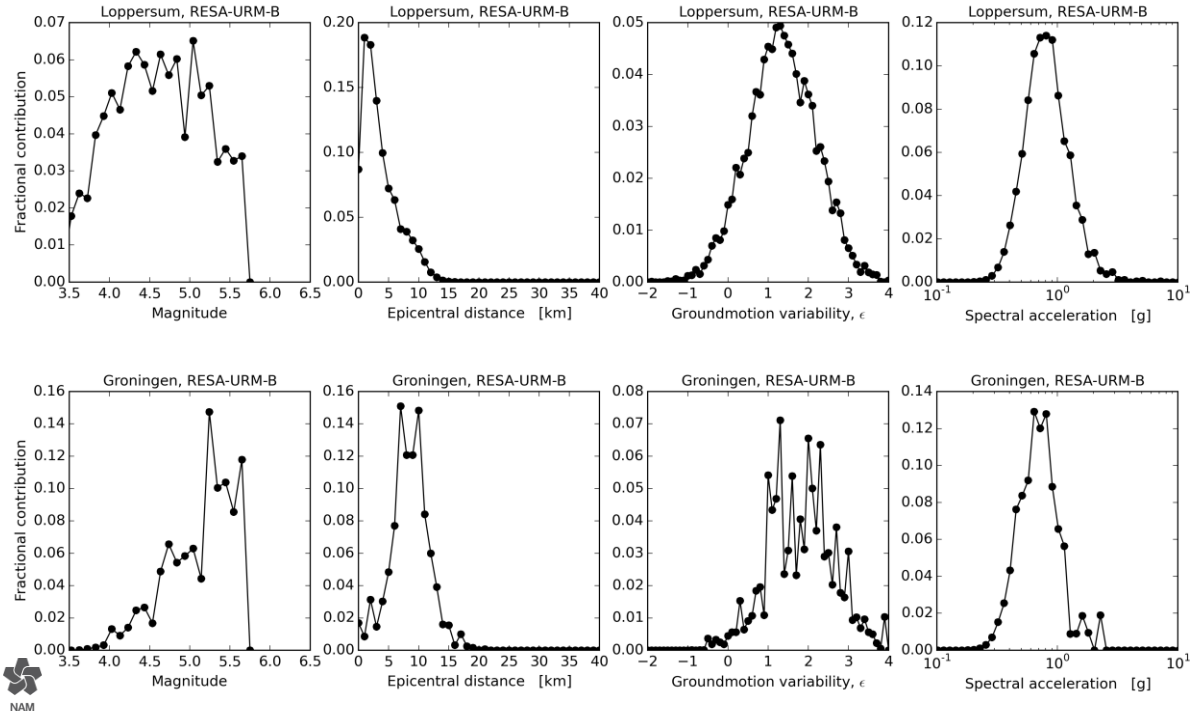

Figure 6.7 *The fractional contribution to ILPR for the RESA-URM-B building typology at two locations: Loppersum (top row) and Groningen city centre (bottom row). This result was obtained for the 2016 to 2021 assessment period under the 33 bcm/year production scenario and the base-case scenario of the risk logic tree. Fluctuations between neighbouring points are due to finite sampling effects of the Monte Carlo procedure; nonetheless the underlying trends are clear.*

As for hazard, earthquakes in the Loppersum area (i.e. at epicentral distances less than 5 km) contribute most to the risk for this area. For Groningen city, earthquakes at an epicentral distance of 10 km (*i.e.* in the Loppersum area) are the most important contribution to the risk.

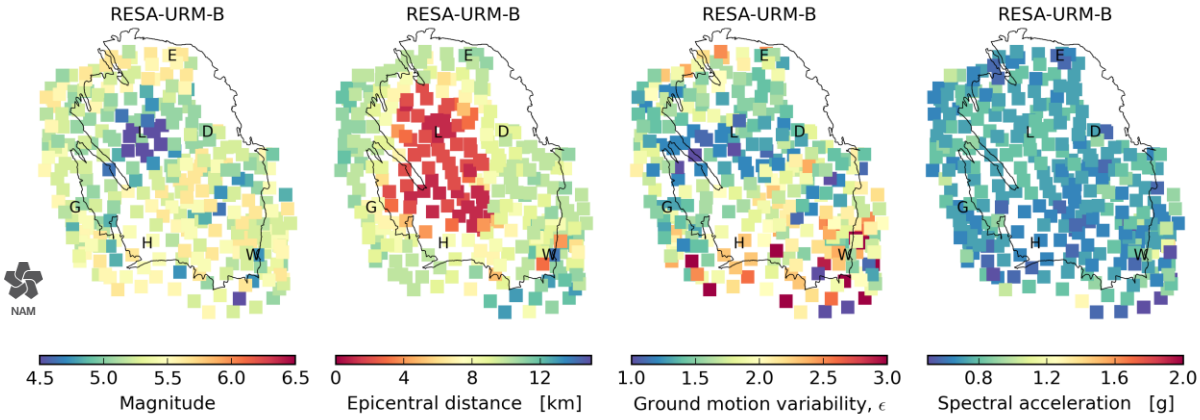

Figure 6.8 *Risk disaggregation maps showing the modal contribution to ILPR at each map location for the period 2016 to 2021 under the 33 bcm/year production scenario and the base-case logic tree scenario.*

The areal representation of the risk disaggregation is shown in figure 6.8. For areas with low hazard (like the South East of the field) the risk disaggregation in this figure is not reliable due to finite sampling effects of the Monte Carlo process for these especially small values of ILPR.

Impact of the Production Scenarios

The influence of future production scenarios on the number of buildings and people exceeding a given level of mean inside local personal risk (ILPR) is shown in figure 6.9 for the three production scenarios, for two assessment periods; two years from 2016 to 2018 and five years from 2016 to 2021.

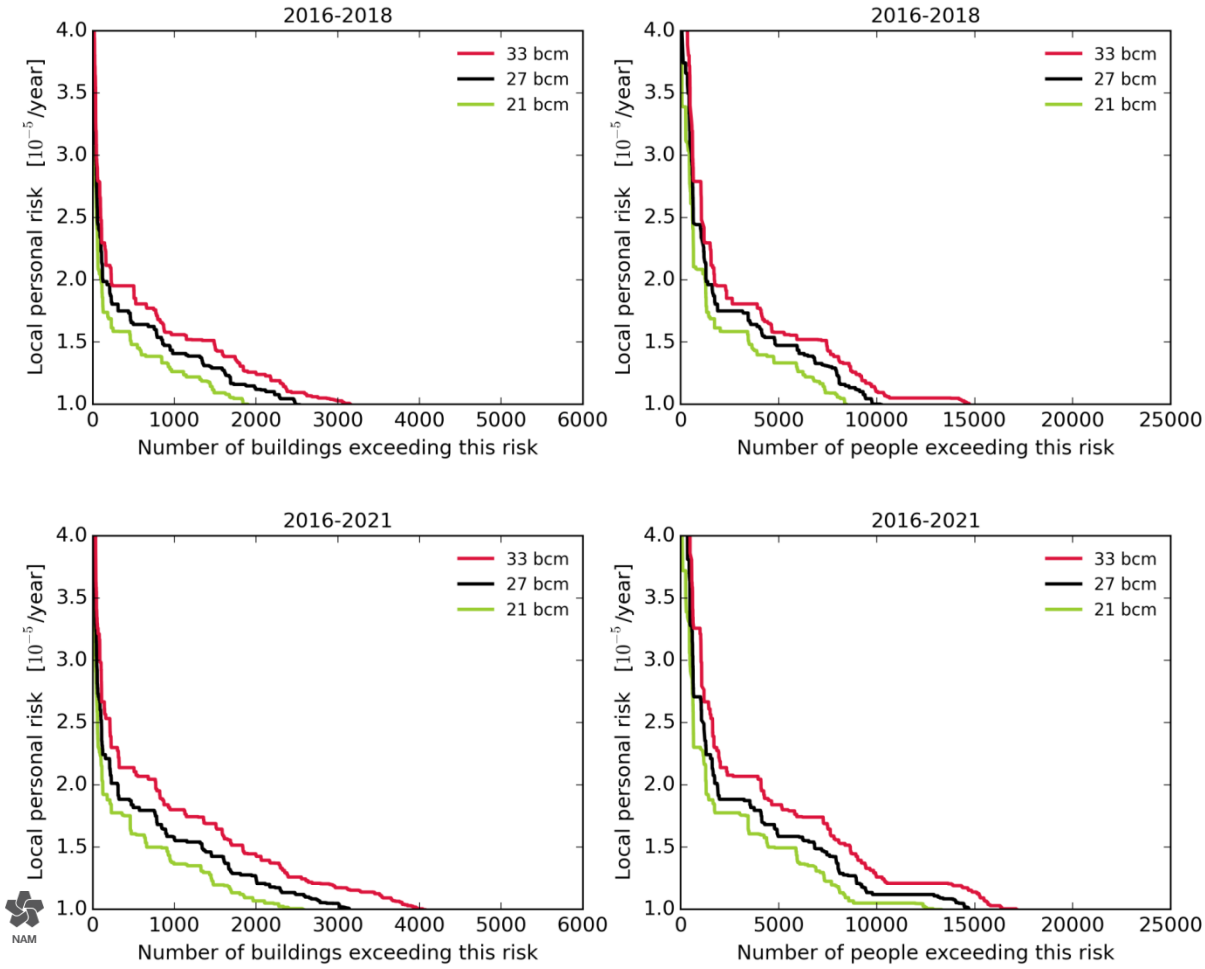

Figure 6.9 *Number of buildings (left) and people (right) exposed to mean inside local personal risk evaluated for two periods; top row: 2 years (2016 – 2018) and bottom row: 5 years (2016 – 2021).*

For a production scenario of 33 Bcm/annum, some 3,000 buildings have ILPR exceeding 10^{-5}/year during the 2-year period from 2016 to 2018. If the production level is reduced to 21 Bcm/annum, this number reduces to some 2,000 buildings.

The PHRA results indicate that with 33bcm/annum production the level of risk is currently within the norm recommended by Commissie Meijdam (accounting for the transition period), in that there are zero buildings with mean inside LPR >10^{-4}/year. However, to ensure the LPR for all buildings is below the 10^{-5}/year norm, some structural upgrading work is required within the transition period to reduce the risk of buildings with above 10^{-5}/year. Accordingly, structural upgrading scenarios have been included in the PHRA, and these are described in the following section.

Structural Upgrading Program

A structural upgrading program is ongoing in the Groningen Area. As of the end of September 2015, work carried out in this program includes more than 19,000 building inspections and 1,000 structural upgrades (including both temporary strengthening, and permanent measures to reduce building collapse risk and to secure potential falling objects). The rate of structural upgrading is planned to continue increasing over the coming years.

Three different structural upgrading scenarios have been included in the PHRA, a mid-case scenario of 10,000 buildings with total scope based approximately on twice the number of buildings with mean inside Local Personal Risk (LPR) > 10^{-5}/year (as calculated by the PHRA), and two sensitivities. The scenarios are considered to be realistic in terms of the pace and efficiency of upgrading work that can be achieved given expected practical and social constraints, and reflect actual progress/experience in the program to date. Within each scenario, the structural upgrading work is prioritised based on the objective to reduce risk as fast as practically possible.

Responsibilities for the planning and execution of the structural upgrading program have been changing in 2015. In mid-2015, the Centrum Veilig Wonen (CVW) assumed responsibility (from NAM) for execution of the program including delivery of the overall number of upgrades per year, while adhering to the principles of risk-based prioritisation. The new National Coordinator Groningen (NCG) organisation publishes their first plan, including structural upgrading, in December 2015.

The structural upgrading scenarios in the PHRA can be further summarised as follows:

- The mid case scenario assumes that a total of 10,000 buildings will be upgraded to protect against collapse risk over a 7 year period (2015-2021). This scope is based upon the PHRA results which indicate that the number of buildings with mean inside LPR >10^{-5} is approximately 4000. For the mid case scenario, the number of buildings to be upgraded has been rounded up to the nearest order of magnitude (10,000), considering that this scenario is an approximate (rather than precise) estimate, and to allow for some degree of inefficiency in the identification of buildings with mean inside LPR >10^{-5} for upgrading (as outlined below, in practice it is expected that the degree of inefficiency will be relatively small). For this upgrading scenario, the level of risk is continuously maintained within the risk acceptance criteria recommended by Commissie Meijdam (including transition period), since there are zero buildings with mean inside LPR >10^{-4}, and all buildings with mean inside LPR between 10^{-4} and 10^{-5} are upgraded within 5 years.
- The pace of work in the mid-case scenario is assumed to increase significantly over the next four years due to the anticipated “learning curve” and increasing execution capacity, reaching a plateau of just under 2,000 buildings per year by 2018. The two sensitivity scenarios assume a total of 5,000 and 20,000 buildings to be upgraded, and have been developed by “scaling” relative to the base case. The scenarios include upgrading of both residential and non-residential buildings (such as schools, hospitals and offices).
- In addition to upgrading measures to protect against collapse risk, the base case scenario also includes other activities to improve building safety, known as L0/L1 measures. These measures are primarily focused on the securing of potential falling objects such as chimneys or gables. The scenarios assume a total scope of 4,000 upgrades, which is deemed to be sufficient to mitigate all falling object risks to an acceptable level (the total falling object scope is expected to be of the order of a few thousand or less). The scenario assumes circa 1,750 L0/L1 measures per year in 2015 and 2016, and 500 in 2017.
- The scenarios include assumed constraints on the amount of work that can be executed in a village in any year. Such constraints are expected to occur due to the need to carry out

structural upgrading work at each location safely and efficiently while minimizing social disruption.

- The upgrading work is prioritised based on the objective of reducing risk as fast as practically possible. Consistent with this approach, in the near term, the work is focused on upgrading the most fragile buildings (particularly terraced houses) starting in the centre of the PGA map. The basis for prioritisation will be continuously updated/optimised as new information and insights become available.

To illustrate the base case structural upgrading scenario and sensitivities, figure 6.10 shows an overview of the scenarios by year.

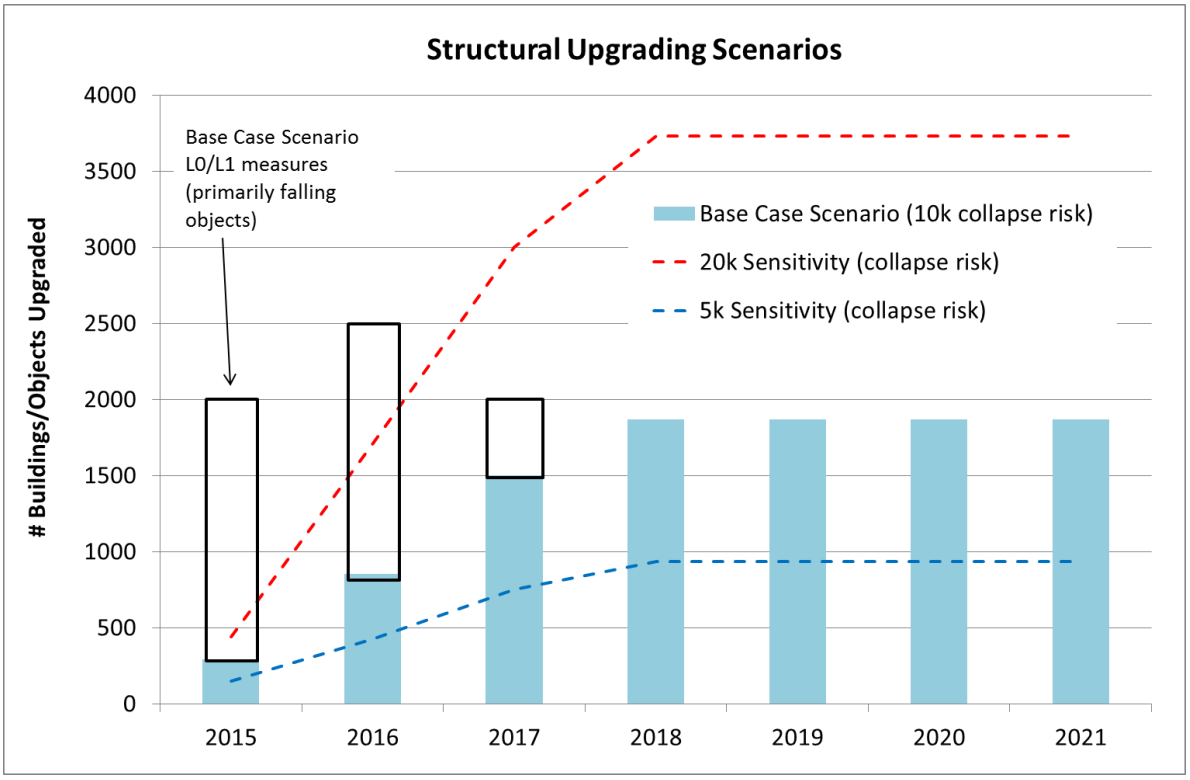

*Figure 6.10 Overview of the structural upgrading scenarios**

**Note – it is recognised that the base case scenario of 2500 upgrades (collapse risk and falling objects) in 2016 is lower than the CVW production plan (5000 upgrades). If the CVW plan is achieved, risk reduction will occur faster than the base case.*

Consistent with the near-term planned structural upgrading program, the results of the PHRA indicate that buildings with mean ILPR >10^{-5} are primarily located in the "core area" of Loppersum and surrounding municipalities (area of highest seismic hazard), and that more than 50% of these buildings are terraced houses. The building inspections carried out to date focused on this "core area", which when combined with damage inspections (which cover a wider area, and help to identify particularly fragile buildings) means that it is likely that the majority of the higher risk buildings have already been inspected.

The results from this PHRA will be used to guide inspection priorities outside the "core area", considering the combinations of building typologies and soil conditions that influence risks in these areas. In practice, once a building has been inspected, detailed structural modelling and/or the application of an "expert system" (such as the catalogue approach recommended in the 2nd Commissie Meijdam advice, Ref. 76) will be used to complete the risk assessment for the building, and a decision on upgrading will be made in consultation with the owner of the building. By

following this process, it is expected that a relatively high degree of efficiency at identifying and upgrading buildings with mean ILPR > 10^{-5}/year will be achieved.

During the early phases of the structural upgrading program, the focus will be on terraced houses in the "core area", and it is expected that there will be a low probability of upgrading any buildings with mean inside LPR below 10^{-5}/year. By the time the program moves outside the core area, significant additional knowledge and expertise will have been developed to enable efficient selection of buildings for upgrading.

Impact of the Structural Upgrading Scenarios

The numbers of buildings and people exceeding a given value of local personal risk is shown in figure 6.11 for four structural upgrading scenarios. These structural upgrading scenarios are for four different numbers of building upgrades; no building upgrades and 5,000, 10,000 and 20,000 buildings upgrades.

No Structural Upgrading

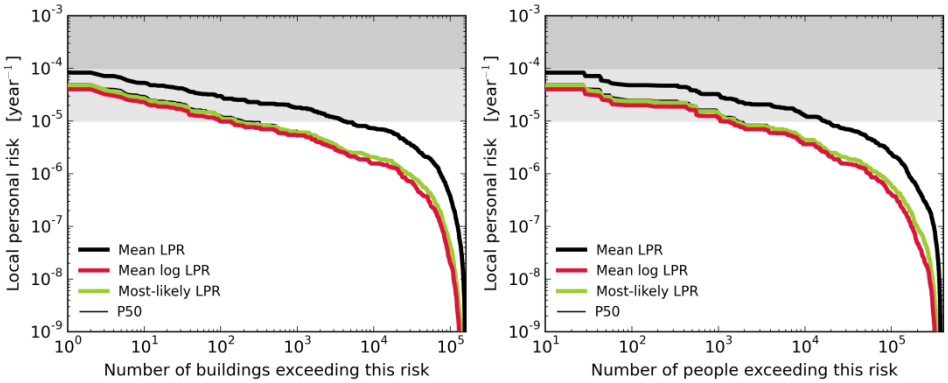

Structural Upgrading Program of 5,000 buildings

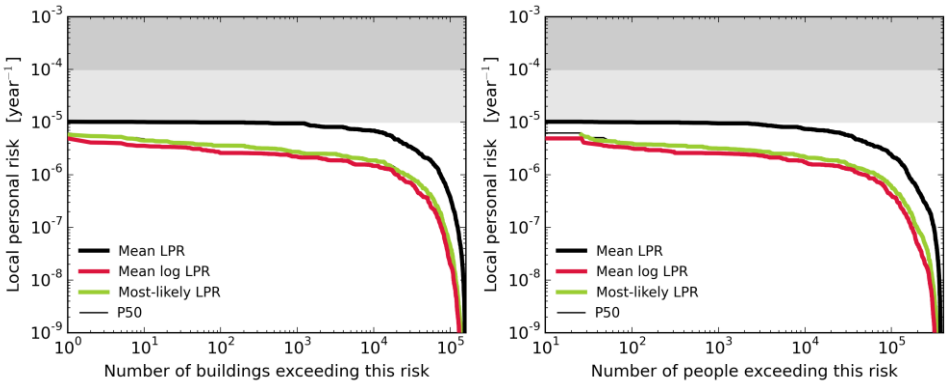

Structural Upgrading Program of 10,000 buildings

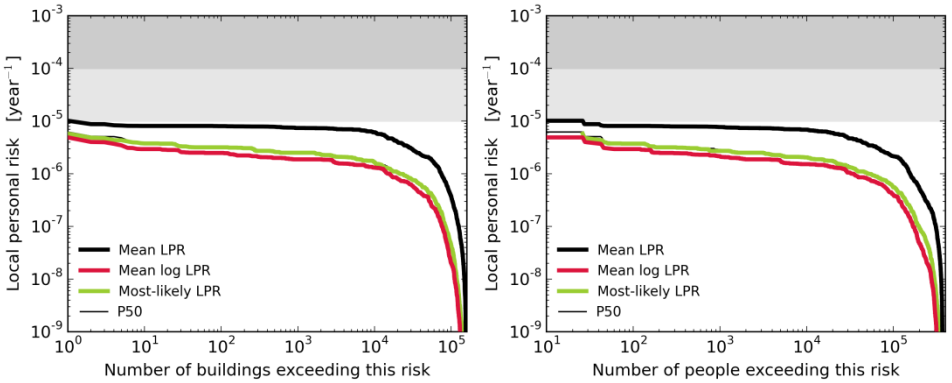

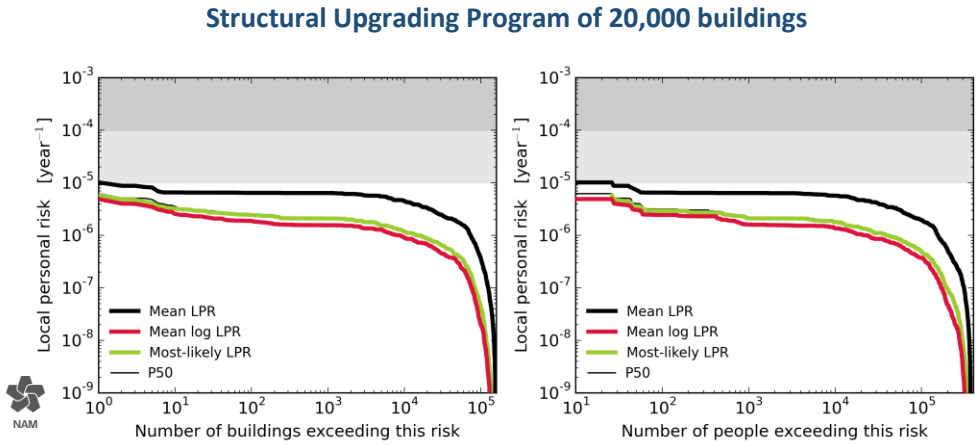

Figure 6.11 *Number of buildings (left) and people (right) exposed to inside local personal risk evaluated for four scopes of the structural upgrading programs (for 0, 5,000, 10,000 and 20,000 buildings). This assessment is for the 33 Bcm/annum production scenario and the 2016 – 2021 assessment period.*

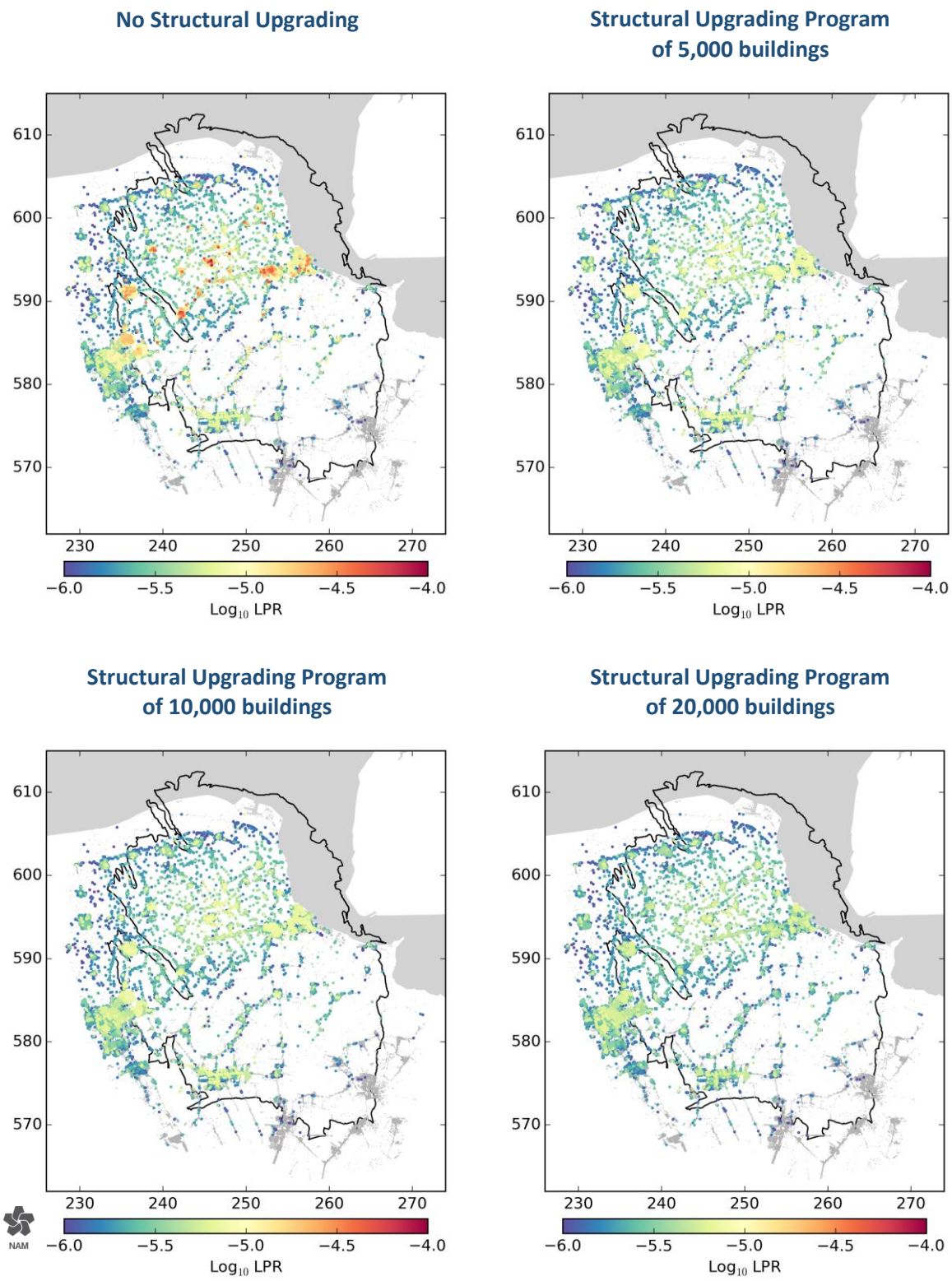

Figure 6. 12 *Mean inside local personal risk maps for different upgrading plans between 2016 and 2021: (top left) no buildings upgrades, (top right) 5,000 building upgrades, (bottom left) 10,000 building upgrades, and (bottom right) 20,000 building upgrades. This assessment is for the 33 Bcm/annum production scenario for the period 2016 – 2021.*

To obtain a sense of the areal spread of the higher risk buildings maps of the LPR for individual buildings were prepared (Fig. 6.12). Each of the approximately 160,000 occupied buildings within the exposure area is represented by a single dot. These are plotted in order of increasing risk so that the largest risks plot on top. Grey dots denote risks smaller than 10^{-6}/year.

7 References

1. Hollands Welvaren, De geschiedenis van een Nederlands Bodemschat, Aad Correljé, Tros/Teleac/NOT.
2. Nederlandse Aardolie Maatschappij BV (Jan van Elk and Dirk Doornhof), Study and Data Acquisition Plan for Induced Seismicity in Groningen - Planning Report, November 2012, http://www.rijksoverheid.nl/documenten-en-publicaties/rapporten/2013/01/25/planning-report-study-and-data-acquisition-plan-for-induced-seismicity-in-groningen.html
3. Staatstoezicht op de Mijnen, Reassessment of the probability of higher magnitude earthquakes in the Groningen gas field, 16th January 2013 http://www.sodm.nl/sites/default/files/redactie/rapport%20analyse%20aardbevingsgegevens%20groningse%20gasveld%2016012013.pdf
4. Nederlandse Aardolie Maatschappij BV, Update of the Winningsplan Groningen 2013, 29th November 2013. http://www.rijksoverheid.nl/documenten-en-publicaties/rapporten/2014/01/17/winningsplan-groningen-wijziging-2013.html
5. Nederlandse Aardolie Maatschappij BV (Jan van Elk and Dirk Doornhof, eds), Technical Addendum to the Winningsplan Groningen 2013; Subsidence, Induced Earthquakes and Seismic Hazard Analysis in the Groningen Field, http://www.rijksoverheid.nl/onderwerpen/aardbevingen-in-groningen/documenten-en-publicaties/rapporten/2014/01/17/bijlage-1-analyse-over-verzakkingen-geinduceerde-aardbevingen-en-seismische-risico-s.html
6. Nederlandse Aardolie Maatschappij BV (Jan van Elk and Dirk Doornhof, eds), Supplementary Information to the Technical Addendum of the Winningsplan 2013. http://www.rijksoverheid.nl/documenten-en-publicaties/rapporten/2014/01/17/toelichting-op-gewijzigd-winningsplan-groningenveld.html
7. Arup Project Title: Groningen 2013, Implementation Study http://www.rijksoverheid.nl/onderwerpen/aardbevingen-in-groningen/documenten-en-publicaties/rapporten/2014/01/17/arup-rapport.html and http://www.rijksoverheid.nl/onderwerpen/aardbevingen-in-groningen/documenten-en-publicaties/rapporten/2014/01/17/oplegnotitie-van-de-nam-op-het-arup-rapport.html
8. TNO, A general framework for rate dependent compaction models for reservoir rock, 2013, Report TNO 2013 R11405.
9. TNO, Eindrapport - Toetsing van de bodemdalingsprognoses en seismische hazard ten gevolge van gaswinning van het Groningen veld, 2013, Report TNO 2013 R11953. http://www.rijksoverheid.nl/onderwerpen/aardbevingen-in-groningen/documenten-en-publicaties/rapporten/2014/01/17/toetsing-tno-van-de-bodemdalingsprognose-en-seismische-hazard-tgv-gaswinning-van-het-groningen-veld.html
10. Staatstoezicht op de Mijnen, Advies Staatstoezicht op de Mijnen: Winningsplan Groningen 2013. http://www.sodm.nl/sites/default/files/redactie/advies%20sodm%20winningsplan%20groningen%202013.pdf
11. Staatstoezicht op de Mijnen – Advies Winningsplan 2013 / Meet- en Monitoringsplan NAM Groningen gasveld. http://www.rijksoverheid.nl/documenten-en-publicaties/rapporten/2014/01/17/adviezen-sodm.html
12. SodM, Risico Analyse Aardbevingen Groningen, 2013
13. Ministry of Economic Affairs, The cabinet decision on production from the Groningen field. http://www.rijksoverheid.nl/onderwerpen/aardbevingen-in-groningen/documenten-en-publicaties/kamerstukken/2014/01/17/gaswinning-in-groningen.html
14. Nederlandse Aardolie Maatschappij BV, Jan van Elk & Dirk Doornhof, Study and Data Acquisition Plan Induced Seismicity in Groningen for the update of the Winningsplan 2016, December 2014, submitted in March 2015, EP 201503202325.
15. Bourne, S. J., S. J. Oates, J. van Elk, and D. Doornhof (2014), A seismological model for earthquakes induced by fluid extraction from a subsurface reservoir, J. Geophys. Res. Solid Earth, 119, 8991–9015, doi:10.1002/2014JB011663.) http://onlinelibrary.wiley.com/enhanced/doi/10.1002/2014JB011663/ or http://www.namplatform.nl/mediatheek/documentatie-van-verder-onderzoek-naar-gaswinning-en-aardbevingen.html

16. S.J. Bourne, S.J. Oates, J.J. Bommer, B. Dost, J. van Elk, D. Doornhof, A Monte Carlo method for probabilistic hazard assessment of induced seismicity due to conventional gas production, Bulletin of the Seismological Society of America, V.105, no. 3, June 2015 in press.
17. Magnitude, Barnavol, J., Belayouni, N., Daniel, G. and Fortier, E., Seismic Monitoring, Delivery of location Results – Groningen field, January 2015.
18. Nederlandse Aardolie Maatschappij BV, Risk Methodology; Back to the region, February 2015, (forwarded to the national committee on earth quake related risks in April 2015) (EP 201504200668).
19. Nederlandse Aardolie Maatschappij BV, Hazard Assessment for the Eemskanaal area of the Groningen field, November 2014.
20. Besluit van de Minister van Economische Zaken: Instemming gewijzigd Winningsplan Groningen veld, Ministerie van Economische Zaken, February 2015, ETM/EM/13208000.
21. Stephen Bourne and Steve Oates, An activity rate model of induced seismicity within the Groningen Field, (Part 1), February 2015.
22. Letter from the Minister of Economic Affairs: Reductie van de productie van het Groningen veld eerste helft 2015, 10th February 2015.
23. Matt Pickering, A re-estimate of the earthquake hypo-centre locations in the Groningen Gas Field, March 2015.
24. Regularised direct inversion to compaction in the Groningen reservoir using measurements from optical levelling campaigns, S.M. Bierman, F. Kraaijeveld and S.J. Bourne, March 2015.
25. Development of Version 1 GMPEs for Response Spectral Accelerations and for Strong-Motion Durations, Julian J Bommer, Peter J Stafford, Benjamin Edwards, Michail Ntinalexis, Bernard Dost and Dirk Kraaijpoel, March 2015.
26. Introduction to the Geology of Groningen, Erik Meijles, April 2015.
27. Geological schematisation of the shallow subsurface of Groningen (For site response to earthquakes for the Groningen gas field), Deltares Pauline Kruiver and Ger de Lange.
28. Report on software verification against experimental benchmark data, Mosayk, November 2014
29. Report on structural modelling of non-URM buildings, Mosayk, April 2015
30. URM Modelling and Analysis Cross Validation – Arup, EUCENTRE, TU Delft, Reference 229746_032.0_REP127_Rev.0.03 April 2015.
31. Plan of approach for URM material testing, ARUP, Eucentre and TU Delft, March 2015.
32. Analysis of deep compaction measurements in the Groningen field, Pepijn Kole, Dirk Doornhof and Antony Mossop, May 2015
33. TNO, "TNO 2013 R12071, Safety considerations for earthquakes (2013); Steenbergen, R.D.J.M.; Vrouwenvelder, A.C.W.M.; Scholten N.P.M. (ERB)"
34. SodM, Letter on reporting requirements as part of the final decision on the winningsplan, annex "SodM expectations for NAM 1st of May risk report", 31 March 2015, 15046197
35. Risk Analysis of Groningen Earthquakes by SoDM (P500 Engels ref-06-risico-analyse-aardgasbevingen-groningen.docx)
36. Bevingen, Aardbevingen in Groningen, Gevolgen Ervaringen Emoties, Mike Tomale, Uitgevery Leander, 2015
37. Meijdam, "First advise", Committee on risks associated with induced earth quakes, 23 June 2015
38. A guideline for assessing seismic risk induced by gas extraction in the Netherlands, Muntendam-Bos, Roest, De Waal, The Leading Edge, June 2015
39. Journal for "Ruimtelijke Veligheid en Risicobeleid", Ale, Hagoort and Vlek, september 2015
40. Deltares / TNO (Piet Meijers, Rafael Steenbergen, Henk Kruse), Handreiking voor het uitvoeren van studies naar het effect van aardbevingen voor bedrijven in de industriegebieden Delfzijl en Eemshaven in Groningen, Report number 1209036-000), 4 July 2015.
41. Deltares / TNO (Bert Sman), Aardbevingen bedrijven Groningen - Procedure prioritering onderzoek, Concept report 1209036-000-GEO-0050, xxx 2015
42. Deltares (Mandy Korff et al.), Effecten aardbevingen op kritische infrastructuur Groningen, Samenvatting resultaten onderzoek Deltares, Report number 1208624-002, January 2014
43. An activity rate model of seismicity induced by reservoir compaction and fault reactivation in the Groningen gas field, S.J.Bourne, S.J. Oates, June, 2015
44. Monitoring Network Building Vibration, TNO 2015 R10501, April 2015
45. Developing an Application-Specific Ground-Motion Model for Induced Seismicity, Julian J Bommer, Bernard Dost, Benjamin Edwards, Peter J Stafford, Jan van Elk, Dirk Doornhof, and Michail Ntinalexis, Bulletin of the Seismological Society of America, September 2015

46. Development of Version 2 GMPEs for Response Spectral Accelerations and Significant Durations for Induced Earthquakes in the Groningen field, Julian Bommer et. Al, October 2015
47. Review of proposed seismic risk study – Groningen field, R. O. Hamburger, Simpson, Gumpertz & Heger Inc., September 2015
48. Review of "An Activity rate model of seismicity induced by reservoir compaction and fault reactivation in the Groingen gas fields", Ian Main, September 2015
49. Induced seismicity in the Groningen field - statistical assessment of tremors along faults in a compacting reservoir, Rick Wentinck, July 2015
50. Impact of various modelling options on the onset of fault slip and fault slip response using 2-dimensional Finite-Element modelling, Peter van den Bogert, July 2015
51. Arup, Eucentre, TU-Delft (2015) "Laboratory component testing: Modelling predictions and analysis cross validation," Draft Rev. 0.01, July 2015.
52. Crowley H., Grant D. (2014) "Report on v0 partial collapse fragility functions," October 2014.
53. Crowley H., Grant D., de Vries R. (2015) "Development of v1 fragility functions for structural failure," July 2015.
54. Crowley H., Pinho R., Polidoro B., Stafford P. (2015) "Development of v2 fragility and consequence functions for the Groningen Field," October 2015.
55. Eucentre (2015a) "Protocol for shaking table test on full scale building," Draft Rev. 2, July 2015.
56. Eucentre (2015b) "Experimental campaign on cavity walls systems representative of the Groningen building stock," October 2015.
57. Eucentre, P&P, TU-Delft, TU-Eindhoven (2015) "Material characterisation," Draft Rev. 1.1, October 2015.
58. Mosayk (2014) "Report on software verification against experimental benchmark data," Deliverable D1, October 2014.
59. Mosayk (2015a) "Report on structural modelling of non-URM buildings - v2 Risk Model Update," Deliverable D2 update, October 2015.
60. Mosayk (2015b) "Report on soil-structure interaction (SSI) impedance functions for SDOF systems," Deliverable D3, October 2015.

Additional References:

61. Alexander D. (1996) "The Health Effects of Earthquakes in the Mid-1990s," Disasters 20(3), pp. 231-247.
62. Baker H., So E., Spence R., Pickup F. (2015) "Debris from collapsed and partially collapsed buildings in earthquakes: a study based on damage photographs," Cambridge Architectural Research Ltd and TTAC Ltd, Internal report submitted to NAM.
63. Coburn A., Spence R. (2002) Earthquake Protection, 2nd Edition, John Wiley & Sons Ltd, Chichester
64. Coburn A.W., Spence R.J.S., Pomonis, A. (1992) "Factors Determining Casualty Levels in Earthquakes: Mortality Prediction in Building Collapse," Proceedings of the 10th World Conference on Earthquake Engineering, Madrid, Spain.
65. Furukawa A. and Ohta Y. (2009) "Failure process of masonry buildings during earthquake and associated casualty risk evaluation," Natural Hazards, 49, 25-51.
66. Jaiswal K., Wald D.J., Hearne M. (2009) Estimating Casualties for Large Worldwide Earthquakes using an Empirical Approach, US Geological Survey Open-File Report 1136.
67. Okada S. (1996) "Description for indoor space damage degree of building in earthquake," Proceedings of 11th World Conference on Earthquake Engineering, Paper no. 1760.
68. Samardjieva E., Badal J. (2002) "Estimation of the expected number of casualties caused by strong earthquakes," Bulletin of Seismological Society of America, 92, pp. 2310–2322.
69. Seligson H.A. (2008) Casualty Consequence Function and Building Population Model Development, Primary resource document for the "FEMA P-58 Seismic Performance Assessment of Buildings", FEMA, Washington.
70. So E. (2015) Derivation of fatality rates for use in building collapse-based earthquake loss estimation models, USGS Internal File Report, under review.
71. So E., Pomonis, A. (2012) "Derivation of globally applicable casualty rates for use in earthquake loss estimation models," Proceedings of the 15th World Conference on Earthquake Engineering, Lisbon, Portugal paper no. 1164.

72. So, E., Spence, R. and Baker H. (2015) “Volume loss in collapsed and partially collapsed buildings in earthquakes: a study based on damage photographs,” Cambridge Architectural Research Ltd, Internal report submitted to NAM.
73. Spence R., So E. (2009) Estimating Shaking-Induced Casualties and Building Damage for Global Earthquake Events, NEHRP Grant number 08HQGR0102, Final Technical Report
74. Pradhan, S. (2010). Failure Processes in Elastic Fiber Bundles. Rev. Mod. Phys., 82, 449–.
75. Rundle, J. B. (2003). Statistical physics approach to understanding the multiscale dynamics of earthquake fault systems. Reviews of Geophysics, 41(4), 1019. doi:10.1029/2003RG000135
76. Adviescommissie ‘Omgaan met risico’s van geïnduceerde aardbevingen’, “Tweede advies - Omgaan met hazard en risicoberekeningen in het belang van handelingsperspectief voor Groningen”, 29 October 2015

Note: For each document the link to the document on the web-site, where the document was issued has been provided. Some of these links might have become obsolete.

NAM documents without a link can be found at the web-site www.namplatform.nl.

8 Appendix A - Partners

The main partners in the research program into induces seismicity in Groningen are listed below:

Partner	Expertise
Deltares	Shallow geology of Groningen, soil properties and measurements of site response/liquefaction.
University Utrecht (UU)	Measurements of rock compaction and rupture on core samples, understanding of physical processes determining compaction.
University Groningen (RUG)	Shallow geology of Groningen.
ARUP	Modelling of building response to earthquakes, management of the program to measure strength of building materials.
Technical University Delft (TUD)	Measure strength of building materials and building elements.
Eucentre, Pavia, Italy	Measure strength of building materials, building elements and shake table testing of full scale houses.
Mosayk	Modelling of building response to earthquakes.
Magnitude (A Baker Hughes & CGG Company)	Seismic Monitoring (determination of location results deep geophones)
TNO	Potential for earthquakes resulting from injection. Building sensor project.
Avalon	Supplier of geophone equipment permanent seismic observations wells.
Baker-Hughes	Supplier of geophone equipment temporary observation wells.
Anthea	Management of the extension of the geophone network.
Rossingh Drilling	Drilling of the shallow wells for the extension of the geophone network.

9 Appendix B - Experts

Apart from scientist, engineers and researchers in NAM and the laboratories of Shell (Rijswijk) and Exxonmobil (Houston), NAM has also sought the advice of internationally recognised experts. Some of the experts involved in the research program on induced seismicity in Groningen, led by NAM, are listed below.

External Expert	Affiliation	Role	Main Expertise Area
Gail Atkinson	Western University, Ontario, Canada	Independent Reviewer	Ground Motion Prediction
Sinan Akkar	Bogazici, University Istanbul	Collaborator	Ground Motion Prediction
Hilmar Bungum	NORSAR, Norway	Independent Reviewer	Ground Motion Prediction
Jack Baker	Stanford University, US	Independent Reviewer	Building Fragility
Julian Bommer	Independent Consultant, London	Collaborator	Ground Motion Prediction and Site Response
Tijn Berends	Student; University Groningen	Independent Reviewer	Site Response and Shallow Geological Model
Loes Buijze	University Utrecht	Collaborator	Rock Physics / Core Experiments
Fabrice Cotton	GFZ Potsdam, Germany	Independent Reviewer	Ground Motion Prediction
Helen Crowley	Independent Consultant, Pavia	Collaborator	Building Fragility and Risk
John Douglas	University of Strathclyde, UK	Independent Reviewer	Ground Motion Prediction
Ben Edwards	University Liverpool	Collaborator	Ground Motion Prediction
Paolo Franchin	University of Rome “La Sapienza”	Independent Reviewer	Building Fragility
Damian Grant	ARUP	Collaborator	Building Fragility
Michael Griffith	University of Adelaide, Australia	Independent Reviewer	Building Fragility
Russell Green	Virginia Tech, USA	Collaborator	Liquefaction Model
Brad Hager	Massachusetts Institute of Technology	Independent Advisor	Geomechanics
Curt Haselton	California State University, US	Independent Reviewer	Building Fragility
Rien Herber	University Groningen	Independent Facilitator	General
Rob van der Hilst	Massachusetts Institute of Technology	Independent Advisor	Geomechanics
Jason Ingham	University of Auckland	Independent Reviewer	Building Fragility
Adriaan Janszen	Exxonmobil	Independent Reviewer	Shallow Geological Model
Mandy Korff	Deltares	Collaborator	Site Response, liquefaction and Shallow Geological Model

Table continued:

External Expert	Affiliation	Role	Main Expertise Area
Marco de Kleine	Deltares	Collaborator	Site Response and Shallow Geological Model
Pauline Kruiver	Deltares	Collaborator	Site Response and Shallow Geological Model
Florian Lehner	University of Vienna	Independent Reviewer	Rock mechanics
Ger de Lange	Deltares	Collaborator	Site Response and Shallow Geological Model
Nico Luco	United States Geological Survey	Independent Reviewer	Building Fragility
Eric Meijles	University Groningen	Independent Reviewer	Shallow Geological Model
Guido Magenes	EUCentre Pavia	Collaborator	Building Fragility
Ian Main	University Edinburgh	Independent Reviewer	Seismogenic Model / Statistics and Member SHACC Committee
Piet Meijers	Deltares	Collaborator	Site Response, liquefaction and Shallow Geological Model
Michail Ntinalexis	Independent	Collaborator	Ground Motion Prediction
Barbara Polidoro	Independent Consultant, London	Collaborator	Ground Motion Prediction
Matt Pickering	Student; Leeds University	Collaborator	Seismic Event Location
Rui Pinho	University Pavia	Collaborator	Building Fragility
Adrian Rodriguez -Marek	Virginia Tech, USA	Collaborator	Site Response Assessment
Emily So	Cambridge Architectural Research Ltd	Collaborator	Injury model
Robin Spence	Cambridge Architectural Research Ltd	Collaborator	Injury model
Chris Spiers	University Utrecht	Collaborator	Rock Physics / Core Experiments
Joep Storms	TU Delft	Independent Reviewer	Shallow Geological Model
Jonathan Stewart	UCLA, California, USA	Independent Reviewer	Ground Motion Prediction
Peter Stafford	Imperial College London	Collaborator	Ground Motion Prediction
Peter Styles	Keele University	Independent Advisor	Geomechanics
Tony Taig	TTAC Limited	Collaborator	Risk
Dimitrios Vamvatsikos	NTUA, Greece	Independent Reviewer	Building Fragility

Table continued:

External Expert	Affiliation	Role	Main Expertise Area
Ivan Wong	AECOM, Oakland, USA	Independent Reviewer	Ground Motion Prediction and Member SHACC Committee
Stefan Wiemer	ETHZ Zurich	Independent Advisor	Geomechanics
Teng Fong Wong	University Hong Kong	Independent Reviewer	Rock mechanics
Bob Youngs	AMEC, Oakland, USA	Independent Reviewer	Ground Motion Prediction Member and SHACC Committee
Mark Zoback	Stanford University	Independent Reviewer	Seismological Model and Geomechanics
Kevin Coppersmith	Geomatrix Consultants Inc.	Independent Advisor	Chaiman SHACC Committee
Jon Ake	US Nuclear Regulatory Commission	Independent Advisor	Member SHACC Committee
Hilmar Bungun	Norsar Norway	Independent Advisor	Member SHACC Committee
Torsten Dahm	GFZ Potsdam	Independent Advisor	Member SHACC Committee
Art McGarr	US Geological Survey	Independent Advisor	Member SHACC Committee

10 Appendix C – Description Groningen dynamic model status update 2015

Subsidence proxy details

Figures A1-A2 below show the theory and schematic representation of the subsidence proxy.

$$u_z(x,y,0) = \frac{1-v}{\pi} \sum_{n=1}^{N} c_{mn}\, \Delta P_n \frac{L_{zn} l_{xn} l_{yn} l_{zn}}{\left[(x-L_{xn})^2+(y-L_{yn})^2+L_{zn}^2\right]^{\frac{3}{2}}}$$

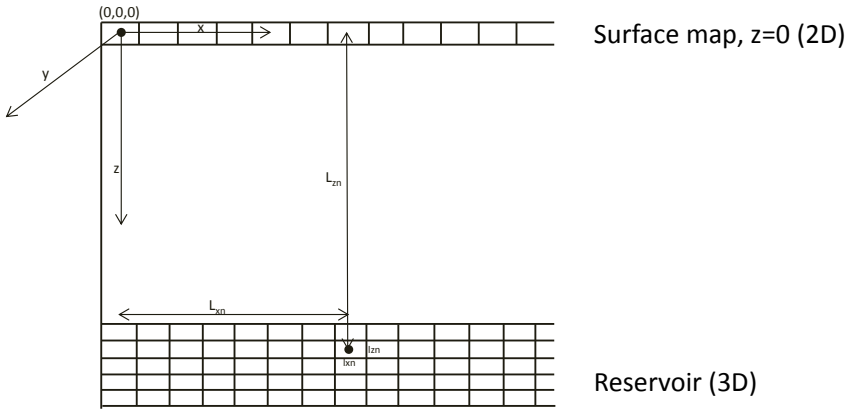

Figure A.1 Subsidence modelling schematic

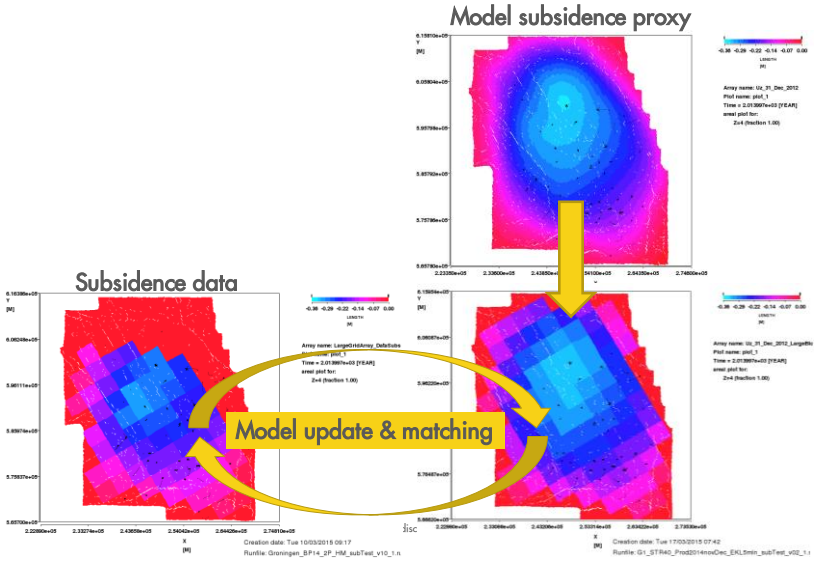

Figure A.2 Subsidence proxy implementation and workflow

Dynamic compartments modelling

The approach has been to first define segments in the updated static Petrel model (83 in total), using all relevant dynamic information provided by reservoir engineering. This is to ensure that Petrel segments have dynamically meaningful boundaries. This allows for direct comparison of static and dynamic modelling results such as in-place volumes and more control if tuning in certain areas is required. In Mores, the 83 Petrel segments were combined into 45 dynamic compartments. Figure A.3 shows the static Petrel segments and the dynamic Mores compartments.

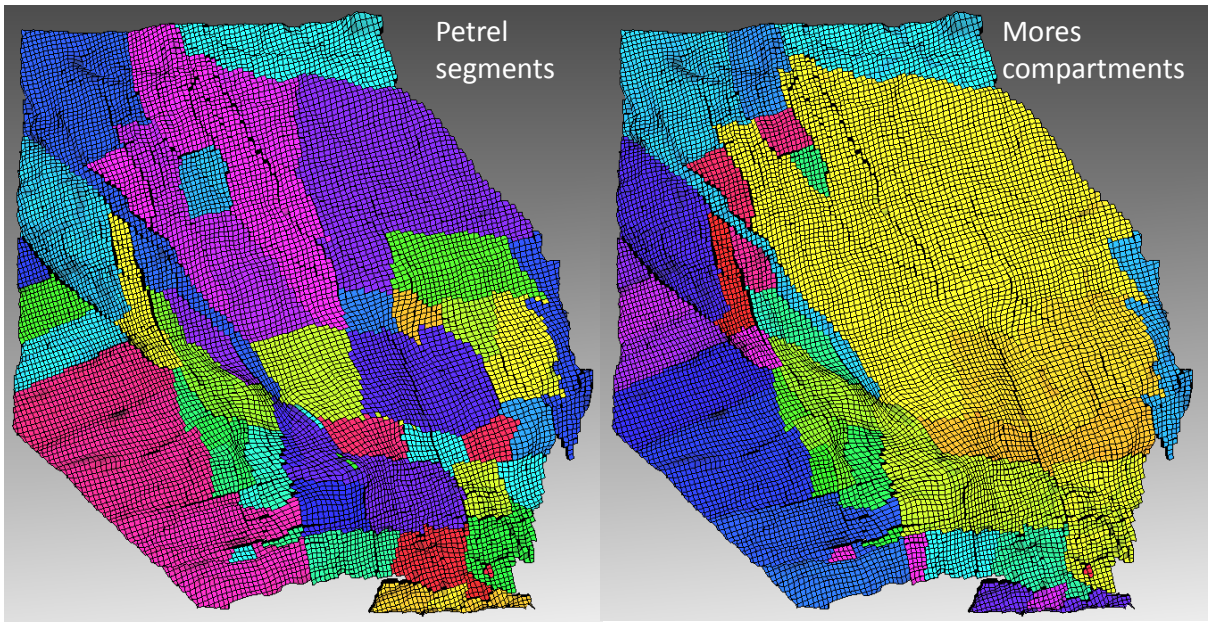

Figure A.3 Comparison between Petrel static model segments and Mores dynamic model compartments

Aquifers

To date, aquifers connected to the Groningen reservoir have shown a weak response and do not cause high gas-water ratio production. There is little direct pressure data available from the aquifers.

The GFR2015 aquifer work is based mainly on Ref **Error! Reference source not found.**], and sources used to analyse aquifer activity are:

- Groningen seismic data have been used to establish juxtaposition relationships between the Groningen field and surrounding aquifers
- Regional seismic data has been used to estimate the lateral extent and volume of the aquifers
- Pressure data from surrounding fields has been used to establish depletion prior to field production (from SPTG and RFT data), which can be linked to Groningen depletion
- Performance data from surrounding fields has been used to establish the likelihood of communication with the Groningen field
- PNL information has been used to assess water influx within the field

Figure A.4 illustrates the aquifers surrounding the Groningen field.

Reference 11 (NAM200304000817, Study of Aquifer Activity around the Groningen Field, by L.L. Vos, D.N.H. Lee, A.P. van der Graaf, February 2003)

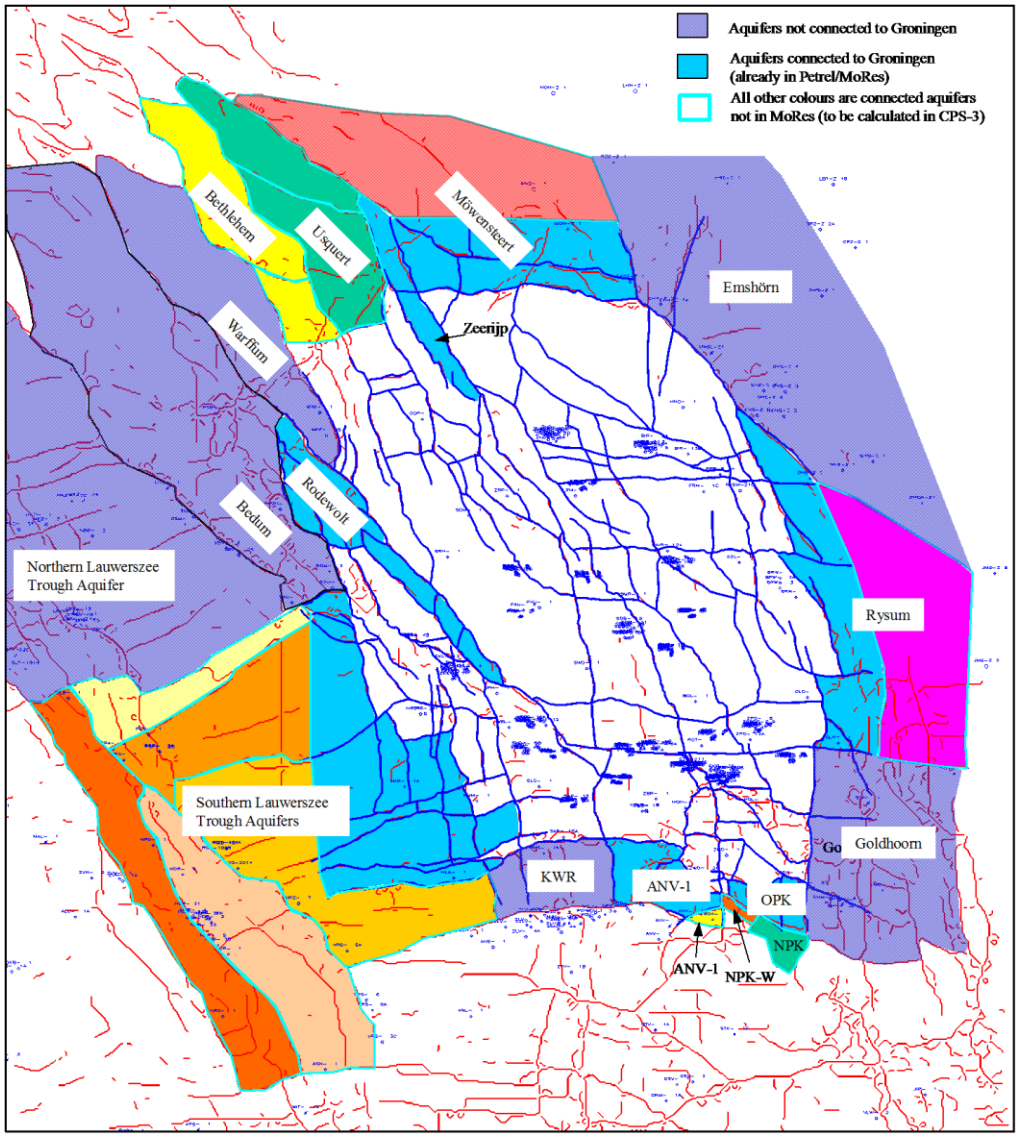

Figure A.4 Aquifers attached to the Groningen field

Revised model input properties

The saturation-height function has been reviewed and calibrated with SCAL data and fluid properties such as mercury injection and centrifuge core experiments. Another change is the application of a Brooks-Corey function which is considered to be physically more meaningful than the Lambda function used in 2012. Additionally, the residual gas saturation (Sgr) was given a fixed zero value in 2012 but is now included as a function of porosity, see Figures A.5 below.

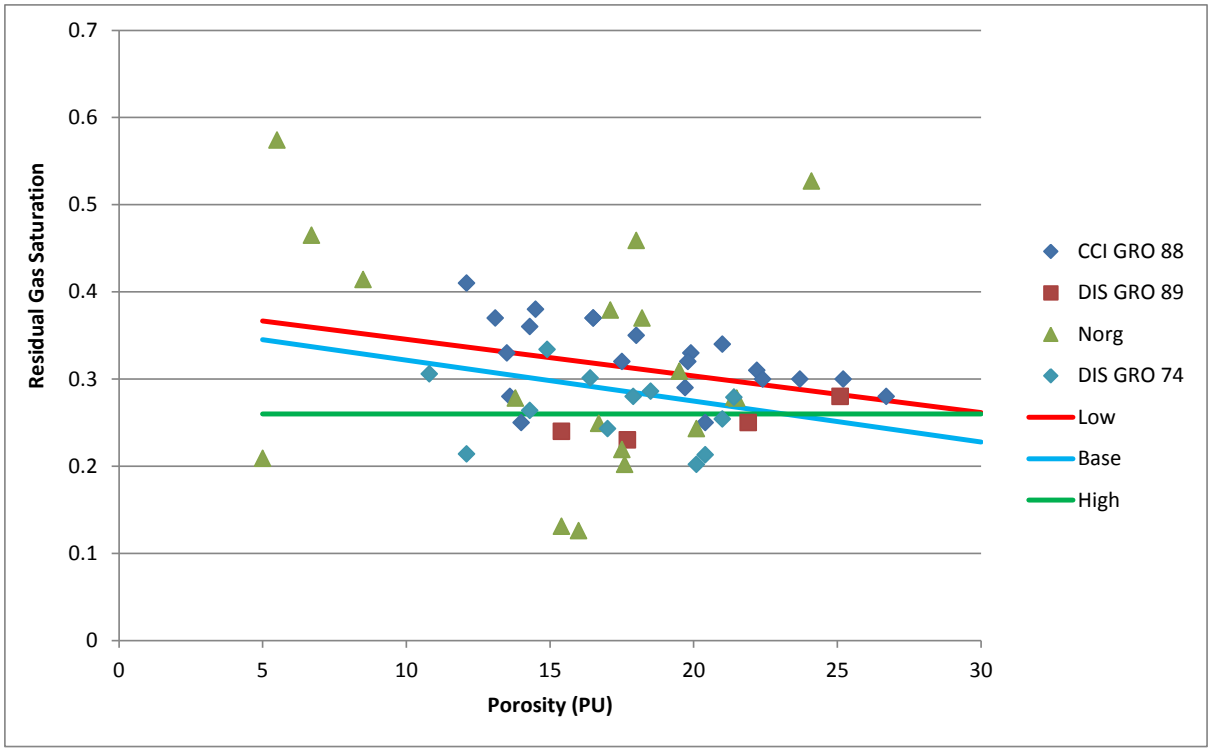

Figure A.5 *S_{gr} dependence on porosity for Low, Mid and High cases.*

Relative permeability data have been reviewed but only very minor changes were applied. The old curves generally seem to be consistent with core data currently available (Figure A.6).

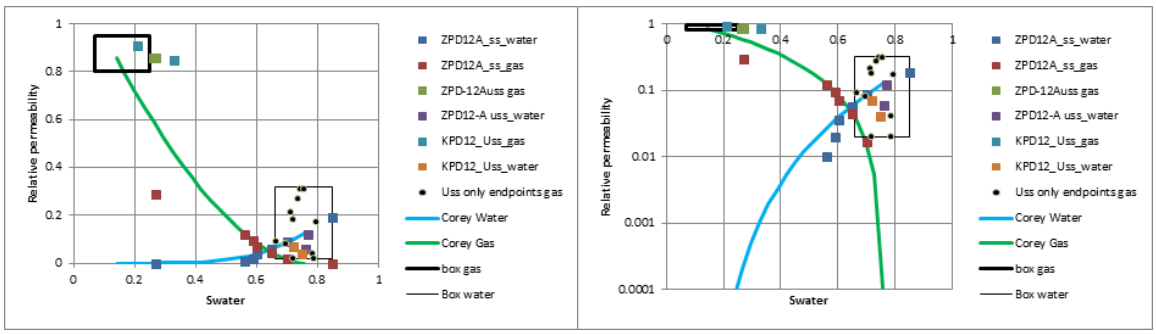

Figure A.6 Corey function fit for 14% porosity Swc (same as steady state experiment) to SCAL data on Groningen cores from steady state (ss) and unsteady state (uss) experiments

PVT data have been reviewed and the model found to be stable despite the temperature differences over the field. The water-gas ratio (WGR) now includes both formation and dissolved water. In the previous model both dissolved water and condensate-gas ratio (CGR) were constant despite the fact that the historical data suggests the changing trend. Both of them are now modelled in GFR2015 (Figures A.7-A.8).

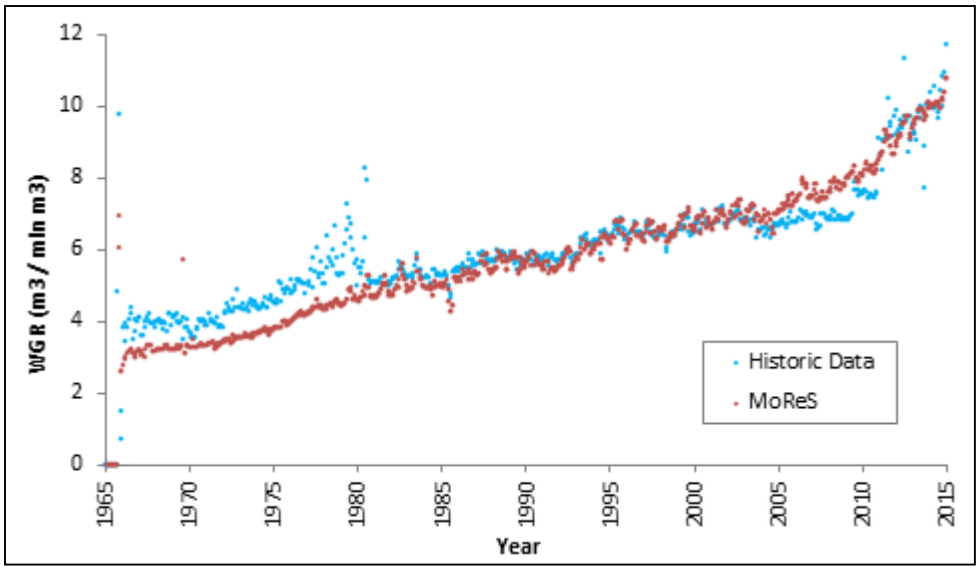

Figure A.7 *Achieved model match of the water gas ratio to the measured ratio*

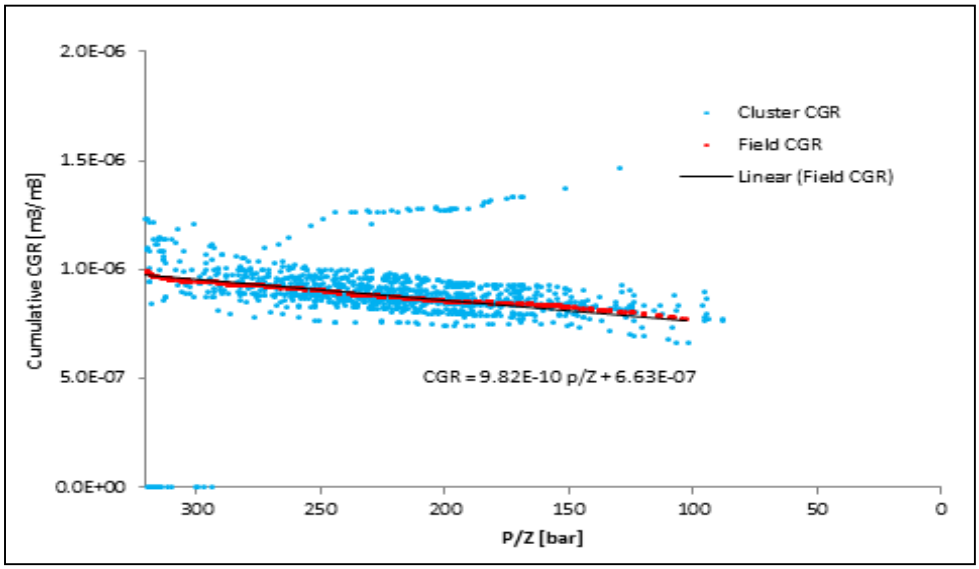

Figure A.8 *In blue ratio of cumulative produced condensate over cumulative produced gas (from EC) as function of p/z (from Siesta). In red Groningen field cumulative CGR as function of average field pressure excluding EKL data due to changing gas composition.*

Pore compressibility

The GFR2012 dynamic model used uniaxial compressibility (C_m) obtained from the first cycle core data and a third polynomial fit with porosity. The same curve has been used in the history matching process of GFR2015 to date (Figure A.9).

Additional work on pore volume compressibility is ongoing and may be incorporated in new updates of the dynamic model.

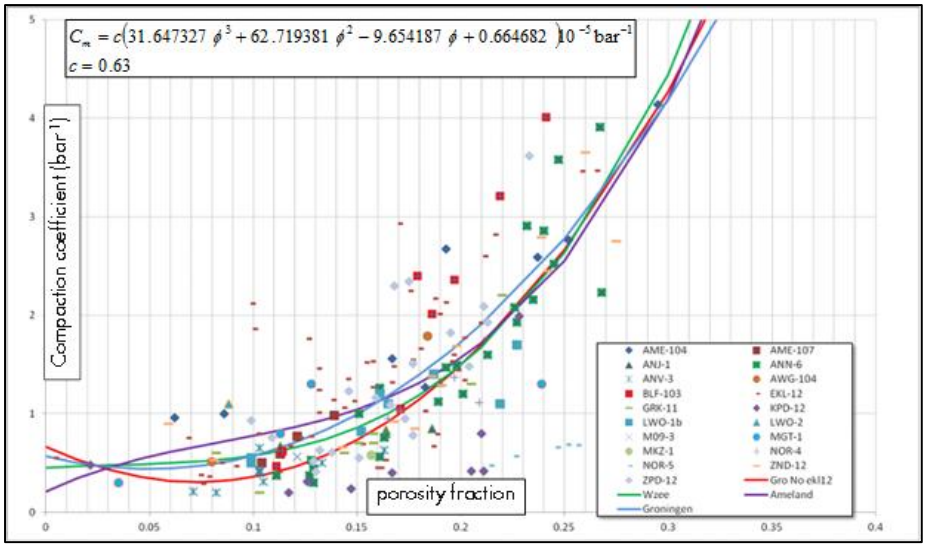

Figure A.9 Compressibility coefficient relation versus porosity based on first cycle cm core data, from Ref [5[5[5]. The constant which has been used in the GFR2012 models is c=0.55 instead of the c=0.63 as noted in the plot

Reference 5: EP201202215894. Groningen Field Review 2012 – Dynamic Modelling and History Matching Results, by Jort van Jaarsveld, February 2012

Assisted history matching workflow details

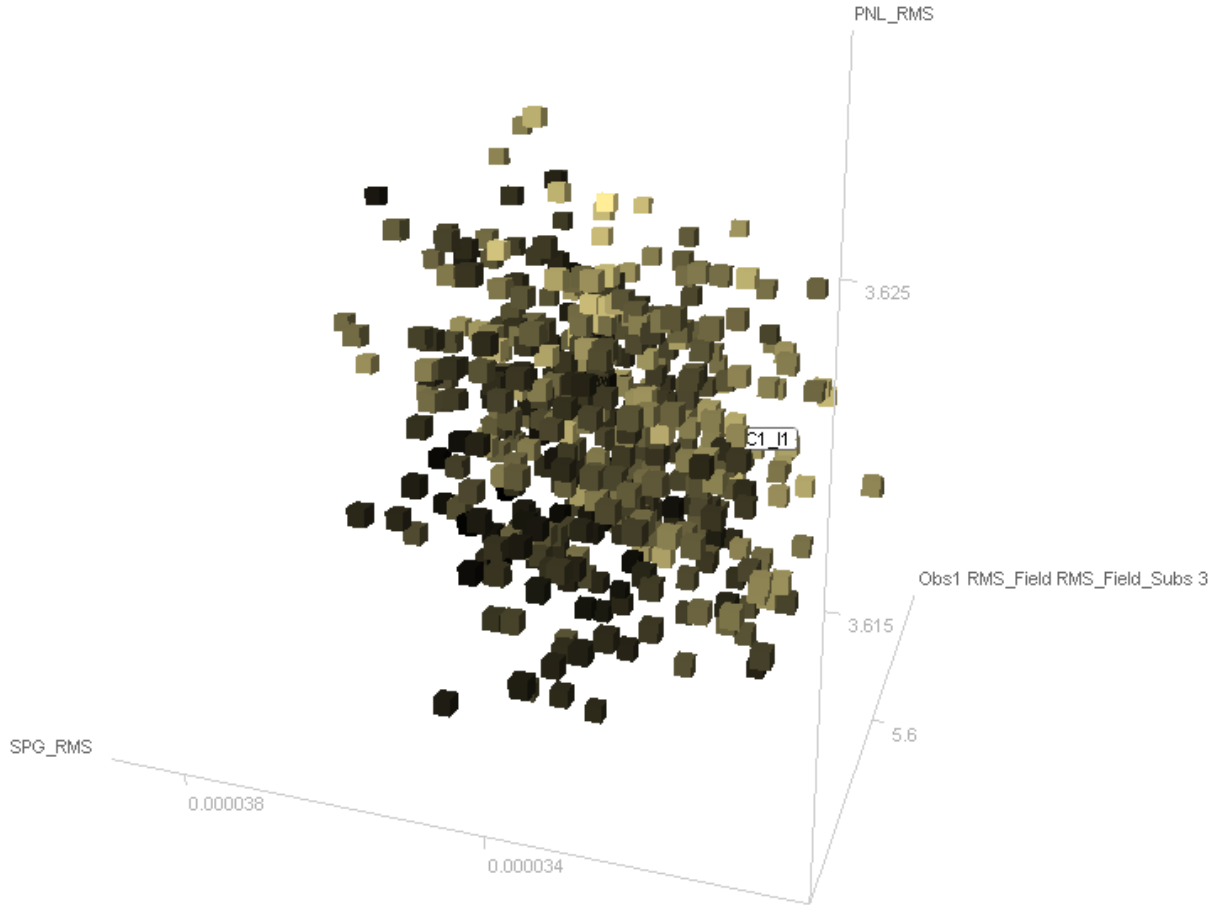

Figure A.10 AHM quality indicators based on 3 criteria.

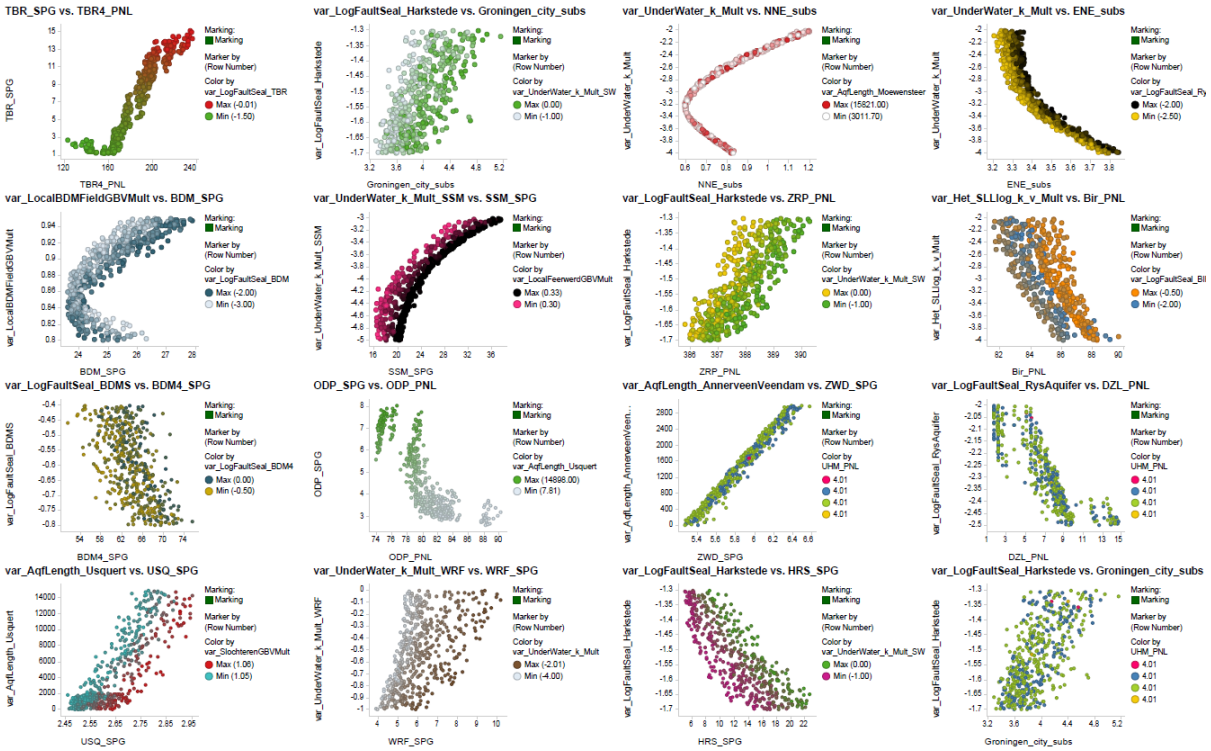

Figure A.11 Local history matching correlations provided by the AHM workflow.

Uncertainty analysis

The calibrated dynamic model provides reservoir pressures for the selected production scenarios and possibly includes the uncertainty range in reservoir pressures associated with subsurface uncertainty.

For a description of the Groningen dynamic model uncertainty workflow see Reference 16. In this workflow the subsurface uncertainty in ultimate recovery should be assessed, and not the GIIP as was done for the GFR2012 and GFR2013 models in the ARPR to date. Previously, the GIIP was considered a substitute of UR because of practical constraints. However, it is very important to use UR instead of GIIP because late field life uncertainty parameters are screened out when only using the history match period, e.g. aquifers or relative permeability parameters, see Figure A.12.

For reserves booking purposes the uncertainty in field UR at the end of economic field production life is important. For infill projects the uncertainty in project UR or project value is considered, and for hazard and risk assessment of earthquakes the uncertainty in maximum subsidence may be the preferred parameter. This would imply that a different set of P90/P50/P10 models is found for each parameter and this is not very practical.

Ideally all subsurface parameters should be assessed in the GFR2015 starting from a number of different static realisations followed by the dynamic uncertainty parameters tested from history match to forecast. This means that Reduce++, Mores for the history match, and HFPT for the forecast all need to be run into one Experimental Design for which DynaShell (Shell internal software) is the preferred platform.

This exercise will be performed once the alternative static models will be provided.

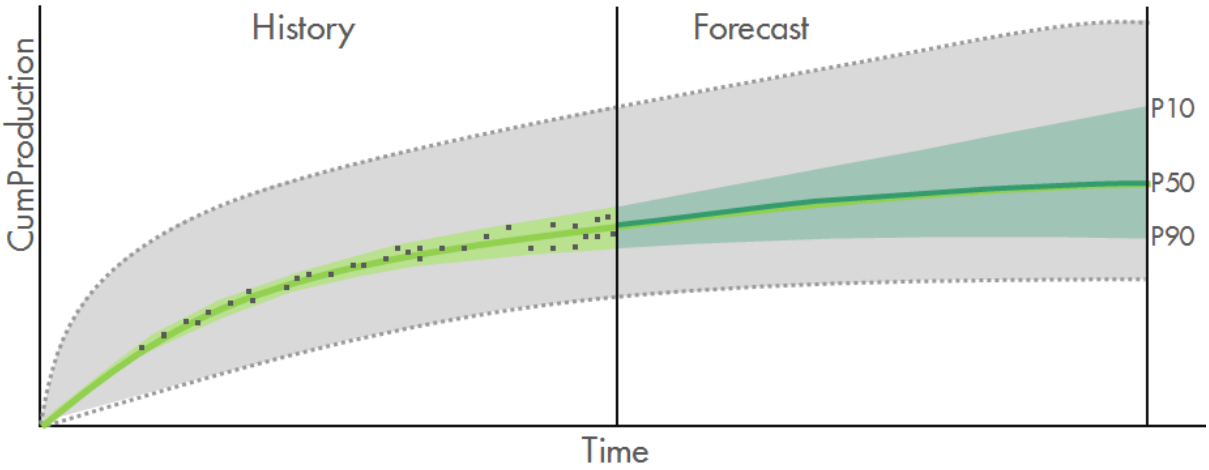

Figure A.12 *Schematic forecast uncertainty for ultimate recovery (UR). The uncertainty in subsurface parameters (ranges) result in the large grey uncertainty band. The dynamic data reduce this band by history matching and the light green uncertainty band remains.*

11 Appendix D – Review of the Activity Rate Seismological Model by Prof. Ian Main

'An activity rate model of seismicity induced by reservoir compaction and fault reactivation in the Groningen gas field'

by S.J. Bourne & S.J. Oates (2015)

Review by Ian Main, University of Edinburgh, Sep 30 2015

Summary

This paper builds on an earlier activity rate model by the same authors by (a) developing a full tensor strain field model for the amount of compaction, (b) explicitly adding information on the location and offset of faults, (c) including variability in reservoir thickness, also from seismic data, and (d) incorporating high-resolution surface deformation data (InSAR) for the first time. Importantly these improvements require a minimum number of additional free parameters in the activity rate model, instead adding the extra information as a set of additional constraints. The authors achieve significant improvements over the more empirical approach of Bourne and Oates (2014, c.f. their Fig 15), notably in reducing the bias and improving precision of the best fit activity rate model in Figures 24,25 of the current manuscript. The precision (statistical error) remains of a similar order of magnitude to the previous paper, likely as a consequence of the dominant effect of the finite sampling of the underlying population of earthquakes (and related uncertainty in the seismic strain partition coefficient), as captured in the stochastic simulations of the uncertainty bounds by similar methods in both reports. The precision will only be improved significantly when a larger sample of the earthquake population is available from the new networks, both as time progresses and as the magnitude detection threshold is lowered.

The paper presents the most comprehensive operational forecasting model to date for seismicity rate and seismic moment release rate in the Groningen field (or perhaps for any hydrocarbon field world-wide that I am aware of), together with forecasts of the uncertainty based on planned future production rates. The authors are aware these formal uncertainties (in Fig 26) for medium and longer-term time scales are likely to be underestimates, and sensibly stress the model should be used for now in shorter-term forecasting, for example for risk assessment and management under different production scenarios.

Overview

First the paper presents a novel theory for the upper bound to seismic moment expected from fault reactivation and variability in thickness, including a hybrid model which weights the contribution of the two components. There is no citation to prior art, and I think the theory is novel. It provides a natural mechanism for seismic slip within the reservoir, even in the case of relatively uniform or at last slowly-varying horizontal compaction due to pressure depletion in the producing horizon. The fault reactivation model includes scenarios where seismic slip is limited to parts of the fault where offset is only across the reservoir horizon, for example due to juxtaposition of the producing horizon with a more ductile overburden and/or under-burden, as well as for the general case where the strain partition coefficient is less than 1 for other reasons, for example due to smearing of such material along faults by episodic slip in past geological times.

At this stage there is no explicit feedback into modelling of the observed pressure field itself, or the implied variability in compaction rate that might be expected from the implied horizontal variability in compaction stiffness implied by some of the surface subsidence observations.

The model is then applied to the Groningen field. First the paper presents many maps of the relationship between seismicity, subsidence, the estimated compaction, the distribution of fault offset or throw, and topographic gradients. The compaction modelling is presented separately (Bierman et al., 2015) so I cannot comment on its validity or otherwise. The results show several of the largest fault offsets (a minority of the data) have a throw/thickness ratio greater than one (Fig 7). The authors don't comment on this directly, but this result implies that the total seismic moment (if such slip on such 'juxtaposition' faults is aseismic) may be dominated by intermediate-offset mapped faults.

The authors then apply this model to calibrate the past seismicity data with the model variants constrained by the new observations, including the discrete fault strain model and the thin sheet model. Importantly they consider retrospective 'smoothed seismicity' models (incorporating temporal clustering due to triggering of aftershocks) that have also proven relatively successful even in prospective mode for natural seismicity in the work of the ongoing CSEP testing centre (http://www.scec.org/research/projects/CSEP/scec3.html) The smoothed seismicity model does not just account for uncertainty in epicentre location, but also the variability that might occur in terms of finite sampling of a small number of events from a large number of spatially-distributed faults.

By carrying out a sensitivity analysis the authors conclude that the observed seismicity is best explained by a model where the dominant effect is due to localised fault reactivation. This is consistent with the fact that deformation inferred from of natural seismicity is likewise dominated by the largest faults, despite the larger numbers of smaller faults, in the case $b^{\sim}1$ (e.g. Main, 1993, Bull. Seismol. Soc. Am. 85, 1299-1308). They also show a strong co-variance in the activity rate model parameters for seismicity rate that propagates into the statistical uncertainties in the best fit model of Figures 24 and 25. They account for spatiotemporal earthquake clustering as in Bourne and Oates (2014), showing similar stochastic uncertainty in the model fits.

The present paper also includes a model variant where the Gutenberg-Richter *b*-value is dependent on strain, though the gains are marginal and it is not possible to reject the hypothesis that *b* is constant. The best fit history match and uncertainty envelope is presented in Figures 24 and 25 for these two scenarios, and a combined history match for 1995-2015 and operational forecast for 2015-2040 is presented in Fig 26. However, in the abstract and conclusions the authors stress the model is likely to be more reliable as a short-term forecasting tool. Given the epistemic uncertainties in any longer-term forecast ('known unknowns' or even 'unknown unknowns') this is quite sensible.

The conclusion and discussion are brief but follow logically from the main results, and the suggestions for further work also arise logically from the work presented.

Comments and suggestions

Presentation. The new conceptual model of Fig 1 could be described with a bit more motivation and detail for a general reader. It was not until I did the maths explicitly that I really understood it. In the

end it is quite simple, as many good ideas are, but key facts, such as the cross-hatched areas representing fixed positions (at least relative to each other) are omitted, making the reader work a bit harder than necessary. Maybe some time-lapse diagrams would be useful rather than simply a static picture, with some tracker horizons explaining the sense of slip that emerges. There may also be an inherent paradox between regarding the lower layer as both much stiffer than the reservoir rock and also more ductile in one of the model variants that should be addressed.

Throughout the text the cross-references to models or model parameters are made in too general a way. The reader is expected to hold a lot in memory for such a complex model. Much more detailed cross referencing to actual equations, for model parameters the equations where they are defined, and a glossary of parameters/ terms that can be updated in future work, would be really helpful. To provide just one example

Term	Symbol	Units	Comments
Compaction	ΔV or c	m	Change in reservoir volume per unit area

The abstract could usefully emphasise other novel aspects of the paper (e.g. tensor modelling, constraints from new data, a new fault reactivation model etc).

Model assumptions. Despite the acknowledgement of variability in reservoir response attributed to horizontal variations in stiffness, this is not addressed explicitly in the model at this stage. This may improve the model fit even further (particularly the more detailed spatio-temporal behaviour), but will come at a cost in terms of developing the model. For example if the under-burden is regarded as fixed in relative position, the shear stiffness at the juxtaposed contact may be different from the spatially uniform assumption in the current model. The juxtaposed contact also has the potential of forming a pressure seal if throw exceeds thickness, and this would have to be accounted for in a fully coupled poro-elastic model for reservoir pressure.

The model also assumes the deformation is dominated by compaction within the reservoir. This is internally consistent with the success of the history match of the model for induced seismicity rate. This does not rule out the potential for longer-range poro-elastic triggering of stress release outside the reservoir, but this can only be tested when the new high-resolution seismicity data are available. The prospect of long-term high-resolution InSAR data is also a very positive development, since it will increase the spatio-temporal resolution of the model.

Model validation. The main claim rests on the improved accuracy of the annual event rate and seismic moment in the history match. My impression is that this has been done without significantly increasing the number of tuneable parameters, and replacing empirical model parameters with constraints based on observation. However, I think it would be good to make this explicit with a one-to-one comparison of the model parameters that are common or unique to the activity rate models of Bourne & Oates (2014 and this report respectively), and then a calculation of a relative Information Criterion, taking explicit account of any differences in the number of parameters as well as the improvement to the residuals (e.g. as in Main et al., Geophys. Res. Lett. 26, 2801-2804), including the differences between the constant and variable *b*-value models.

Model development. At this stage the model is restricted to annual sampling. This is sensible given the even larger large uncertainties that would result from sampling smaller data sets at higher

temporal resolution. Nevertheless there does exist the potential to adapt the model for rate-dependent effects, for example annual flow rate cycling due to the demand cycle. Again this would have to be tested by formal model comparison, taking account of differences in the number of tuneable parameters, and the large sampling error introduced by the relatively small number of seismic events recorded annually.

12 Appendix E – Review of the Fragility Descriptions Version 1 by Prof. Ron O. Hamburger

The work supporting the development of Fragility Curves was independently reviewed by Ron O. Hamburger, an internationally recognised experts this field. Below the conclusions section of his review report.

The approach taken by NAM's consultants to characterize the risk of earthquake-induced structural collapse and fatalities due to induced seismicity in the Groningen region adopts the best current practices for such studies currently undertaken worldwide by both government and private parties. However, this state of practice is not perfect and has been known in past studies to over-predict potential losses, particularly for low level events. In specific we offer the following comments:

1. Benchmarking of analytical work against laboratory specimens undertaken by NAMS's consultants is admirable and appropriate. However, for reasons previously discussed, this benchmarking appears to be occurring for relatively low levels of nonlinear response. Collapse is a result of extreme nonlinear response. Benchmarking of the type undertaken by NAM's consultants does not necessarily demonstrate that analytical predictions of collapse are correct in that it is not clear if the modeling approaches will track well at extreme response.

2. As noted in some of the benchmarking studies for masonry buildings, the several analytical approaches undertaken did not agree well with each other. This is indicative of the significant uncertainty associated with predicting response for complex, highly nonlinear systems.

3. Although the proposed study conforms to present best practices, it inherently incorporates a number of conservative biases common to all such studies. The result of these biases is that study will tend to over-predict the true risk of building collapse and life endangerment. Conservative biases we identified include:

    a. For structures with fundamental periods less than about half second or so, nonlinear dynamic analyses, and static procedures calibrated to dynamic analyses, including so-called R-μ-T relationships developed by Miranda and others, predict very large displacement ductility demands at relatively modest values of the inelastic demand ratio, R. As a result, nonlinear analyses inherently predict collapse of such structures at ground motions modestly larger than those that load these structures to their elastic limits. Observation of real structures in earthquakes suggests this behavior is not correct. The profession generally recognizes this and ascribes this discrepancy between analytical predictions and observed behavior to soil-structure interaction, modeling simplifications and other effects.
    b. Analytical prediction of collapse is very difficult. Often, analysts will use somewhat arbitrary indicators of structural failure, such as reduction in strength to a defined fraction of peak strength to signal collapse. These indicators are typically conservative and prematurely predict true structural failure.
    c. Analytical models often neglect many structural and nonstructural elements that add substantial stiffness and strength to buildings. This results in under-prediction of actual stiffness, over-estimation of period, and consequently, over-estimation of displacement demands induced by earthquake shaking.
    d. Fragility curves are assumed to have lognormal distribution. While commonly for this purpose, many believe that the lower tails of lognormal distributions predict small, but significant probability of failure at demand levels that would

not credibly cause structural failure. When applied to large portfolios of buildings this inevitably produces large potential losses at levels of ground motion less than that at which damage has historically been observed.

4. The capacities predicted for some building archetypes including single-story, high bay industrial buildings and detached single family residences appear credible. Capacities predicted for other archetypes including some of the URM and concrete archetypes appear to be unreasonably low particularly when compared against fragilities that have typically been developed by others for similar building archetypes. In particular for the URM archetypes of wood diaphragms, the indicated capacities appear very low. Studies of similar buildings in the U.S. has indicated that seismic response is typically dominated by response of the flexible wood diaphragms which exhibit displacement capacities considerably in excess of those indicated in the URM fragility reports reviewed. Spectral demand will more closely approximate the diaphragm deflection of such buildings than the wall deflection. It does not appear this has been accounted for in the studies undertaken to date.

5. It is essential to benchmark the fragilities ultimately derived for this study against engineering judgment and to examine predicted HCLPF points from the fragilities against credible values based on observational data.

6. The life safety goals suggested as a basis for retrofit would seem to be aggressive compared with standards for both new and existing buildings deemed acceptable in seismically active regions of the U.S.

The full text of the review report prepared by Ron Hamburger, is available on:

http://feitenencijfers.namplatform.nl/onderzoeksrapporten/.